Development of Vertical Welding Technology on Thick Steel Plate

Using Hot-Wire Laser Welding Method

(ホットワイヤ・レーザ溶接法による

厚鋼板立向き溶接技術の開発)

September, 2015

WARINSIRIRUK EAKKACHAI

Department of Mechanical Science and Engineering

Graduate School of Engineering

Hiroshima University

Abstract

Recently, larger container ships have been built for more efficiency of maritime transportation, consequently by the thicker of steel plates that have been used for its structure. Generally, "electrogas arc welding" (EGW) process, a single-pass vertical welding process having very high efficiency, has been used to join heavy-thick steel plates on the vertical direction in a ship building industry, especially in the part of a container ship structure such as a hatch side coaming. However, the EGW process causes very high heat input, which affects seriously on toughness deterioration of a welded joint, since it makes grains coarse and a heat affected zone (HAZ) width wide. Therefore, the novel vertical welding process with lower heat input is strongly demanded to join heavy-thick steel plates having high strength and high toughness.

The present research proposes the novel vertical welding process for thick steel plates, using the laser diode as a heat source in combination with the hot-wire method, in order to achieve much lower heat input compared with the EGW process. This proposed welding process with low heat input should prevent grain growth and widening HAZ width and maintain toughness of a welded joint. In addition, the proposed process needs high efficiency by single-pass welding for thick steel plates in the vertical direction as with the EGW.

In the proposed welding process, a high-power laser diode is used as a main heat source and the hot-wire method is used for efficient deposition. A large rectangular spot shape of a laser beam, which fits a groove width (gap) and plate thickness, is employed. The laser is irradiated continuously from the above the joint into the groove to create and keep a molten pool during welding. A reflected laser on a molten pool surface is utilized for melting groove surfaces efficiently. Filler wires are fed from both sides of the groove, and filler wires are heated up to its melting point by Joule heating using the hot-wire system before entering the molten pool. YP-47 steel material for hull structure was used as base metal to joining for this research.

Firstly, feasibility study of welding phenomena of the proposed process was performed. The Initial melting of base metal was observed by in-suite observation during the stationary laser beam irradiate and hot-wire feeding. It was verified that the reflected laser beam form the molten pool really affected initial melting of the groove surfaces. Melting phenomena were investigated by basic experiment of single-pass vertical joining by hot-wire laser method. Gap width size of 5 mm with base metal thickness of 26 mm was joint dimension to study. The high-speed observation shows the result of stable weld pool formation during the vertical joining. The power density of laser irradiation is principle parameter to obtain an adequate fusion of the base metal. The critical power densities which depended on welding speed were successfully determined with 25 and 35 W/mm^2 for welding speed of 1.7 and 3.3 cm/min, respectively. Therefore, it was idealized for design and provide an appropriate laser

irradiating method to maintain high power density of laser beam to obtain the sound joint.

Laser irradiating methods were investigated on melting phenomena. Gap dimension of 10 mm (width) x 26 mm (thickness) was used as a target for joining. The couple parameter of power density is ratio of laser beam width per groove width, namely W_L/W_G ratio was used to investigate the joining ability. For the length dimension of the beam is almost equal base metal thickness. The stationary laser beam with W_L/W_G = 1.0 was used, but irradiated by low power density (23 W/mm^2) has a result of low melting amount, more accumulated imperfections of incomplete fulfill, and lack of fusion. It was revealed that joining by the low-power-density laser beam does not provide an adequate reflected laser energy to create the initial melting of the base metal. On the other hands, the final fusion of the weld joint that was formed by weld pool heat conduction.

Consequently, the weaving laser irradiating method was used instead of the stationary laser beam method in case of the laser power source is a limitation of the maximum power irradiation. Methodology of the weaving laser beam is an irradiation of the narrow-width long-length laser spot-shape to maintain high power density (higher than the critical power density) and sweep this beam along the groove width direction. The appropriate weaving frequency and waveform was obtained; it is 5 Hz exponential wave to set for the weaving condition. The weaving irradiating condition was optimized by varies 2 beam width sizes of 2 mm and 4 mm over gap width of 10 mm and W_L/W_G = 0.2 and W_L/W_G = 0.4. The wide laser spot size of W_L/W_G =0.4 could maintain a high temperature weld pool and result on a larger melting volume (larger weld bead size). Meanwhile, laser beam size of W_L/W_G = 0.2 was resulted on larger difference of liquid weld pool energy when laser beam moving, although narrower laser beam width irradiated by higher power density. It was mentioned that using long-length laser beam size for joining resulted in much lower energy on the beam tails (edge region). Frequently imperfection of incomplete fulfill or lack of fusion was occurred on this region. An important idea of this problem is a compensation of laser energy on the both tails for troubleshoot the occurring of imperfection.

Therefore, the twin laser method was performed to improve welded joint quality for sound weld achievement. Twin laser method has been successfully applied on one pass vertical joining. Imperfection on edge region could be fixed by compensate laser power on the edge region. For one side of compensate laser power, laser power levels strong affected the melting amount of base metal. At 3 kW compensate laser power provided complete fulfill weld metal and complete fusion of welded joint under fixed welding speed of 3.33 cm/min (2 m/h). It was performed to study of welding speeds effects to optimized welding parameters. The optimized welding speed for twin laser with one side compensation is 5.00 cm/min (3 m/h). It provided complete fulfill and adequate weld penetration. From the information of this chapter, it can be suggested that homogenizer for create laser beam shape should distribute higher energy on the

edge tails on the laser beam. The center region can irradiate by lower energy since during joining heat conduction from both tail sides can provide adequate energy for fusion base metal.

The weld metal properties were studied. Cooling transformation time of Δt8/5 were obtained and related with microstructure and toughness. The cooling characteristic of the twin laser method has Δt8/5 range of 84 to 200 second. The selected filler metal of JIS3312 G78AUMN5C1 M3T provided martensitic-bainitic base of microstructures transformation. The increasing of welding speed resulted in cooling time became short and resulted in the fine martensite phase formed. On the other hand, long cooling time by lower welding speed resulted in coarse upper bainite formed. The finest microstructure of cooling time of 84 second was performed on the Charpy V-notch test. Absorbed energy more than 100 Joule at test temperature of -20 °C could be obtained by high-speed condition.

According to the main proposes of low heat input delivered to base metal, heat input effects on HAZ's characteristics was investigated. Heat input of twin laser method was controlled by welding speed ranges. Increasing welding speed resulted in heat input was decreased thereby grain size on CGHAZ became smaller. CGHAZ width of the proposed process has narrower to 1,600 micron and could become narrower than 700 micron by using the welding speed of 5.00 cm/min which was optimized welding speed for sound weld condition. Compare HAZ's characteristics of the proposed process with two electrode VEGA, the proposed process has an advantage of both of grain size and CGHAZ over two electrode VEGA. It was clearly evidence that the proposed process provide low heat input welding for single-pass vertical joining. The requirement of heat input of the proposed process has the lower level of heat input when comparatively compared with other vertical welding processes.

Table of Contents

Chapter 1

Introduction

1.1 Research background

1.1.1 Background

In recent years, marine transportation has been considered as high efficiency for shipping large numbers of container in one time. In particular, container ships rapidly increase in size progressing against the background of the traffic volume increase. Fig.1.1 shows the trend of container loading capacity of container ships [1]. 6,000~8,000 TEU (Twenty-feet Equivalent Unit: 20-foot containers in terms of the number) capacity of container ship is conventional size for economical transportation. However, on the present, 10,000 TEU class or higher container ship is built, 20,000 TEU class that have also been planned for construction.

During loading of container, a structure is characterized with a large opening in the deck unit. So, for a large containership must ensure the strength for carry on load due to the wave applied to the hull structure. Critical part structures such as hatch side coaming, strength deck, broadside plank, longitudinal bulkheads that are made of high strength steel plate having a heavy thickness (Fig. 1.2) [2].
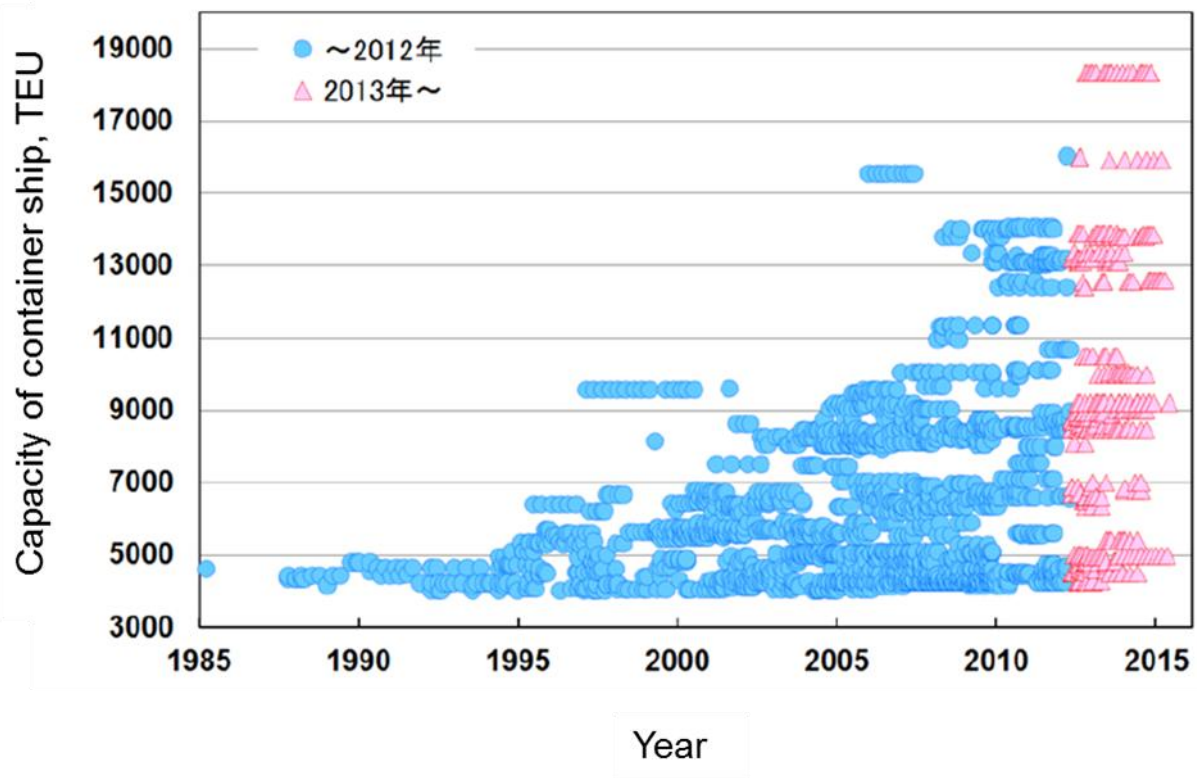
Fig. 1.1 Transition of capacity of container ship (Sea-web).

1
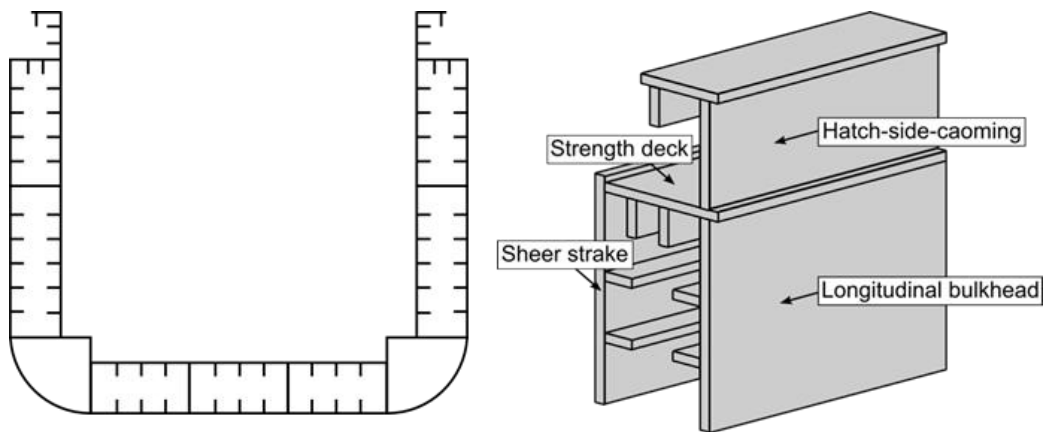
Fig. 1.2 Cross section of container ship and strength deck structure.

These structure has meet requirement of ensuring the toughness property of steel plate and welded joint. However, it was very difficult for heavy thickening the steel plate to obtain good toughness. Moreover, thermal affects the toughness degradation when high heat input welding was applied. Therefore, YP47 steel plate is a new high-strength steel plate, which has a specified yield point of 47 kgf/mm^2, for heavy thickening class has been developed and applied for large containership [3-10]. YP47 steel plate is a high strength steel grade, good toughness property, and good property of crack arresting. Currently, it has become possible to produce for the maximum thickness about 70 mm.

Currently, hatch side coaming, the welding of thick plates, electro-gas arc welding is applied as a high-efficiency one-pass vertical welding. Electrogas arc welding (here after will call as EGW) is a fusion welding process for continuous vertical joining, especially for thick steel plates. Continuous arcing between a consumable electrode and base metal make a weld joint. A shielding gas is used for controlling arc environment [11, 12]. This welding method has been applied for joining an extra-thick steel plate of about thickness 70mm. High heat input welding of more than 500 kJ/cm necessary applies to achieve sound joint [13]. It was resulted in toughness deterioration that is a severe problem in the weld metal and heat affected zone [7].

YP47 steel toughness ensuring the weld is developed and can reduces the thickness for hull structure. Reduced thickness can reducing the amount of heat input for joining. However, in the case of using a further containership, capacity more than 20,000 TEU, the thickness is considered to be more than 100 mm. Then, YP47 steel must be produced and used by having more plate thickness. The amount of heat input is still considered on heavy thickness on the aspect of toughness deterioration.

1.1.2 Background statements of high heat input welding

In recent years, in shipbuilding and construction of steel structure, thickening of the steel due to the increase in the size of the structure, high strength has progressed. At the same time, shortening the construction period, submerged arc welding for the purpose of construction cost reduction, electro-gas arc welding, the high heat input welding of electro-slag welding has been applied widely. For high heat input welding, the welding heat affected zone slow cooling rate is exposed to high temperature for a long time, toughness degradation due to grain coarsening of the weld joint is a major problem [14]. Various investigations have been taken metallurgical and mechanical aspects for toughness ensure on the heat-affected zone. In the welding process with heat input 10 kJ/mm or higher, grain coarsening suppression technology of the heat-affected zone utilization the pinning effect of TiN particles it has been applied [15-17]. Fine TiN particles suppressing the growth of austenite grains, refining the ferrite transformation structure (Grain boundary ferrite). However, further large heat input welding, there is a problem that TiN particles cannot be obtained that sufficient pinning effect of solid solution [18]. Therefore, new oxides and sulfides as pinned particles Mg and Ca are utilized, it is possible to be stable held at a high temperature to suppress the growth of austenite grains [18, 19]. Also, toughness ensuring the heat affected zone utilizing a diffusion phenomenon current B is being performed [13, 20-22]. It was mechanism of fine ferrite generation by B diffusion from fusion zone to heat affected zone. Free N disassociated from TiN and then it forms as BN. This phenomena can success by balancing an adequate amount of B in filler metal and TiN in base metal. Toughness securing welds have been carried out by material development, as mentioned above.

1.1.3 Electro-gas arc welding for the very thickening of steel plate

Conventional electrogas arc welding [23] which was developed in the 1960s. This welding process has widely used in the shipbuilding and other heavy industries. Because of large groove section to be joined due to heavy plate thickness, high heat input of arc necessary applied. Many reports of brittle crack occurred over theses joints. The safety of the joint structure reliability became low. Then one electrode VEGA (Vibratory Electro-gas Arc Welding) welding process in the 1970s has been developed. The welding is made possible heat input decreased by carrying out and narrow groove using thin wire [24]. Heat affected zone toughness and construction efficiency were significantly improved by the application of one electrode VEGA welding method. Also, it is possible to obtain a sound joint without causing fusion defects even in steel sheet having a thickness 50 mm. However, heavy thickening of the steel plate in the containership as described above proceeds rapidly, the maximum thickness is in the order of 70~100 mm. Development [24, 25] has been made of two-electrode VEGA welding method as a response to the thickness. Capable of electrode 1 pass vertical the steel sheet with a thickness of 50~70 mm in

VEGA welding, on having a stable penetration and adequate joint properties, construction efficiency is also improved. However, the steel plate are very thicker by increasing the size of the container ships. Corresponding with multi-electrode does not become a ready solution. The development of new low heat input vertical welding method is priority goal.

1.1.4 Current state of the thick steel plate vertical welding in other fields

For weld joint properties of the skyscraper, especially they are placed on the earthquake filed, is required high fracture toughness than conventional building. The Charpy absorbed energy higher than 70 J at 0 ℃ in the weld joint properties of the skyscraper is meet requirement [26, 27]. In addition, high strength steel plates having thickness up to 50 mm have been implemented on the large span structure [19]. On these construction fields, electroslag welding (ESW) has been adapted is equally one-pass vertical welding likes electrogas arc welding. Large amount of heat is generated by resistance heat between consumable electrode and slag obtain large fusion volume of the weld joint. Toughness deterioration of the heat-affected zone by the extremely heat become a problem in this welding method.

For the protection of the global environment, the demand of an alternative fuel such as liquefied natural gas (LNG) has increased. Currently, the effective use of the site area, in progress increase in the size of the domestic onshore LNG tank from reducing such as construction cost. The inner tank material of LNG tank (shell parts) is applied the cryogenic material of 9% Ni steel [28]. A large volume of a tank, the 50 mm thick plate that exceeds conventional thickness (about 30 mm) greatly is used [29]. Multi-pass welding with high-quality welding capable of TIG welding is being carried out to vertical welding at the LNG tank construction. Multi-pass welding ensures the quality of the joints has been made but poor construction efficiency. There is a need for efficiency improvements for low- heat input vertical welding.

1.2 Development of hot-wire method and the thick steel plate vertical welding method which is a combination of a laser heat source

Hot-wire method is Joule heating method to heats a filler wire in a state of just below the melting point is energized heating the addition of wire. The parent material melting can be controlled by a main heat source such as a laser or an arc. The weld metal deposition rate can be arbitrarily controlled by the wire feed control. It high-efficiency weld deposition as a feature of the hot wire method can be formed. The degree of freedom in selection of additives wire is high it can be mentioned.

Hot-wire TIG welding is widely applied to high quality joining. However, blowing arc of magnetic, arcing from the wire, is difficult problems such as proper wire current adjustment. Thus, on the present, various studies to improve [30, 31], which enables stable wire feeding. Laser welding, high-quality, low deformation, high speed, use is expanding in various industrial fields as a joining method of deep

penetration [32, 33]. However, it has a drawback of the small groove tolerance. Welding defects frequently occur. There is a problem such that the characteristic control of the weld metal is difficult. Hybrid laser-arc welding has advantage of groove tolerance than normal laser welding process [34]. In the shipbuilding that the hybrid welding can achieve joining over thin steel plate or less of the plate thickness 13 mm. General cargo ship, butt welding is actually applied in the industry [35]. However, Hybrid laser-arc welding difficulty success joining to extra-thick steel plate because generally use a relative small spot size of laser beam as a heat source. It was mismatching to the joint dimension. So, nowadays, the diode (semiconductor) laser capable of laser beam shape control is used as a laser heat source in the welding and using a rectangular laser suitable for groove shape. By that laser beam is possible way for joining over extra-thickness plates.
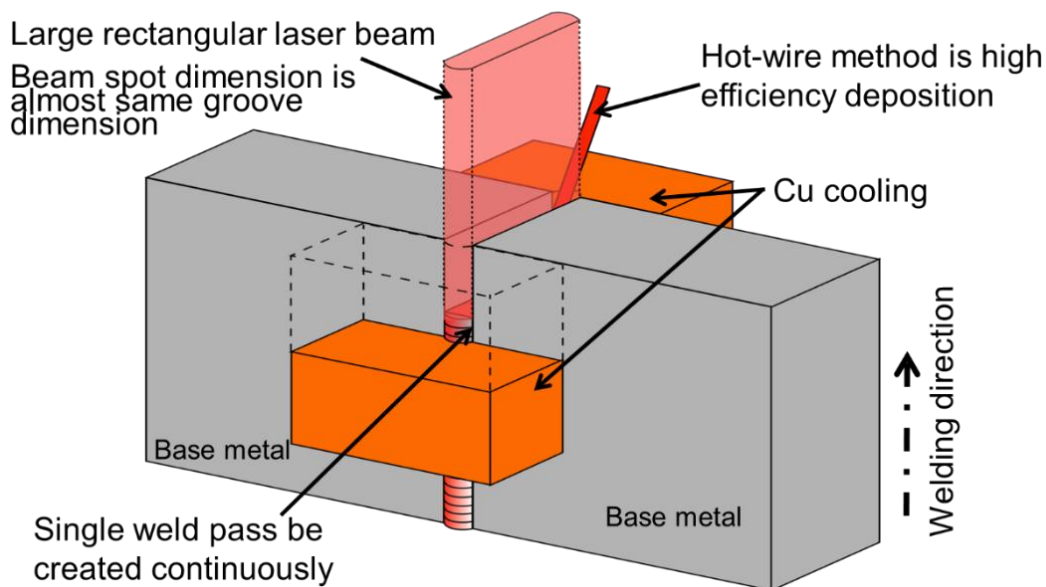
Fig. 1.3 Schematic illustration of novel welding process.

Fig. 1.3 shows a schematic diagram of the proposed welding method. A high-power laser diode is used as a main heat source and hot-wire method is used of efficient deposition. A large rectangular spot shape laser beam, which fits a groove width (gap) and plate thickness, is used. The laser irradiated continuously from above the joint into the groove to creates and maintain a molten pool during welding. A reflected laser on the molten pool surface is used to melt groove surfaces in front of the molten pool surfaces efficiency. Filler wire fed on beside of groove is heated to their melting point by Joule heating using hot-wire system before entering the molten pool. Copper jig and motion are similar to those of an EGW process. By significantly lower heat input of the present welding method, prevent softened and

embrittlement in the heat affected zone, it is possible to reduce the welding deformation (distortion). Also due to the low dilution, it is possible to control the characteristics of the weld metal by adding wire. In addition, cost reduction due to relaxation of design conditions of a higher efficiency of steel, welding material due to the hot wire or the like can be expected. High quality in this welding method, it is possible to achieve both high efficiency and low cost, it is considered to be a very valuable welding.

1.3 Objective and Construction of Thesis

In this research, we proposed novel vertical welding for thick steel plates using a laser diode as the heat source in combination with the hot-wire method to achieve a much lower heat input compared with the EGW process. This welding process, with low heat input should prevent grain coarsening and widening HAZ width and maintain the toughness of a welded joint. In addition, the proposed process requires a high efficiency by single-pass welding for thick steel plates in a vertical direction such as with EGW process.

This thesis dissertation is emphasized explanations for the basic idea of the proposed process, welding phenomena during vertical welding, development of the proposed process for particular joining site, optimization welding condition, metallurgical characteristics and weld joint properties under effects of welding parameters, competitively evidence of low heat input process. Fig 1.4 shows the flow chart of the construction of the thesis.

Chapter 1 discusses the background of research as well as the objective and construction of thesis.

Chapter 2 reviews the theoretical background and the present researches on high performance structure of steel types, joining process for vertical heavy joint, problem on service properties from high heat input applying, advanced EGW method and its limitation. The evolution of hot-wire welding method is discussed. Laser welding method is considered on laser beam irradiating method and material processing.

Chapter 3 is a basic idea of single pass vertical joining on the heavy joint which using a combination of hot-wire method and laser heat source. Methodology of laser irradiation for the large rectangular beam with stationary laser irradiating method is explained. In this chapter, a narrow gap of width relative with plate thickness is the proposed study. The process phenomena are investigated on groove surfaces melting by the reflected laser heating. Basic experiment to study the effect of laser power and welding speed can obtain the critical power density for fusion weld.

Chapter 4, Investigation of melting phenomena and optimization of laser irradiating condition is an objective in this chapter. Gap width size of 10 mm is a

target to achieve of joining. Laser irradiating methods are considered to provide an appropriate power density for make a sound weld. Weaving laser irradiating method is developed for joining on large gap size by narrow-width long-length beam sweep on gap width dimension. Weaving parameters and laser beam spot size are optimized to achieve completed fusion on weld joint. Laser access methods are also develop to make of most realization for actual field joining.

Chapter 5, Improvement of novel welding process by laser power compensation with twin laser method is an objective in this chapter. Compensate laser power on edge region by fiber laser is a possible study to obtain an idea of design an appropriate optical laser beam shaping. This chapter has two main parts for study. First, the experiment for parameters screen out of twin laser by the effect of fiber laser power and welding speed on weld joint characteristics. Second, optimization the laser parameters to achieve sound joint.

Chapter 6, fusion zone characteristic is obtained by monitoring of weld metal cooling history. Welding speed ranges which were obtained from the twin laser method by sound weld results are monitored the weld metal cooling curves. Cooling transformation time: $\Delta t8/5$ of the selected filler metal is obtained and related to microstructure outcomes and hardness. Effect of cooling rate is investigated on phase constituents, phase sizes, hardness and toughness properties.

Chapter 7, Heat Affected Zone (HAZ) characteristic affects by heat input levels is investigated. Grain size and the width of coarse grain HAZ (CGHAZ) are obtained and compared their behavior. Evidence of the low heat input process can be shown by smaller grain size and narrower CGHAZ width of the proposed process compare with advanced EGW such VEGA®. The proposed process has a good potential to be used single pass vertical joining by low heat input condition. High welding speed can be provided and controlling minimize heat input for joining.

Finally, the conclusions of this thesis are summarized in Chapter 8.

Chapter 1: Introduction and Research Objectives

⇩

Chapter 2: Literature Reviews

⇩

Chapter 3: Feasibility study of single pass vertical joining by using hot-wire laser method

- Introduction to the novel welding process and its methodology
- Preliminary experiments to study welding phenomena on vertical joining using hot-wire laser method (gap width of 5 mm)
- Basic experiment to study effect of laser power and welding speed by stationary laser beam
- Determination of the critical power density for fusion welding

⇩

Chapter4: Investigation of melting phenomena and optimization of laser irradiating condition

- Investigate effect of stationary laser beam on the wide gap size (gap width of 10 mm)
- Improvement the process efficiency by weaving laser irradiating beam method
- Optimization of laser beam parameters for weaving laser irradiating method

⇩

Chapter5: Improvement the novel welding process by laser power compensation with twin laser method

- Effect of laser power compensation and welding speed on weld joint characteristics with twin laser method
- Achievement of sound weld-vertical joining on heavy thickness by optimized energy profile using twin laser method
- Optimization of welding parameters on sound weld criteria

⇩

Chapter6: Weld metal characteristic

- Weld metal cooling curves under influenced of welding speed ranges
- The relation of $\Delta t8/5$ and microstructure constituents, phase sizes and weld metal hardness
- Toughness properties of weld metal comprehensively test on NK rules

⇩

Chapter7: Heat affected zone characteristic

- Effects of heat input on grain size distribution and CGHAZ width
- Comparison the proposed process and other EGW process on HAZ's characteristics
- Competitively comparison of the requirement of heat input with other welding process

⇩

Chapter8: Conclusions and future works

Fig. 1.4 Construction of the thesis

Chapter 2

Literature review

2.1 Introduction

This chapter is an additional review of the related research and technical report from chapter 1. There are consists of the performance of constructions of steel structure in the present and meet requirement on the future, high-performance steel grade and technology of joining process with specified vertical weld joint. The evolution of hot-wire welding method was discussed on various sub techniques. The related phenomena of laser heat source during welding were shown and explained by clearly evidenced from in-situ observation.

2.2 Brief Innovation of high-performance steel structure

Since 20th century, steel structures possible reduced manpower and construction time by engineering evolution [40]. High rise building, skyscrapers, large volume tank farm, high performance bridge and container ship were constructed by high process efficiency with both sides of high-strength lighter-weight materials and high efficiency manufacturing process. For high strength steel has advantage of lighter-weight by reduced a section to carry load as equal of higher. Thermomechanical Controlling Process or TMCP technology [41] can provide high strength and excellent fabricated properties. Then, the structure could be made as larger sizes and more loading capacity. From steel making evolution, possible demand to design and construct more performance structures, continuously. Especially, marine transportation business, large container ship which up more 18,000 TEUs loading is a target of economical transportation. Fig 2.1[42] shows gradually demands of loading a container from the 19th century to the present. The container ship size becomes larger. Moreover, from its tendency could be seen larger size may be constructed in the future. Loading container capacity depended on cross section size of hull structure which shown as example on Fig. 2.2. It was resulted in steel plate or steel form section become bigger or thicker.

In addition, these steel structure must be able to support or service for carrying a heavy load and external load such as wave load or wind load. Then, steel must be having high performance based on designed strength and fabricated strength. For this section emphasized review research and technical cases for ship building industry.
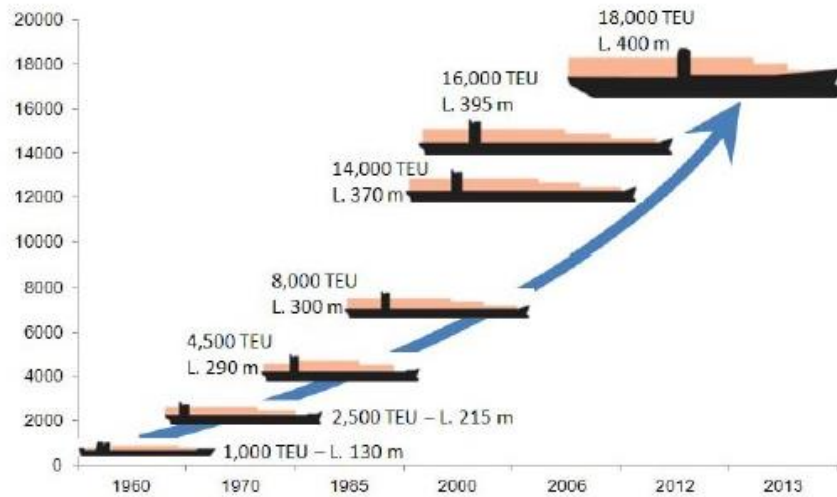
Fig 2.1 Loading demands over historical recorded year.

Fig. 2.2 Example of loading capacity depended on hull sizes [42].

Fig. 2.3 shows the example for various plate thicknesses on hatch coaming side structure are deepened on steel grade. By using high performance steel grade can maintain the weight of the shipbuilding structure. The yield point steel grade of 390 MPa or namely as YP 40 steel was used for the structure of hatch coaming side for capacity of 8000 TEU. The plate having thickness up to 65 mm and it has a problem for produce on heavy thickness 80 mm because good toughness cannot be obtained by the heavy thickness plate for the conventional steel. From this situation, new steel grade has been developed to obtain high strength and high toughness under medium thickness. Yield point 460 MPa or YP 47 steel is steel grade for hatch coaming side structure of ship class of 12,000 TEU or more. Using this steel grade, an example for 12,000 TEU class, the plate thickness are used around 50 mm to 70

mm. Therefore, the ship structure became lighter weight. The transport efficiency on parts of ship speed control and energy consumption can be increased by the light-weight structure.

On the manufacturing process, the light-weight structure has an advantage of setting time, mobile processing, etc. Especially, Thinner steel plate can reduce the processing time and energy for the joining process.
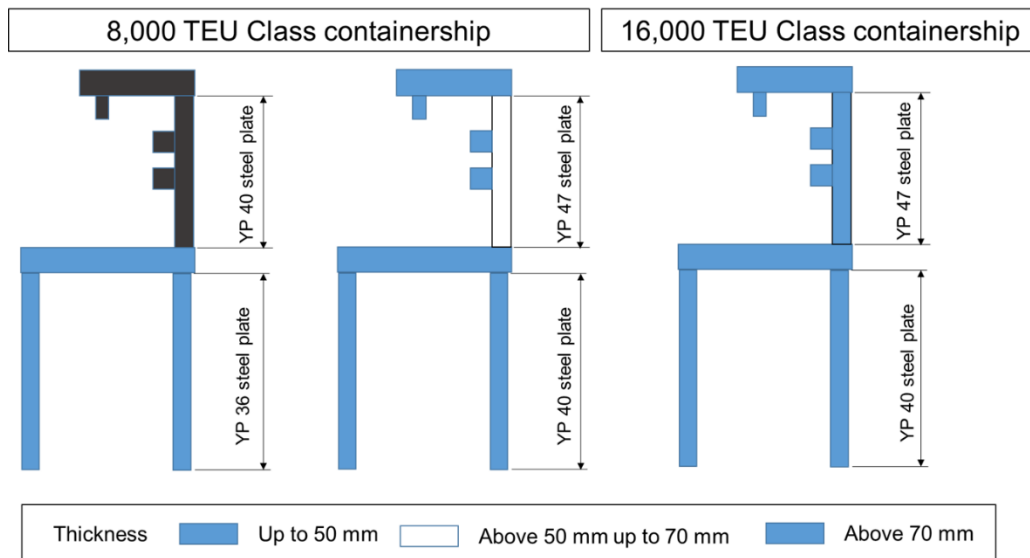
Fig. 2.3 Section of containership for differential capacities were constructed by various class strength of steel grades and various plate thicknesses.

2.3 Evolution of the developed high strength steel

From the previous section was described on the structure size and high strength steel grades were applied for reducing the structure section and reducing the structure weight. However, in the steel manufacturing process does not control only the strength of steel plate but also the homogenization of toughness property in the thickness direction must be obtained for corresponding on fabrication properties. This section will be discussed in the technology of manufacturing process for high strength steel plate in the metallurgical aspect.

Thermo-mechanical Control Process (TMCP) [43-47] has been using for production of high strength and high toughness of steel plate, especially for steel for marine transportation. The concept of technology for controlling the microstructure by mechanical and thermal processing was shown in Fig.2.4 [47]. During austenite nucleated in the recrystallization temperature, plate was rolling in same time and resulted in austenite grain deform by rolling load. Final strength of TMCP' steel plate is controlled by final microstructure which was controlled by an appropriate cooing

rate. As from above mention TMCP's plate has characteristics of grain refinement, controllable microstructure, high toughness and controllable strength.
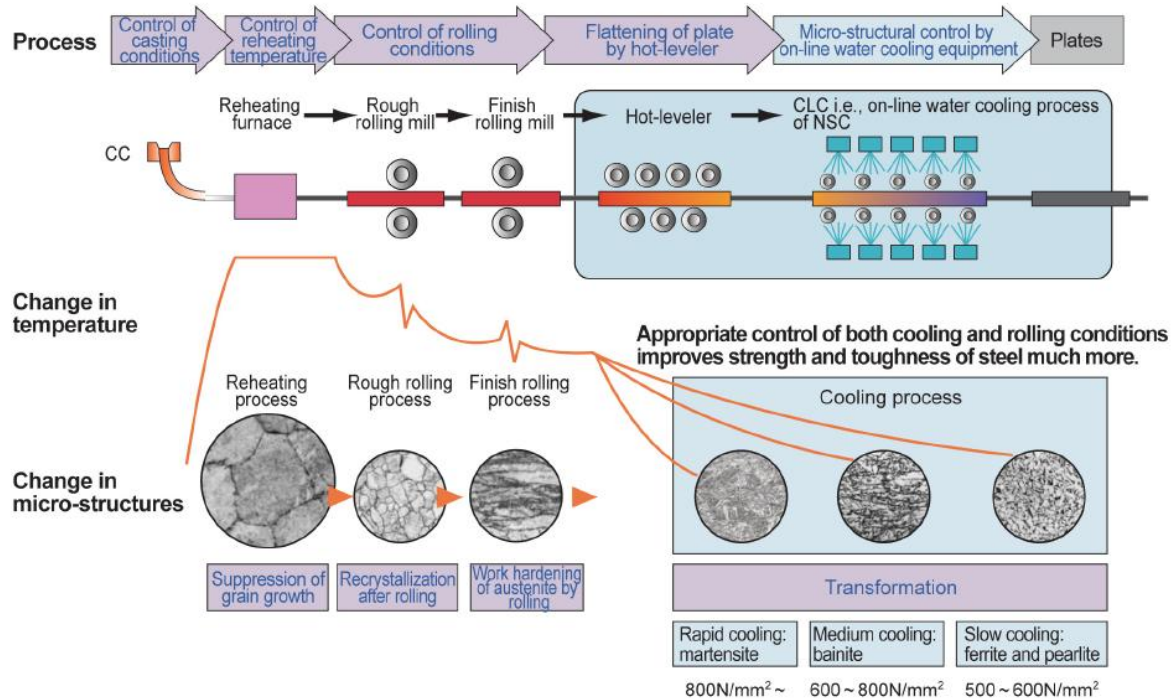
Fig. 2.4 Concept of Thermo-mechanical Control Process.

Technology for development of steel properties has evolution to control behaviors of steel phases by controlling alloying elements on micro-scale and nano-scale. In order to maintain high strength and high toughness after welding process applied by condition of high heat input, alloying element should retards grain growth and resists the toughness deterioration. The brief of particles or alloying elements control steel properties will be discuss as below.

For the developed steel grades are YP 40 steel and YP 47 steel. YP 40 steel is used container ships greater than 6,000TEU and up to 10,000 TEU. It is available made heavier thickness at a maximum of 65 mm or more. For fabricated property, can provide high toughness and retard grain growth on HAZ even though it was welded by high heat input process with EGW. TMCP technology and optimization of TiN formation has been successful controlling excellent HAZ toughness for high heat input EGW. However, when the super-large container with over 10,000 TEU was designed, YP 40 steel must be used plate thickness up to 80 mm and then the problem of the heavy weight of hull structure. Moreover, heavy joint with over 70 mm need to join by large heat input with EGW process thereby grain coarsening on HAZ which leading to the toughness deterioration. As for above mentioned, to reduce plate thickness by keep more strength of steel plate, YP 47[48-53] steel was developed to use in the construction for a large-containership. YP 47 steel has yield point more

than 460 N/mm^2 and it was produced by good TMCP technology, particularly in Japan. YP 47 steel or EH 47 steel has many advantages not only high strength properties but also retard austenite grain growth under large heat input EGW operation, excellent toughness property, high crack-arrestability properties and corrosion resistance. Now a day, YP 47 steel has been produced for thickness up to 70 mm for the large-container ship with over 10,000 TEU.
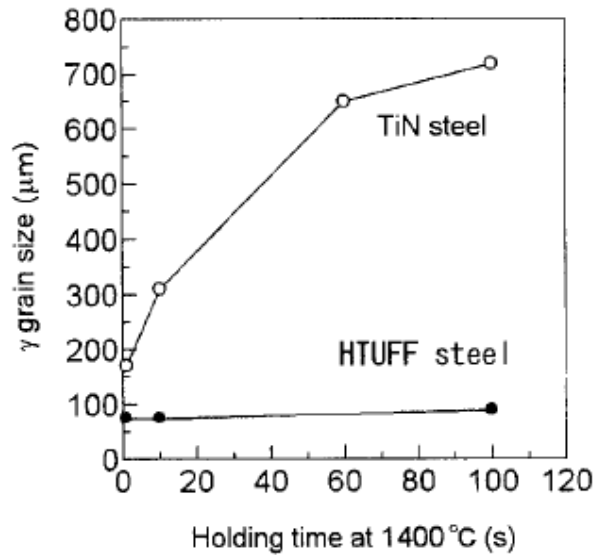
Fig. 2.5 High temperature stable of γ size with HTUFF steel compare with TiN steel.
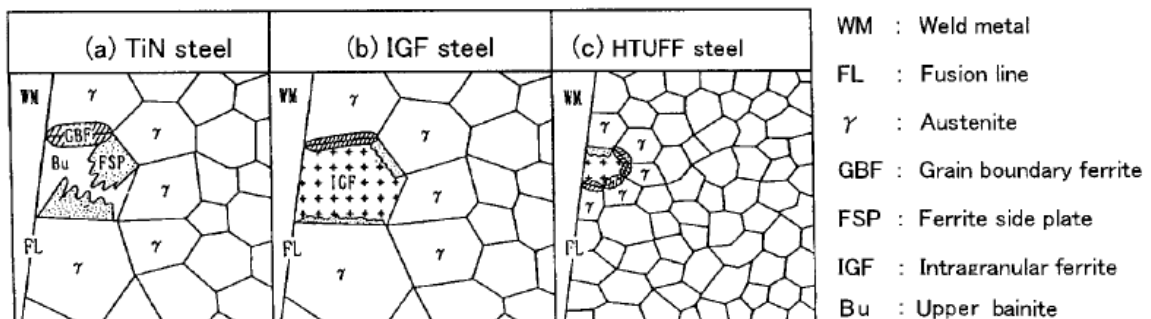
Fig. 2.6 Comparison of HAZ grain growth behaviors between conventional TiN steel, IGF steel and HTUFF steel (ultra-fine particle addition)

Nippon Steel Corporation develops steel plates for service on the large-container ship by super high HAZ technology with fine microstructure imparted by fine particles [54-59]. Steel plates having a tensile strength of 490 MPa to 590 MPa for heavy thickness were made by addition fine particles of thermally stable oxides and sulfides in the plates. Heavy steel plates such HTUFF steel excellent in HAZ toughness and it can reduce the grain growth or γ size stable on longer holding time with high temperature exposed (1400 °C). Fig 2.5 shows stable of γ size on HTUFF steel plate compare with TiN steel [60]. And Fig 2.6 shows comparison of HAZ grain

growth between conventional TiN steel and HTUFF steel. Fig 2.7 shows a concept of HTUFF development, oxide containing Mg, oxide containing Ca and Sulfide containing Mg which have nano-particles were employed as pining particles to retard austenite grain growth. The result of pining particles of HTUFF steel obtains HAZ grain refinement even though it was joined by ESW process. Fig 2.8 shows microstructure of the fusion boundary region of HTUFF having smaller grain size compared with conventional steel.
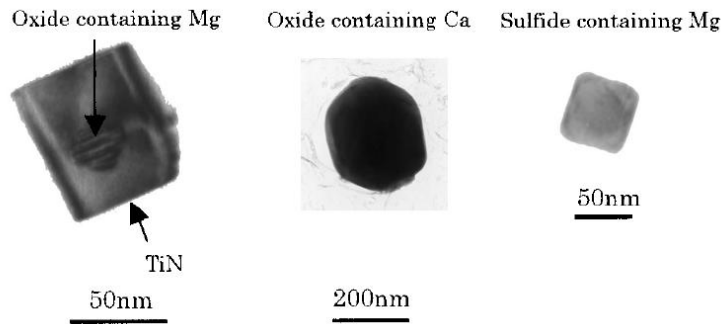
Fig. 2.7 Ultra-fine pinning particle.
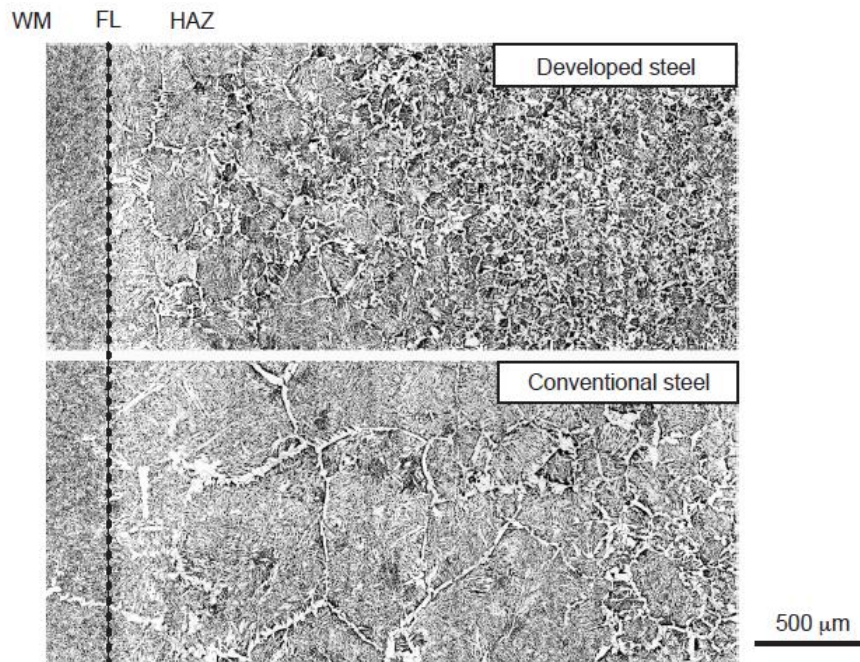
Fig. 2.8 Comparison of fusion boundary between HTUFF (developed) steel and conventional steel which were joined by ESW process.

JFE Steel Corporation also develops steel plate for high heat input joining but has an enhancement of particle formation mechanism to control HAZ grain size. The

combination of TiN in base metal and an appropriate amount of B in welding consumable was used to optimize a weld joint properties [16]. Fig. 2.9 shows the mechanism of particles dissolution and diffusion during high heat input welding. TiN dissolution occurs when exposed on high temperature over 1,450 °C (position near a fusion boundary). Free N is matched with B which diffused from base metal, formed as BN in HAZ. BN has an influence of reducing interganular-microstructure formation. An appropriate amount of Ti from base metal can form as Ti_2O in weld metal and this Ti_2O was employed as nucleation of formation of acicular ferrite. Moreover, remain of B in weld metal (original B amount is high level) can match with Ti and form as TiB which affected grain refinement of weld metal.
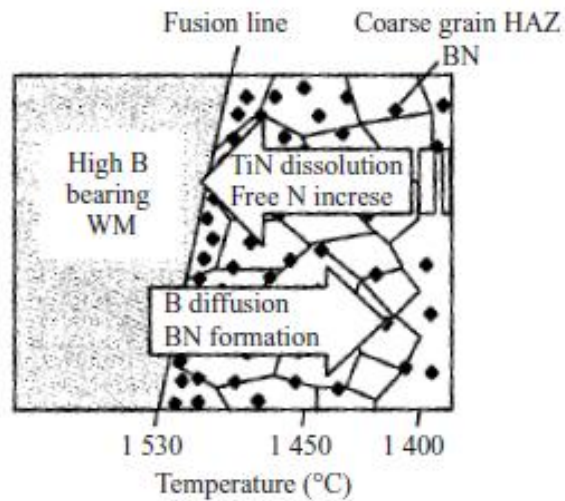
Fig. 2.9 High temperature phenomena showing TiN dissolution and B diffusion during high heat input welding.

2.4 Conventional and special electrogas arc welding (EGW) process

Nowadays, large container ship, hatch coaming side which has heavy thickness joint with vertical joint alignment has been joined by electro gas welding process (Hereafter in a call as EGW). Many issues reported about developing EGW [61] to achieve a sound weld for single pass vertical joining on heavy thickness (Fig. 2.10). High heat input of EGW was required to obtained sound welded result. An example of a plate thickness of 19 mm needs heat input for conventional EGW about 227 kJ/cm. Heat input condition of conventional EGW shows the result in Fig. 2.11 and compared with single vibratory electro-gas arc welding (VEGA ®) process in case of joining on 19 mm plate thickness. Single electrode VEGA could reduce heat input for welding to 72 kJ/cm. However, in case plate thickness over 50 mm must be joined under 258 kJ/cm by single electrode VEGA. Weld defect such as lack of fusion would occur when plate thickness over 50 mm.
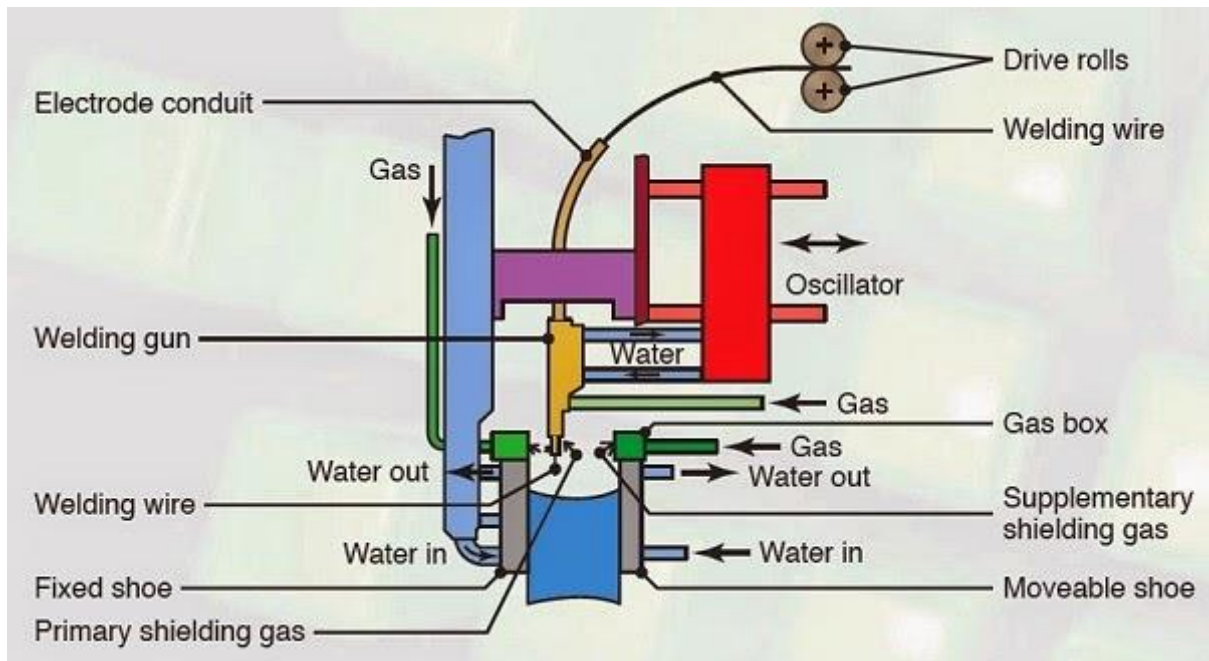
Fig. 2.10 Shecmatic of single-electrode VEGA [61]

Welding processes	Plate thickness	Cross-sections of welds	Heat input
Conventional EGW	19mm		227 kJ/cm
Single-electrode VEGA			72 kJ/cm
	50mm		258 kJ/cm

Fig. 2.10 Comparison welded joint result with differential plate thickness and heat input by conventional EGW and single electrode VEGA® welding process.
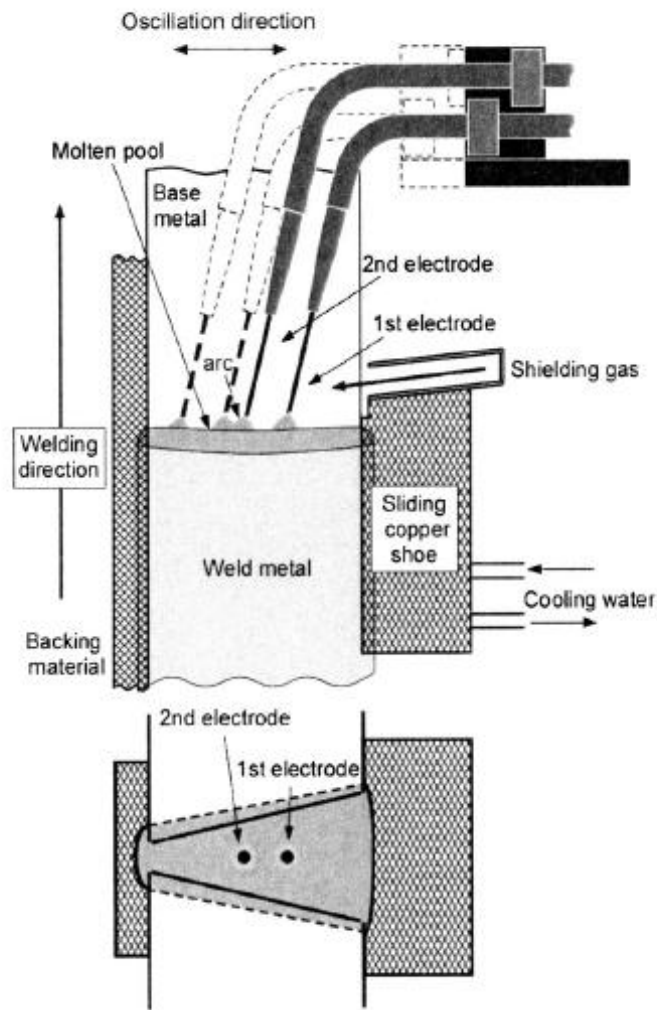
Fig. 2.12 Schematic illustration of two-electrode VEGA®.

Nippon Steel developed the two-electrode VEGA welding process in order to resolve the problem as described above mentioned [62]. Schematic illustration of two-electrode VEGA was shown in Fig. 2.12. Apparatus of this process almost same single electrode VEGA®, a type of polarity on each electrode were differences. This process can improved welding workability clearly, complete fusion for the plate having 50, 60, and 70 mm thickness which results were shown in Fig. 2.13. Heat input levels were also shown and it could be seen that more than 380 kJ/cm must be applied to join in case plate having 70 mm. It was considered about grater heat input when plate thickness having more than 70 mm for the larger container in the future. A deterioration of the toughness of the joint occurred by cause of grain coarsening when large heat input of two-electrode VEGA applied. Then the level of heat input was concerned. In addition, the normal speed of VEGA on plate thickness of 70 mm has a range of 3.3 – 5.0 cm/min (2-3 m/h) because of higher speed would produce imperfection on welded joint.

Plate thickness : 50mm	Plate thickness : 60mm	Plate thickness : 70mm
281 kJ/cm	321 kJ/cm	382 kJ/cm
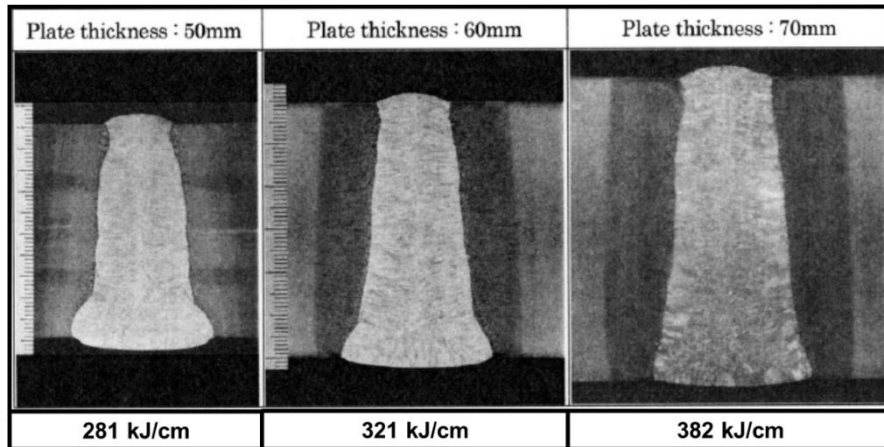
Fig 2.13 Cross sections of welded joint under differential heat input levels of two-electrode VEGA®.

2.5 Hot-wire welding method

Hot-wire method was developed to get high deposition rate of the welding process. A hot-wire system as illustrated in Fig. 2.14, GTAW with a hot-wire filler metal provides an attractive alternative that combines the benefits between increasing deposition rate and independent control of heat input. As for mentioned of a benefit of hot-wire method that it provided on various types of welding application and various types of material to joining. Mechanism of hot-wire feeding under arcing zone were observed by an in-situ high-speed system [64]. Effect of wire current was shown on adequate or inadequate conditions. The result from study was shown in Fig. 2.15. Optimization of hot-wire parameters were obtained from clearly evidenced during welding.
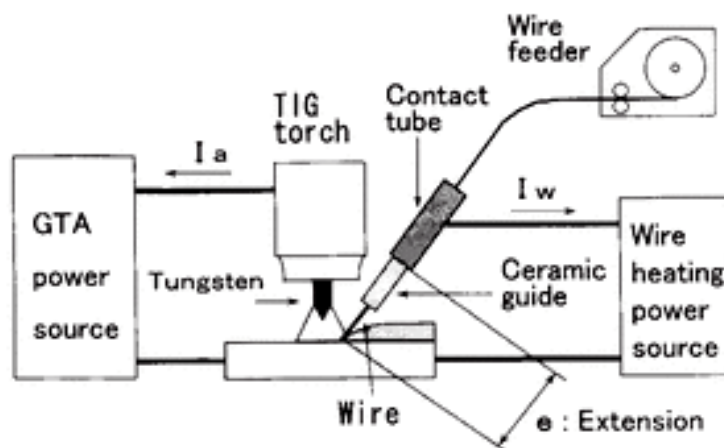
Fig. 2.14 Principle of Hot-wire GTAW [63]

However, hot-wire–GTAW is useful for a narrow gap joint, such technology is still limited in terms of traveling speed and production rate. An alternative to narrow-gap welding is laser-arc hybrid welding, which has a tendency to induce defects due to arcing - although such a process has the advantage of a high traveling speed.
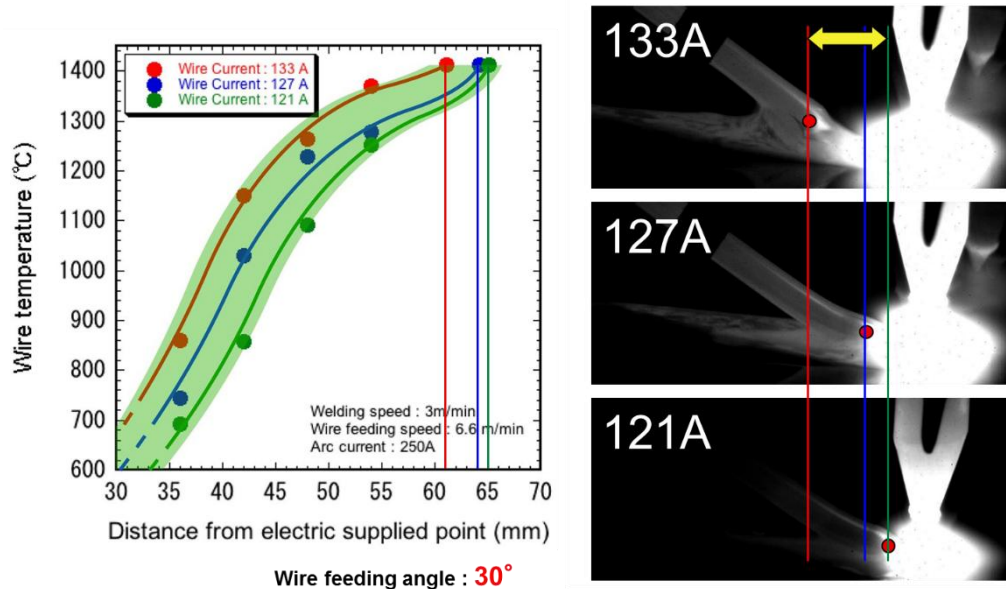
Fig. 2.15 Effect of wire current on feeding phenomena and in-situ observation during operation of TIG Hot-wire.

Laser welding has been using in various industrial since laser beam can be precisely controlled the spot size for heating on the target and precisely control the power density for make a fusion weld [65]. In the automobile industrial, laser beam was developed as the remote laser welding technique for galvanized steel sheets [66]. An advantage of various focus can be adapted and fast irradiation, laser beam can access on the long target distance and provide high speed welding.

For high power laser beam, the beam can be separated by the beam splitter in order to distribute the energy for improvement the weld quality [67]. By this way, welding on aluminum alloy and carbon steel plate can significantly reduce the centerline cracking and porosity.

Recently, hot-wire method was combined with laser heat source for high efficiency joining process [68-70]. Not only narrow groove welding that hot-wire laser welding can be applied but also various type of welding joint can be used. Filet joint for ship building industry has been also joined by hot-wire laser welding method. Sound filet weld could be obtained by extremely low dilution. Various types of welding joint such as fillet weld or lap joint (Fig 2.16) can be joined by hot-wire laser method. The joint strength can be obtained by hit-wire laser method which was optimized the combination parameter of hot-wire parameter and laser beam parameter.
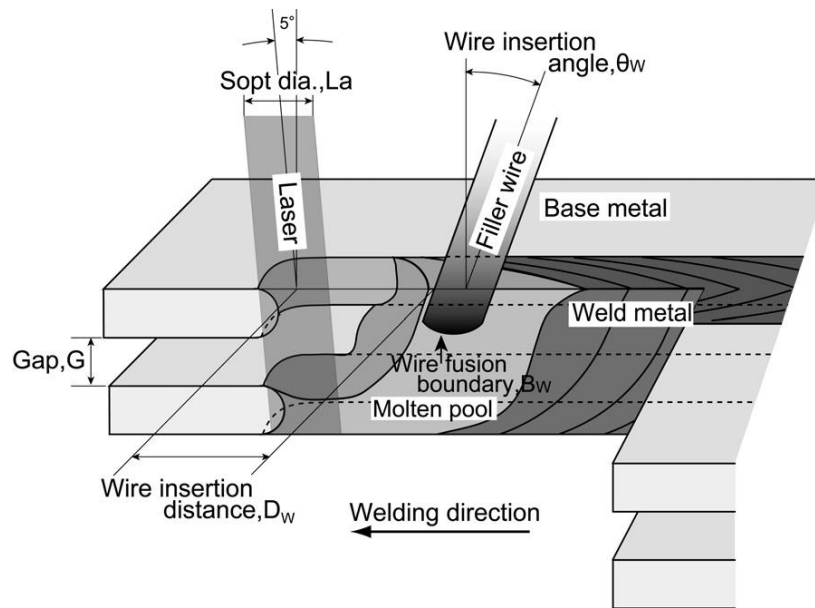
Fig. 2.16 Application of hot-wire laser method for joining on steel sheets with lap-joint condition.

Fig. 2.17 shows hot-wire laser method on a narrow groove of 9Cr-Mo steel [67] for two laser beam spot shapes irradiated. By this method, low dilution weld, a narrow size of HAZ and low distortion could be obtained due to low heat input.
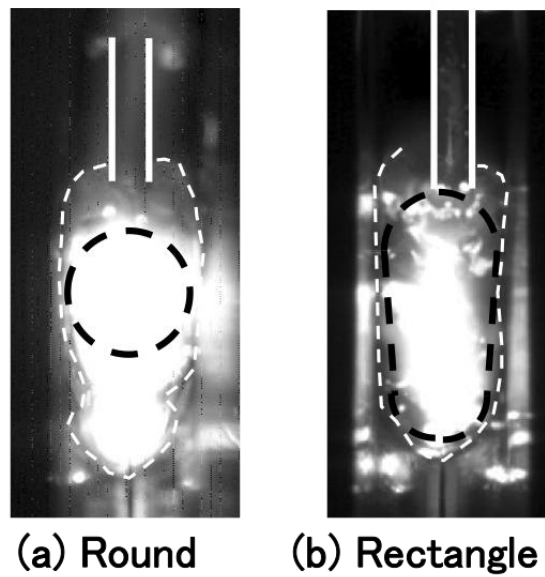
Fig. 2.17 Laser spot shape of (a) round and (b) rectangular type irradiated to join on narrow groove.

2.6 The process phenomena during laser welding by in-situ observation

During laser beam welding, one phenomenon has been investigated [71-78] by in-situ observation with a high-speed camera and high-temperature optical vision. The basis of material processing, the part of reflection (not absorbed) must occur from a surface and that reflected laser exposes out beside region depended on its direction. Fig. 2.10 shows an assumption of reflected laser may occur during hot-wire laser on a narrow gap and this phenomenon could provide low dilution under high-speed welding. Rittichai and et. al., observed the melting phenomena of groove wall surface by reflected laser beam which was shown the result on Fig. 2.11. Obviously, the images of the microscale appearance and the weld bead cross section are examined. It is seen that the metallurgical structure and wall shape is changed substantially. This is remarkable evidence explaining why the energy of scattering laser irradiation can increase the penetration depth at the groove side-wall and the melting of the feeding wire in narrow-gap welding.
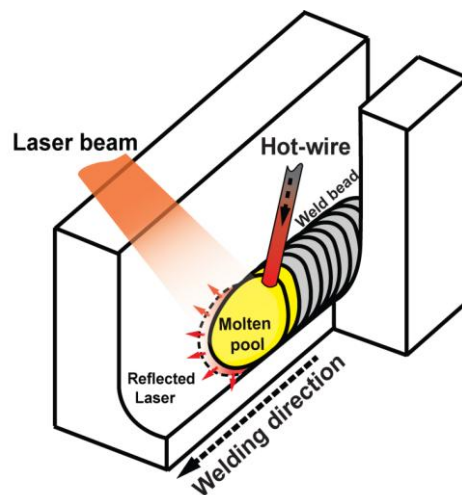
Fig. 2.10 Schematic illustration of Characteristic of hot wire laser welding in a narrow groove.
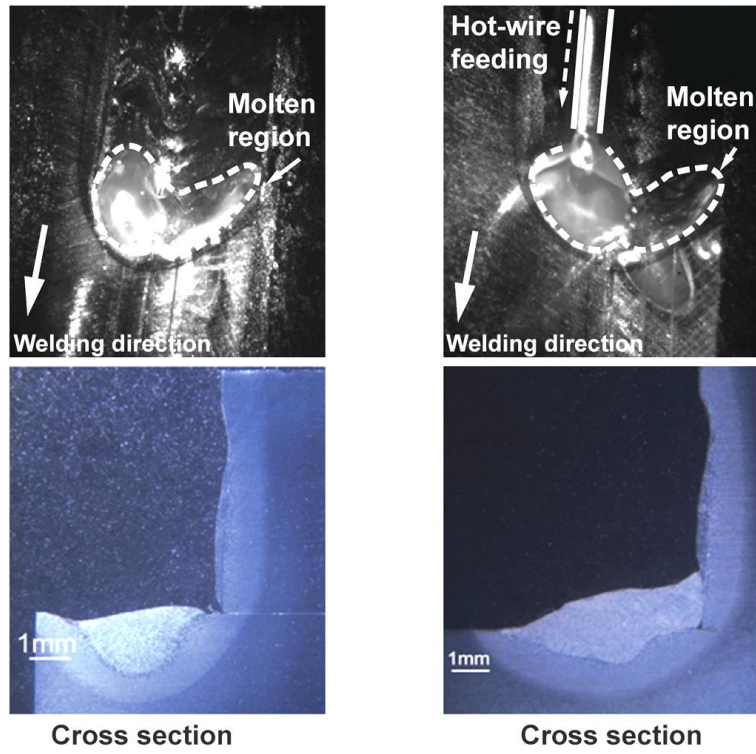
(a) Only laser radiation.   (b) Hot wire Laser welding

Fig. 2.11 Welding phenomena of groove surface melting by reflected laser from molten pool.

Chapter 3

Feasibility study of single pass vertical joining by

using hot-wire laser welding method

3.1 Introduction

According to the aforementioned background statement, the novel welding process is designed for joining on vertical heavy thickness joint. The originality of conceptual idea is the combination of the laser heat source and the hot-wire feeding to a joint gap. This chapter introduces a methodology of the novel process and its apparatus. Main equipment were explained on their specification and typical parameter ranges used. There are three major parts discussing on feasibility and main effect on welding phenomena to achieve fusion joining.

First part introduction of the novel process and investigation of the reflected laser beam inducing the initial melt of base metal were presented. A basic idea was explained on the methodology of a joint configuration, laser power source, laser irradiating method, hot-wire system and hot-wire parameters. The investigation of the reflected laser beam is verifying experiment in order to make clear the mechanism of groove wall melting in the novel welding process. High speed photographs are supporting evidence of process mechanism.

Second part is a basic experiment to determine the critical power density for joining. Joining on 5 mm gap width was a proposed condition. Effects of laser power and welding speed on melting amount of base metal were investigated. The critical power density for melting was determined in this part. It was important for designing of the laser beam parameter for joining in the proposed process.

Third part discusses an investigation on the effect of laser access through joint target to adapt the proposed method on more actual environment and conditions. The effect of a tilt angle of laser head for irradiation of laser beam through the joint target (an oblique laser access) was compared, using weld joint characteristics, to basic vertical laser access method. Finally, gap width of 5 mm was identified that its condition difficulty achieve the weld metal fulfillment on the joint gap. The part emphasizes on designing a wider gap size for more flexibility of joining. By the basis of a critical power density from this chapter experiment, new laser irradiating method is designed and discussed in the next chapter.

3.2 Introduction of the novel welding process methodology and its equipment

This section explains the conceptual idea of the novel process. First, the main idea of vertical single weld pass was explained. And second the descriptions of each equipment were explained their methods and typical set up.

(a)   (b)
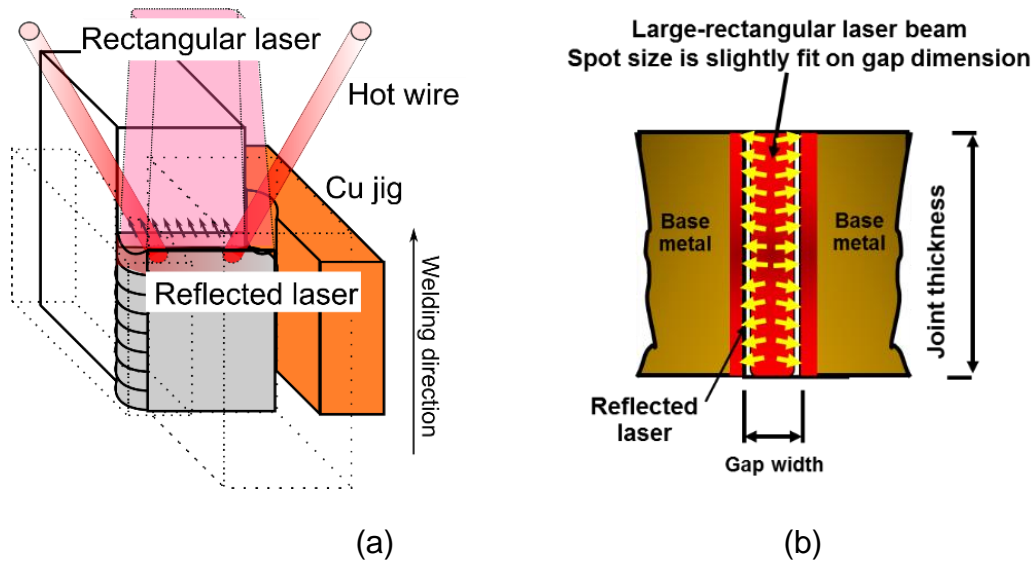
Fig. 3.1 The proposed process methodology (a) process configuration and (b) Schematic illustration on top view of large rectangular laser beam irradiate trough joint target and reflected laser be utilized for melts the groove surface .

Fig 3.2 Laser oscillator

Fig. 3.1 (a) shows the schematic of the proposed welding process. In the proposed welding process, a high-power laser diode is used as a main heat source and the hot-wire method is used for efficient deposition. A large rectangular spot

24

shape of a laser beam, which fits a groove width (gap) and plate thickness, is employed. The laser is irradiated continuously from the above the joint into the groove to create and keep a molten pool during welding. By the assumption, a reflected laser (Fig. 3.1 (b)) on a molten pool surface is utilized for melting groove surfaces efficiently. Filler wires are fed from both sides of the groove, and filler wires are heated up to its melting point by Joule heating using the hot-wire system before entering the molten pool. Jigs and a moving way are almost the same as these of an EGW process. It can be expected from the aforementioned features that the proposed hot-wire laser welding method realizes single-pass vertical welding for a heavy joint with a low heat input, low dilution, high efficiency and reduction of a laser power.

The laser equipment used as a power source was Laserline LDF 6000-40 (6.0 kW) continuous wave (CW) Diode Laser (LD). 4 Wavelengths of 910, 940, 980 and 1030 nm are available irradiation for this laser power source. Fiber core is connected to wafer source and convey the output laser to the laser head. Fiber core sizes of 400 μm and 1,000 μm were available for use in this research. Fig. 3.3 (a) shows the assembly of a normal laser head, procedures of laser generation passing through optic part of fiber core, collimator, homogenizer and focusing lens, respectively. Fig. 3.3 (b) shows the flow chart of typical assembly of laser head for the creation of large-rectangular laser beam used for joint thickness of 26 mm.

Hot-wire system, Power Assist HI-TIG IV662 is a hot-wire power source (Fig. 3.4 (a)) used. Normal electrical polarity setting is positive direct current electrode (torch). In the case using 2 hot-wire feeding, one torch must be set as reversed polarity. Fig. 3.4 (b) shows the hot-wire torch used in the proposed process. For hot-wire parameters setting, essential parameters are wire feed speed (m/min), energization length (mm), wire current (ampere), wire feeding angle (°), and wire feeding position (mm). All of essential parameters were drawn as schematic illustration in Fig. 3.4 (c). In the practical use for the proposed process, a wire feeding speed is adjusted as a function of volumetric feed rate of groove size and welding speed. It also compensates a deposition rate of 1.2 time of calculated result. An energization length (mm) and a wire current direct affects the Joule heating. However, in case of the proposed process, the energy supply length was dependent of wire feed position and wire feed angle. Specifically, wire current is adjusted adequately[62] which depend on wire feed speed, wire diameter, wire material, laser power density or irradiating method etc. In practice, setting of wire feed speed and wire current (power module) can be done on the hot-wire remote control is shown in Fig. 3.4 (d).

(a)

(b)
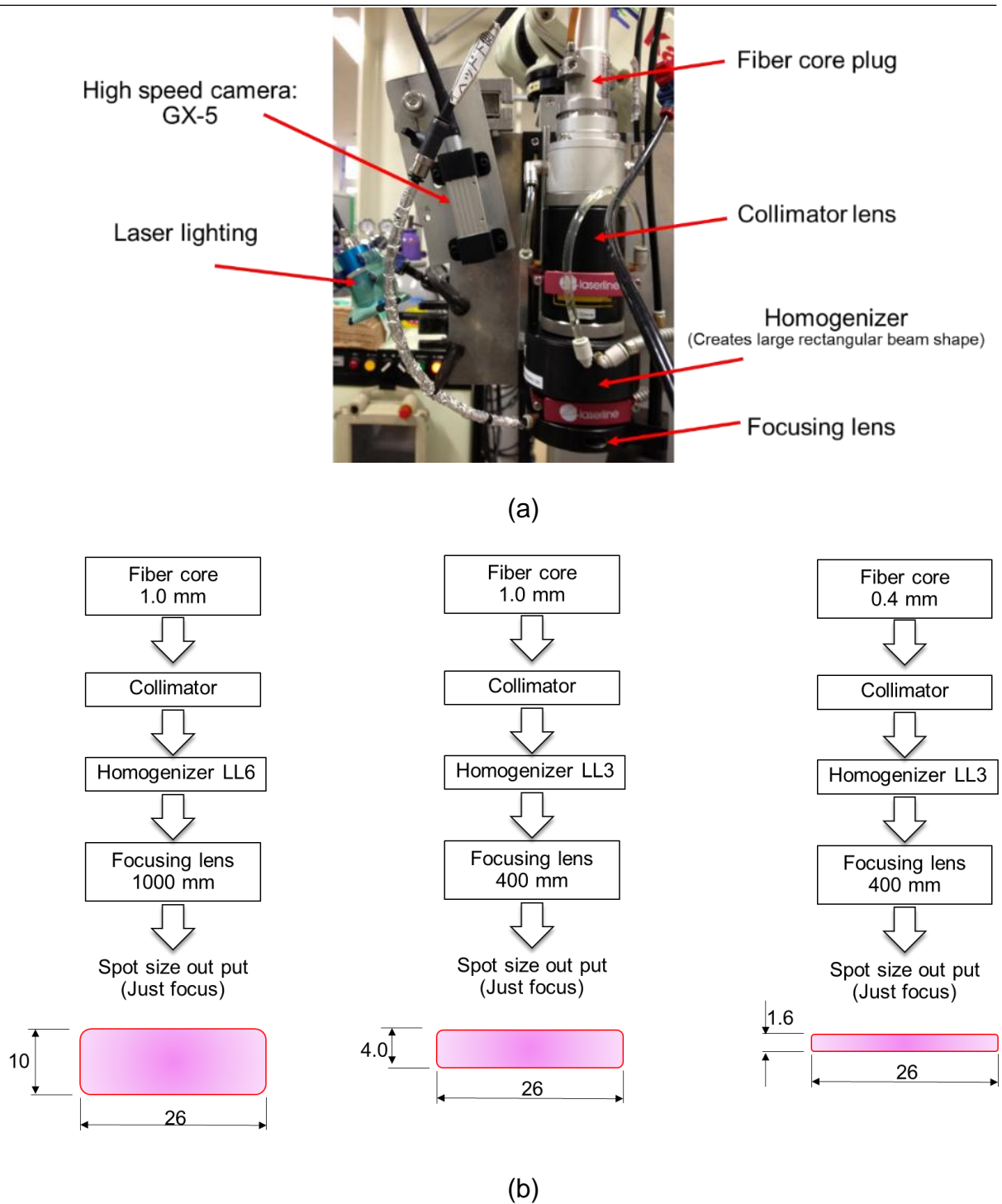
Fig 3.3 Assembly of the laser head for forms the large rectangular laser beam (a) actual laser head assembly and (b) simplified chart of laser head components to create the used large-rectangular laser beam.

Welding jig was designed for vertical movement and also assisting of specimens cooling like a semi-infinite media. Specimens were fixed on cooling copper base by toggle clamp. In this welding jig, specimens were moved by IAI

cylinder which was controlled by specified program. Cooling copper shoes and base use a water flow method for cooling parts. The cooling copper shoes were slotted at the center for installing a gas shielding box and insert a hot-wire torch for feeds in to a joint gap. Typical details will be explained follow the experimental cases.

(a)

(b)

(c)

(d)
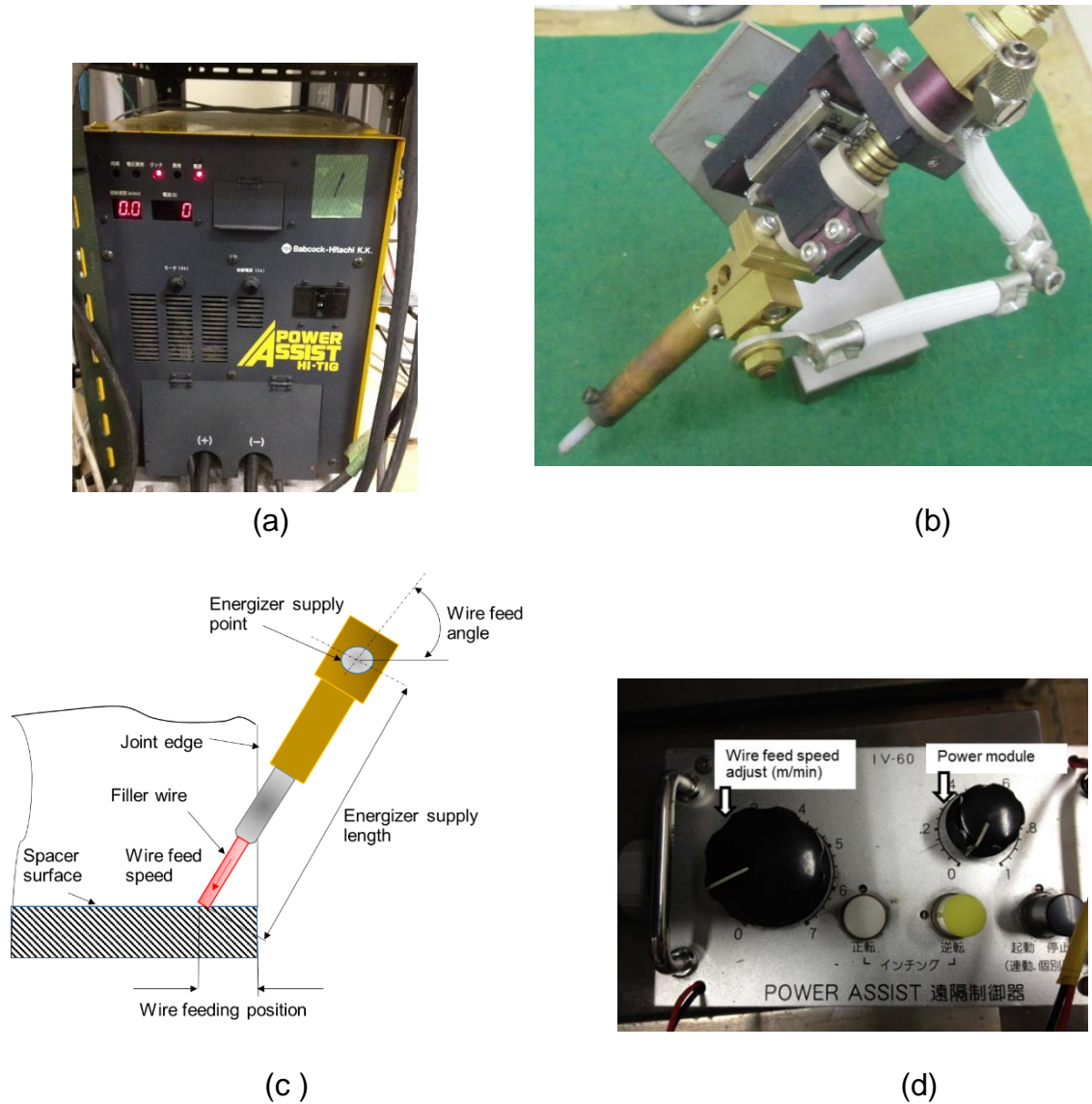
Fig 3.4 Hot-wire (a) machine, (b) hot-wire torch, (c) hot-wire setup parameters and (d) remote controller

A part of this research discusses the study of welding phenomena during process operation in order to make clear the process mechanism. The high speed camera is provided for monitoring tool which has an advantage of spatial information

and temporal information of the weld pool. The camera was used Pencil camera V-193-M1 model connected with NAC: MEMRECAM GX-5 module. The optical apparatus will be discussed later.

3.3 Preliminary experiment to investigate fusion phenomena by reflected Laser heating on groove wall (Instantaneously irradiation)

In order to verify that the reflected laser induce the initial melting on groove surfaces, the experiment using instantaneous laser irradiation and short time hot-wire feeding was performed. The melting phenomena on one side of the groove surface was monitored during the proposed process operation. The stability of weld pool forming under large-rectangular laser beam irradiation and hot-wire feed is also observed to discuss a feasibility of the proposed process. High speed images, which clearly showing phenomena, and macro cross sections will be obtained to shows the fusion evidence.

3.3.1 Material used

Firstly, it must be noted that for material used YP 47 steel has equivalent to KE 47 steel. Hereafter would like to call base metal as KE47 steel.

KE-47 steel plates were used in this study, the dimension of the specimen was 100 (width) x 50 (height) x 26 mm (thickness) is shown in Fig.3.5. Plates were fixed and aligned as a vertical joint configuration. The specimen was slotted by the dimension of 5 mm (width) x 30 mm (depth) x 26 mm (length) to simulate a groove joint. The filler metal of YM-1N (JIS Z 3325 YGL2-6A (AP)) with the diameter of 1.6 mm was used. The chemical composition of base metal and filler metal is presented on Table 3.1.

Table 3.1 Chemical compositions of steel plate and filler wire used

Material	Chemical Composition, wt%											
	C	Si	Mn	P	S	Al	Cu	Ni	Nb	Ti	Cr	Mo
KE-47	0.09	0.07	1.52	0.007	0.002	0.014	0.32	0.69	0.01	0.01	0.02	0.00
YM-1N	0.04	0.46	1.35	0.01	0.007	-	0.17	1.07	-	0.7	-	0.26
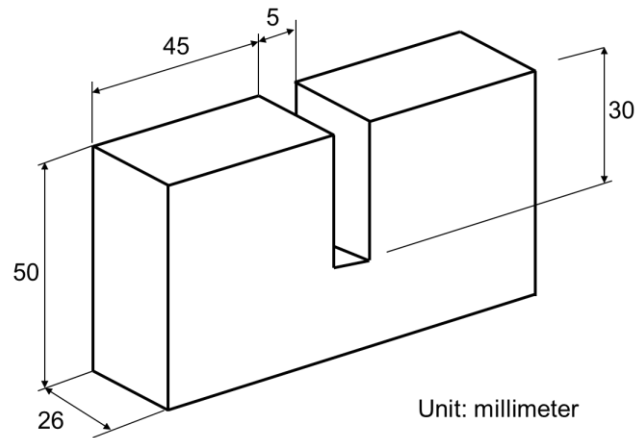
Fig. 3.5 Specimen dimension for the experiment of groove wall melting by instantaneous laser irradiation and hot-wire feeding

3.3.2 Experimental procedure

Welding parameters were shown in Table 3.2 and schematic layout of the experiment was shown in Fig. 3.6. Laser beam irradiates from the top side of the specimen. Laser spot size of 4.5 mm x 27 mm and laser power of 6 kW (CW) was set for irradiation in stationary irradiating method. It can be seen that laser beam width is slightly narrower than groove width, thereby groove wall surface are not heated by direct laser irradiation. 1 hot wire was used and set its parameters range depending on the welding speed of 3.33 cm/min (2 m/h). This experiment was expected to simulate for instantaneous laser irradiation to avoid effect of heat accumulation. Then, the pre-irradiation time of 5 second and hot-wire feeding 15 of second is period for joining.
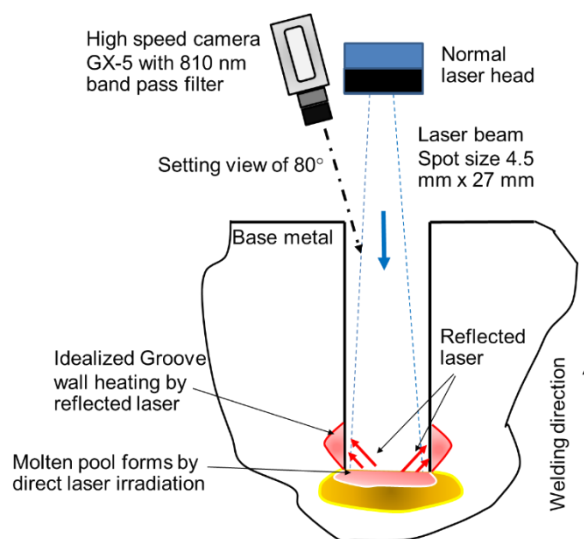
Fig 3.6 Schematic layout of in-situ observation of groove melting phenomena by reflected laser

Table 3.2 Welding parameters

Gap width size, mm	5
Laser type	Diode laser
Laser irradiation type	Stationary
Fiber core, mm	1.0
Homogenizer	LL3
Focus lens, mm	400
Laser power, kW	6
Laser irradiation angle, degree	15°
Defocus, mm	50
Spot size, mm x mm	4.5^w x 27^l
Power density, W/mm^2	49
Filler wire diameter, mm	1.2
Welding speed, cm/min	3.3
Wire feed speed, m/min	4.42
Wire current, A	111
Wire feeding angle, degree	45
Wire feeding position, mm	5
Shielding gas (Argon), LPM	10
Pre irradiation time, s	10
Welding time, s	20

3.3.3 In-situe observation

An optical processing for capturing of welding phenomena was done with high speed camera. The camera of Pencil camera V-193-M1 model connected with NAC: MEMRECAM GX-5 module with focus lens 50 mm with diameter of 25 mm, 810 nm band pass filter. The capturing parameter is the frame rate of 50 fps, shutter speed of 1/20000, and closed aperture. Table 3.3 shows the monitoring condition. By setting camera perspective to see the melting phenomena on the groove wall surface, it was set perpendicular on groove wall in horizontal axis and 80° from the weld pool plan.
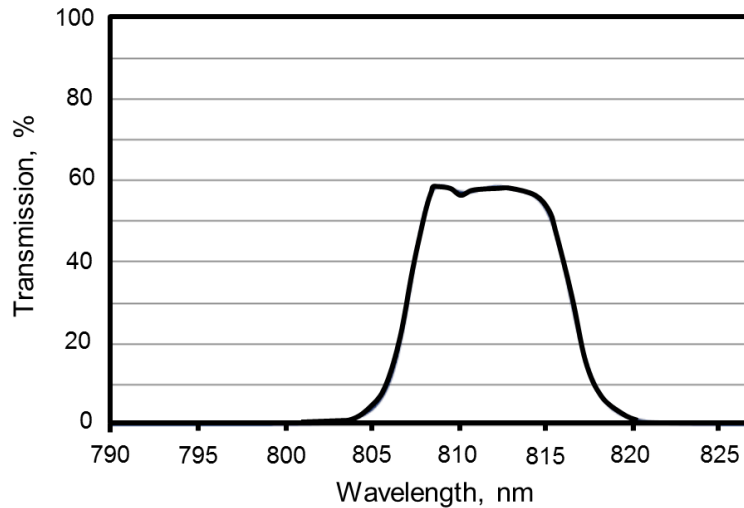
Fig 3.7 Transmission curve of 810 nm band pass filter

Table 3.3 Monitoring conditions of In-situe Observation

High speed camera	GX-5
Frame rate, fps	50
Aperture	Closed
Focus lens, mm	50
Band pass filter, nm/FWHM	810 / 10
Lighting	N/A
Shutter speed	20 k

3.3.4 Melting phenomena on groove surface by the reflected laser energy

Fig. 3.8 (a) shows captured high speed images on the pre-irradiation period (before feeding). Short time of pre-irradiation may less affected heat conduction to melts groove surfaces. It could be expected that only the reflected laser energy heats the groove surface. The results show that the groove surface was heated by the reflected laser from molten pool in small region by starting at the middle region of the joint thickness and the melting propagated fast to left and right directions. It implies that the reflected laser beam induces through groove surface just above weld pool surface, narrowly.

Fig. 3.8 (b) shows the melting and liquid metal wetting phenomena on the groove surface during hot-wire feeding and specimen moving down. It can be seen that the groove surface was melted continuously by the reflected laser. When the

groove surface temperature gets higher and changes to liquid, the liquid metal of the weld pool would runs and fuses together, this is called wetting phenomena. The wetting phenomena indicates that the proposed process has a stable weld pool formation and base metal melting.
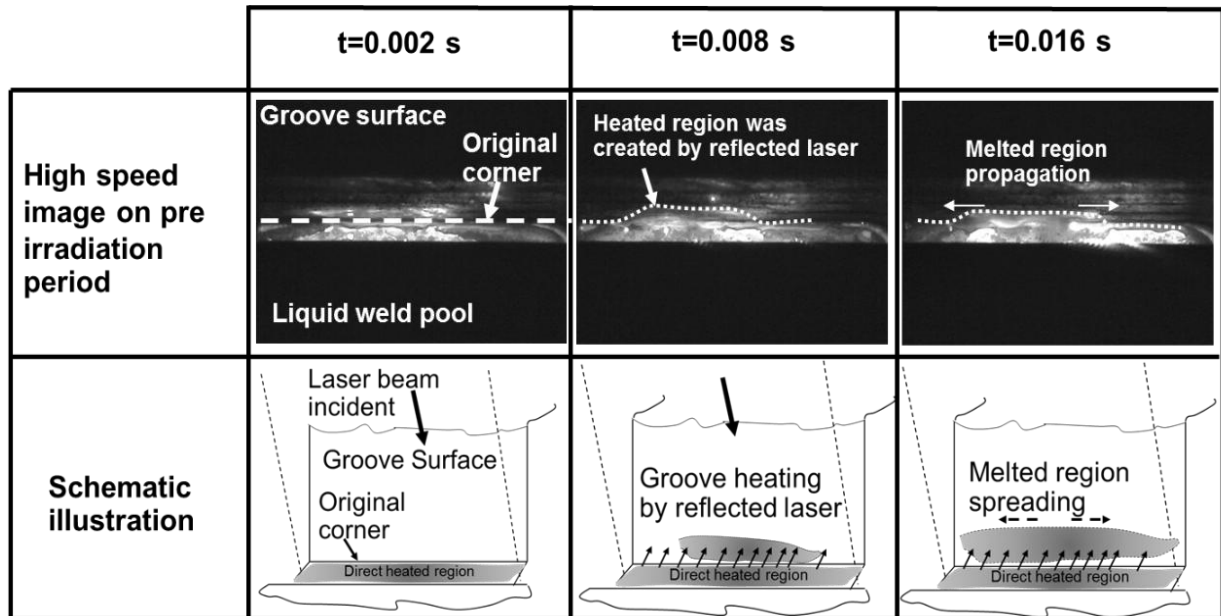
(a)   Pre irradiation period
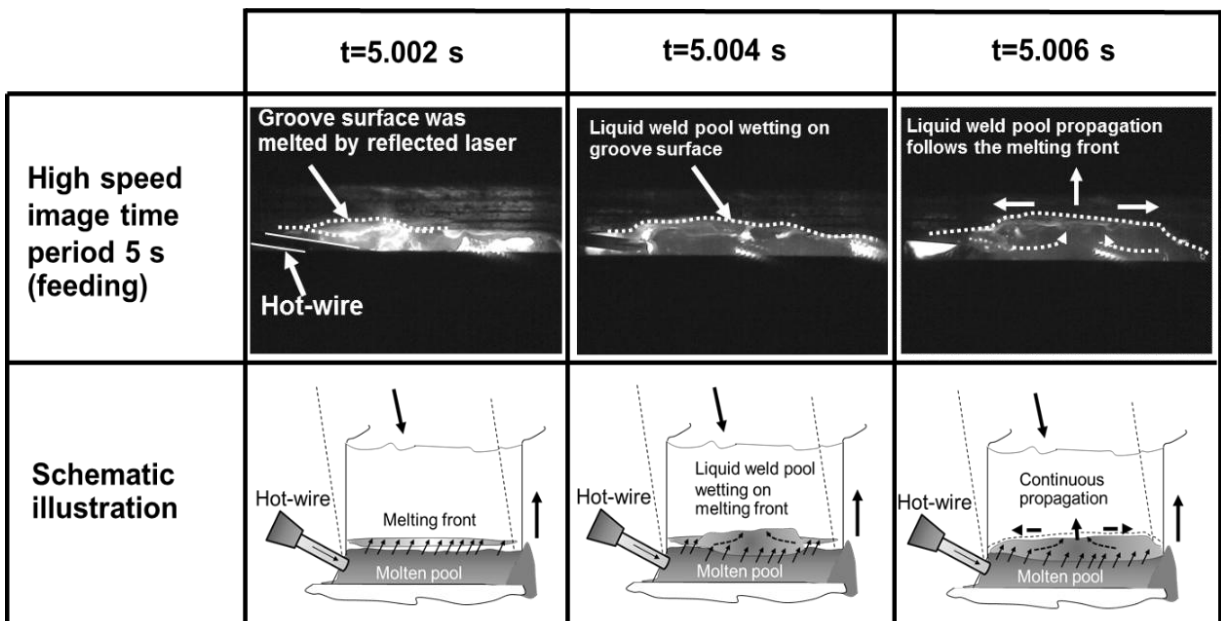
(b)   Continuous hot-wire feeding and specimen moving vertically

Fig 3.8 High speed image results of laser irradiation (Hot-wire laser feeds)

Macro cross section was shown in Fig. 3.9 which was cut in parallel welding direction shows the evidence of the initial melting depth was occurred by the reflected laser energy. The appearance of the fusion line as a straight line from bottom to top of weld pool that imply the specimen was joined by the condition of instantaneously irradiation. As can be seen in the magnified region A, the complete fusion clearly occurred, melting depth shows shallow depth. As a result of last solidified weld metal showed wetting on groove surface is correlation result on the captured high speed images of Fig. 3.8 (b). The wetting phenomena of the proposed process was drawn as schematic illustration on Fig. 3.10.

As a result from this experiment, it can be confirmed that weld pool and base metal melting were created continuously under the large-rectangular laser beam irradiation and hot-wire feeding.
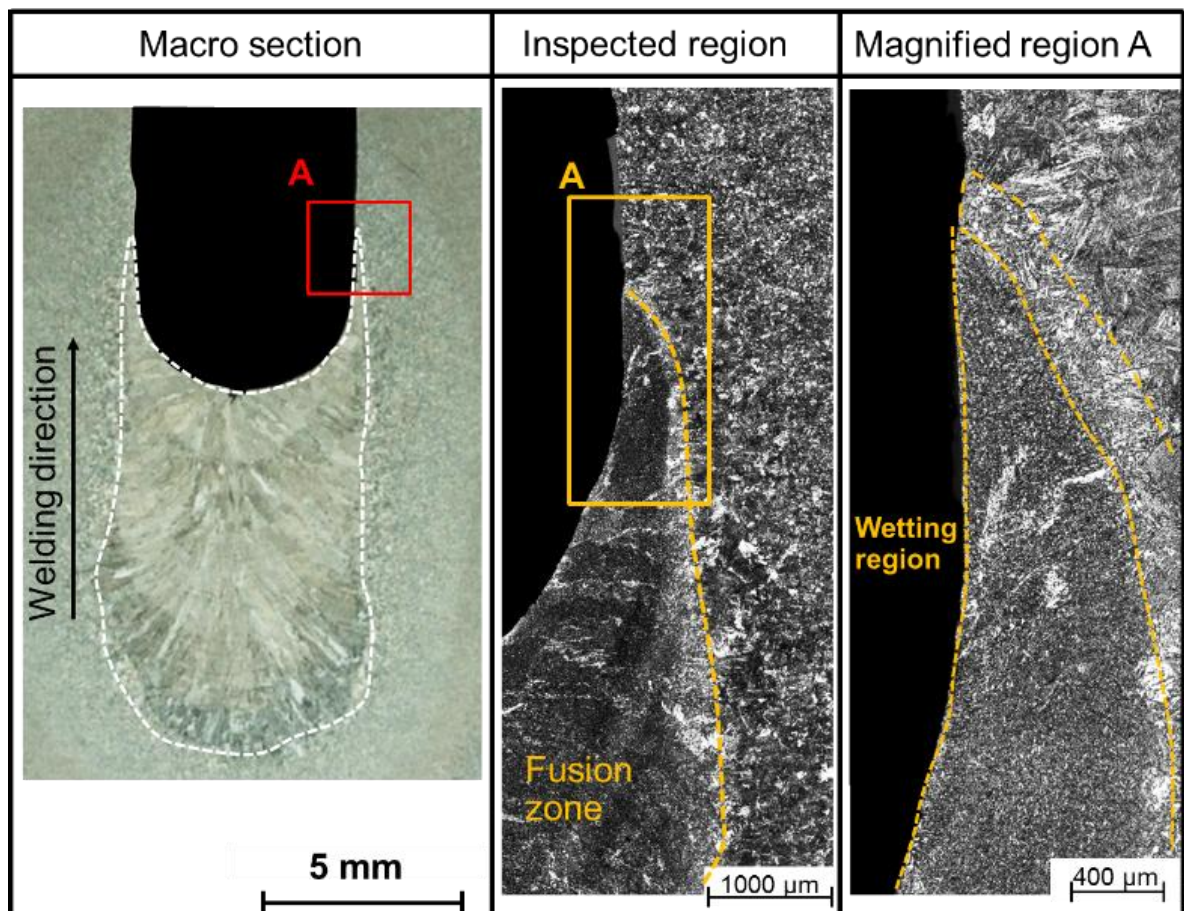
Fig 3.9 Macro section and microstructure on wetting zone (melting by reflected laser energy)

From the first experiment, sub conclusion could be drawn as

- Large-rectangular laser beam irradiation and hot-wire feeding can create weld pool growth in the vertical direction in the stable condition.
- The evidence of captured high speed image confirms that the reflected laser beam has influence of groove surface melting.
- The combination of hot-wire feeding and laser irradiation is possible method for joining on vertical joining process.
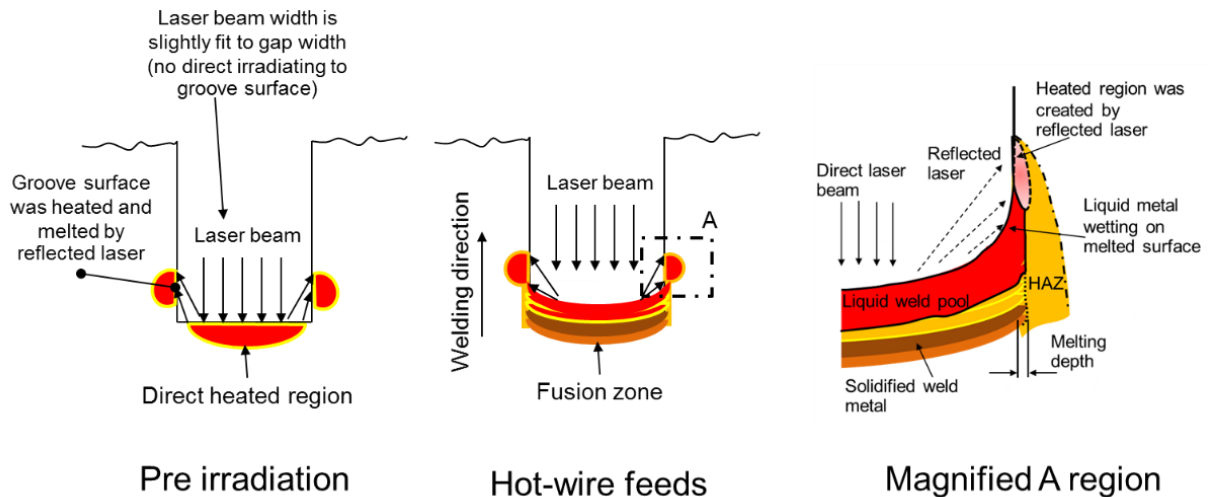
Fig 3.10 Schematic illustration of the groove melting phenomena by reflected laser energy

3.4 Basic experiment of study effect of laser power and welding speed on welding phenomena

3.4.1 Introduction

In this research, welding phenomena of the proposed process was studied and effects of primary parameters on welding phenomena were investigated first. A stationary laser beam and a specimen having a relatively small gap were used for basic investigations. 2 hot wires was used for deposit filler metal. In addition, the potential of the proposed process for a practical use was shown from this investigation.

3.4.2 Material and specimen used

KE47 steel plates and filler wires of YM-1N (JIS Z 3325 YGL2-6A (AP)) with its diameter of 1.6 mm were used in this research. The dimension of a specimen was 50 (width) x 100 (height) x 26 mm (thickness) as shown in Fig. 3.11.
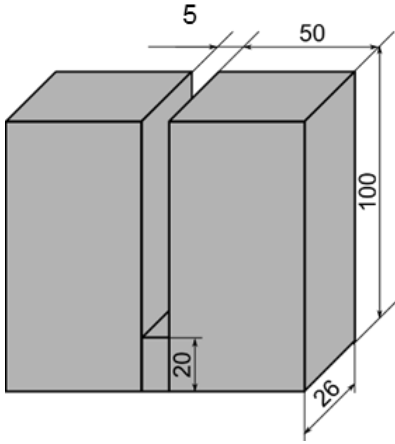
Fig 3.11 Specimen dimension
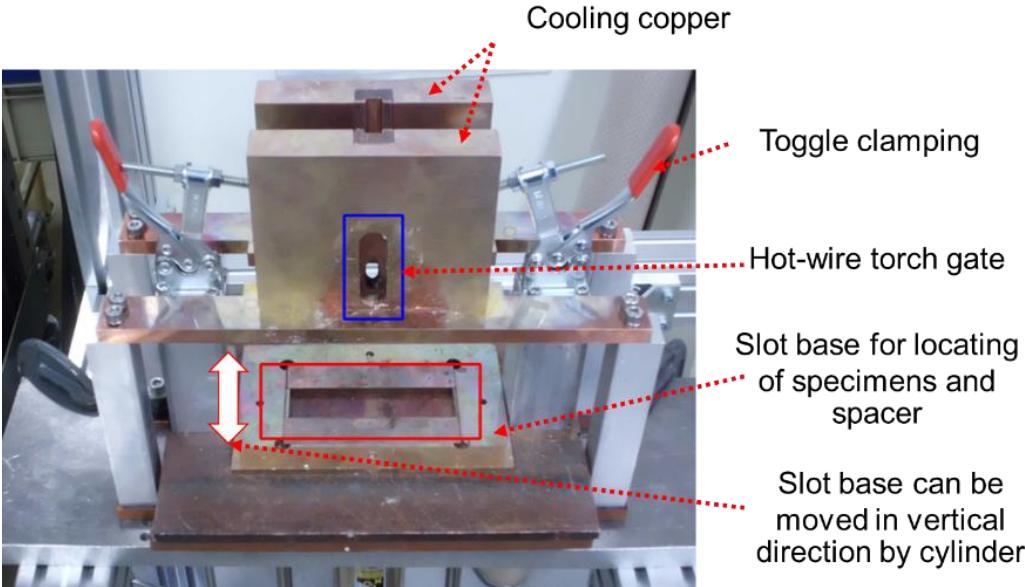
Fig 3.12 Welding Jig
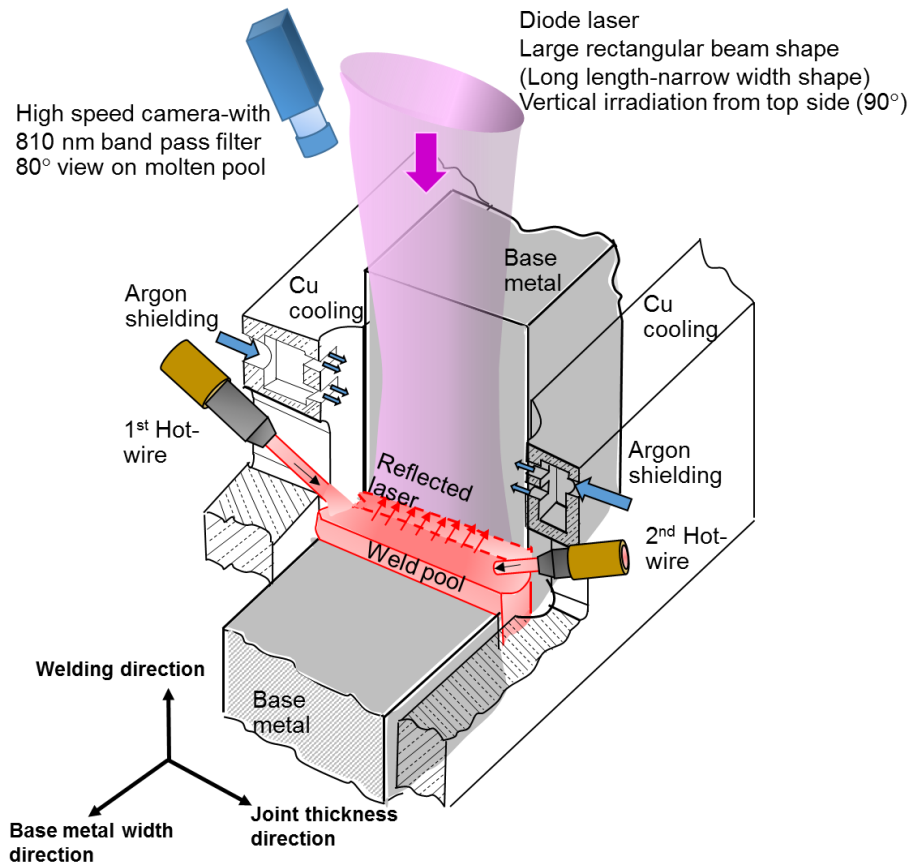
Fig 3.13 Schematic illustration of the experimental set up by 2 hot-wire feeding and vertical laser irradiation.

3.4.3 Experimental procedure

Stationary laser irradiation and a specimen having a relatively small gap (5 mm) were used. Table 3.4 shows the welding conditions used in this experiment. The laser power and welding speed were changed as 4 ~ 6 kW, 1.67 and 3.33 cm/min (1 and 2 m/h) respectively in order to obtain effects of primary parameters on welding phenomena. The rectangular laser spot size of 3.5 x 26 mm and irradiation condition were fixed. The hot-wire feeding speed was adjusted to the welding speed, and the wire current was set to heat a filler wire tip up to just under its melting point appropriately. Two hot-wires were inserted from both sides of the groove. Argon gas was used for shielding. A high-speed camera was used to observe molten pool formation and stability, and filler wire feeding during welding.

Table 3.4 Welding parameter

Gap width size, mm	5
Laser type	Diode laser
Laser irradiation type	Stationary
Fiber core, mm	1.0
Homogenizer	LL3
Focus lens, mm	400
Laser power, kW	4~6
Laser irradiation angle, degree	0°
Defocus, mm	50
Spot size, mm x mm	3.5^w x 26^l
Filler wire diameter, mm	1.2
Welding speed, cm/min	1.6 ,3.3
Wire feed speed, m/min	0.54, 1.12
Wire current, A	51, 113
Wire feeding angle, degree	45
Wire feeding position, mm	1
Shielding gas (Argon), LPM	1
Pre irradiation time, s	120

3.4.4 Effect of Laser Power and Welding Speed on Melting Depth of Groove Wall

In-situ observations using a high-speed camera, Fig. 3.14, indicated stable formation of a molten pool and stable feed of filler wires during welding. It became clear that the proposed hot-wire laser welding method could stably form a large molten pool filling a groove constantly using laser diode with a large rectangular spot as a heat source.
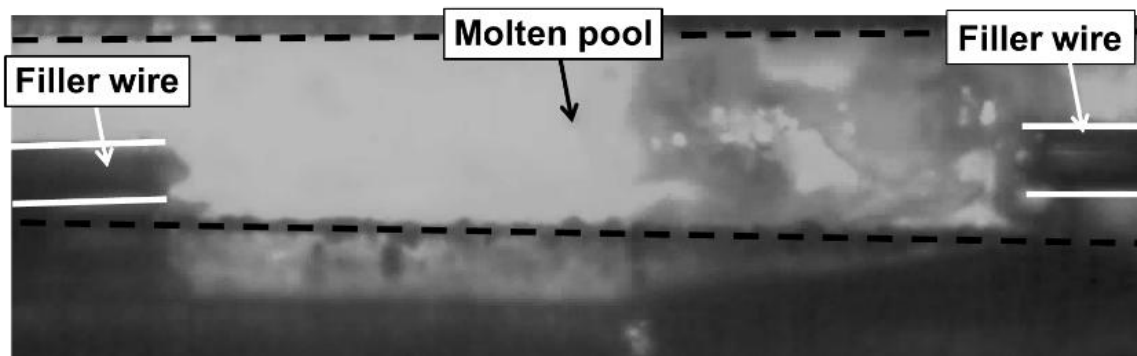
Fig. 3.14 Weld pool was created by the large rectangular laser beam and hot-wire feeds. High speed image viewed perpendicular weld pool surface.

Fig. 3.15 shows macro cross-sections of welded joints at the thickness center in the vertical (welding) direction, and Fig. 3.16 shows the lack of fusion ratio and the width of heat affected zone (HAZ) measured on vertical sections under various welding conditions in the cases of the 5 mm gap. With the increase in the laser power up to 6 kW, the width of weld bead and HAZ increase, nevertheless, the width of HAZ is narrower than that of the conventional EGW process (15~20 mm). It was cleared that the single-pass vertical welding for thick steel plates with low heat input and low dilution could be achieved by using the proposed process.

When the relatively low laser power of 4 or 4.5 kW was applied, only a fairly top region on the groove surface was melted, then lack of fusion occurred under some conditions. On the other hand, when the relatively high laser power of 5 or 6 kW was applied, the wider region on the groove surface was melted, then the lack of fusion decreased and sound weld bead could be obtained.

In contrast with the effect of laser power, and welding speed on melting of base metal and the lack of fusion ratio is very small, as shown in Fig. 3.16 and 3.17. It can be implied from these results that the laser power density affects largely on fusion of the groove surface and sound weld bead formation compared with the welding speed.

Fig. 3.18 shows the relationship between the energy density (laser power / laser irradiating area) and the penetration width on the groove surface in each welding speed using stationary laser irradiation and 5 mm gap. It is clear that there is the critical energy density, which is about 25 and 35 W/mm^2 for each welding speed of 1.7 and 3.3 cm/min (1 and 2 m/h), to begin fusion of the groove surface. Moreover the penetration width on the groove surface increases linearly with the increase of the energy density on both welding speeds. It can be considered that the energy density is the primary factor to obtain sound fusion in the proposed process since the critical energy density does not double even if the welding speed doubles.
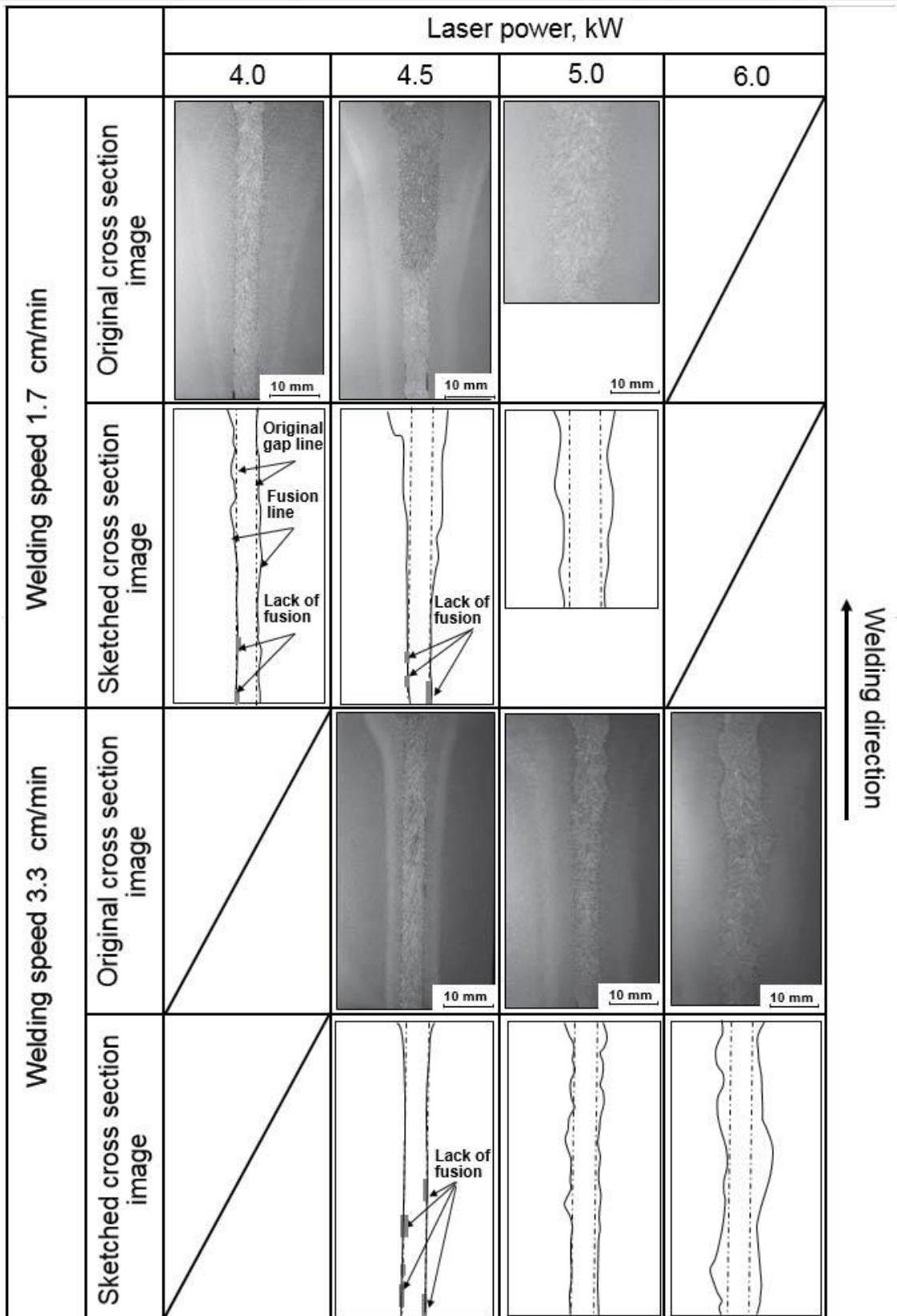
Fig. 3.15 Macro cross-sections of welded specimens in case of 5 mm gap in case of 5 mm gap with stationary laser irradiation.
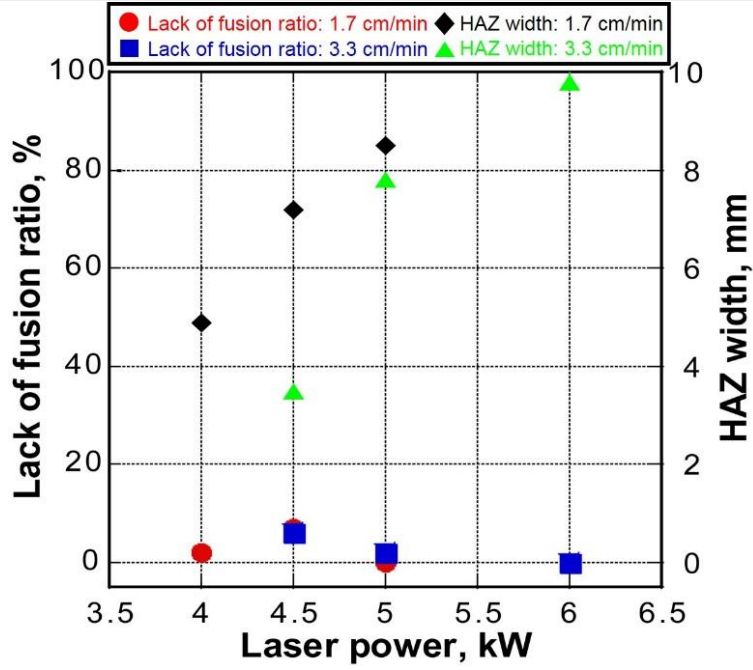
Fig. 3.16 Lack of fusion ratio on vertical sections and HAZ widthof 5 mm gap with stationary laser irradiation
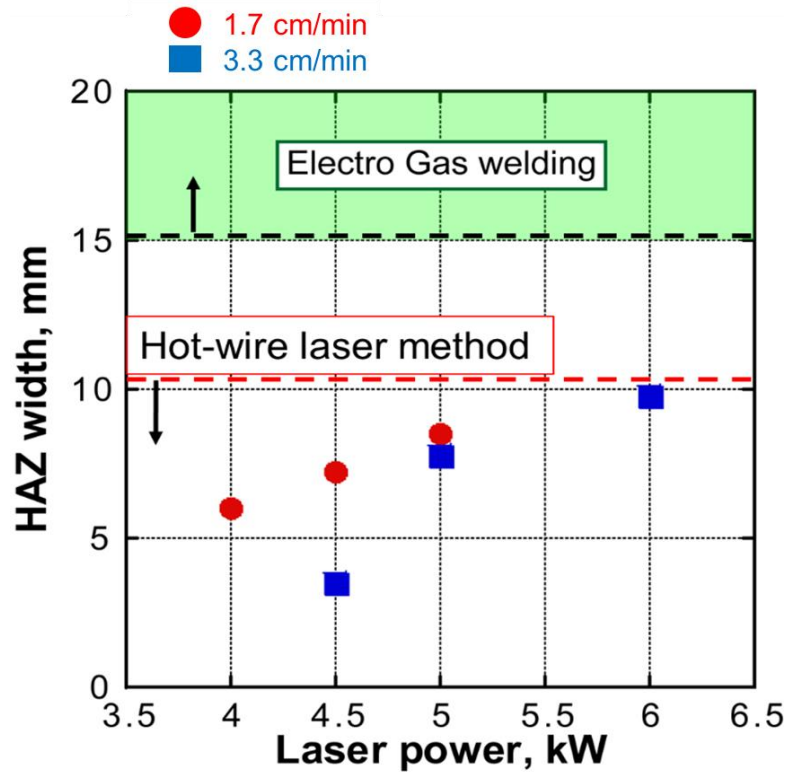
Fig. 3.17 The width of heat affected zone (HAZ) of hot-wire laser method has narrower than common electro gas welding process.
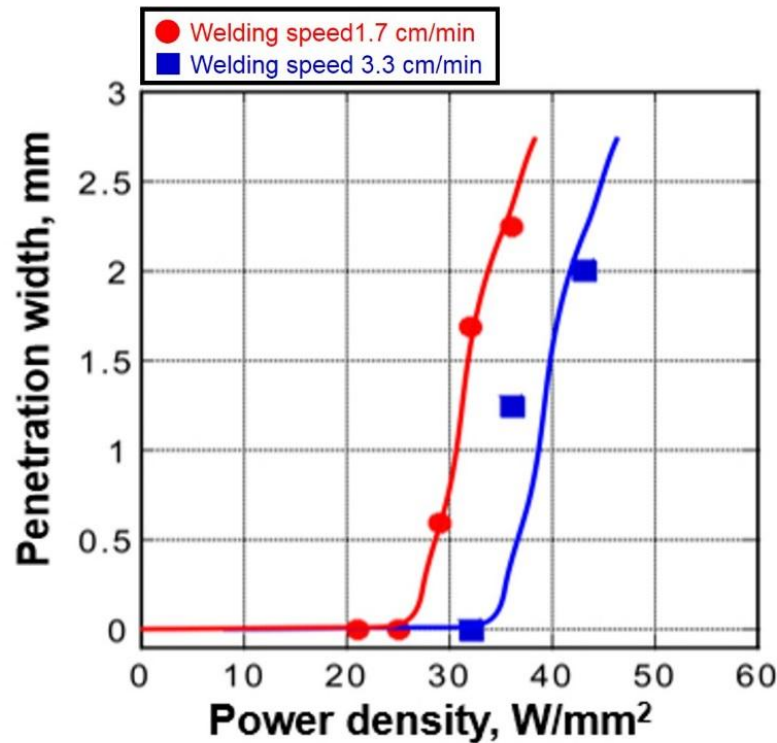
Fig. 3.18 Relationship between energy density, welding speed and penetration width of weld metal.

3.5 Effect of laser access method for joining on gap width of 5 mm

3.5.1 Introduction

In preliminary experiment of using the proposed process, welding was done by utilizing laser irradiation in vertical access through the groove and with 2 hot wires fed from two sides of the weld. It yielded weld with complete melting. Nevertheless, the aforementioned method is merely basic originality idea. In practical applications, it may be necessary to irradiate the joint with laser from the side of the groove, which has the benefit of less adjusting of the laser source and beam. The problem of obstacles or obstruction of laser beam can also be minimized, moreover, the filler metal needs to be fed from only one side. This research presents the idea of how to gain access for laser to the joint from the side. This can be achieved by tilting the laser head so that it focuses and yields beam size that is suitable for the joint. Welding was done under the higher power density than the critical value reported in the previous report. Lastly, the welding speed plays a critical role in defining welding phenomena.

The objective of this report is to investigate the effect of laser access method, consisting of vertical laser access with 2 hot wires and oblique laser access with 1

hot wire, and the effect of the weld speed in each access method. The joint on which the welding was performed has a width of 5mm, which can be considered small comparing to the thickness of 26mm. Both laser access method used the heating by stationary laser irradiating method. The result from high-speed camera recorded during welding is used to analyze the behavior of the process. In the final comparison the effect and the result of investigation of the weld in macro scale is done, with imperfection and weld penetration as the quantitative comparisons.

3.5.2 Material and specimen used

The material used in this study was KE47 steel plates. The filler wires of YM-1N (JIS Z 3325 YGL2-6A (AP)) with its diameter of 1.6 mm was used in this research. The chemical composition of base metal and filler metal were shown in Table 3.5. The dimension of a specimen was 100 (width) x 200 (height) x 26 mm (thickness) as shown in Fig. 3.19.
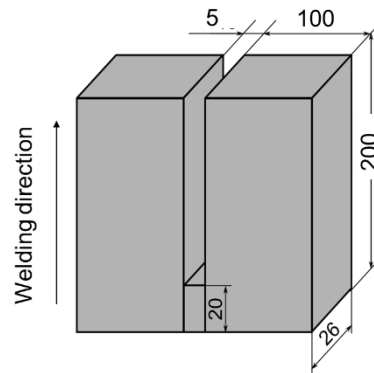
Fig. 3.19 Specimen dimension used

Table 3.5 Chemical compositions of base metal and filler metal

Material	Chemical Composition, wt%											
	C	Si	Mn	P	S	Al	Cu	Ni	Nb	Ti	Cr	Mo
KE-47	0.09	0.07	1.52	0.007	0.002	0.014	0.32	0.69	0.01	0.01	0.02	0.00
YM-1N	0.04	0.46	1.35	0.01	0.007	-	0.17	1.07	-	0.7	-	0.26

3.5.3 Welding process laser access method and welding parameters

The procedures of the proposed process is shown in schematic layout of joint configuration and apparatus in Fig. 3.20: the vertical laser access with 2 hot wires is shown in Fig. 3.20. (a), and oblique laser access with 1 hot wire is shown in Fig. 3.20 (b). The joint configuration is rigged in vertical alignment. Groove configuration is square butt joint for welding with single pass weld.
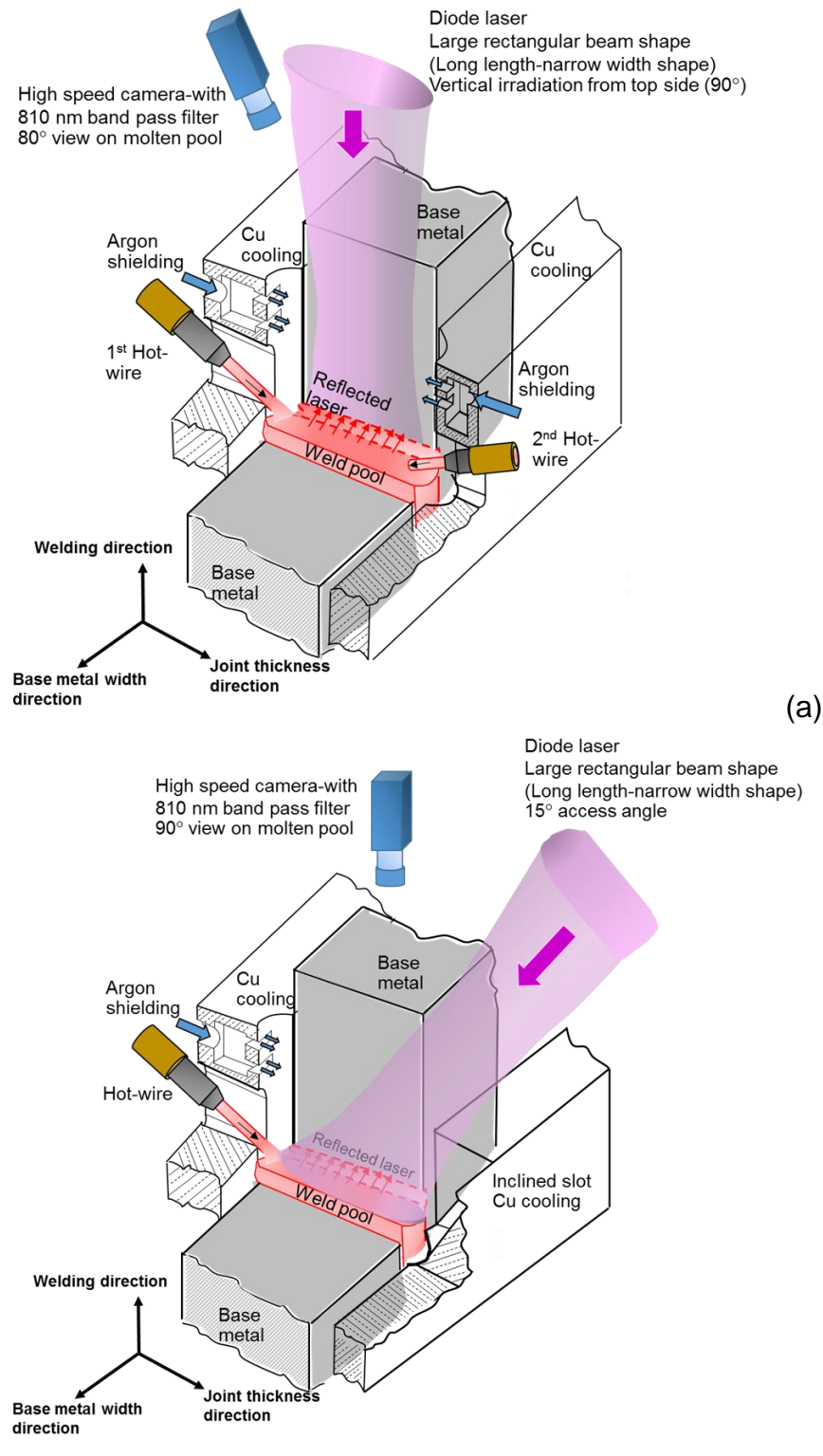
Fig. 3.20 Schematic layout of joint configuration and apparatus of the hot-wire laser method by (a) Vertical laser access-with 2 hot wires and (b) Oblique laser access-with 1 hot wire method.

The laser equipment used as a power source was Laserline LDF 6000-40 (6.0 kW) continuous wave (CW) Diode Laser (LD). It was assembled with colliminater lens of 100 mm, focus lens of 400mm, and fiber diameter of 1 mm. The resulting laser beam has a rectangular beam shape with long-length narrow-width dimension. The spot size will be discussed in the next section. The hot-wire system was used in the proposed process to improve the efficiency of deposition. The hot wire machine used was Hitachi Power Assist HI-TIG series IV662.

The welding parameter of the vertical laser access with 2 hot-wires was shown in Table 3.6. The welding process, which is the basic ideal of this research, irradiates the joint with laser from above with laser spot size of 4.5mm width and 31mm length. The width is narrower than the gap width. The reason of this is that this process focuses on the reflection of laser from weld pool to the surface of the joint to melt the base metal. The laser power used is 6 kW. The resulting power density is 43 W/mm^2, which exceeds critical limit stated in the previous experiment. The experiment of vertical laser access was done to investigate the effect of the welding speed at 3.33 cm/min (2m/h) and 5.0 cm/min (3m/h). The welding speed of 1.7cm/min was not investigated because of the excessive melting of base metal occurred due to too high heat conduction of weld pool. Filler metal is fed from hot-wire torches from both 2 sides of the joint. The hot wire torches is set inside with copper cooling shoes. The wire feeding position and the feeding angle was set at 2mm and 45°, respectively. During the welding, the atmosphere above the molten pool is shielded with argon gas at the flow rate of 10 l/min.

(a) Vertical laser access with 2 hot wires   (b) Oblique laser access with 1 hot wire
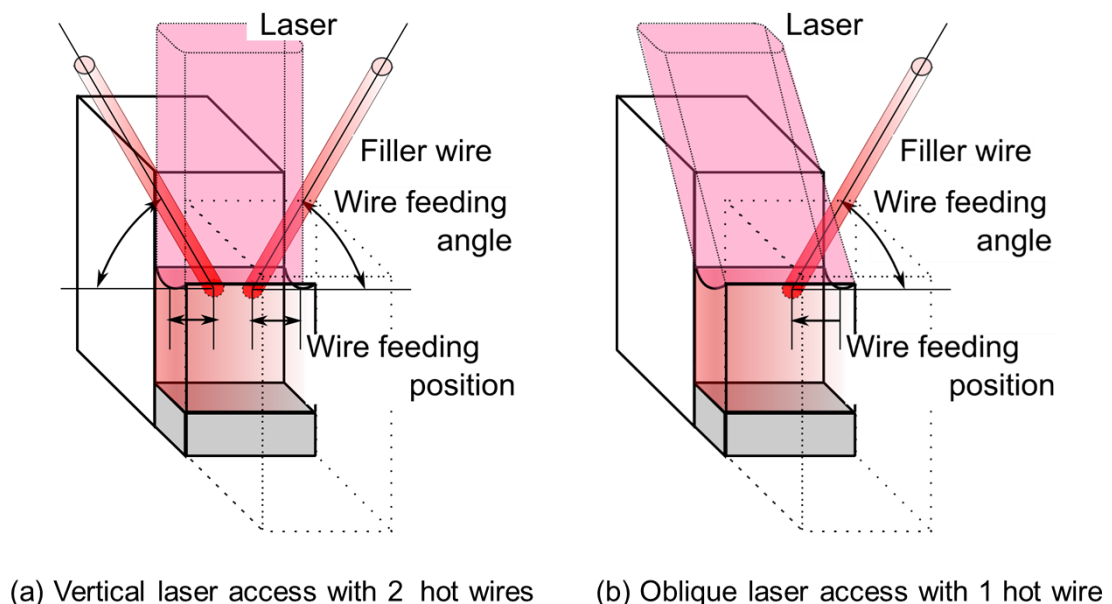
Fig. 3.21 Definition of welding parameter

The oblique laser access with 1 hot-wire shows schematic by Fig 3.20 (b) and its welding parameter was shown in Table 3.6. The laser head was set out of specimen alignment and tilt a laser head by the tilt angle 15°. This angle is proper angle for irradiate laser beam through the joint target. The laser head set is same of the first case. Result of spot size is 4.5 x 27 mm. 1 hot-wire feeds from the opposite side of laser access side. Feeding parameters were consist of feeding position of 2 mm with feed angle of 45°.

Definition of welding parameter setup for two laser access methods were shown in Fig. 3.21.

Table 3.6 Welding parameters

Laser access method	Vertical		Oblique		
Laser irradiation type	Stationary		Stationary		
Fiber core, mm	1.0		1.0		
Homogenizer	LL3		LL3		
Focus lens, mm	400		400		
Laser power, kW	6		6		
Laser irradiation angle, degree	0		15°		
Defocus, mm	50		50		
Spot size, mm x mm	4.5^w x 31^l		4.5^w x 27^l		
Power density, W/mm^2	43		49		
Hot-wire feed numbers	2		1		
Welding speed, cm/min	3.3	5.0	1.67	3.3	5.0
Wire feed speed, m/min	1.16	1.62	2.28	4.42	5.66
Wire current, A	96	111	96	111	150
Wire feeding angle, degree	45		45		
Wire feeding position, mm	2		2		
Shielding gas (Argon), LPM	10		10		
Pre irradiation time, s	60		60		

3.5.4 Process monitoring methodology

Optical processing for capturing of welding phenomena was done with high speed camera. The camera used was a Pencil camera V-193-M1 model connected with NAC: MEMRECAM GX-5 module, focus lens 50 mm with diameter of 25 mm, 810 nm band pass filter. The capturing parameter with frame rate of 50 fps, shutter

speed of 1/20000, and closed aperture. The capturing yielded detailed observation of the welding phenomena.

The setting and rigging of the camera can also be seen in Fig. 3.20 (a) and (b) In the vertical laser access, the camera cannot be set at 90° from the plane of weld pool due to the laser beam. The best viewing angle obtained is 80° from the plane of weld pool. Hence, the visible area is around 60% of the joint thickness, or approximately 15mm. The width axis of the joint is visible entirely. The available access view is shown in Fig. 3.22. In oblique laser process, the camera can be set at 90° from the plane of weld pool, so the behavior of weld pool can be seen entirely in both axes.
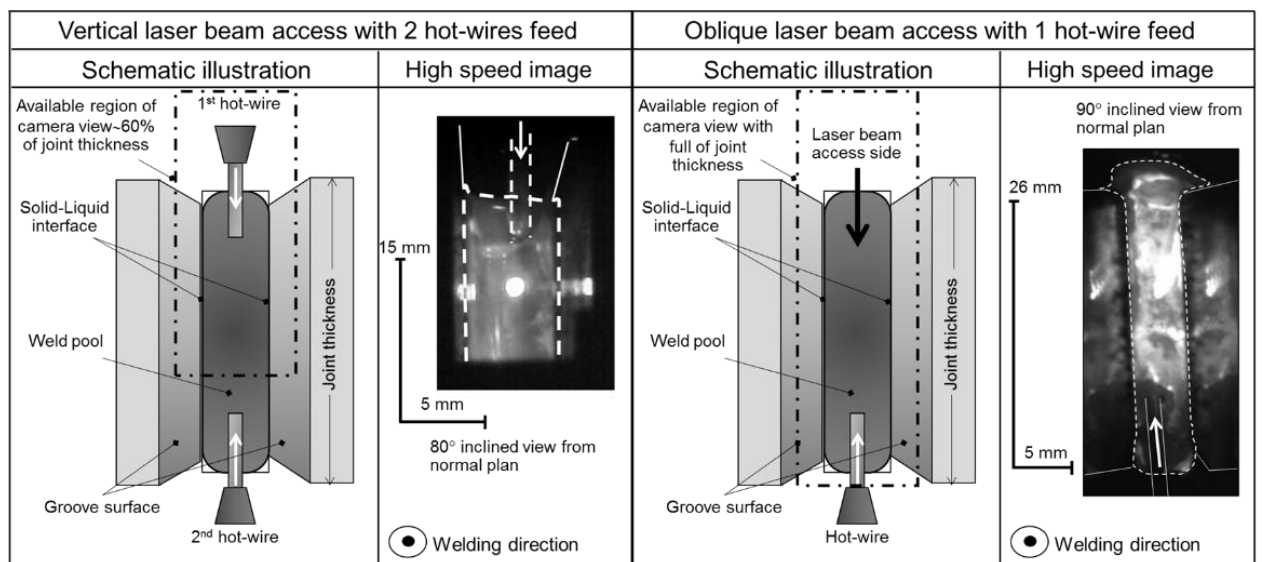
Fig. 3.22 Schematic illustration and high speed image explain available region for vertical and oblique laser beam access

3.5.5 Methodology for evaluation of weld joint characteristics

The imperfection level and the maximum weld penetration of the weld from the aforementioned experiment were evaluated on 2 cut planes: vertical cutting plane cut parallel to the weld direction at the center of the thickness, and horizontal cutting plane which is made perpendicular to the welding direction. The cutting plane are shown in Fig. 3.23. The position to be cut was selected at the area showing steady state behavior. The cut was then polished and etched with 3% nital acid for weld characteristics to be visible.
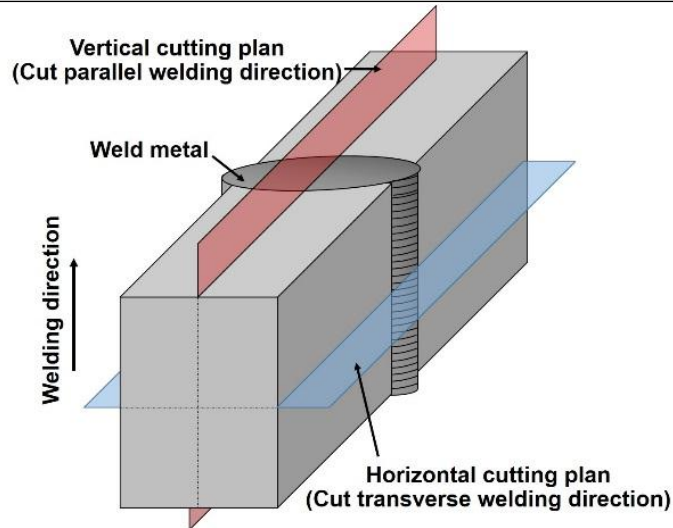
Fig. 3.23 Cutting plan layout and section definition
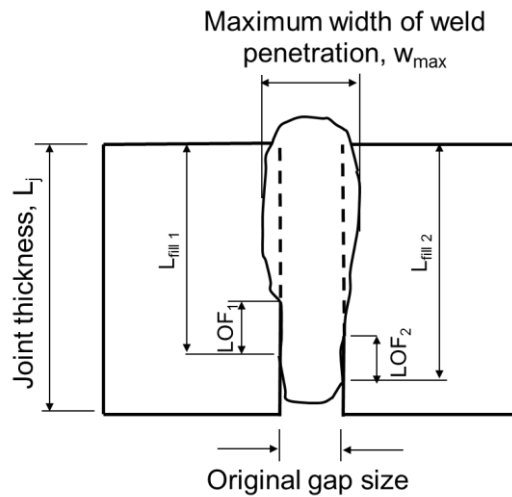
Fig. 3.24 Method of measurement variables for evaluate weld imperfections (for horizontal cutting plan)

The evaluation of weld characteristics is shown in Fig.3.24. The feature shown is measured and calculated for the effective weld metal deposition (L_{fill}), the effective complete fusion on deposited length (L_{fusion}), and maximum width of weld penetration (W_{max}).

L_{fill} is defined as in equation (1). It defines depositing ability and weld ability.

$$L_{fill} = \frac{L_{fill1} + L_{fill2}}{2 \times L_j} \times 100\% \tag{1}$$

In the case that L_{fill} equals to 100%, complete deposited weld is achieved by single pass joining. However, the effective complete fusion on deposited length (L_{fusion}) must also be evaluated. The L_{fusion} is defined as shown in equation (2):

$$L_{fusion} = \left(1 - \left(\frac{Total\ LOF}{L_{fill\ 1} + L_{fill\ 2}}\right)\right) \times 100\% \qquad (2)$$

L_{fusion} defines the melting ability of base metal along the length of effective weld metal deposition (L_{fill}). The reason of additional evaluation is that in many cases the weld can be made on the entire groove size, but lack of fusion (LOF) occurs due to inadequate heating. Finally, W_{max} can be measured directly on the section.

3.5.6 Welding phenomena of vertical laser access with 2 hot-wires

The high-speed photographs of welding phenomena in the weld pool during the weld process are shown in Fig. 3.25 (a) and (b) for the welding speed of 3.33cm/min (2m/h) and 5.0cm/min (3m/h), respectively. The photo before hot wire feeding shows white dash line as a border of the weld pool, white solid line as a border of the work piece, and red centerline as a reference line of joint edge as an aid for observation of the deposition of the weld. Fig. 3.25 (a) shows that the weld pool size is slightly larger than the designated groove site before wire feeding. This is to warm up the weld pool to have consistent heating before welding start. After initial wire fed, hot wire can be seen filling into the weld pool in a stable manner during melting under the heating from the laser and deposition. Regardless of welding duration, there is small incomplete fulfill, but liquid metal was able to fill up the void. Overall, welding speed of 3.33cm/min that yields stable full-size deposition of weld metal. At higher speed of 5.0cm/min, high-speed photos shown in Fig. 3.25 (b) shows that even at 2 times higher a speed, stable weld pool creation can still be achieved.

Comparing and contrasting between 2 welding speeds regime in vertical laser access cases, the effect of the welding speeds is small. This may be due to the laser energy level, the consistency of heating level along the joint, and the hot wire feeding rate from both sides still in suitable limit.
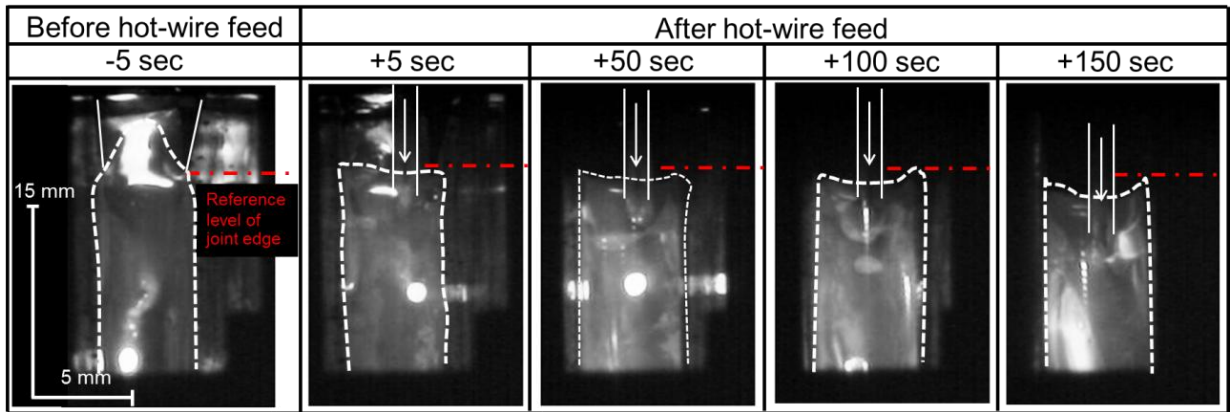
(a) Welding speed 3.33 cm/min (2 m/h)
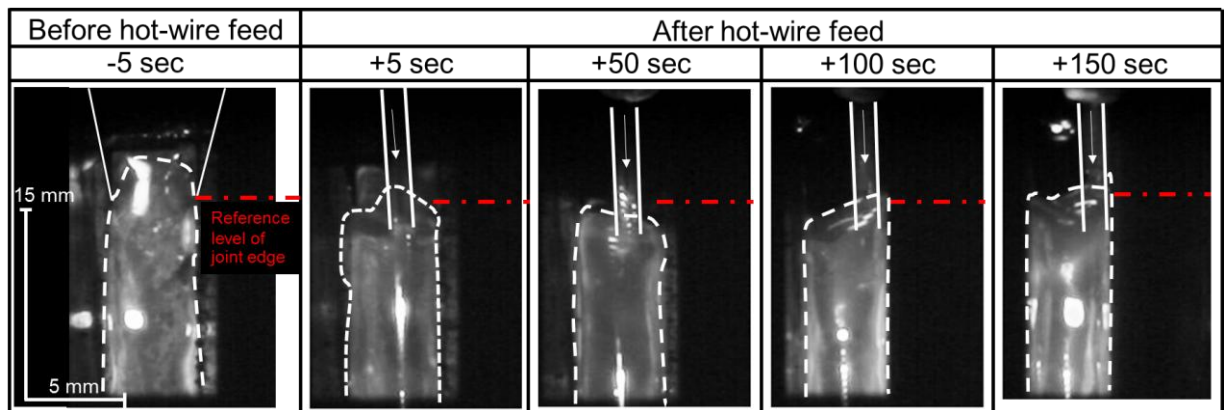
(b) Welding speed 5.0 cm/min (3m/h

Fig. 3.25 High speed photographs (Inclined 80° from weld pool plane) for vertical laser access with 2 hot-wire: centerline is reference level of joint edge.

3.5.7 Welding phenomena of oblique laser access with 1 hot-wire

The result of vertical welding using oblique laser with 1 hot wire is shown in full joint thickness view of high-speed photographs in Fig. 3.26. The weld with welding speed of 1.67 cm/min (1 m/h), 3.33 cm/min (2 m/h), and 5.0 cm/min (3m/h), are shown in Fig. 3.26 (a), (b) and (c), respectively. In this case, the size of the weld can be obtained by using reference length of the both sides of joint edges, which are marked by red centerline.
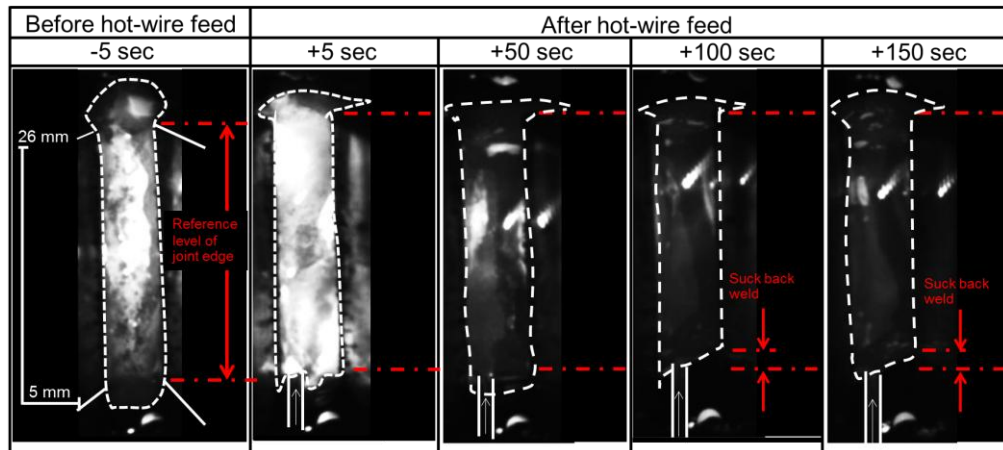
(a)
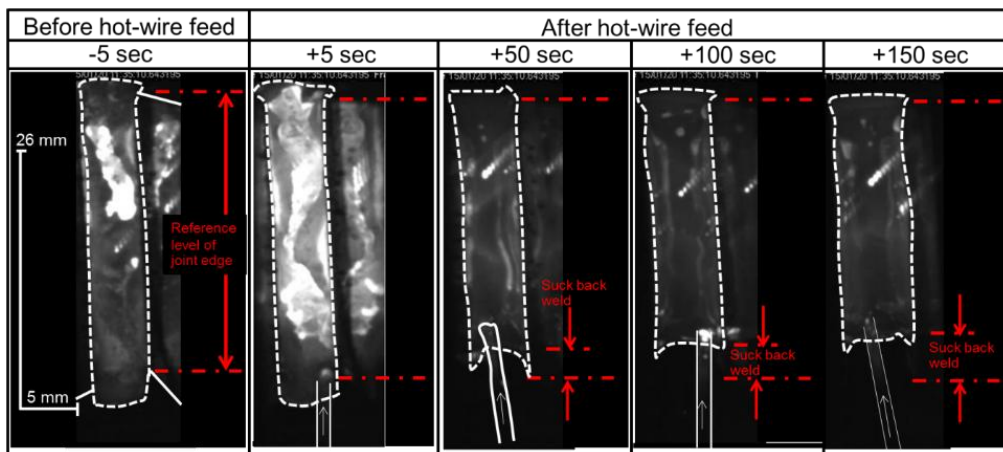
(b)
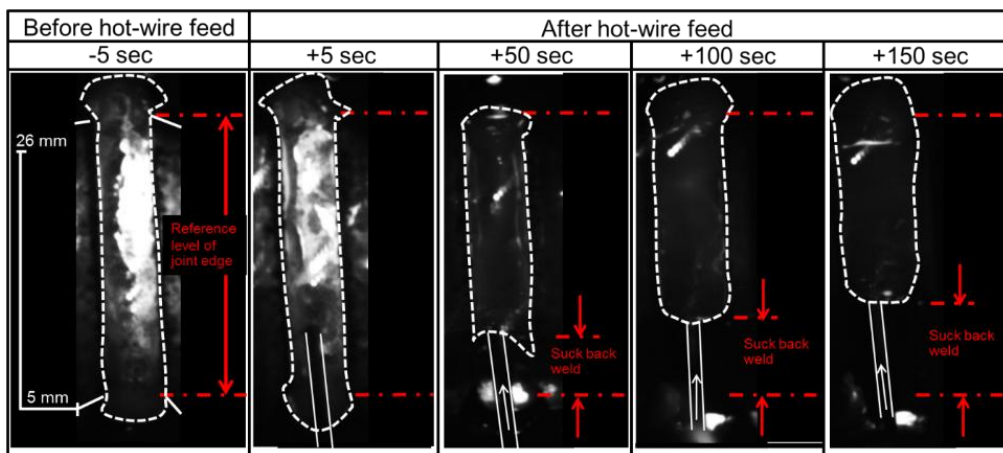
(c)

Fig. 3.26. High speed photographs for oblique laser access with 1 hot-wire (full thickness view) with (a) welding speed 1.67 cm/min (1 m/h), (b) welding speed 3.33 cm/min (2 m/h) and (c) 5.0 cm/min (3m/h), Upper side is laser access side and lower side is hot-wire feeds side: centerline is reference level of joint edge.

At the welding speed of 1.67cm/min shown in Fig. 3.26 (a), the weld pool is consistently created even the weld has relatively narrow gap width at 5mm comparing to 26mm. Incomplete fulfilled weld has a depth of approximately 2mm on the top part of the work piece. Increasing the speed to 3.33 cm/min, Fig. 3.26 (b), Incomplete fulfilled weld increase, meaning that deposition ability decreases. The weld pool shape in the hot wire feeding side can be observed which is a good wetting between it and both groove surfaces can still be achieved. This implies that the weld pool creation heat level is still adequate. However, with increased speed, flow and dissipation of molten metal more difficult to fill in the groove due to boundary constrain. This can be regarded as the characteristic problem in vertical joining, which is drastically different from other welding positions, in that incomplete fulfilled weld creation is severe, especially at the welding speed of 5.0 cm/min, shown in Fig. 3.26 (c). In 100 and 150 seconds of the welding, weld pool flows out through laser access side and no wetting between weld pool and groove surfaces was observed.

From these welding phenomena results of oblique laser access with 1 hot wire, show the welding speed affects the deposition ability greatly. In these cases, faster hot wire feeding rate and travel speed makes it difficult for molten metal to diffuse and flow in horizontal plane in short time. From this problem, the author proposes 2 ideas for future research: makes the laser beam energy level at both ends higher to increase the flow and sweeping of the molten metal to fill the groove using laser weaving method

3.5.8 Evaluation of weld metal cross sections

The welded specimens from aforementioned experiments was evaluated of weld quality using the protocol stated in section 3.5.5. The vertical cutting (cutting plane parallel to the weld direction) is shown in Fig. 3.27. It can be seen that complete fusion occurred at all parameter values. The fusion zone or weld penetration width is inverse proportional to the welding speed. In the case of oblique laser access, weld penetration width dramatically decreased between the case with welding speed of 1.67cm/min and 3.33cm/min. At the speed of 5.0m/min, the weld penetration fits within the width of gap size. Comparing between laser access methods, vertical access with 2 hot wires yields better melting, and change of weld speed affects only slightly to the melting and weld phenomenon. However, it can be observed that melting and weld phenomenon of 3.33cm/min weld speed is more consistent than 5.0cm/min weld speed.

The result from horizontal cutting plane (perpendicular to weld direction) is shown in Fig.3.28. In this section, weld characteristics can be thoroughly observed. Vertical laser access yields successful sound joint at both weld speed, which can be observed from the high-speed photographs that the width of weld penetration is maximum at the middle of the joint, which indicates the heat conduction from the

weld pool. In oblique laser access, the deposition from the laser access side is complete, but on wire feed side is plagued with incomplete fulfilled weld.
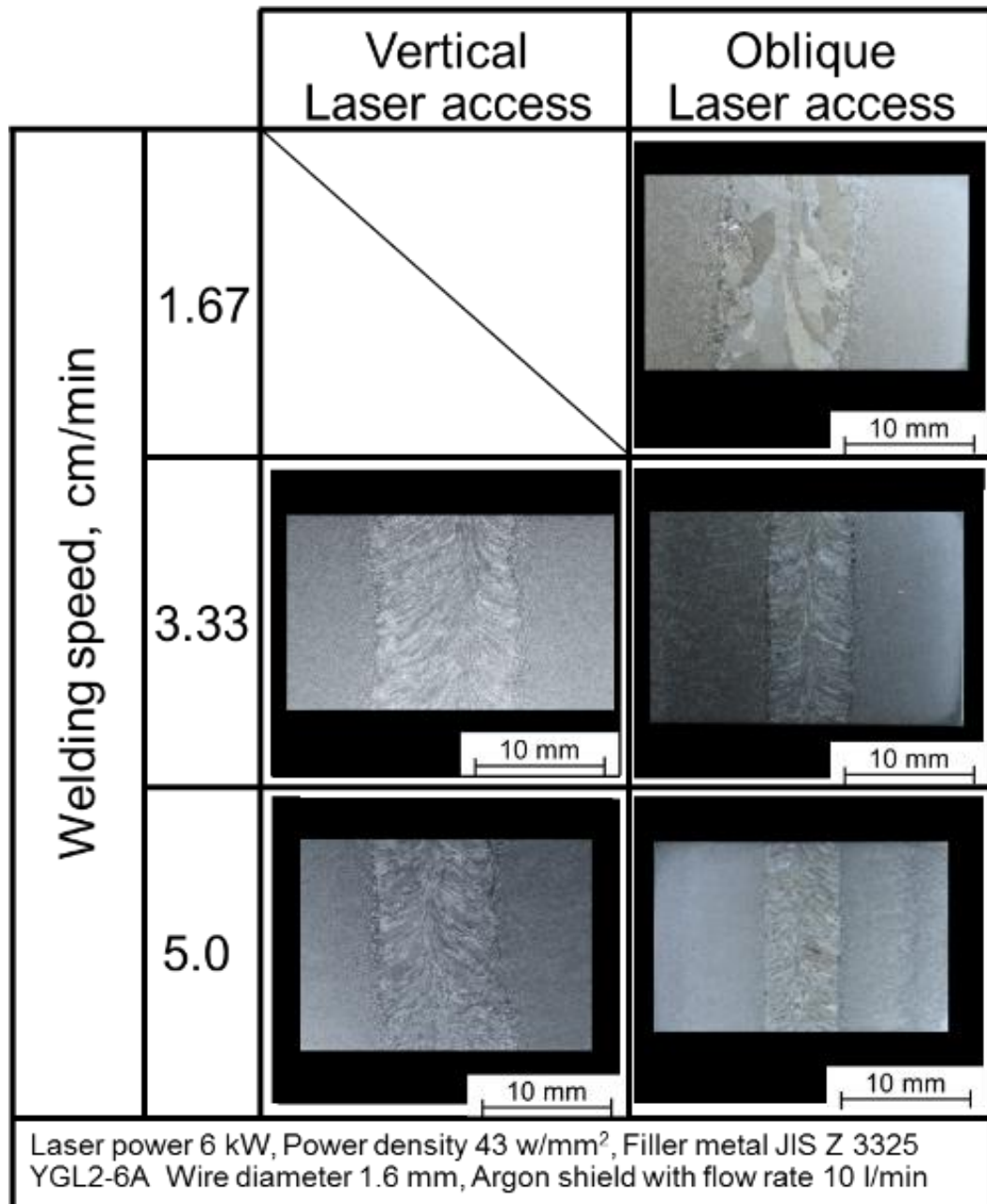
Fig. 3.27 Macro photographs of center thickness cross section with parallel welding direction
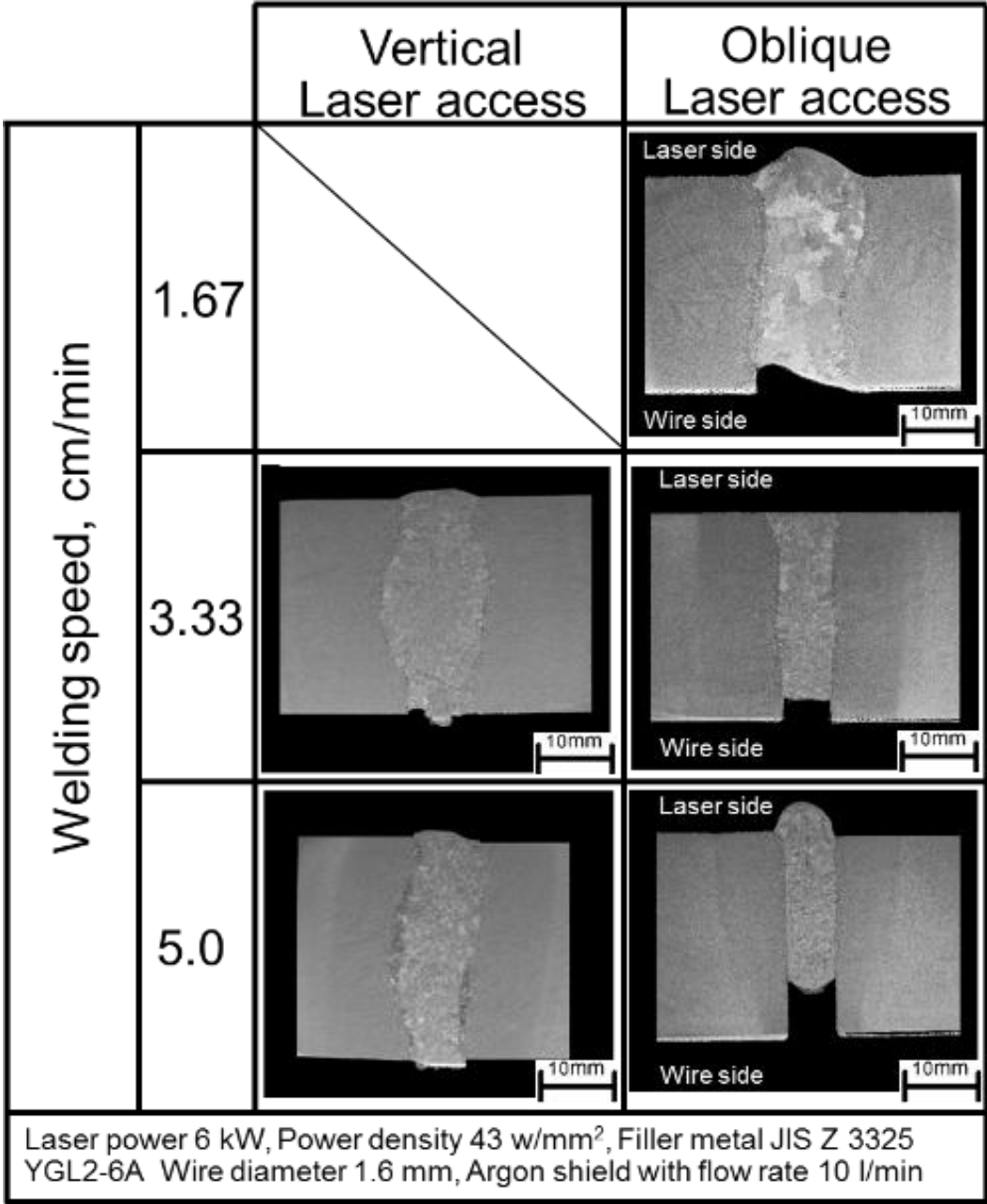
Fig. 3.28 Macro photographs of cross sections with transverse welding direction

The analytic result of the weld evaluation consists of maximum width of weld penetration W_{max}, effective weld metal deposition L_{fill}, and effective complete fusion on deposited length L_{fusion}. They are shown in Fig. 3.29. (a), (b) and (c), respectively. The W_{max} of vertical laser access is higher than oblique laser access in all cases. Increasing the welding speed from 3.33cm/min to 5.0cm/min decreases the width slightly from 13 mm to 10 mm. Comparison of the results at same welding speed, oblique laser access yields 1.25 times smaller width than that of vertical laser access.
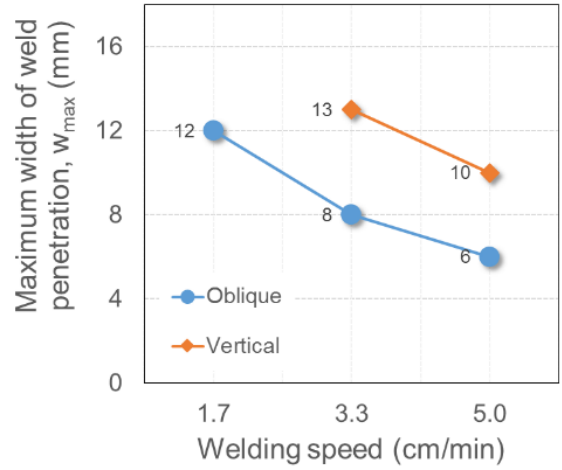
(a)
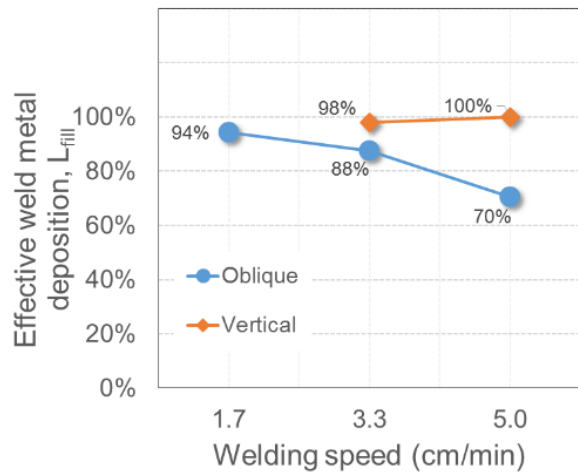
(b)
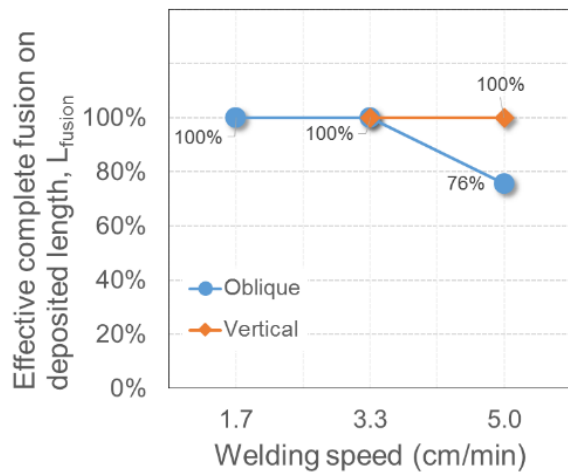
(c)

Fig. 3.29. Measured weld characteristic for (A) maximum width of weld penetration, w_{max} (B) effective weld metal deposition, L_{fill} and (C) effective complete fusion on deposited length, L_{fusion}

The evaluation of L_{fill} and L_{fusion} is coupled. It can be seen that the vertical access yields consistent and complete melting on the entire length of deposition. It is more interesting however, that in the oblique welding at the speed of 1.67cm/min and 3.33cm/min, even L_{fill} is at 98% and 88% level respectively, the ability to melt, or L_{fusion}, is at 100% on both cases. This demonstrates that the energy level is adequate for melting. To improve the quality of the weld, the efficiency of dissipating heat at joint edge has to be increases. This phenomenon can be confirmed using high-speed photographs shown in Fig. 3.26 (a) and (b). Nevertheless, the result at 5.0cm/min welding speed is non preferable, with L_{fill} of 70% and L_{fusion} of 76%, which means the melting length of only 7mm per side of base metal. This shows that at welding speed higher than 3.33cm/min, irradiation method and welding procedure has to be adjusted to achieve successful weld.

In practical welding situation where fit-up and shrinkage of the weld may occur, the optimized procedure is oblique laser access with laser spot size of 4.5mm×26mm, laser power density of 43 W/mm^2, and welding speed of 3.33cm/min (2m/h). The reason of this is because it benefits from lower heat input than at weld speed of 1.67cm/min with no excess melting of base metal, high deposition ability, and consistent melting over the entire deposition length.

The present section is investigation of the basic welding phenomena of the proposed welding process. The groove size of 5mm (groove width) × 26mm (thickness) was a target for joining. The effect of laser access method is investigated. The access methods consist of vertical laser beam access and oblique laser beam access. The investigation result can be concluded as follows:

- The proposed method welded successfully with both access method. Oblique laser access is more practical in welding field than vertical access method even though the useful weld speed range is narrower due to narrower gap size.
- The oblique laser access giving optimized procedure has a laser spot size of 4.5 mm x 26 mm, laser power density of 43 w/mm^2, and welding speed of 3.33 cm/min (2 m/h). It yields weld with complete fusion on deposited area and low dilution level.

3.6 Summary

The single-pass vertical joining using hot-wire laser welding method was developed. The basic idea of the proposed process was explained and investigated the welding process phenomena. The weld joint dimension of 5 mm (gap width) x 26 mm (joint thickness) was used as a target for the feasibility study. From the experiment of this chapter, it could be draw as summary for this chapter as:

1) Irradiating of large rectangular laser spot size to crates weld pool is possible and able to make weld joint by hot-wire feeding as single-pass vertical joining.

2) The reflected laser beam was investigated and obtained the evidence. The high speed images during laser irradiation showed that it could made the initial melting on groove surfaces.

3) Stable formation of a molten pool and stable feed of filler wires during single-pass vertical welding on a joint of 26 mm thick steel plates were achieved using the laser diode with a large rectangular beam spot and hot-wire system.

4) The power density is the principal parameter to obtain adequate fusion and a sound weld bead, and it affects largely on melting phenomena compared with a welding speed. Critical power densities with relative to welding speeds were determined, which is about 25 and 35 W/mm^2 for each welding speed of 1.67 and 3.33 cm/min, respectively.

5) Although the energy distribution in the thickness direction must be optimized to obtain the sound bead at bead surfaces, it can be said that the proposed hot-wire laser welding process has the potential to be used as the single-pass vertical welding process for thick steel plates with low heat input and low dilution.

6) The oblique laser access with 1 hot wire feeding giving optimized procedure has a laser spot size of 4.5 mm x 26 mm, laser power density of 43 w/mm^2, and welding speed of 3.33 cm/min (2 m/h). It yields weld with complete fusion on deposited area and low dilution level.

Chapter 4

Investigation of melting phenomena and

optimization of laser irradiating condition

4.1 Introduction

According to successful determination of the critical laser power density with respect to the welding speed for melting base metal on the gap width of 5 mm. And the laser access method was also studied to make of the proposed process more realize practical process for fabrication industries, the results have a good tendency on the narrow gap. However, the situation of narrow gap width affected a difficulty of flow of the liquid weld metal due to the long distance the joint thickness. As for set narrow gap width before welding that is an undesirable for heat source access and liquid metal fulfill through another side joint target. The gap tolerance in the width dimension were varied from 5 mm to 15 mm, preferentially. Then, the laser irradiating method must be fit to the gap dimension and get the sound joint result.

The gap feature relative large due to the limit power density of laser be which can be irradiated. The laser beam parameters must be considered to success joining base on a maximum efficiency and optimization of the proposed process. It was a statement in this chapter to study a methodology to achieve joining on the large gap size.

There are two main parts for studies in this chapter which consists of the stationary laser irradiating method and the weaving laser irradiating method. The 1st study has an objective to investigate welding phenomena on joining by a low power density laser beam. The melting amount of base metal and other weld joint characteristics were investigated the effect to clarify main factor of the base metal fusion. It was research strategy by using same power density with differential weld pool (heating) volume for the clarified experiment. The 2nd part is an improvement of the proposed process and optimization of the high efficiency of the laser beam was designed an adequate power density and distributes energy along groove area. Beam motion in the groove width dimension was specified a method for the study.

In-situ observation by high-temperature optic apparatus and high-speed detection was provided to be used for explain the process phenomena. A visualized energy image is supporting evidence for comparing the effect of laser beam parameters.

4.2 Investigation of main effect of base metal melting for low power density laser beam

4.2.1 Material used

KE-47 steel plates were used in this study, the dimension of the specimen was 50 (width) x 100 (height) x 26 mm (thickness). Plates were fixed and aligned as a vertical joint configuration. The gap widths were set by spacer which are dimension of 5 (width) x20 (height) x 26 (thickness) and 10 (width) x20 (height) x 26 (thickness) for study the effect of differential heating volume. The filler metal of YM-1N (JIS Z 3325 YGL2-6A (AP)) with a diameter of 1.6 mm was used. The chemical composition of base metal and filler metal were presented on Table 4.1.
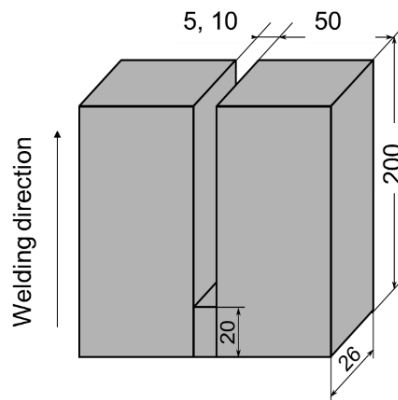
Fig. 4.1 Specimen dimension and weld joint configuration

Table 4.1 Chemical compositions of materials used

Material	Chemical Composition, wt%											
	C	Si	Mn	P	S	Al	Cu	Ni	Nb	Ti	Cr	Mo
KE-47	0.09	0.07	1.52	0.007	0.002	0.014	0.32	0.69	0.01	0.01	0.02	0.00
YM-1N	0.04	0.46	1.35	0.01	0.007	-	0.17	1.07	-	0.7	-	0.26

4.2.2 Experimental procedure

The procedures of the proposed process are shown in the schematic illustration of joint configuration and apparatus in Fig. 4.2: the stationary laser beam method by using the oblique laser access (tilt angle of 15°) with 1 hot-wire for joining. The joint configuration is rigged in vertical alignment. Groove configuration is a square butt joint for welding with single pass weld.

For verifying the main effect of fusion phenomena weld pool volume was varied by modulating the laser spot sizes. By controlling the same level of the power density, the experiment was designed different spot sizes and the modulated laser power for joining as showed in Fig. 4.3. The laser spot size for create weld pool on the groove size of 5 mm x 26 mm was 4.5 mm x 31mm, laser power of 3 kW was resulting on irradiated power density of 23 W/mm^2 (Fig. 4.3 (a)). Once, the laser spot size of 10

mm x 26 mm, laser power of 6 kW was resulting on irradiated power density of 23 W/mm^2 for create the weld pool on the groove size of 10 mm x 26 mm (Fig. 4.3 (b)). Table 4.2 shows the welding parameter of laser and hot-wire for all conditions.
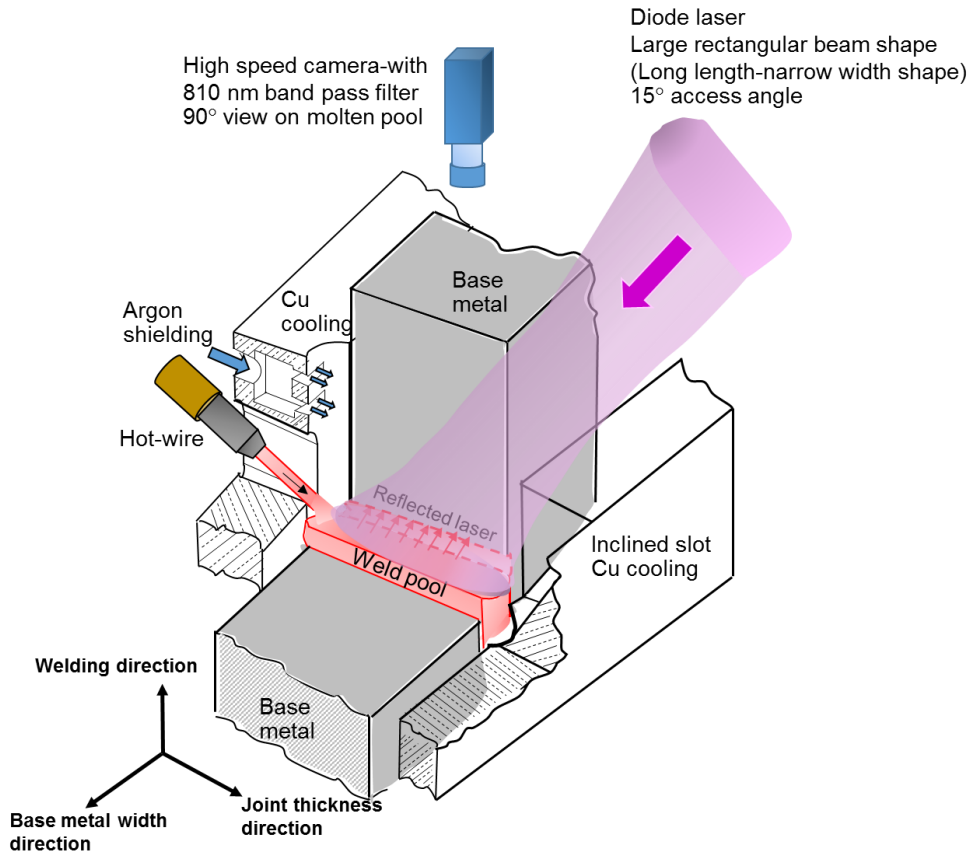
Fig. 4.2 Schematic illustration of the oblique laser access for the stationary laser beam experiment.
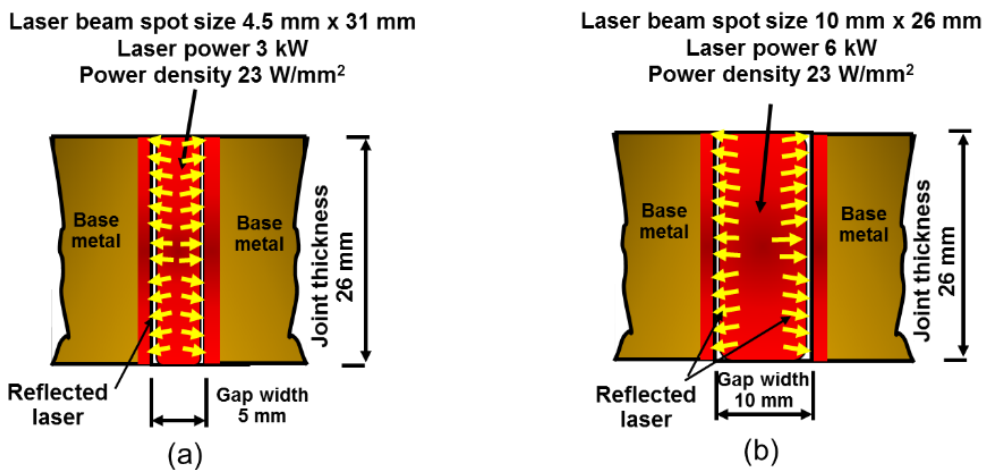
Fig. 4.3 Schematic illustration the stationary laser beam of 23 W/mm^2 which are different weld pool volumes by modulation the spot size of (a) 4.5 mm x 31 mm and (b) 10 mm x 26 mm

Table 4.2 Welding parameters for verify the effect of weld pool volume on melting phenomena

Gap width size, mm	5	10
Laser type	Diode laser	Diode laser
Laser irradiation type	Stationary	Stationary
Fiber core, mm	1.0	1.0
Homogenizer	LL3	LL6
Focus lens, mm	400	1000
Laser power, kW	3	6
Laser irradiation angle, degree	15°	15°
Defocus, mm	50	0
Spot size, mm x mm	4.5^w x 26^l	10^w x 26^l
Power density, W/mm^2	23	23
Filler wire diameter, mm	1.2	1.6
Welding speed, cm/min	3.3	3.3
Wire feed speed, m/min	4.42	5.31
Wire current, A	111	161
Wire feeding angle, degree	45	45
Wire feeding position, mm	510	5
Shielding gas (Argon), LPM	10	
Pre irradiation time, s	120	120

4.2.3 Methodology of in-situ observation

Optical processing for capturing of welding phenomena was done with a high-speed camera. Pencil camera V-193-M1 model connected with NAC: MEMRECAM GX-5 module, measured with focus lens 50 mm with diameter of 25 mm, 810 nm band pass filter (Fig. 4.4 showed the characteristic of transmission curve of 810 nm used). The capturing parameter is the frame rate of 50 fps, the shutter speed of 1/20000 s and closed aperture. The capturing yielded the detailed observation of the welding phenomena. Fig. 5 shows a schematic layout and the explanation of the weld pool view. The camera can be set at 90° from the plane of the weld pool, so the behavior of the weld pool can be seen entirely in both axes.
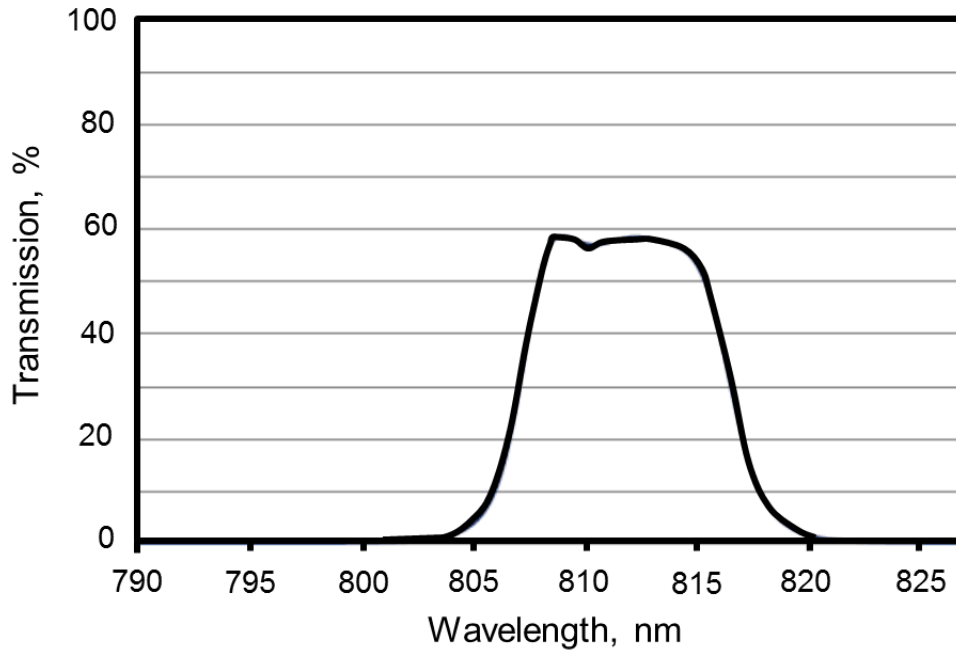
Fig. 4.4 the characteristic of transmission curve of 810 nm
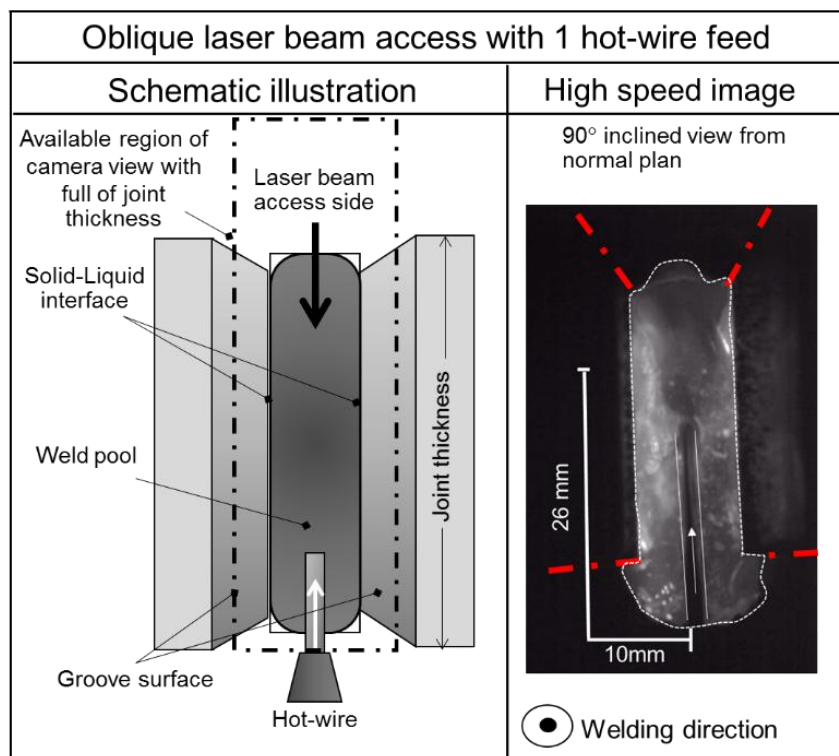
Fig. 4.5 Schematic layout and high speed image explain available region for oblique laser beam access

Table4.3 Monitoring conditions of In-situe Observation

High speed camera	GX-5
Frame rate, fps	50
Aperture	Closed
Focus lens, mm	50
Band pass filter, nm/FWHM	810 / 10
Lighting	N/A
Shutter speed, s	1/20 k

4.2.4 Methodology for evaluation of weld joint characteristics

The imperfection level and the maximum weld penetration of the weld from the aforementioned experiment were evaluated in 2 cut plane: vertical cutting plane cut parallel to the weld direction at the center of the thickness, and horizontal cutting plane which is made perpendicular to the welding direction. The cutting plane are shown in Fig. 4.6. The position to be cut was selected at the area showing steady state behavior. The cut was then polished and etched with 3% nital acid for weld characteristics to be visible.
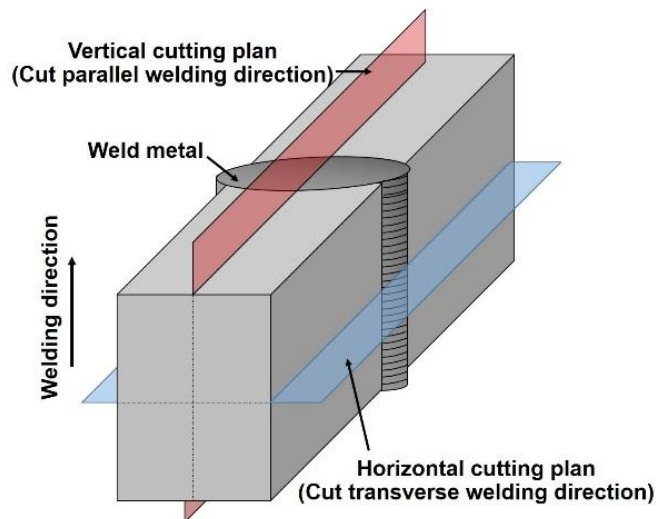
Fig. 4.6 Cutting plan layout and section definition
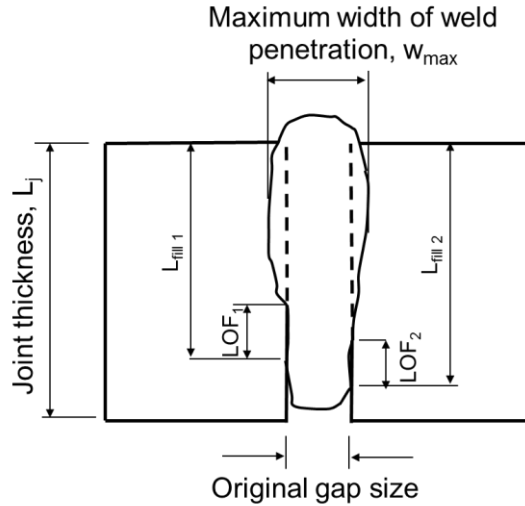
Fig. 4.7 Method of measurement variables for evaluate weld imperfections (for horizontal cutting plan)

The evaluation of weld characteristics is shown in Fig. 4.7. The feature shown is measured and calculated for effective weld metal deposition (L_{fill}), effective complete fusion on deposited length (L_{fusion}), and maximum width of weld penetration (W_{max}). L_{fill} is defined as in equation (1). It defines depositing ability and weld ability.

$$L_{fill} = \frac{L_{fill1} + L_{fill2}}{2 \times L_j} \times 100\% \qquad (1)$$

In the case that L_{fill} equals to 100%, complete deposited weld is achieved by single pass joining. However, the effective complete fusion on deposited length (L_{fusion}) must also be evaluated. The L_{fusion} is defined as shown in equation (2):

$$L_{fusion} = \left(1 - \left(\frac{Total\ LOF}{L_{fill\ 1} + L_{fill\ 2}}\right)\right) \times 100\% \times L_{fill} \qquad (2)$$

L_{fusion} defines the melting ability of base metal along the length of effective weld metal deposition (L_{fill}). The reason of additional evaluation is that in many cases the weld can be made on the entire groove size, but lack of fusion (LOF) occurs due to inadequate heating. Finally, W_{max} can be measured directly on the cut.

4.2.5 Effect of weld pool volume on melting amount of base metal

Fig. 4.8 and 4.9 show the results of captured high-speed images and cross section of the joint by the stationary laser beam of 23 W/mm^2-with gap size of 5 mm x 26 mm and 23 W/mm^2 with gap size of 10 mm x 26 mm, respectively. Measured results of the effective weld metal deposition (L_{fill}), the effective complete fusion on deposited length (L_{fusion}) were shown as main effect plot in Fig. 4.10.

Observed position	High speed image	Cross section of transverse welding direction	
Laser Side ↓ 50 mm ↑ Wire Side		Severe separated part	Laser Side ↓ ↑ Wire Side
Laser Side ↓ 70 mm ↑ Wire Side		Severe separated part	Laser Side ↓ ↑ Wire Side
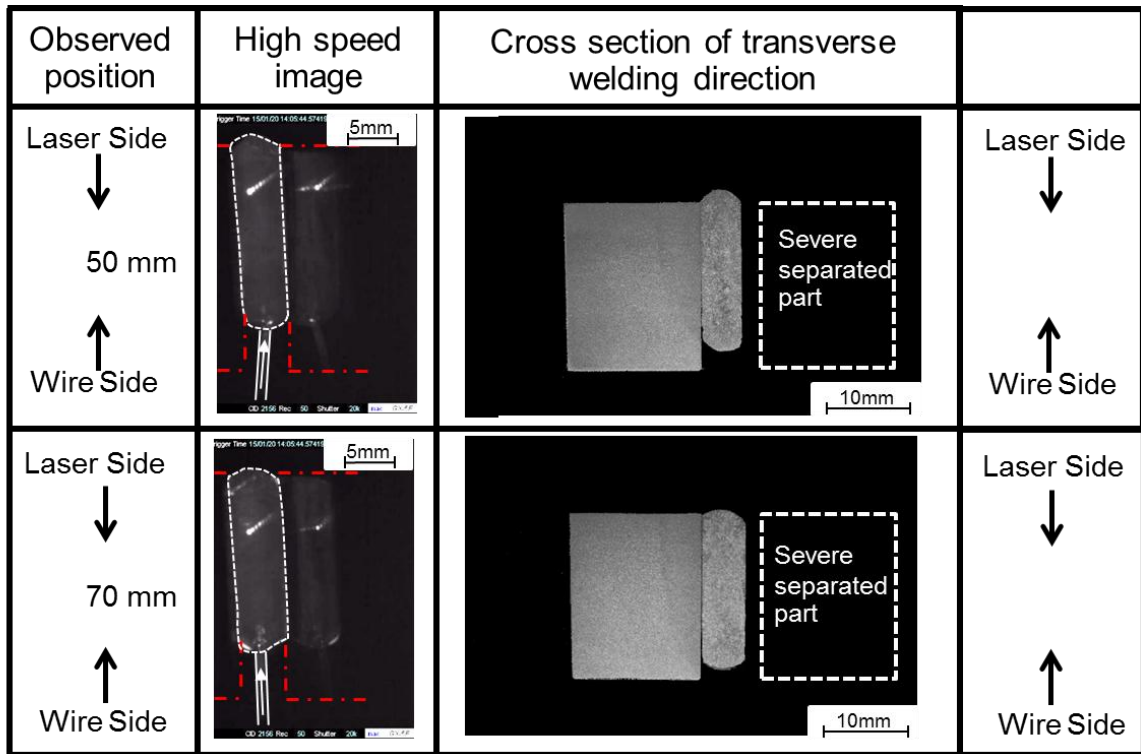
Fig. 4.8 High speed images and cross sections of joining by the stationary laser beam of 23 W/mm^2-with gap size of 5 mm x 26 mm: showed unable fusion the base metal.

Observed position	High speed image	Cross section of transverse welding direction	
50 mm			Laser Side ↓ ↑ Wire Side
70 mm			Laser Side ↓ ↑ Wire Side
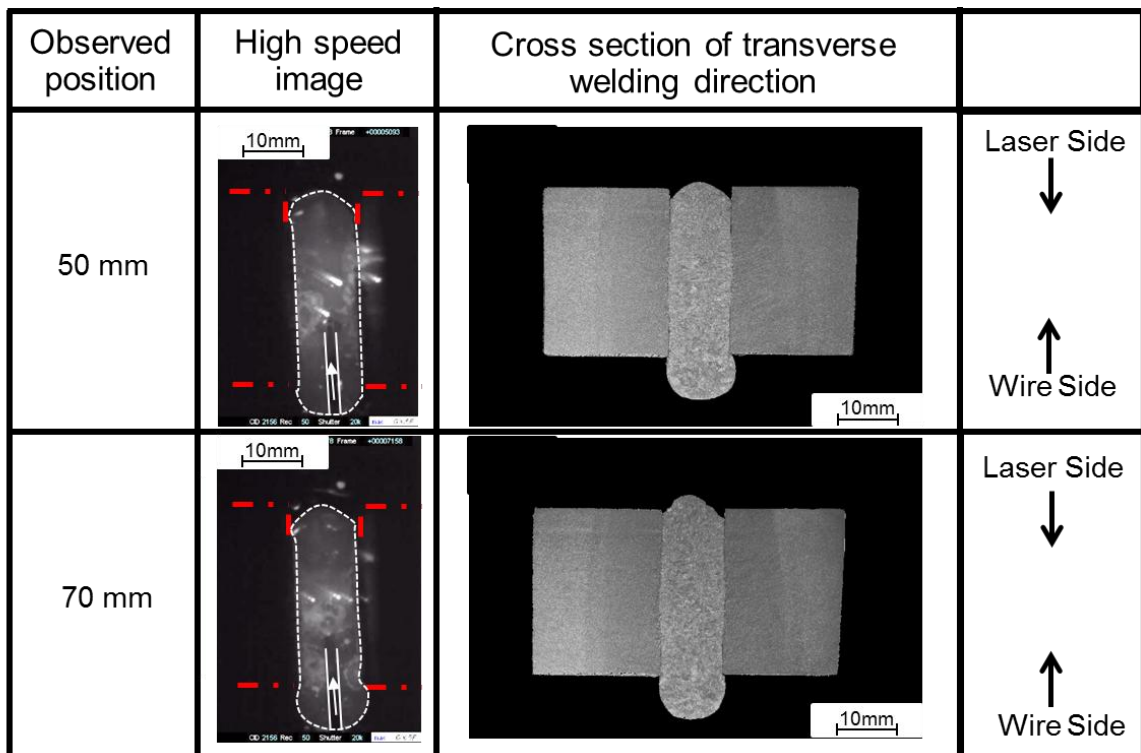
Fig. 4.9 High speed images and cross sections of joining by the stationary laser beam of 23 W/mm^2-with gap size of 10 mm x 26 mm.

In the result of the laser irradiation of 23 W/mm^2 with a relative small gap size of 5 mm x 26 mm (Fig. 4.8), it can be observed on high speed images that incomplete fulfilled weld occurred large area on wire feed side. Although the weld pool could be created stable along 180 mm weld length, average L_{fill} has only 58%. Results of the cross section showed incomplete fusion by severe separated between weld metal and base metal (L_{fusion} = 0%). It was identified that joining by laser irradiation of the lower power density than the critical value (~30 W/mm^2, result from section 3.3) could not obtain the fusion weld joint.

While joining by laser irradiation of 23 W/mm^2 with a relative large gap size of 10 mm x 26 mm which has a double volume of weld pool due to the first case show a better result. The high-speed image showed high volume deposited through large gap joint and weld pool was stable created along weld length of 180 mm even though low power density irradiated. Incomplete fulfilled weld still occurred but reverse side on the laser access side. The result of cross sections shows fusion appearance better than the case of small gap size joining. Measured results of L$_{fill}$ and L$_{fusion}$ are 88% and 68%, respectively.
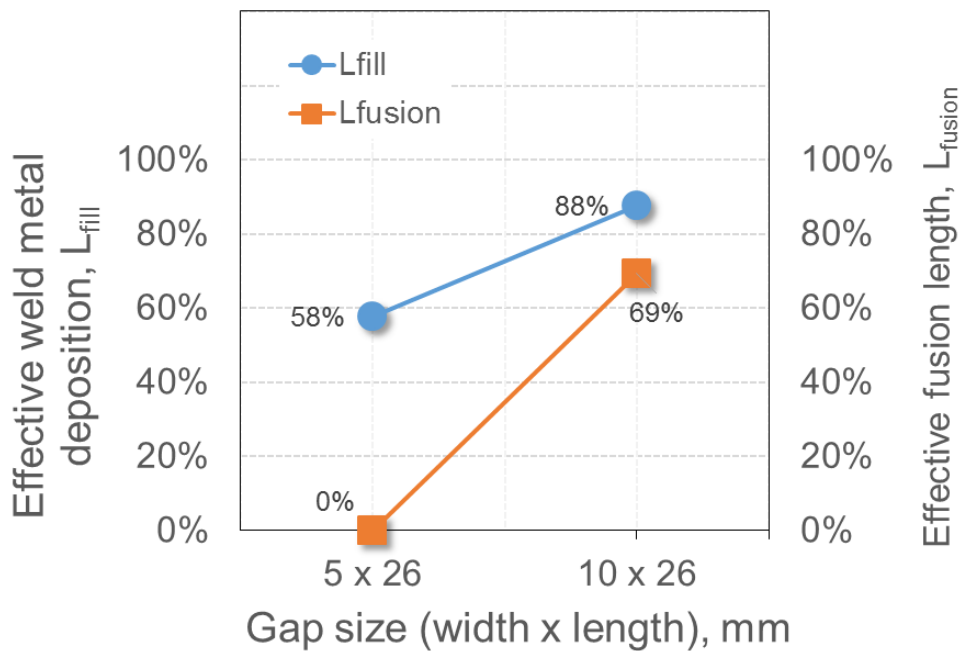
Fig. 4.10 Main effect plot

Comparison the difference melting results on different weld pool volume by the same power density irradiation can be discussed by two mechanisms of base metal melting on the proposed process. First, the initial melting on base metal by reflected laser could not occur by low power density irradiation. The result has been already proof by the first case of 5 mm x 26 mm gap size. On the other hand, the second

mechanism, the relative large volume of weld pool could obtain fusion (melting) between weld metal and base metal. The supporting theory [79-80] of the large volume of the weld pool effect on base metal phase changes can use the integral volume energy and the solid-liquid phase change to discuss the phenomena. The Large volume of the weld pool has a high accumulated energy than small volume even though they received the same level of energy input. The large volume of weld pool has a higher heat flux flow (conduction mode) through base metal thereby cause of base metal phase changes (solid to liquid) by high driving force.

The information of this experiment could be used to explain the melting phenomena of the proposed process. The initial melting of groove surface could be created by adequate laser power density. The final melting amount of base metal depends on the accumulated energy of the weld pool. Therefore, this section could be drawn sub conclusion as

1)   The level of a power density of reflected laser beam strongly affected to induce the initial melting the groove surface. The power density value must be higher than the critical value with respect to welding speed. Chapter 3, for the gap width of 5 mm, the critical value was determined for welding speed 3.33 cm/min (2m/h) as 30 W/mm^2.

2)   The main effect on the final melting amount on large gap size that depend on an amount of heat energy with depended on weld pool volume. The large weld pool size strongly affected the final melting amount of base metal.

3)   Since as using only the heat energy of liquid weld pool to joining is a low-efficiency process and it was missing the concept of the proposed process for using reflected laser energy to melts the base metal, initially.

Then, advance irradiating method by using high power density laser beam sweeps on the groove width direction to distribute appropriate energy for joining is provided. The weaving laser irradiating method is the originality for the vertical joining will be explained in the section.

4.3 Development of weaving laser irradiating method

4.3.1 Methodology and equipment

Assembly between the normal laser head and the weaving head were shown in Fig. 4.11. The normal laser head creates the large rectangular beam. The laser beam size in width dimension can be changed by changing fiber core size and focusing lens. For a length dimension of the beam can be changed by changing homogenizer lens. The large-rectangular laser beam was shoot out from the normal laser head to the weaving head and incident on weaving blade. Since the weaving blade is made of the perfect reflecting coating material, thus the laser beam is complete reflected out to the

target. The weaving blade is swept by harmonic motor for weaving the lager-rectangular beam. The harmonic motor is controlled by using harmonic generator and the controller for changing a weaving amplitude and a weaving frequency. It is noted that a limit maximum frequency for oscillating is 15 Hz.

An advanced waveform weaving control to distribute laser energy can be provided by design on specified program as AFG and connect to weaving system. To investigate the effect of waveforms and weaving frequencies will be discussed on the next part.
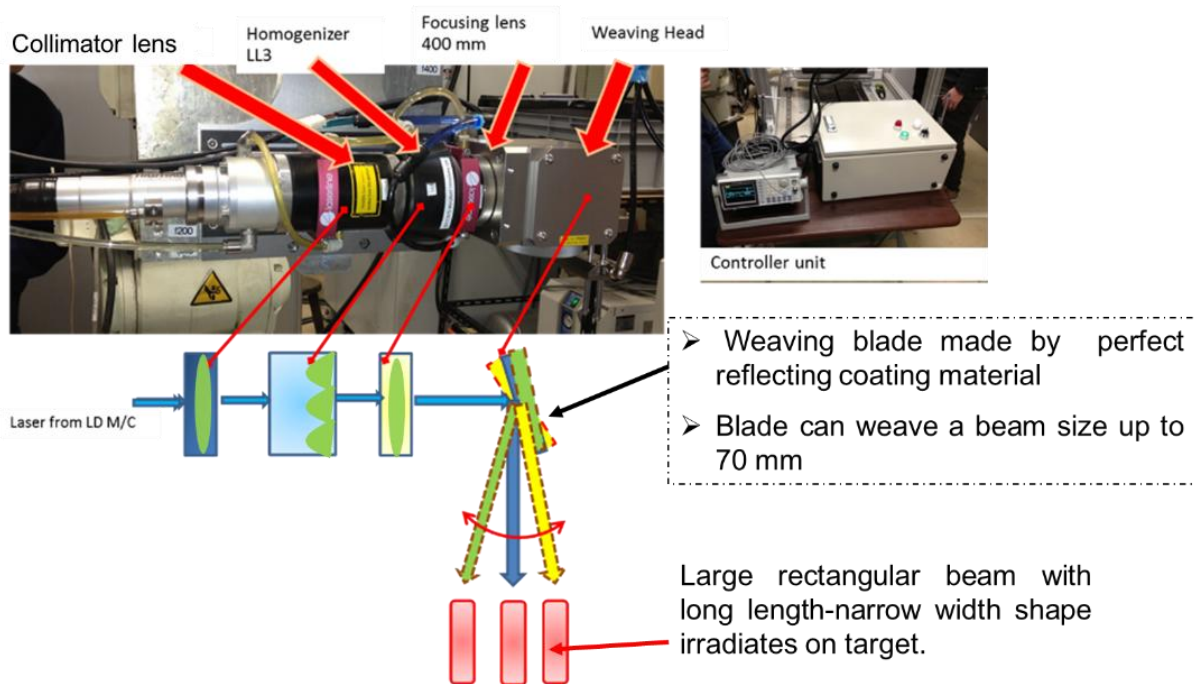
Fig. 4.11 Layout of (a) assembly of laser normal head to weaving head and (b) schematic illustration of laser weaving system

The vertical laser access is a basic studied method for the weaving laser irradiating method. The laser beam was irradiated from the top side of the specimen vertically through the joint. Fig. 4.12 shows the schematic illustration of process methodology and table 4.4 showed the welding parameters. In this basic experiment , the welding speed of 3.33 cm/min (2m/h) was used for joining.
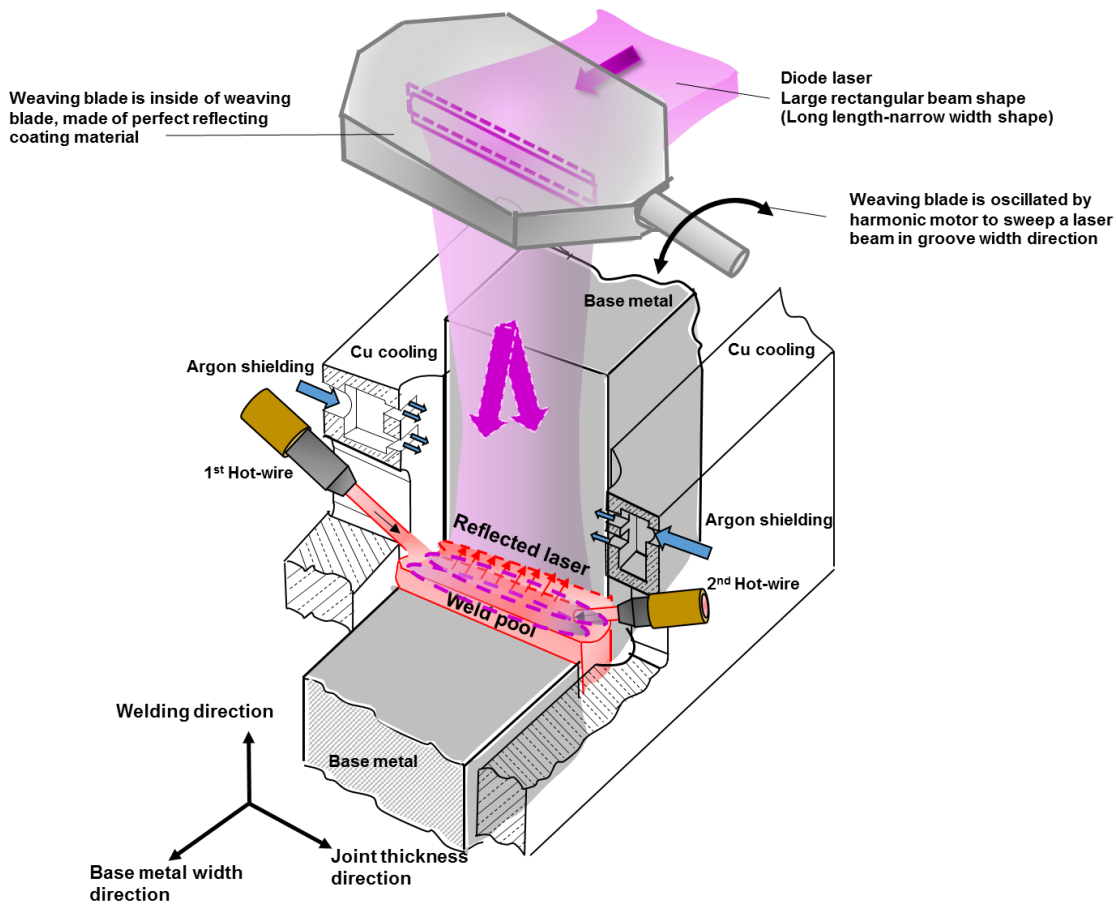
Fig. 4.12 Schematic illustration of process methodology of the weaving laser irradiating method by vertical laser access with 2 hot-wires feed.

4.3.2 Effects of weaving frequency and waveform

This experiment used 2 types of waveforms to study. Sine wave and exponential wave are investigated. Frequencies of 5 Hz and 15 Hz are investigated to obtain the effect on periodically reflected laser heating on groove surface. In case of lower frequency, such 2.5 Hz was not considered because too low repetition rate that would affect heat conduction loss for wide gap size. It this section, study has been emphasized the time interaction on groove wall region more than the center region of the groove. Effects of welding parameters on the weld metal deposition and the fusion length along groove wall were investigated.

Firstly, Characteristics of waveforms versus frequencies were measured the oscillating signal from the PCD's box. Fig. 4.13 (a), (b), (c) and (d) showed waveforms versus frequency of (a) 5 Hz-sine wave, (b) 15 Hz-sine wave, (a) 5 Hz-exponential wave, and (c) 15 Hz-exponential wave, respectively, as a function of time. Interaction time data for each weaving condition were also showed in table 4.5.

Table 4.4 Welding parameters for the weaving laser irradiating method by vertical laser access with 2 hot-wires feed.

Weaving method	See in the details
Fiber core, mm	0.4
Homogenizer	LL3
Focus lens, mm	400
Laser power, kW	6
Laser irradiation angle, degree	90°
Defocus, mm	20
Spot size, mm x mm	2^w x 27^l
Power density, W/mm^2	111
Filler wire diameter, mm	1.6
Welding speed, cm/min (m/h)	3.3 (2)
Wire feed speed, m/min	1.24
Wire current, A	93
Wire feeding angle, degree	45
Wire feeding position, mm	0
Shielding gas (Argon), LPM	20
Pre irradiation time, s	120

Table 4.5 Interaction time for typical waving conditions

Weaving waveform	5 Hz				
	1 cycle	Interaction time on groove wall	For 1 s	Interaction time on middle zone	For 1 s
	ms	ms	ms	ms	ms
Sine wave	200	34	170	132	660
Exponential wave	200	72.5	362.5	55	275
Weaving waveform	15 Hz				
	1 cycle	Interaction time on groove wall	For 1 s	Interaction time on middle zone	For 1 s
	ms	ms	ms	ms	ms
Sine wave	66.67	11.5	172.5	44	660
Exponential wave	66.67	25	375	17	255
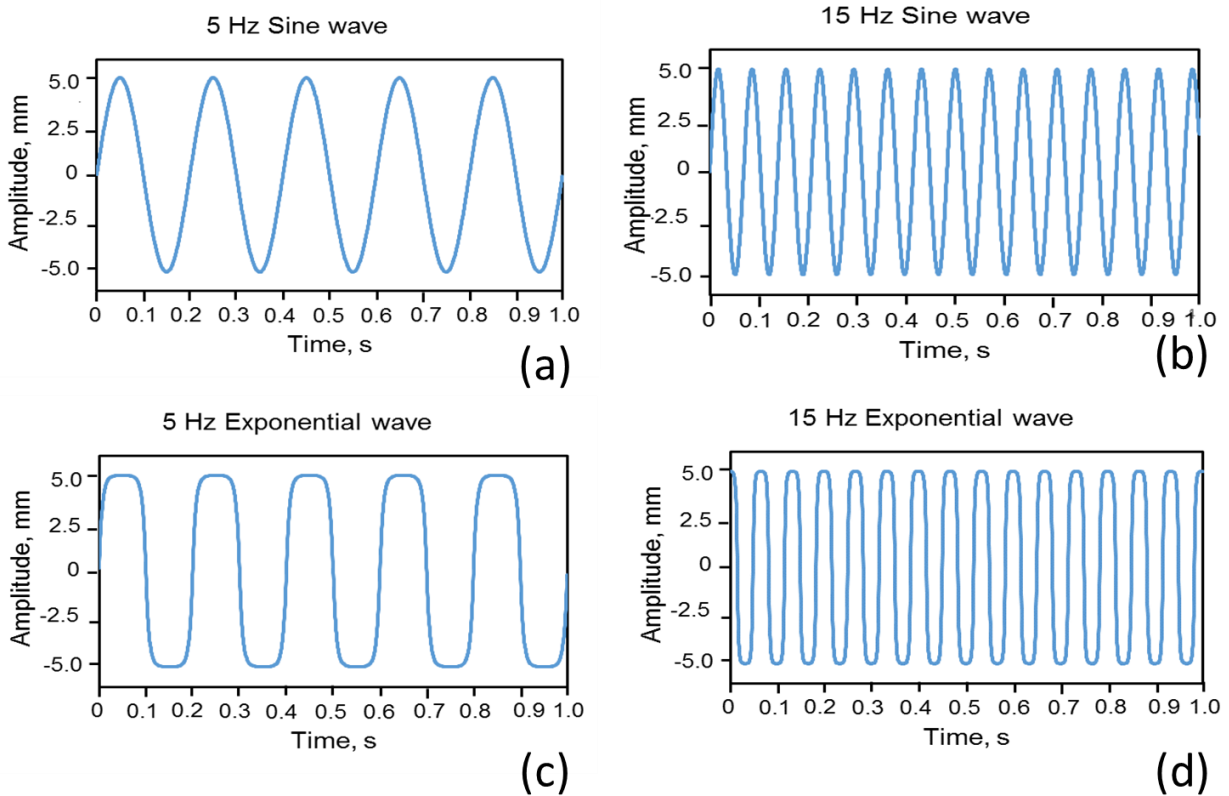
Fig. 4.13 Wave forms were obtained from the PCD's signal during weaving motor oscillating by wave from versus frequency of (a) 5 Hz-sine wave, (b) 15 Hz-sine wave, (a) 5 Hz-exponential wave, and (c) 15 Hz-exponential wave,
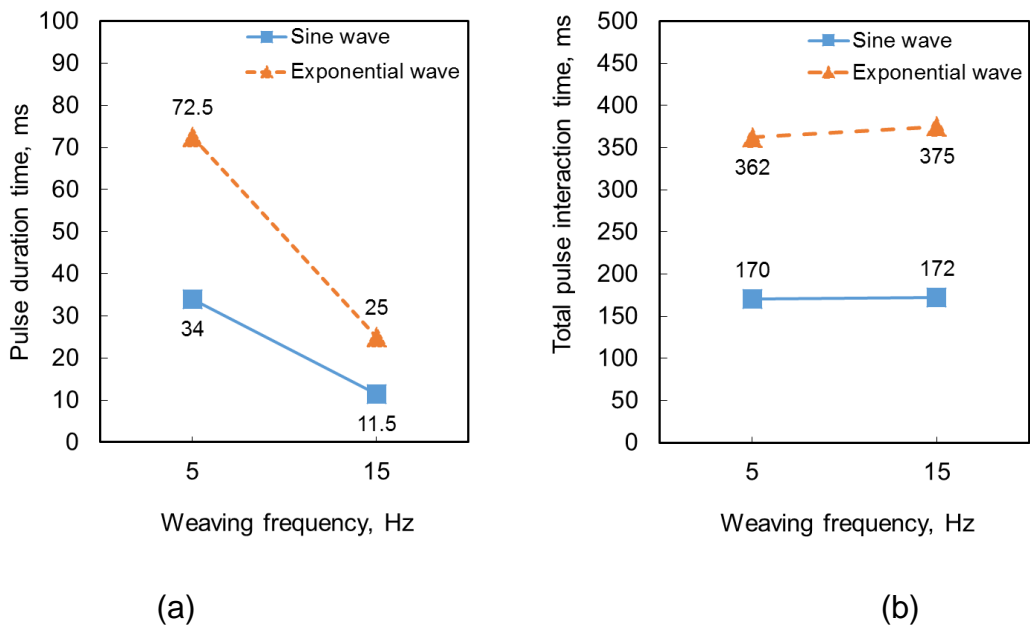
Fig. 4.14 plot of (a) pulse interaction time and (b) total interaction time (1 s) as a function of weaving frequency and wave form.

In order to clarify the effects of the waveform and weaving frequency, preliminary analysis of pulse duration time is discussed for select appropriate parameters. Table 4.5 showed the numerical data and Fig. 4.14 showed the differences of duration time as a function of frequency and waveform. On the Fig. 4.14 (a), it was shown that 15 Hz- exponential has no large differences of the weaving pulse duration time compared with 5 Hz-sine wave. On the Fig. 4.14 (b) showed the total interaction time on 1 second for weaving. The exponential waveform has longer total interaction time than that of a sine wave. Moreover, J.T. Lui and D.C. Wu [80] had investigated and evaluated the effect of pulse duration, it strongly affected the melting efficiency. It was summarized by the basis that pulse interaction time per round was considered rather a total pulse interaction in 1 second. Thus, 5 Hz-exponential, 5-Hz sine, and 15 Hz-sine which have a difference interact time were selected for the present study.

The pulse duration time on groove wall (tp) of 72.5, 34 and 11.5 ms were parameter of 5 Hz-exponential, 5-Hz sine, and 15 Hz-sine, respectively.

Fig. 4.15 shows the sections on horizontal direction (transverse welding direction), vertical direction (parallel welding direction) and microstructure on fusion boundary on the vertical cross section. They were cut at middle zone of welded specimen as a quasi-steady state. The results showed that the weaving laser irradiating method on relative larger gap size has a good potential for joining. By observation on the horizontal cross section, the weaving waveform and frequency have affect weld metal fulfill and melting morphology. 5-Hz exponential has a better result of the weld metal fulfill than others weaving conditions. The vertical cross section which were cut at the middle of joint thickness by macro scale showed the perfect fusion all of the specimens. However, high magnified investigation, microstructure on fusion boundary for all conditions obtained from vertical cross section show lack of fusion occurred on the joining by short period of weaving pulse duration time of 11.5 ms (5 Hz-sine) and 34 ms (15 Hz-sine). On the other hand, result of a long period of weaving pulse duration time of 72.5 ms (5 Hz-exponential) showed a complete fusion.

Results of measured fulfill percentage and fusion percentage were shown in Fig. 4.16. The method of measurement of L_{fill} and L_{fusion} have been defined as equation (4.1) and (4.2). Under the condition of tested weaving frequencies, when the pulse duration time at the groove surface increases, effective weld metal deposition not different significant (L_{fill} average of 82%) but effective fusion length increased. By controlling pulse interaction time of 72.5 ms (5 Hz-exponential wave) complete fusion over available weld deposited length was obtained. On the other hands, using sine wave for weaving has lower effective fusion of welded joint. Therefore, it was hereby the study effect of weaving frequency and waveform, optimization weaving frequency and waveform is the condition of 5 Hz-exponential wave.

Frequency (Hz) – wave form		
15 Hz-sine	5 Hz-sine	5 Hz-exponential
Weaving pulse duration time, msec		
11.5	34	72.5
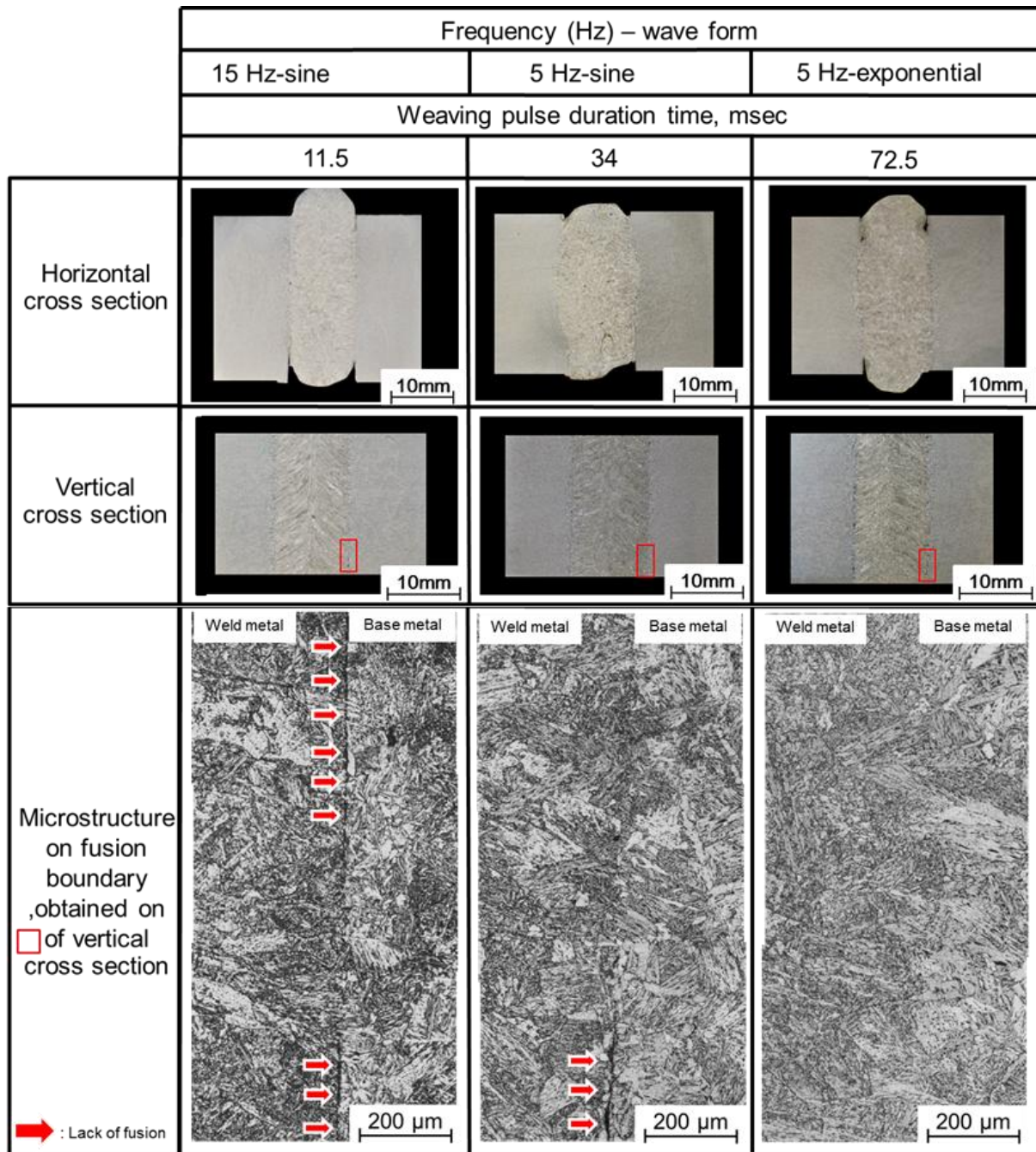
Fig. 4.15 Investigated sections of welded specimens
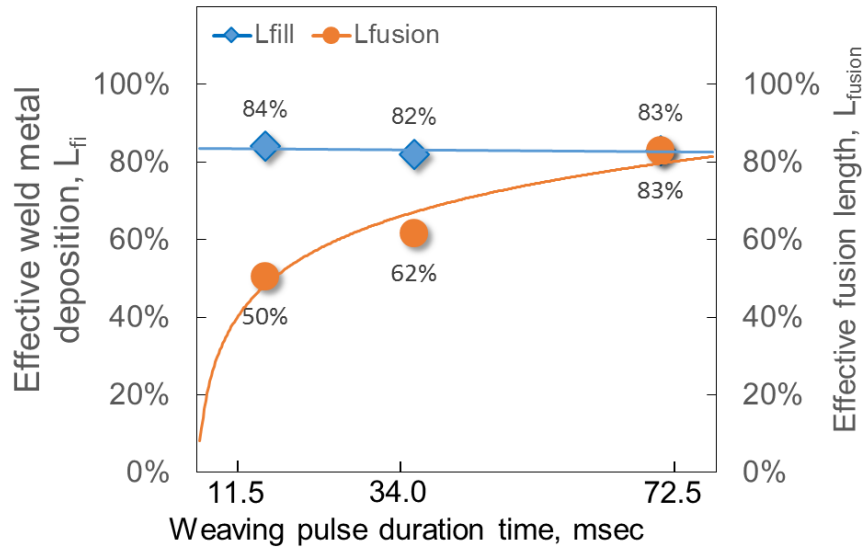
Fig. 4.16 Effect of weaving pulse duration time on effective weld metal deposition and effective fusion length.

4.4 Oblique laser irradiation technique and effect of irradiating angle

In preliminary experiment of using the proposed process, the welding was done by utilizing laser irradiation in vertical access through groove weld and with hot wire fed from two sides of the groove weld. It yielded weld with complete melting. Nevertheless, the aforementioned method is merely basic originality idea. In practical applications, it may be necessary to irradiate the joint with laser from the side of the joint, which has the benefit of less adjusting of the laser source and beam. The problem of obstacles or obstruction of laser beam can also be minimized, moreover, the filler metal needs to be fed from only one side. This section presents the idea of how to gain access for laser to the joint from the side. This can be achieved by tilting the laser irradiator so that it focuses and yields beam size that is suitable for the joint. The welding was done under higher power density than the critical value reported in the previous chapter.

The objective of this section is to investigate the effect of laser access method, consisting of vertical laser access with 2 hot wires and oblique laser access with 1 hot wire, and the effect of irradiating angle (tilt angle of laser head). Both laser access method used the heating by weaving laser irradiating method. In the final comparison the effect and the result of investigation of the weld in macro scale is done, with imperfection and weld penetration as the quantitative comparisons.

4.2.1 Material and specimen used

KE-47 steel plates were used in this study, Fig. 4.17 shows the dimension of specimen. The dimension of specimen was 50 (width) x 100 (height) x 26 mm (thickness). Plates were fixed and aligned as a vertical joint configuration. The gap width was set by spacer (dimension of 10 (width) x20 (height) x 26 (thickness)). The filler metal of YM-1N (JIS Z 3325 YGL2-6A (AP)) with diameter of 1.6 mm was used. The chemical composition of base metal and filler metal were presented on Table4.6.
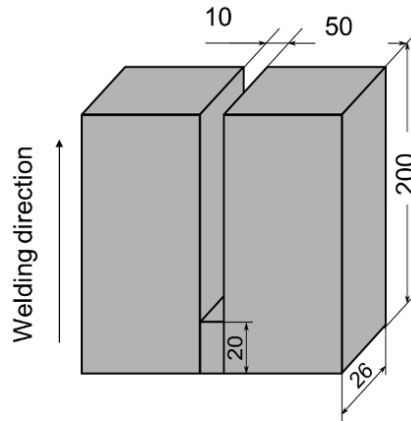
Fig. 4.17 Specimen dimension used for hot-wire laser welding shows configuration of vertical joint alignment.

Table 4.6 The chemical composition of base metal and filler metal

Material	Chemical Composition, wt%											
	C	Si	Mn	P	S	Al	Cu	Ni	Nb	Ti	Cr	Mo
KE-47	0.09	0.07	1.52	0.007	0.002	0.014	0.32	0.69	0.01	0.01	0.02	0.00
YM-1N	0.04	0.46	1.35	0.01	0.007	-	0.17	1.07	-	0.7	-	0.26

4.4.2 Welding process, laser access method and welding parameters

The methodology of the proposed process is shown in schematic layout of joint configuration and apparatus in Figure 4.18: the vertical laser access with 2 hot wires is shown in Figure1.8 (a) , and oblique laser access with 1 hot wire is shown in Figure 4.18 (b). The joint configuration is rigged in vertical alignment. Groove configuration is square butt joint for welding with single pass weld.

The laser equipment used as a power source was Laserline LDF 6000-40 (6.0 kW) continuous wave (CW) Diode Laser (LD). It was assembled with colliminater lens of 100mm, focus lens of 400mm, and fiber diameter of 400mm. The resulting laser

beam has a rectangular beam shape with long-length narrow-width dimension. The spot size will be discussed in the next section. Hot wire was used in the proposed process to improve the efficiency of deposition. The hot-wire system used was Hitachi Power Assist HI-TIG series IV662. It generates current and passes it into and heats up the filler wire in the process known as Joule heating. The filler wire is heated up to the temperature near the melting point.
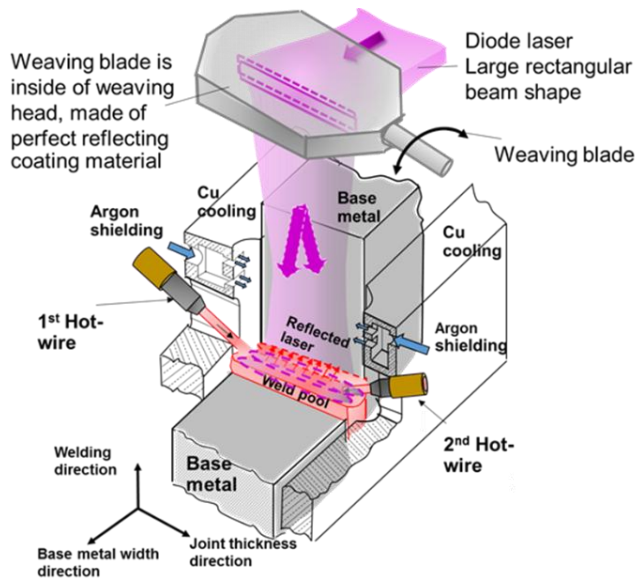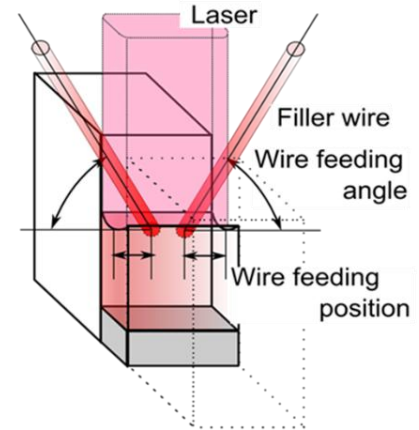
Schematic of laser access   Parameter setup definition

(A) Vertical laser access-with 2 hot-wires
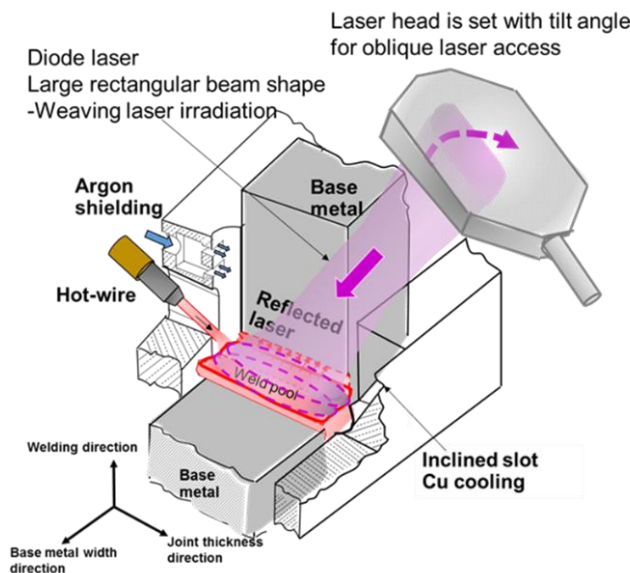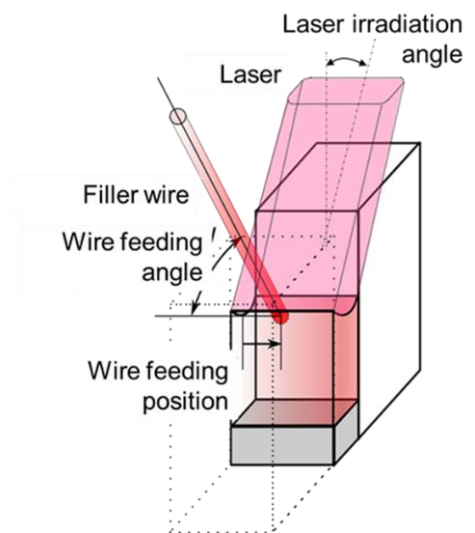
Schematic of laser access   Parameter setup definition

(B) Oblique laser access-with 1 hot-wire method

Fig.4.18 Schematic layout of joint configuration and parameter setup of the hot-wire laser method.

Welding parameters of 2 laser access methods were presented in Table 4.7. The studied parameter is laser irradiating angle. The effect of tilt angles of 0, 15 and 30 degree are investigated. For 0 degree of laser irradiation, vertical laser access with 2 hot wires was employed as shown schematic in Fig. 4.18 (a) and the parameter definition is also shown in Fig. 4.18 (a). For 15 and 30 degree of tilt angle are oblique laser access-with 1 hot wire and it was shown its schematic of method in Fig. 4.18(b).

The weaving frequency and weaving waveform in this study was 5 Hz-exponential waveform. Fig. 4.19 shows the time-distance characteristic of the exponential wave in one cycle. By weaving distance of 10 mm, the holding time of laser near groove surface is 72.5 ms for frequency of 5 Hz and time for moving through other side is only 27.5 ms. It is advance supply reflected laser to get appropriate heat energy through the base metal side during holding time and appropriate repetition rate on weld pool center can keep liquid weld pool during continuous welding.

The parameters of vertical laser access with 2 hot-wires (Figure 4.18 (a)) are shown in Table 4.7. The welding process, which is the basic idea of this research, irradiates the joint with laser from above with laser spot size of 5.0 mm width and 30 mm length. The laser power used is 6kW. The resulting power density is 40 W/mm^2, which exceeds critical limit stated in the chapter 3. The experiment of vertical laser access was done to investigate the effect of welding speed at 3.33 cm/min (2m/h). Filler metal is fed from hot-wire torches from both 2 sides of the joint. The hot wire torches is set inside with copper cooling shoes. The distance of wire feeding and the feeding angle was set at 2mm and 45°, respectively. During the welding, the atmosphere above the molten pool is shielded with argon gas at the flow rate of 10 l/min.
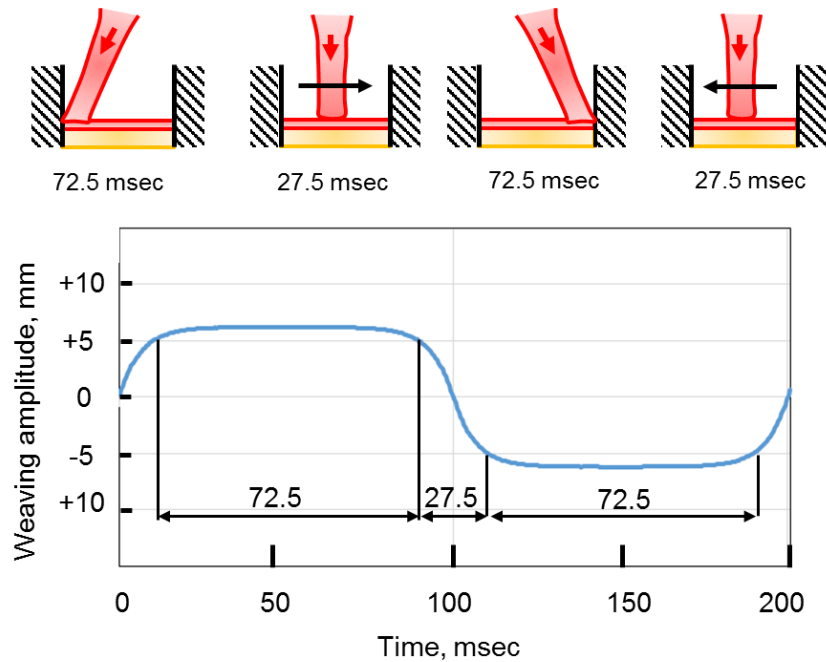
Fig. 4.19 Time characteristics of the exponential-wave 5 Hz weaving method, shows one cycle.

In oblique laser access-with 1 hot wire (Figure 4.18 (b)), the parameters used are shown in Table 4.7. This welding process is the main objective of this study. The laser is irradiated from the side of the joint with laser source angle from vertical reference axis. Two laser source angle of 15°, 30 °are studied. The laser beam parameter as same as the vertical laser access method. For this part, the copper cooling shoe on the laser side is designed to be angled for transmitting laser into joint target. For comparison purpose, the laser spot size, laser power, and power density used are the same as vertical laser access with 2 hot wires process. The hot-wire parameter was showed in Table 4.7.

Table 4.7 Welding parameters of the 2 method of laser access methods.

Laser access method	Vertical	Oblique	
Laser irradiation angle, degree	**0**	**15°**	**30°**
Laser irradiation type	Weaving 5 Hz exponential wave		
Fiber core, mm	0.4		
Homogenizer	LL3		
Focus lens, mm	400		
Laser power, kW	6		
Defocus, mm	80		
Spot size, mm x mm	5^w x30^l		

Power density, W/mm^2	40	
Hot-wire feed numbers	**2-wire**	**1-wire**
Welding speed, cm/min	3.3	
Wire feed speed, m/min	2.48	4.98
Wire current, A	155	181
Wire feeding angle, degree	45	30
Wire feeding position, mm	0	10
Shielding gas (Argon), LPM	20	
Pre irradiation time, s	120	

4.4.3 Methodology for evaluation of weld joint characteristics

The imperfection level and bead width of the weld from the aforementioned experiment were evaluated in the horizontal cutting plane which is perpendicular to the welding direction. The cutting plane are shown in Fig 4.20. The position to be cut was selected at the area showing steady state behavior. The cut was then polished and etched with 3% nital acid for weld characteristics to be visible.

The width of the weld bead was measure on every 2 mm distance along joint thickness. Imperfection will be recorded to show its occurring position. The effect of laser irradiating angle will be plot versus result of weld bead width and accumulated imperfection.
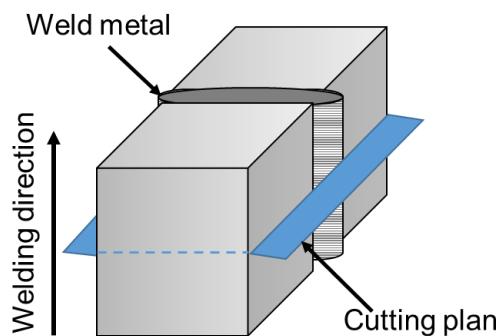
Fig. 4.20 Cutting plan layout and section definition

4.4.4 Effect of laser irradiating angle

Figure 4.21 shows macro cross-sectional observation of welded joints in the horizontal direction on different laser irradiating angle. When the laser irradiating angle was 0°, the rectangular laser beam was irradiated vertically from the top of the specimen and double hot-wires fed from both sides of groove. When the laser irradiating angle was 15° and 30°, the rectangular laser beam was irradiated obliquely from the side of groove (upper side in Fig. 4.21) and single hot-wire fed from the

opposite side of groove (lower side in Fig. 4.21). The accumulated imperfection ratio was also shown in Fig. 4.21. From observations of macro cross-sections, all joints have imperfections occurred at joint edge regions of groove. On the other hands, the inside of welded joint shows complete fusion with low dilution and uniformity of fusion lines when the laser irradiating angle is 0˚ and 15˚.
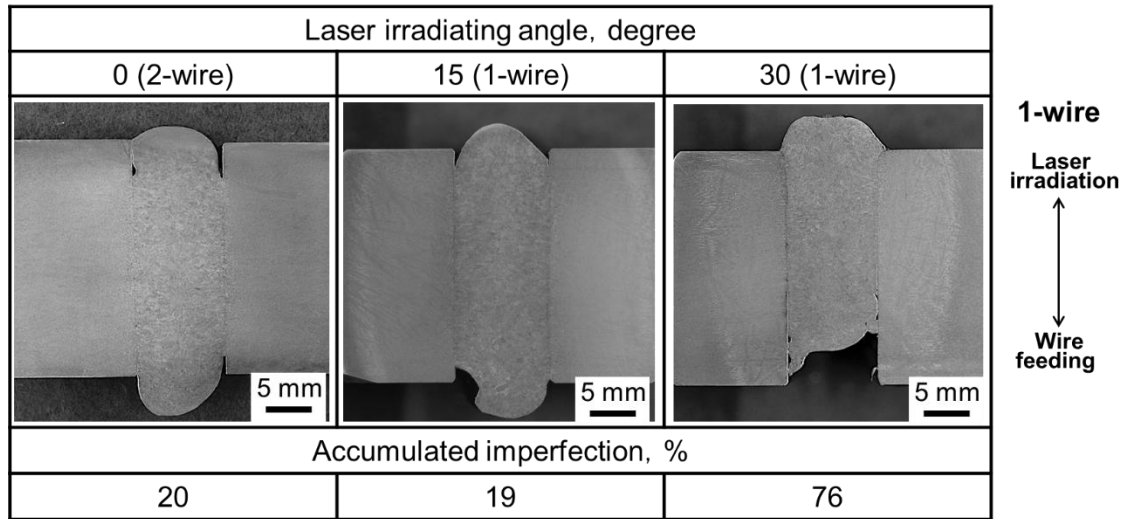
Fig. 4.21 Horizontal cross section (Perpendicular cut of welding direction)

Firstly, in comparison between 0˚ and 15˚ of laser irradiating angle, it is clear from Fig. 5 that there is not significant difference of bead shape, imperfection ratio. It is also clear that the filler wire feeding method, double hot-wires feeding and single hot-wire feeding, does not strongly affect on weld bead formation and base metal melting. It can be noticed that the oblique laser irradiation with single hot-wire feeding can be used for single-pass vertical joining.

Next, in comparison between 15˚ and 30˚ of laser irradiating angle, it is clear from Fig. 5 that severe incomplete fulfill of weld metal and large imperfection occurs on the wire feeding side of groove when the laser irradiating angle is 30˚. It can be noticed that the oblique laser irradiation with relatively large angle affects obviously on molten pool and weld bead formations, and base metal melting. In other words, too large laser irradiating angle causes severe imperfections (incomplete fulfill of weld metal and luck of fusion), therefore relatively small laser irradiating angle should be applied for the proposed hot-wire laser welding process.
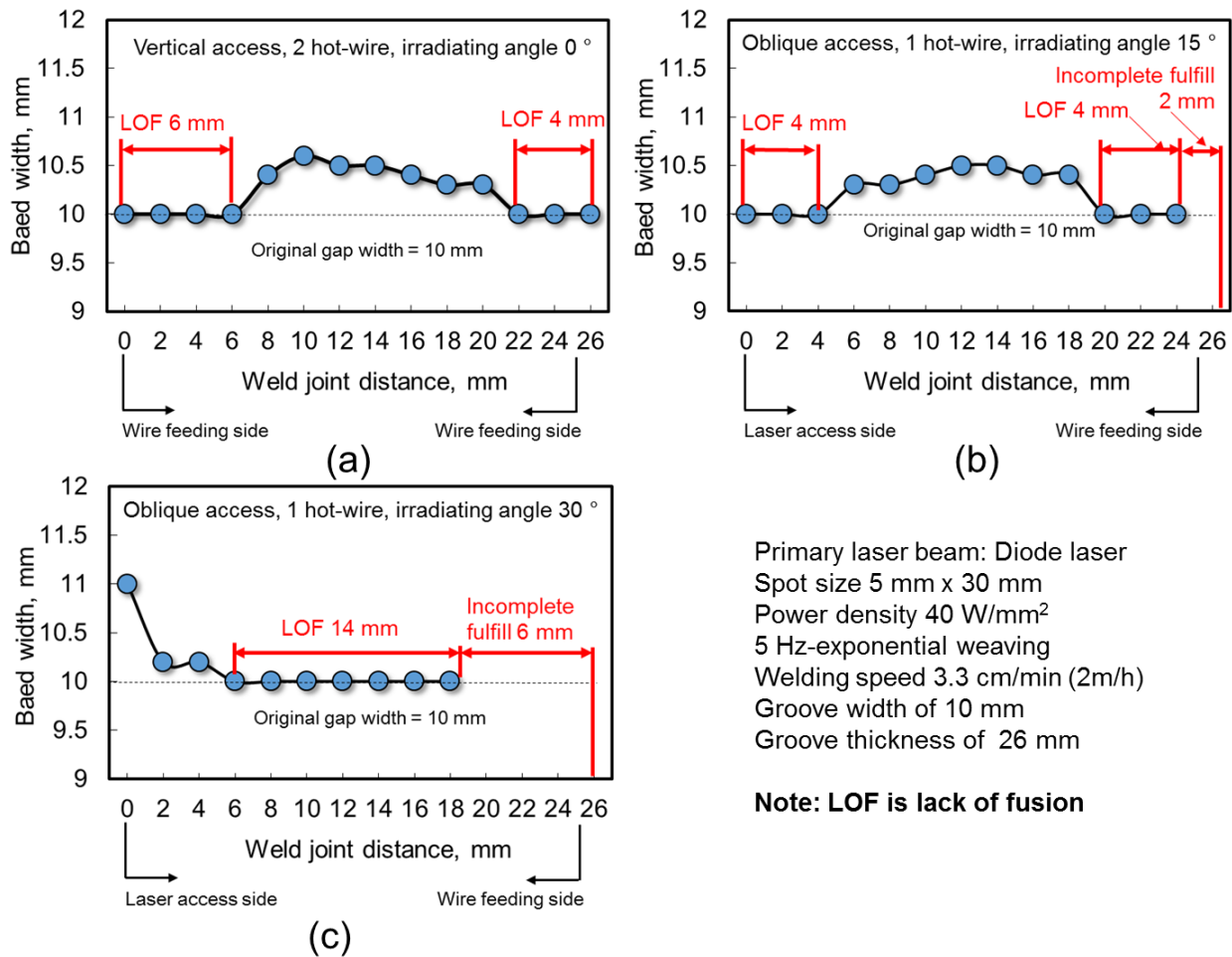
Fig 4.22 Measured results of the width of the weld bead and imperfection size on the horizontal cross sections.

Measured results of the width of the weld bead and the imperfection size were shown in Fig. 4.22. Fig 4.22 (a) is result of irradiating angle of 0 degree (Vertical). Lack of fusion on the both sides of the groove which have accumulated size of 10 mm. The maximum width of bead is 10.6 mm occurred at middle of the joint thickness. Fig 4.22 (b) is result of 15 degree irradiating angle (Oblique), it has almost the same result of irradiated by angle of 0 degree. Accumulated size of imperfection is 10 mm but has a different characteristic. Incomplete fulfill with length of 2 mm had occurred at the wire feeding side and then lack of fusion occurred. The tendency of incomplete fulfill was increased when irradiating angle increasing to 30 degree as showed in Fig. 4.22 (c). It has incomplete fulfill length of 6 mm at the wire feeding side. Moreover, irradiating angle of 30 degree has a poor result of base metal melting. Because the result of 30 degree irradiation showed a long length of lack of fusion up to 14 mm and has a small bead size.

The effect of laser irradiating angle on vertical joining ability was summarized by Fig. 4.23.The average bead width and accumulated imperfection were plotted as a

function of laser irradiating angle. It could be summarized that irradiating by tilt angle of the laser head between 0 degree to 15 degree can obtain a good weld result. Accumulated imperfection of 20 % was resulted from the effect of low laser energy of especially on the edge of the laser beam. New optical homogenizer to provide high energy on the edge sides need to design to achieve the sound weld. As for improvement of base metal melting amount or more weld penetration, the possible ways by increasing power density or optimize the laser beam parameters, can be considered. In case of laser irradiating angle more than 15 degree is improper condition because it contains large size of imperfection up to 79%.

For discussion on the practical perspective, 15 degree is the optimized and realized condition for joining as regardless for the height of the weld joint. Since as the laser head can be set on out of plate alignment. It has no obstruction during process operation. From this study, it was identified that the proposed process has a flexibility of laser beam access through the joint gap, practically.
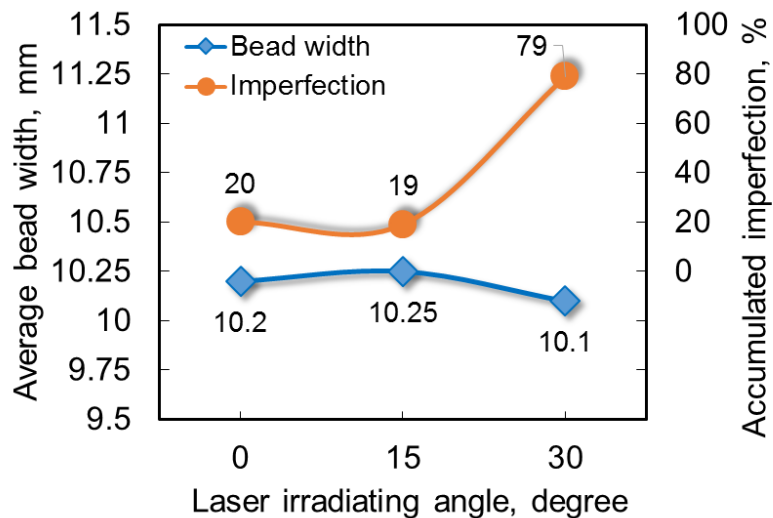
Fig. 4.23 Average bead width and accumulated imperfection as a function of laser irradiating angle.

4.5 Investigation of the reflected laser creates the melting on groove surface during weaving laser irradiating method

This experiment has an objective for verifying that the reflected laser beam of high power density during weaving could create melting on groove surfaces. The experimental result of section 3.2 showed clear phenomena of groove wall melting, same methodology was performed in the case of weaving. In-situe observation by a high speed camera with 810 nm band pass filter provides laser weaving phenomena.

Two spot sizes of laser beam were used for modulation of power density in order to investigate the effect of power density on the initial melting depth.

4.5.1 Material and specimen used

KE-47 steel plates were used in this study, the dimension of specimen was 100 (width) x 50 (height) x 26 mm (thickness) is shown in Fig. 4.24. Plates were fixed and aligned as a vertical joint configuration. The specimen was slot by dimension 10 mm (width) x 30 mm (depth) x 26 mm (length) to simulate a groove joint. The filler metal of YM-1N (JIS Z 3325 YGL2-6A (AP)) with diameter of 1.6 mm was used. The chemical composition of base metal and filler metal were presented on Table 4.8.
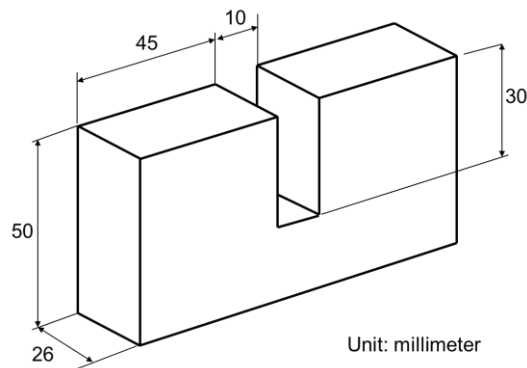
Fig. 4.24 Specimen dimension

Table 4.8 Chemical composition of specimen and filler wire

Material	Chemical Composition, wt%											
	C	Si	Mn	P	S	Al	Cu	Ni	Nb	Ti	Cr	Mo
KE-47	0.09	0.07	1.52	0.007	0.002	0.014	0.32	0.69	0.01	0.01	0.02	0.00
YM-1N	0.04	0.46	1.35	0.01	0.007	-	0.17	1.07	-	0.7	-	0.26

4.5.2 Experimental procedure

Welding parameters were shown in Table 4.9 and a schematic layout of the experiment was shown in Fig. 4.25. The laser beam was irradiated from the top side of the specimen. The weaving laser irradiation was employed for investigation. A 5 hz-exponential waveform which optimized from previous section was used for the study. In this experiment, the effect of power density was studied by changing laser beam width size. Changing fiber core size, beam spot width was changed. Fiber core size 0.4 mm and 1.0 mm created beam spot size of 4 x 27 and 2 x 27 mm, respectively, under setting the homogenizer of LL3 and the focusing lens of 400 mm. The laser spot

size of 4 x 27 and 2 x 27 mm have power density of 55 W/mm^2 and 111 W/mm^2 nnder 6 kW laser power irradiation.

1 Hot-wire was used and set its parameters range depending on welding speed 3.33 cm/min (2 m/h). In this experiment, instantaneous laser irradiation was performed to avoid the effect of heat accumulation. Then the pre-irradiation time of 5 seconds and hot-wire feeding 20 seconds is the period for joining.
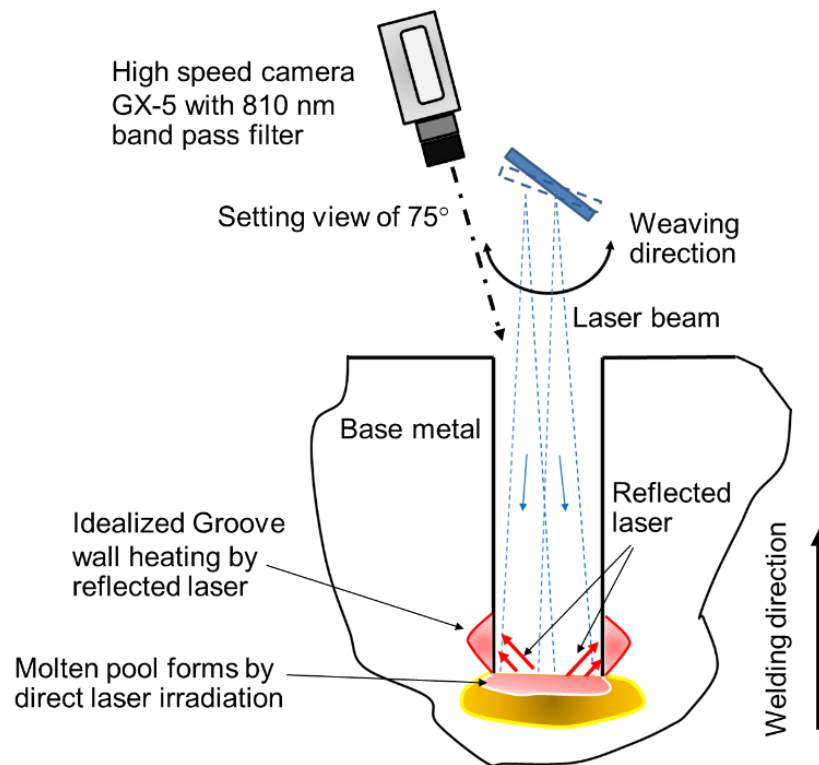
Fig. 4.25 Schematic lay out of process methodology and monitoring setup of high speed camera

Optical processing for capturing of welding phenomena was done with a high-speed camera. Pencil camera V-193-M1 model connected with NAC: MEMRECAM GX-5 module was used with, a focus lens 50 mm with a diameter of 25 mm, 810 nm band pass filter. The capturing parameter is the frame rate of 50 fps, the shutter speed of 1/20000 s and an aperture is closed. Table 4.10 shows the monitoring condition. In order to see the melting phenomena on the groove wall surface, the camera was set perpendicular on groove wall in the horizontal axis and 75° from weld pool plan.

Table 4.9 Welding parameters

Laser irradiation method	Weaving 5 Hz-exponential wave	
Fiber core, mm	1.0	0.4
Homogenizer	LL3	LL3
Focus lens, mm	400	400
Laser power, kW	6	6
Laser irradiation angle, degree	15°	15°
Defocus, mm	20	20
Spot size, mm x mm	4^w x 27^l	2^w x 27^l
Power density, W/mm^2	55	111
Filler wire diameter, mm	1.6	1.6
Welding speed, cm/min	3.3	3.3
Wire feed speed, m/min	5.31	5.31
Wire current, A	181	164
Wire feeding angle, degree	45	45
Wire feeding position, mm	5	5
Shielding gas (Argon), LPM	10	10
Pre irradiation time, s	5	5

Table 4.10 High speed camera and apparatus condition

High speed camera	GX-5
Frame rate, fps	50
Aperture	Closed
Focus lens, mm	500
Band pass filter, nm/FWHM	810 / 10
Lighting	N/A
Shutter speed, s	1/20 k

4.5.3 Welding phenomena on groove wall heating by instantaneous laser irradiation

Fig. 4.26 and 4.27 show the melting phenomena using weaving laser with the condition of 2 x 27 mm spot size. The high-speed image shows the achievement of detection of groove wall (one side) and groove bottom, clearly. During the pre-irradiation period (without feeding) laser swept along the width direction of the groove. There are three major steps in the exponential wave weaving as laser moving to groove surface, laser holds on groove surface (duration 72.5 ms per cycle) and laser moving out from groove surface. The weaving distance was set at 9.5 mm, it was slightly narrower than the groove width size. The only the reflected laser could heat on the groove surface. In a period of 1 second pre-irradiation that show during laser beam hold near groove surface, they showed that birthing color on groove surface and became dark when laser beam moves out from groove surface. Longer irradiation time of 5 s period shows a larger area and residue heating zone when laser move out. One specimen with only laser irradiation without feeding was obtained to investigate the transformation on the groove surface. It will be discussed on the next part.

	Laser moving to groove surface	Laser holds at the groove wall	Laser moving out from groove surface
High speed image time period 1 s (pre irradiation)			
Schematic illustration			
High speed image time period 5 s (pre irradiation)			
Schematic illustration			
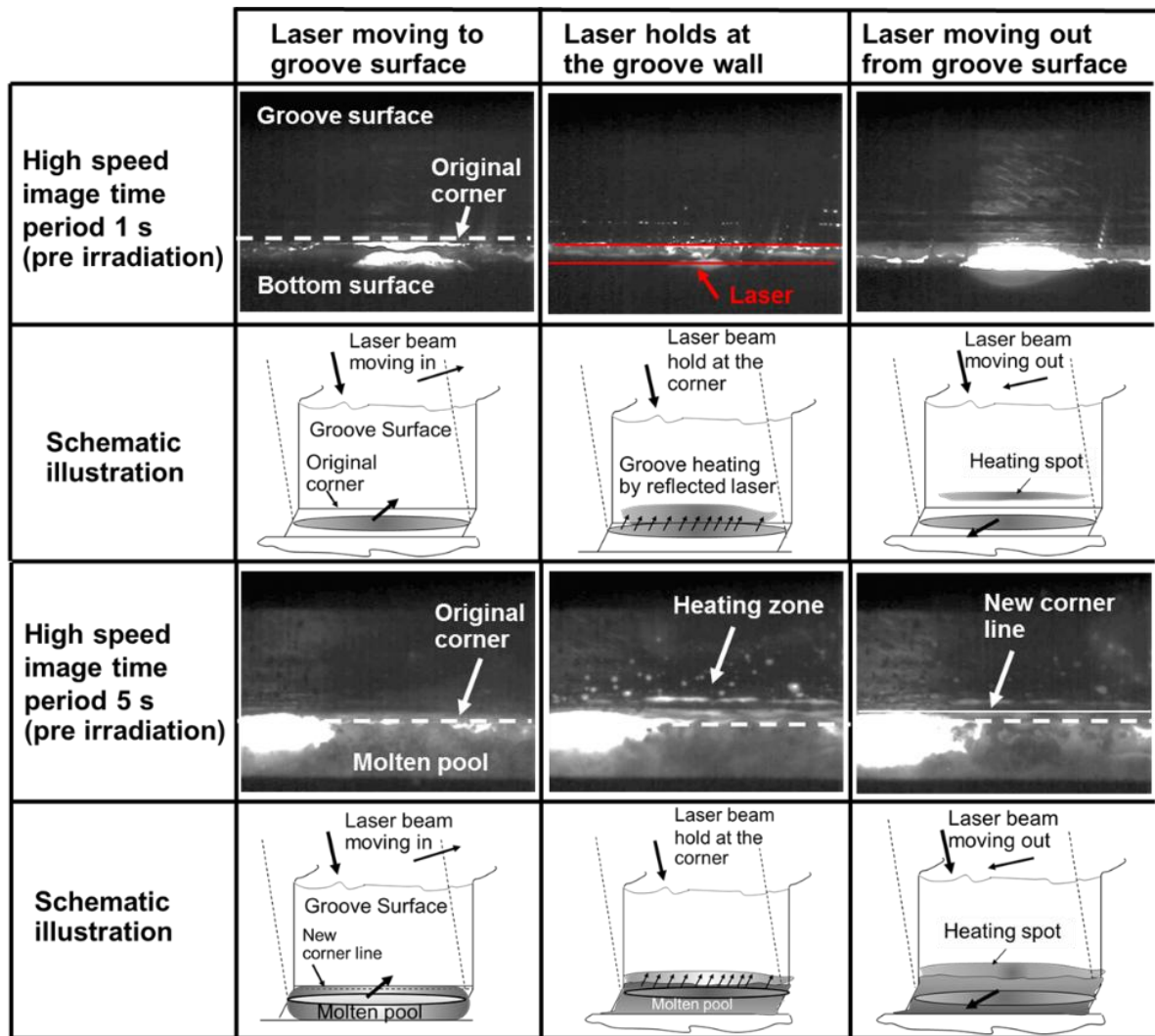
Fig. 4.26 High speed image results of weaving laser irradiation (Pre irradiation)

Fig. 4.27 shows the melting phenomena during hot-wire feeding and specimen was moving down. It can be seen that the weld pool was created in groove joint under weaving irradiation by long-length narrow-width laser beam. In the period of 5 seconds during laser hold on the groove surface, the large melted region occurred clearly as be shown in white dash line. That melted region became show darker when laser moving out and the region became smaller. By continuous of irradiation and feeding, period of 10 second shows residue heating zone clearly on both before laser moving in and after laser moving out. And the melted region obviously occurred when laser hold near groove surface.

	Laser moving to groove surface	Laser holds at the groove wall	Laser moving out from groove surface
High speed image time period 5 s (feeding)		Melt by reflected laser	Residue heating zone
Schematic illustration	Laser beam moving in / Hot-wire / Welding direction	Laser beam hold at the corner / Groove surface is melted by reflected laser / Molten pool	Laser beam moving out / Hot-wire / Residue heating zone
High speed image time period 10 s (feeding)	Residue heating zone	Melt by reflected laser	Residue heating zone
Schematic illustration	Laser beam moving in / Hot-wire / Residue heating zone / Welding direction	Laser beam hold at the corner / Groove surface heats by reflected laser / Hot-wire / Molten pool	Laser beam moving out / Hot-wire / Residue heating zone

Fig. 4.27 High speed image results of weaving laser irradiation (Hot-wire laser feeds)

Fig. 4.28 shows macro cross sections of the specimen were irradiated without hot-wire feeding (pre-irradiation period of 5 seconds) and with hot-wire feeding (20 seconds). For irradiation without wire feeding, the molten pool separate from the groove surface since the laser beam was set slightly narrower than the groove width to avoid direct laser irradiates on groove surface. It could be confirmed that this experiment has only the reflected laser incidence on groove surface. As investigation on a micro scale as shown in Fig. 4.29. Region A was inspected the transformation of steel. It can be seen that small part of transformation occurred and region B shows the transformed region separated from direct heat conduction, obviously. Schematic of the partial transformed region was drawn to explain the heating phenomena on groove wall by reflected laser energy during weaving.
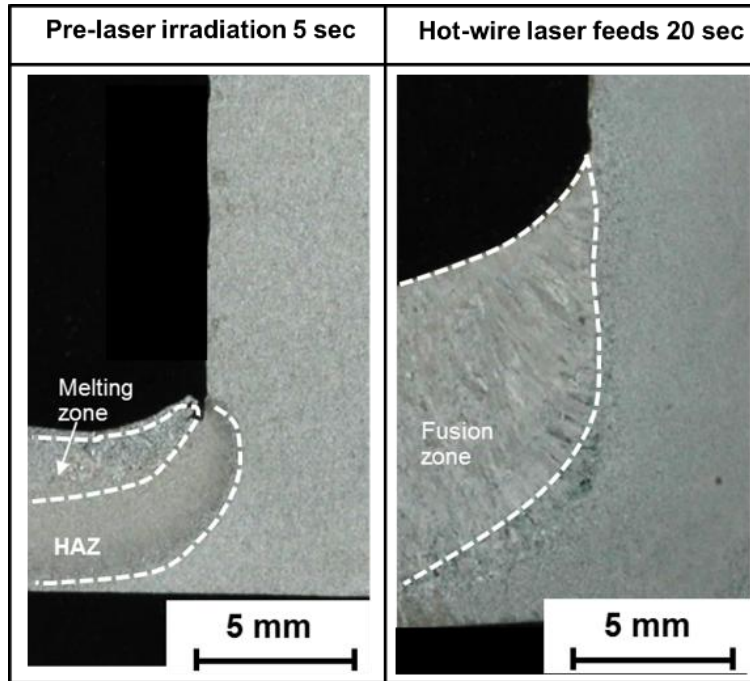
Fig. 4.28 Macro cross section of pre irradiation and hot-wire laser feeds.
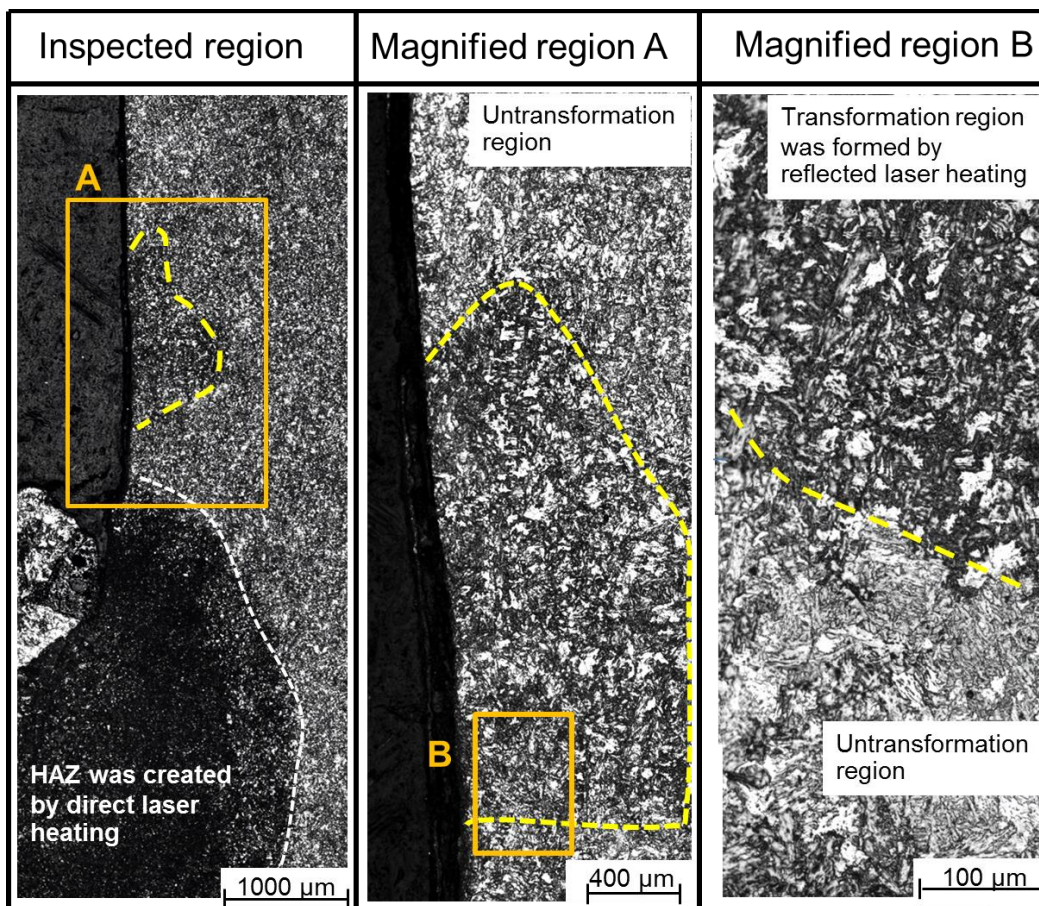
Fig. 4.29 Magnified section of melting region front with pre-irradiation
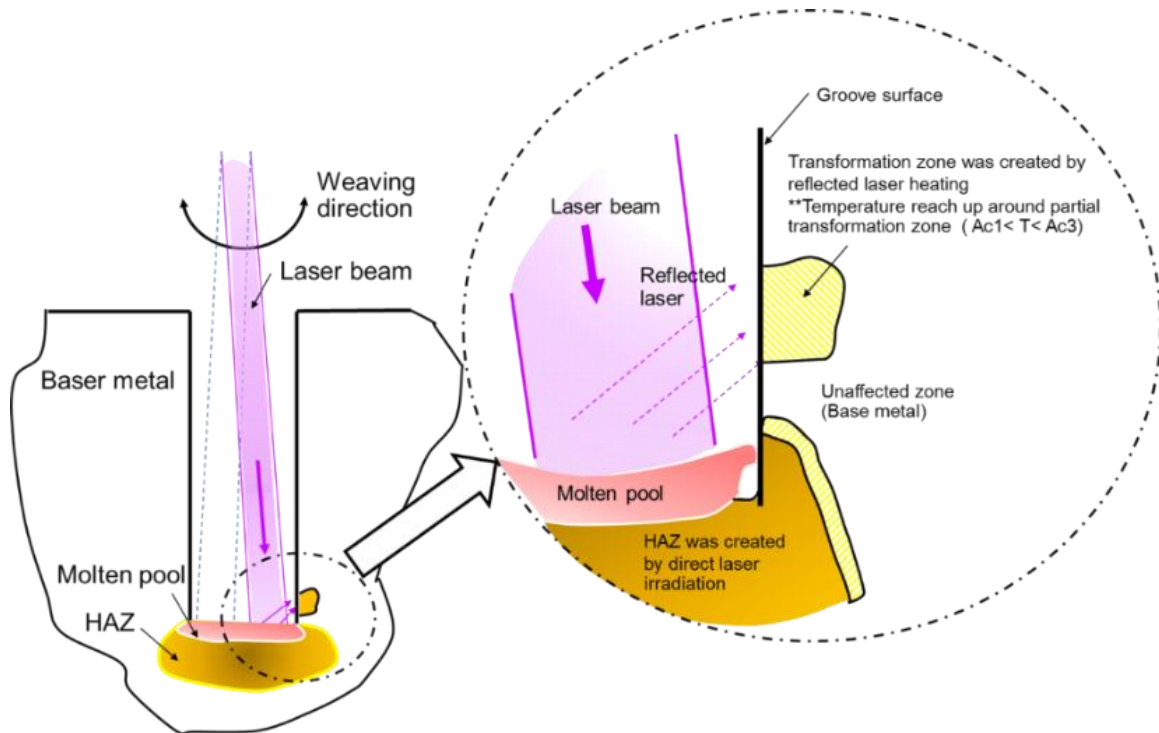
Fig. 4.30 Schematic illustration of mechanism of groove wall heating by
reflected laser (Instantaneous laser irradiation)

4.5.4 Effect of power density on melting depth

Specimens which joined by laser power density of 55 W/mm2 and 111 W/mm^2
were obtained, and a macro scale cross sections were shown in Fig. 4.31.The
specimens were joining by a period of 20 s. Complete fusion was seen on the both
condition and wetting of weld metal also shows. The result of groove wall melted that
confirmed as the previous investigation of the pre-irradiation specimen as the reflected
laser energy only affect melting on groove wall. Comparison of macro scale clearly
showed irradiated by the power density of 111 W/mm^2 has wetting better than the
case of power density of 55 W/mm^2. It implies that high power density irradiation more
affect groove wall heating.
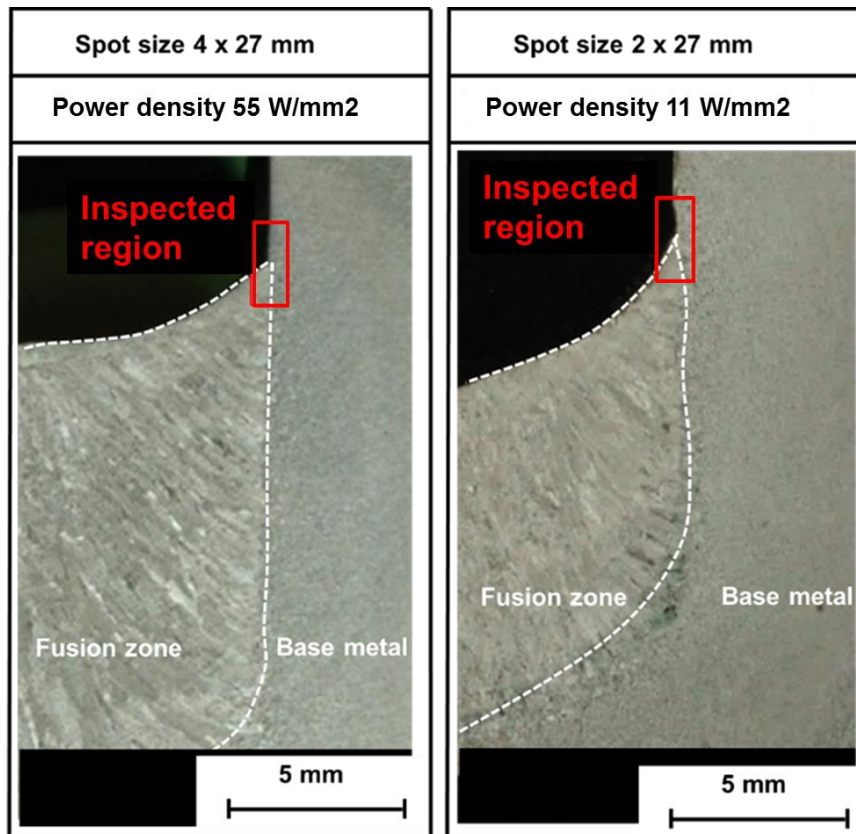
Fig. 4.31 Macro cross section (cut in parallel welding direction) of hot-wire laser feeds with irradiated power density of 55 and 111 W/mm^2.

In order to compare the effect of power density on melting depth, evidence of micro scale were obtained. Fig. 4.32 (a) shows the investigated result of the power density of 55 W/mm^2 and Fig. 4.32 (b) shows the result of the power density that of 111 W/mm^2. It can be seen that the power density of laser beam affected the initial melting depth, high power density could get deeper melting depth than low power density. Moreover, the interesting point of irradiated by the power density of 111 W/mm^2 shows a small melting part without wetting of weld pool.

The measured melting depth as a function of power density was shown in Fig. 4.33. The melting depth of the power density of 55 W/mm^2 is 400 μm and that of the power density of 111 W/mm^2 is 800 μm. It must be noted that this experimental result is simulated to get the initial melting depth. In case of the final melting depth of welded joint will be discussed on the next section.
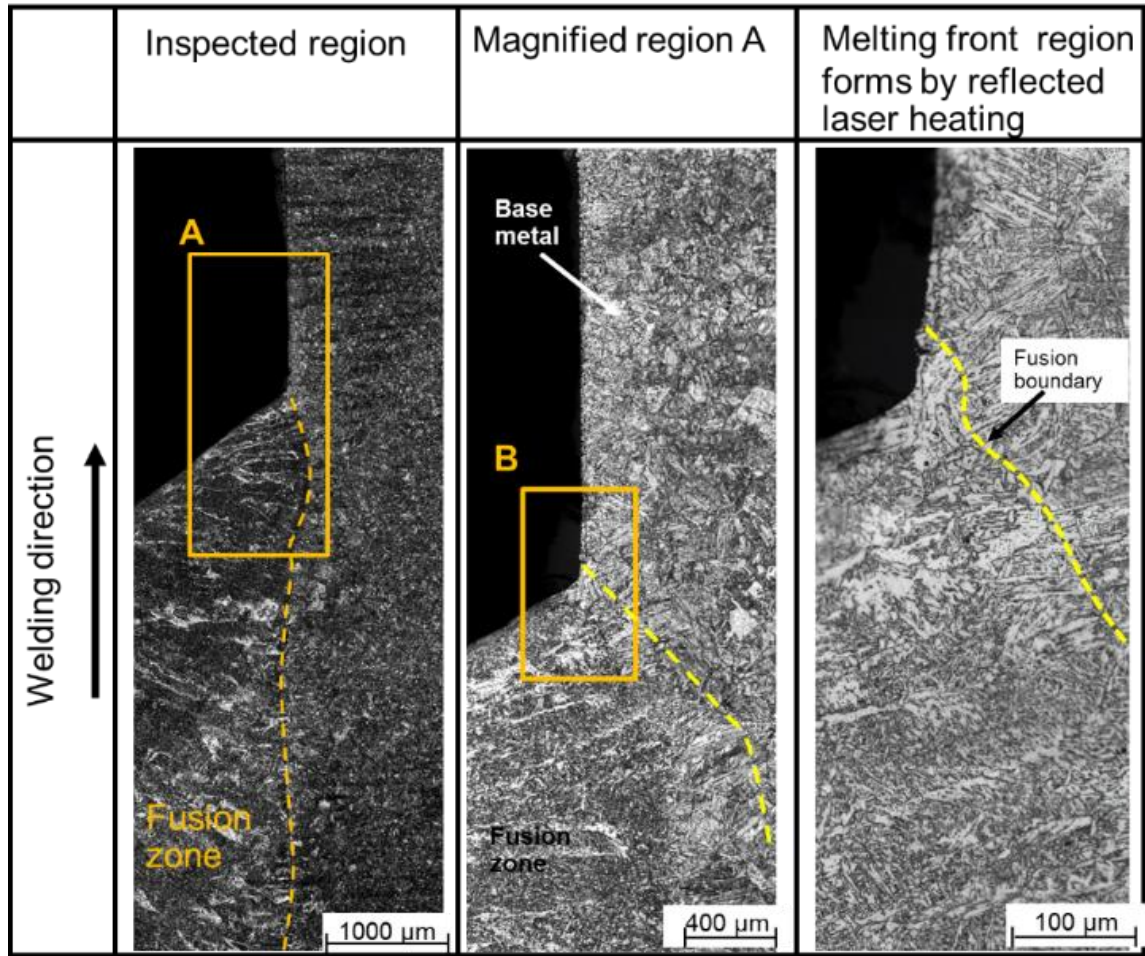
(a) Power density of 55 W/mm^2
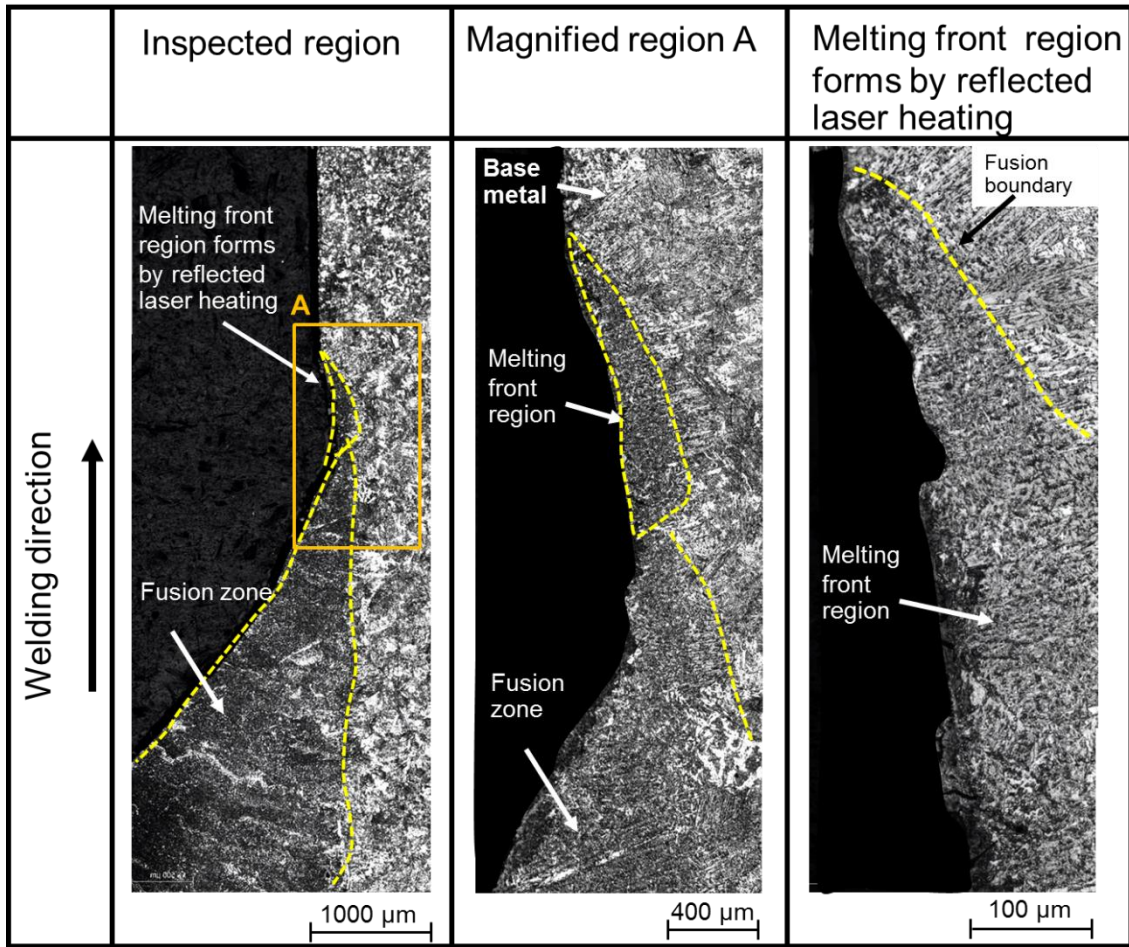
(b) Power density of 111 W/mm^2

Fig. 4.32 Magnified section of melting region front with hot-wire laser feeding
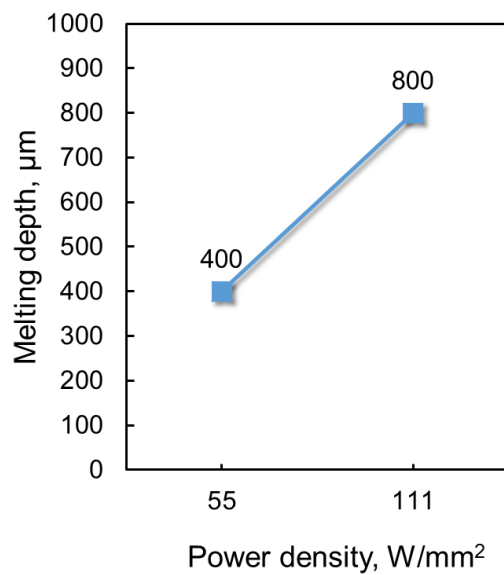
Fig. 4.33 Effect of power density on the initial melting depth by instantaneous laser irradiation.

4.6 Optimization of joining on relative large gap size

According to a large gap size joining, the weaving laser irradiating method was developed in order to improve the process weldability. Result of the weaving method by vertical laser access method and oblique laser access (15°) method have good tendency on the effective weld deposition and the effective fusion length on small specimens. The objectives in this section are improvement joining performance and optimization laser beam parameters.

The laser irradiating conditions are optimized studied by changing laser spot width and laser power density. The welding phenomena during joining was detected by in-situ observation by a high-speed camera. Result of weld pool formation was described by normal high speed image. Relative intensity from the high-speed image was used to make clear the spatial effect of weld pool under difference laser beam parameter as the qualitative method. The results of macro weld joint characteristics were related by all of the evidences.

4.6.1 Materials and specimen used

KE-47 steel plates were used in this study, the dimension of specimen was 50 (width) x 100 (height) x 26 mm (thickness). Fig. 4.34 shows the dimension of specimen. Plates were fixed and aligned as a vertical joint configuration. The gap width was set by spacer (dimension of 10 (width) x20 (height) x 26 (thickness)). The filler metal of YM-1N (JIS Z 3325 YGL2-6A (AP)) with diameter of 1.6 mm was used. The chemical composition of base metal and filler metal were presented on Table 4.11.
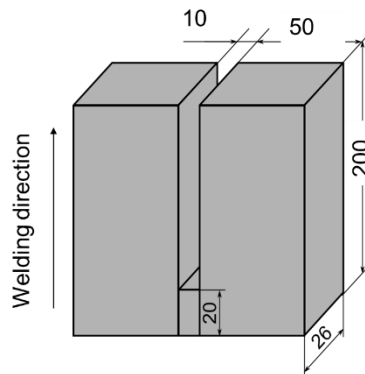
Fig. 4.34 Specimen dimension and weld joint configuration

Table 4.11 Chemical compositions of materials used

Material	Chemical Composition, wt%											
	C	Si	Mn	P	S	Al	Cu	Ni	Nb	Ti	Cr	Mo
KE-47	0.09	0.07	1.52	0.007	0.002	0.014	0.32	0.69	0.01	0.01	0.02	0.00
YM-1N	0.04	0.46	1.35	0.01	0.007	-	0.17	1.07	-	0.7	-	0.26

4.6.2 Methodology of the proposed process

The procedures of the proposed process are shown in the schematic illustration of joint configuration and apparatus in Fig. 4.35: the stationary laser beam method is shown in Fig. 4.35 (a), and weaving laser beam method is shown in Fig. 4.35. (b). For both methods the oblique laser access (tilt angle of 15°) with 1 hot-wire for joining. The joint configuration is rigged in vertical alignment. Groove configuration is a square butt joint for welding with single pass weld. Table 4.12 shows the welding parameter of laser and hot-wire for all conditions.

The laser equipment used as a power source was Laserline LDF 6000-40 (6.0 kW) continuous wave (CW) Diode Laser (LD). For the stationary laser method, it was assembled with collimator lens of 100 mm, the focus lens of 1000 mm, and a fiber diameter of 1 mm. The resulting laser beam has a rectangular beam shape with the narrow-width long-length dimension of 10 x 26 mm (Fig. 4.36 (a)). The power density for this case is 23 W/mm^2 by laser power of 6 kW.

The weaving laser beam, it was assembled on two main parts of the normal laser head and weaving head. The normal laser head was assembled with collimator lens of 100 mm and focus lens of 400 mm. The laser beam was shoot out from laser head and run into weaving head. In the side of the weaving head has a weaving blade which was made by perfect reflection coating material and it was oscillated under desired frequency by the harmonic motor and wave form controller. The Large rectangular laser beam was sweep along the joint target in gap width direction.

The weaving laser method was varied power densities by modulation of laser spot size. Since the maximum laser power of 6 kW was used, the spot size 4 x 27 mm irradiates the power density of 55 W/mm^2 by used the fiber core size of 1.0 mm (Fig.4.36 (b)) and the spot size of 2 x 27 mm irradiates the power density of 111 W/mm^2 by used the fiber core size of 0.4 mm (fig 4.36 (c). By modulation of laser spot size, beam width change with smaller gap width, it was defined laser parameter for the weaving method by laser beam width (W_L) and gap width (W_G) ratio (hereinafter referred to simply as W_L/W_G ratio) . There are resulted of W_L/W_G ratio = 0.4 for the spot size 4 x 27 mm, power density 55 W/mm^2 and W_L/W_G ratio = 0.2 for the spot size 2 x 27 mm, power density 111. W/mm^2. The W_L/W_G ratio is one parameter, which is considered for the effect on weld joint characteristics. The weaving frequency and weaving waveform in this study was 5 Hz-exponential waveform.

Hot-wire was used in the proposed process to improve the efficiency of deposition. Hot-wire machine used was Hitachi Power Assist HI-TIG series IV662. It generates current and passes it into and heats up the filler wire in the process known as Joule heating. The filler wire is heated up to the temperature near the melting point.
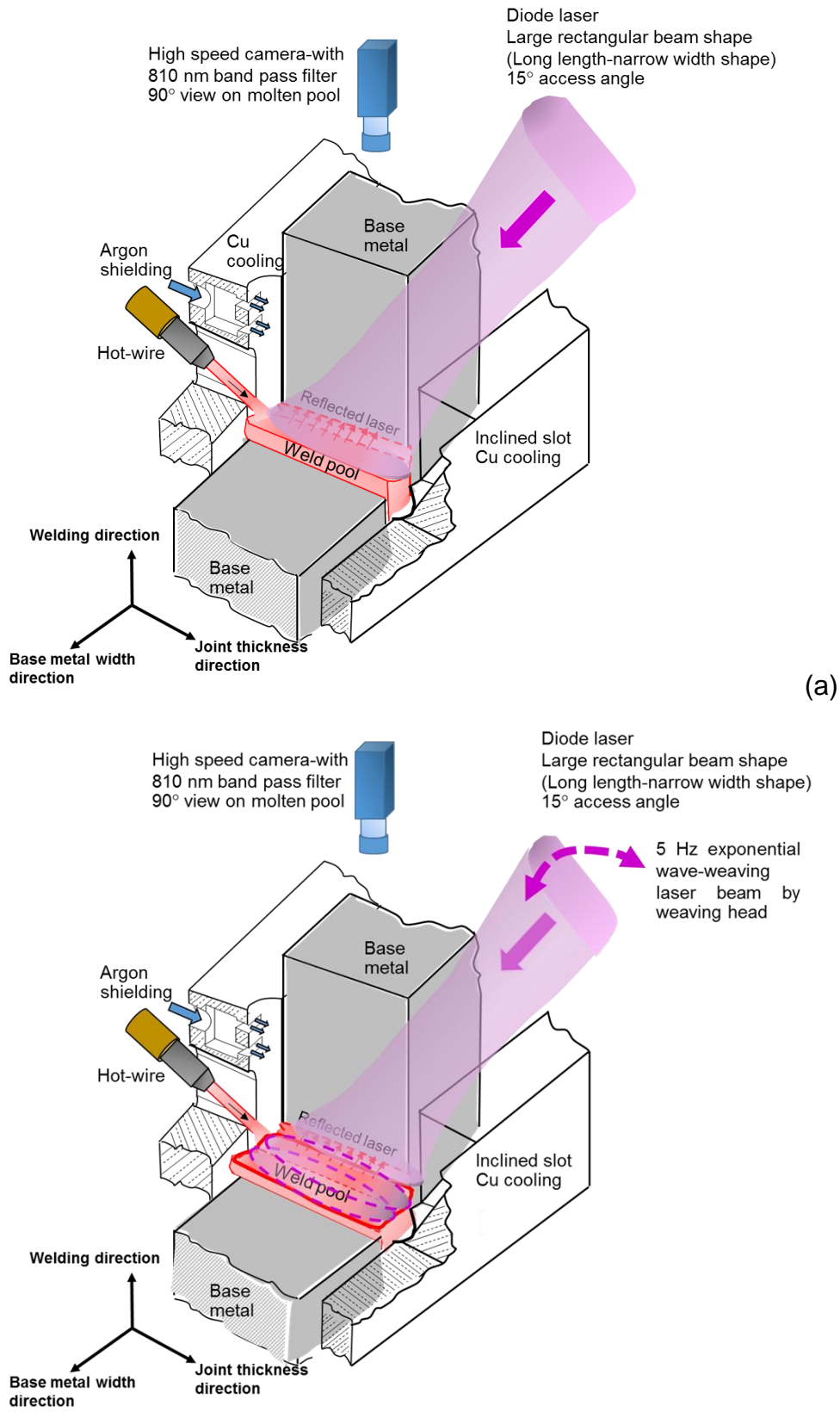
Fig. 4.35. Schematic illustration of the vertical welding process using hot-wire laser (oblique laser access) on gap width of 10 mm (a) stationary laser irradiating method and (b) weaving laser irradiating method

(a) 23 W/mm^2 W$_G$/W$_L$ ratio 1.0   (b) 55 W/mm^2 W$_G$/W$_L$ ratio 0.4   (c) 111 W/mm^2 W$_G$/W$_L$ ratio 0.2
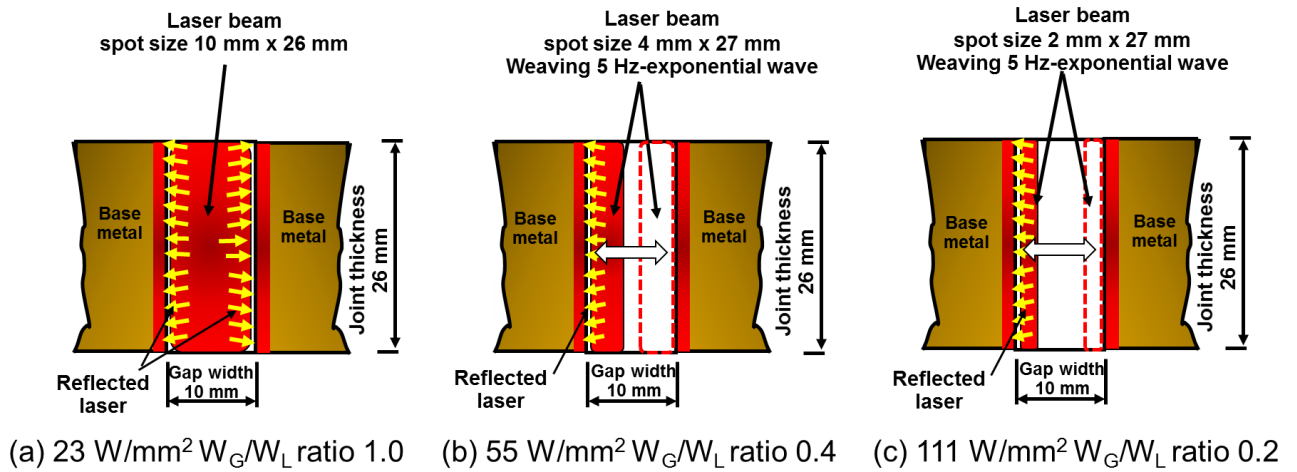
Fig. 4.36. Schematic illustration of the 10 mm gap width

Table 4.12 Welding parameters

Laser irradiation method	Stationary	Weaving 5 Hz-exponential wave	
Fiber core, mm	1.0	1.0	0.4
Homogenizer	LL6	LL3	LL3
Focus lens, mm	1000	400	400
Laser power, kW	6	6	6
Laser irradiation angle, degree	15°	15°	15°
Defocus, mm	0	20	20
Spot size, mm x mm	10^w x 26^l	4^w x 27^l	2^w x 27^l
Power density, W/mm^2	23	55	111
Filler wire diameter, mm	1.6	1.6	1.6
Welding speed, cm/min	3.3	3.3	3.3
Wire feed speed, m/min	5.31	5.31	5.31
Wire current, A	161	181	164
Wire feeding angle, degree	45	45	45
Wire feeding position, mm	5	5	5
Shielding gas (Argon), LPM	10	10	10
Pre irradiation time, s	120	120	120

4.6.3 Methodology of in-situ observation

Optical processing for capturing of welding phenomena was done with a high-speed camera. Pencil camera V-193-M1 model connected with NAC: MEMRECAM GX-5 module was used with a focus lens 50 mm with a diameter of 25 mm, 810 nm band pass filter. The capturing parameter is the frame rate of 50 fps, the shutter speed of 1/20000 and an aperture is closed. The capturing yielded the detailed observation of the welding phenomena. Fig. 4.37 shows a schematic layout and explanation of weld pool view. The camera can be set at 90° from the plane of the weld pool, so the behavior of weld pool can be seen entirely in both axes.

By using a high-speed camera and 810 nm band pass filter (Edmund) that has two phenomena to be discussed. Frist, the original high-speed photograph of the weld pool be discussed on weld bead formation and process stability. Second, the relative intensity image of the weld pool radiation be discussed for qualitative temperature distribution on the weld pool. The relative intensity image was converted from the original high-speed photograph to intensity jet color image for visualized information. It was noted that the intensity data (0-255 intensity scale) can be used only each condition, it is properly is used only separation low energy region and high energy region on the same weld pool.
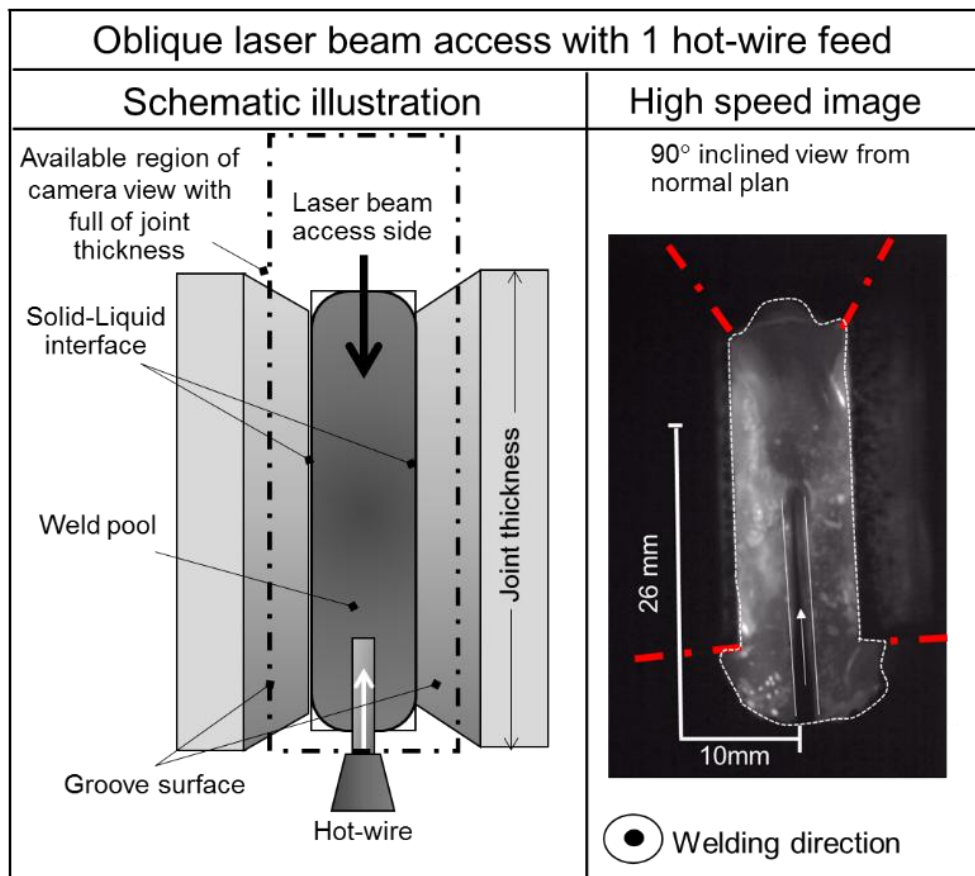

Fig. 4.37 Schematic layout and high speed image explain available region for oblique laser beam access

4.6.4 Methodology for evaluation of weld joint characteristics

Welded specimens were cut in the perpendicular to the welding direction in order to investigate weld joint characteristics in joint thickness. Sections of welding distance at 50 mm and 70 mm were preferentially investigated. The specimen observation were performed by standard metallurgical procedure and etched by 3% nital solution to get clear weld bead section appearance. The bead width and imperfection were measured on every 2 mm in the joint thickness direction from laser side through wire side.

4.6.5 Weld pool phenomena results by in-situ observation

Fig. 4.38 shows the high-speed image of welding phenomena in each weld condition at propagate times of 90 and 125 seconds, or at the observed positions of weld length 50mm and 70mm from the spacer surfaces. The weld pool is shown as a dashed line, hot wire being fed into the weld pool is shown as solid line and arrow, and the joint edge, which is base metal, is shown as red centerline.

The high-speed photographs show the feeding of the hot wire into the weld pool under the laser irradiation and the stable weld pool generation. For stationary laser method, which is irradiated with the low power density of 23 W/mm^2, it is observed that the weld pool has low wetting. This implies that the weld pool has low temperature, and it showed that the propagation of molten metal not thoroughly over entire length of joint, especially on the edge of laser access side. Incomplete fulfilled weld can obviously be observed at the edge region. And when the welding duration increases, the size of the weld tends to decrease.

The laser weaving method has a higher ability to deposit on the weld pool because of the higher power density of the laser beam comparing to the case of stationary laser method. The weaving of the high laser power density makes the molten metal propagates better. Comparing the laser parameters, laser spot size of 4mm x 27mm and W_L/W_G ratio of 0.4 yields better result than the laser spot size of 2mm x 27mm having W_L/W_G of 0.2 even the ratio of 0.4 has a lower power density. From the high-speed photograph, it can be seen that WL/WG of 0.4 achieved fulfill of the joint entirely, especially on the wire feed side which has more suitable amount of molten metal than on the laser side. As welding duration increases, small size of incomplete fulfill is observed on the laser side. Incomplete fulfill also occurs on the laser side for the case using laser spot size of 2mm x 27mm even at laser power density of 111 W/mm^2.
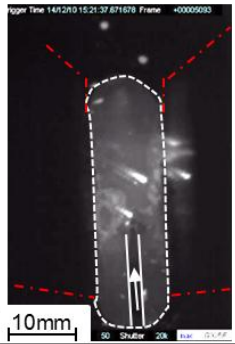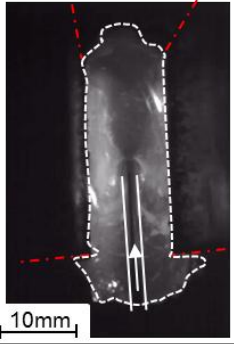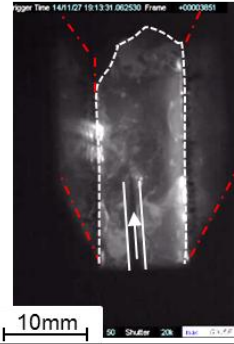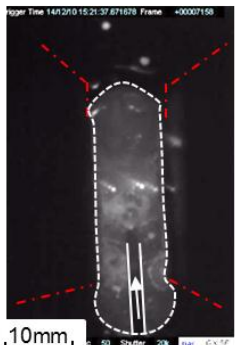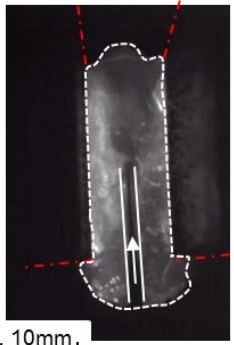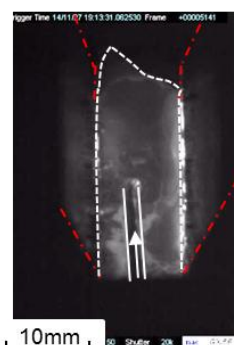
	Laser irradiating method		
	Stationary	Weaving 5 Hz-exponential wave	
	Laser spot size, width x length (mm x mm)		
	10 x 26	4 x 27	2 x 27
Observed position	Power density, W/mm^2 (W$_L$/W$_G$ ratio)		
	23 (1.0)	55 (0.4)	111 (0.2)

Fig. 4.38 High speed image during welding

4.6.6 Results of relative intensity image of weld pool responsibility by 810 nm band pass filter (qualitative method)

The contour of the relative intensity of weld pool transformed from the high-speed photograph, shown in jet color scale in Fig. 4.39. The objective of this conversion is to make an spatial comparison between each weld condition. The result of the stationary method shows more dark color, which means the weld pool is at a lower temperature due to low laser power density used. Only the middle zone has brighter color indicating higher weld pool temperature. This shows that there is melting in this area more than in edge regions.

For the weaving method, the result from irradiation with the exponential wave with the duration at groove boundary of 72.5 ms for 5 Hz frequency is also shown in Fig. 4.39. A clear responded area under the laser weaving irradiation with high laser power density. Comparison between the power densities of 55 W/mm^2 and 111

W/mm^2 in the direction parallel to the joint, the power density of 111 W/mm^2, shows narrow and long response, or the rise in temperature of weld pool on the entire length. The rise in temperature in 111 W/mm^2 condition is also more than that using the power density of 55 W/mm^2. This phenomenon shows that the area of fusion interface using the power density of 111 W/mm^2 is affected largely the temperature than using the power density of 55 W/mm^2. It implies that using the power density of 111 W/mm^2 yields more stable weld bead width along the direction parallel to the joint.

Observed position	Laser irradiating method		
	Stationary	Weaving 5 Hz-exponential wave	
	Laser spot size, width x length (mm x mm)		
	10 x 26	4 x 27	2 x 27
	Power density, W/mm² (W_L/W_G ratio)		
	23 (1.0)	55 (0.4)	111 (0.2)
50 mm			
70 mm			

Note: Relative intensity image of the weld pool radiation was detected by 810 nm filter.

Qualitative expression   Low ◄— Radiation energy —► High

Relative intensity   0   50   100   150   200   250
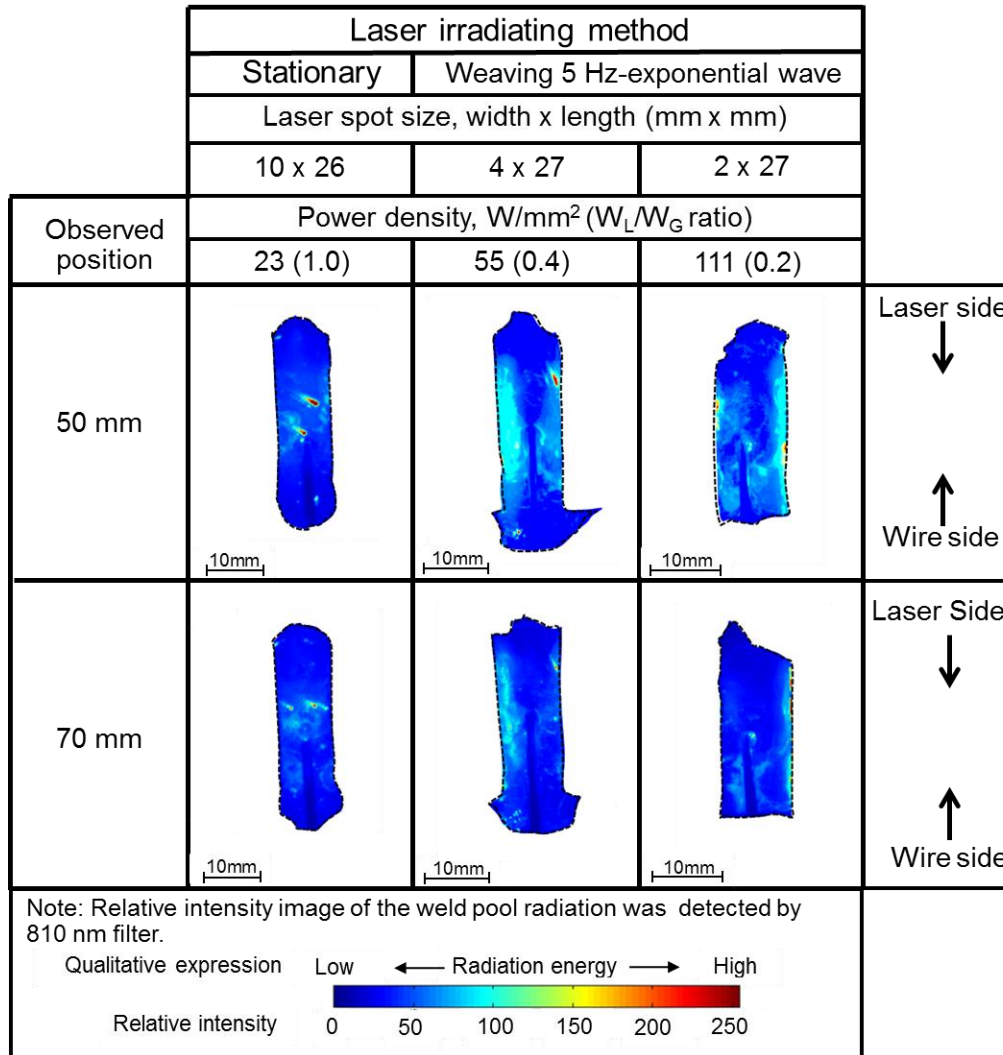
Fig. 4.39 The image by relative intensity of weld pool radiation (Spatial information)

Viewing the weld pool of weaving method in the overall scale, it can obviously be seen that the result using 4 mm laser width on the 10 mm-wide joint (W_L/W_G ratio of 0.4) has relative intensity less than that of using 2 mm laser width on the 10mm-wide joint (W_L/W_G ratio of 0.2). However, the 4 mm width of laser beam condition having a width of the higher temperature region is wider than the 2 mm width of laser beam condition. This quantitatively shows that using W_L/W_G ratio of 0.4 with 5 Hz exponential wave yields stable weld. In the direction parallel to the joint, it is found that the area of the joint edge has lower relative intensity, which results in increased

chance of imperfection on the area. This can be seen at the observed position of 50 mm and 70 mm of both cases, shown as the darker area in Fig. 4.39.

4.6.7 Result of weld joint characteristics

Weld joint characteristics are shown in Fig. 4.40 as a macro cross section in the cross section to the weld direction, which can be seen along the entire length of the joint. The welding using single pass vertical joining process on a gap width of 10mm was successful. Welding duration has no effect on the rate of melting of base metal, demonstrating the stability of the weld pool creation and melting of the method. The weaving method also increases the efficiency of the process, both weld metal deposition and melting stability.

Fig. 4.41 shows the result of weld size and lack of fusion generation. It is found that stationary (Fig. 4.41 (a)) has low melting: maximum bead width of only 10.2mm under the final gap width of 9.2mm, which indicates gap shrinkage. The lack of fusion level is also high on the joint edge.

The laser weaving method shows interesting results in the characteristics of melting in the direction parallel to the joint. Using laser power density of 111W/mm^2, spot size of 2mm x 27mm, and WL/WG ratio of 0.2 yields stable and consistent melting depth on the entire length of the joint in the form of low dilution weld. The characteristic of the weld is shown in Fig. 4.40 (c-1) and (c-2) and the weld size result is shown in Fig. 4.41. It can be seen that the widest weld is at 11.2 mm, but with the lack of fusion with the total length of 2mm at the laser side. In contrast, irradiation with the laser power density of 55W/mm^2, the spot size of 4 mm x 27 mm, and WL/WG of 0.4, of which the result is shown in Fig. 4.40 (b-1), (b-2) and Fig. 4.41 (a), yields more melting than the aforementioned case. The maximum weld width is 13mm, but the lack of fusion still occurred with the length of 2 mm, as a result from suck back during the welding on the 70 mm joint.

4.6.8 Discussion of the effect of laser irradiating method on joining performance

From the result discussed above, weaving laser method with long-length narrow-path laser beam maintaining high power density over the critical density yields increased deposition ability and melting ability over the stationary laser method. This is due to the modulation of the laser beam size to be near to the gap dimension (of 10mm x 26mm), resulting in low power density (of 23 W/mm^2). The maximum laser power of the source is 6 kW.

4.6.9 Discussion of the effect of laser spot size over wide gap width size for weaving laser method

Using the power density of 111W/mm^2 with laser beam size modulation at 2 mm x 27mm has an effect on base metal melting. The effect is mainly from reflected laser beam while weld pool heat conduction contribute less. This makes weld characteristics

on the direction parallel to the joint having consistent penetration depth and low dilution weld. The power density of 55 W/mm^2 with laser beam size modulation at 4 mm x 27 mm has the highest effect on final melting depth, which is due to weld pool heat conduction. The weld yielded has maximum penetration point at the center of the weld, and the overall effect of melting is more than the result with laser spot size of 2 mm x 27 mm.

Observed position	Laser irradiating method		
	Stationary	Weaving 5 Hz-exponential wave	
	Laser spot size, width x length (mm x mm)		
	10 x 26	4 x 27	2 x 27
	Power density, W/mm² (W_L/W_G ratio)		
	23 (1.0)	55 (0.4)	111 (0.2)
Laser Side ↓ 50 mm Wire Side ↑	(a-1) 10mm	(b-1) 10mm	(c-1) 10mm
Laser Side ↓ 70 mm Wire Side ↑	(a-2) 10mm	(b-2) 10mm	(c-2) 10mm
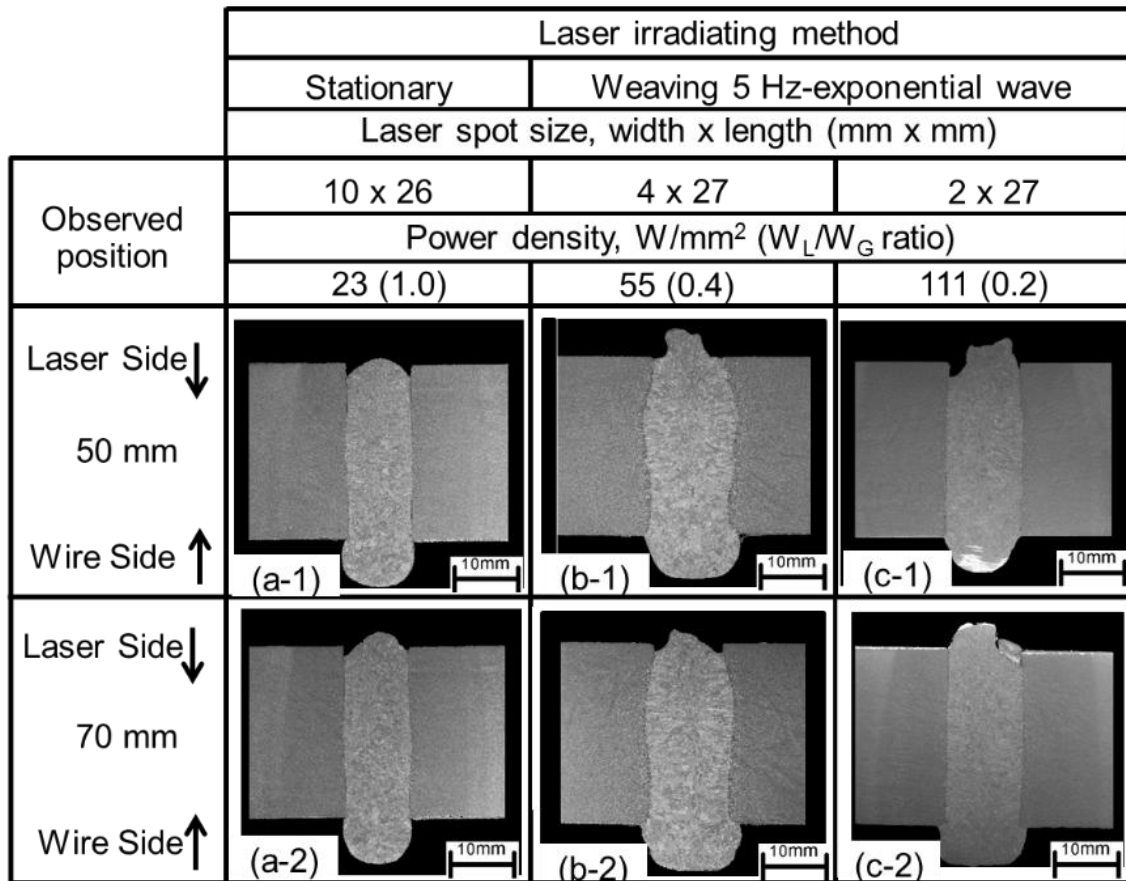
Fig. 4.40 Macro cross section of transverse welding direction cut

In the discussion of the effect of weld pool heat conduction, W_L/W_G ratio is best used in the evaluation of laser parameter. The result of weld pool penetration or bead width, shown in Fig. 4.40 is the supporting evidence with good correlation. Weaving with W_L/W_G ratio of 0.4 shows the higher heat conduction than with WL/WG ratio of 0.2. Relative intensity image also shows the high concentration of heat at the center of the joint, consistent with the final melting depth shown in Fig. 40 (b-1) and (b-2). Relative intensity image of W_L/W_G ratio of 0.2 (Fig. 40 (c-1) and (c-2)) shows heat concentration in the narrow band but consistent in the direction parallel to the joint. The percentage of low-temperature area is higher, implying low weld pool heat effect.
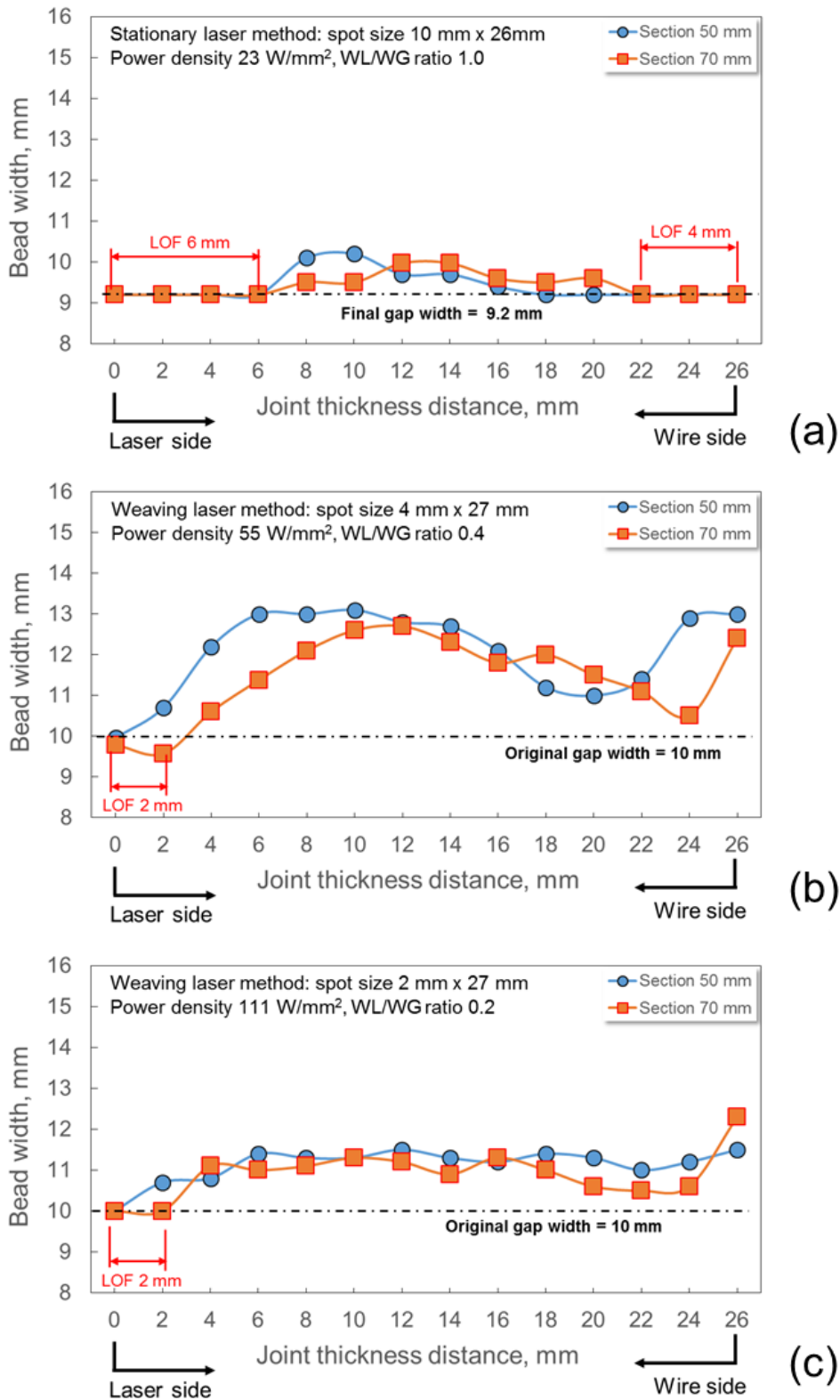
Fig. 4.41. Measured bead width and lack of fusion (LOF) of (a) stationary laser method [23 W/mm^2, W_L/W_G ratio =1.0], (b) weaving laser method [55 W/mm^2, W_L/W_G ratio =0.4] and (c) weaving laser method [111 W/mm^2, W_L/W_G ratio =0.2]
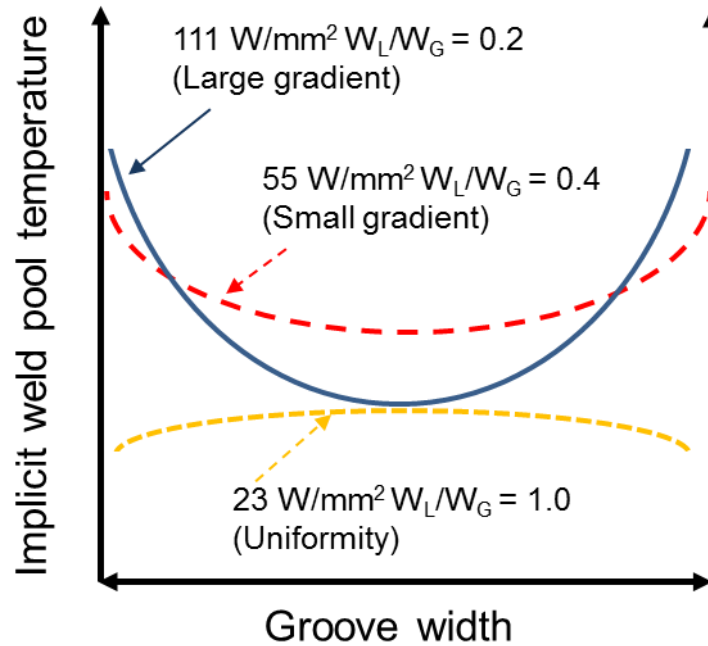
Fig. 4.42 Schematic of qualitative description for weld pool temperature (steady state) under influence of combination of power density and W_L/W_G ratio.

The actual weld pool temperature could not be detected now. But in the future, multi-sensor high-speed camera will be used for observation on full area of the weld pool. However, the relationship between relative intensity image and horizontal cross section can be summarized welding phenomena by the qualitative method. Weld pool phenomena on steady state under influence of power density and W_L/W_G ratio was shown as schematic in Fig. 4.42. High power density with narrow beam width (111 W/mm^2, W_L/W_G ratio =0.2) has a result of large gradient of weld pool temperature then an average weld pool temperature has a low level. The complete fusion can obtain but the melting amount of base metal is very small.

Wider beam with an appropriate power density (55 W/mm^2, W_L/W_G ratio =0.4) can provide high temperature and small gradient thereby an average weld pool temperature has a higher level. It is result in large amount of base metal melting.

Beam width size fit on the gap width size which irradiated by low power density 23 w/mm^2, W_L/W_G ratio =1.0) has a result of uniformity of weld pool temperature but the level of temperature is very low. It difficult obtained complete fusion because low power density cannot create the base metal melting by reflected laser energy.

4.6.10 Optimization of W_L/W_G ratio

The novel welding process has two factors for consider in order to achieve sound joint, adequately. First, the power density shall be higher than the critical power density to primary melts groove surface. Second, the laser spot size under the adequate power density shall provide adequate weld pool energy distribution on both directions of joint thickness direction and width direction.

Using laser beam irradiated by power density more than 55 W/mm^2, joining by W_L/W_G of 0.4 is optimized laser beam parameter which achieved sound joint and obtain adequate melting amount of base metal.

Fig. 4.43 shows summarized result for optimization of laser irradiating method by objective function of minimized imperfection and maximized weld bead width. It can be seen that the weaving laser irradiating method by power density 55 W/mm^2 with W_L/W_G of 0.4 reaches the objective function.
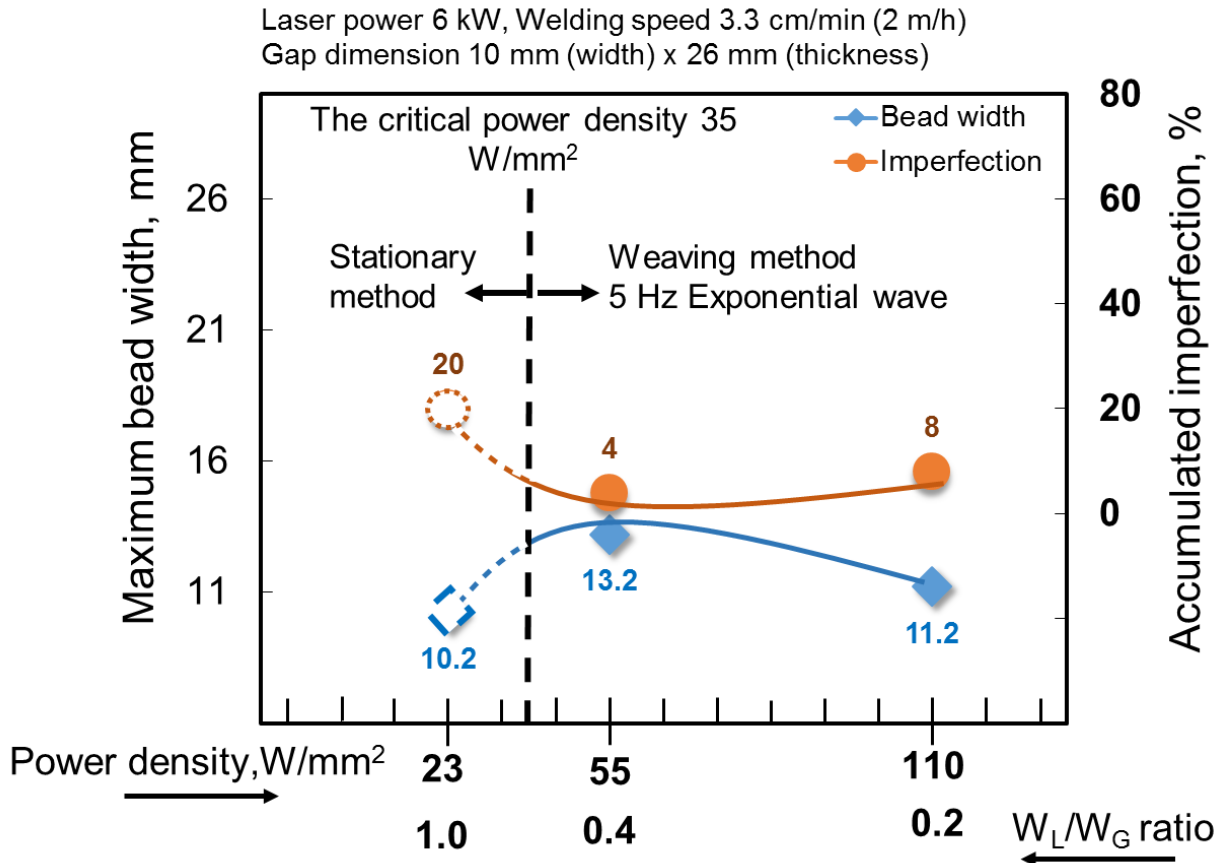

Fig 4.43 Optimization of laser irradiating methods versus maximum bead width and imperfection on the weld joint.

4.7 Summary

The single-pass vertical joining by hot-wire laser method was studied and has been successfully welds due to large gap size of 10 mm (width) x 26 mm (length). The effect of welding parameters could be drawn as

1)   The weaving laser method by using appropriate laser power density of large rectangular laser beam can improve a joining fulfill and amount of base metal melt. While the stationary laser beam has a low power density over wide laser spot width due to a limit of laser power source, resulting the low melting amount of base metal and large size of lack of fusion occurred.

2)   An appropriate weaving condition is weaving frequency of 5 Hz with the exponential waveform. The adequate combination of an exponential waveform and weaving frequency supplies enough laser irradiating time near the groove surface side to obtain appropriate base metal melting during holding time and appropriate repetition rate on a weld pool center to keep a stable weld pool formation.

3)   Oblique laser irradiation with the angle of 15˚ achieved the almost same weld bead of vertical laser irradiation (0˚) with low dilution and uniformity of fusion. The larger laser irradiating angle of 30˚ causes extremely large imperfection and small amount of base metal melting. Oblique laser irradiation and single hot-wire feeding could be used practically, and the combination with laser weaving method could provide large gap tolerance.

4)   The welding phenomena of weaving laser method, the value of power density has effect initial melting of base metal however large amount of base metal or final melting volume of weld metal was strongly affected by the weld pool heat conduction. The wide laser spot size-WL/WG =0.4 could maintained a high-temperature weld pool and resulting on large melting volume (larger weld bead size). On the other hand laser beam, WL/WG = 0.2 has resulted on the large difference the liquid weld pool energy when laser beam moving, although narrower laser beam width irradiated by higher power density.

5)   It was mentioned that using long length laser beam size for joining resulted of much low energy on the beam tails (edge region). Frequently imperfection such incomplete fulfill or lack of fusion occurred on this region. An important idea that the problem is a compensation the laser energy on the both edge sides for troubleshooting the imperfection occurrence.

Chapter 5

Optimization of laser beam energy distribution

to achieve sound joint

5.1 Introduction

According to the previous chapter, when the laser oblique access method was developed, the imperfection such incomplete fulfill and a lack of fusion frequently almost occurred on the joint edge region. The supporting evidence by the high-speed camera with relative intensity image showed that on the edge region has lower temperature than the middle region. Then in this chapter has objective to compensate/ balance the energy of the applied laser energy on the weld pool for improve the process capability and process capacity. The method of twin laser beams was provided to investigate the feasibility and effect of welding parameters.

It must be noted that the twin laser method does not meaning of add more laser energy to achieve sound weld or increasing melting ability. The twin laser method is the experiment to study and optimize the laser beam parameters for basic design for the new optic beam profile in the future.

This chapter has two main parts for study. First, the experiment for parameters screen out of twin laser by the effect of fiber laser power and welding speed on weld joint characteristics. Second, optimization the laser parameters to achieve sound joint.

In-situ observation by high speed camera with preferential 810 nm band pass filter was performed to monitor weld pool phenomena. Welded specimens were investigated by macro cross section scale to compare and evaluate the effect of welding parameters.

5.2 Experiment of the effect of compensation of laser energy on joint edge by fiber laser access on one region

5.2.1 Materials used and specimen dimension

KE-40 steel plates were used in this study, the dimension of the specimen was 100 (width) x 200 (height) x 27 mm (thickness). Plates were fixed and aligned as a vertical joint configuration. The gap width was set by spacer (dimension of 10 (width) x20 (height) x 27 (thickness)). The filler metals are used 2 sizes and type of filler wires, YM-1N (JIS Z 3325 YGL2-6A (AP)) with diameter of 1.2 mm was used for experiments of low-speed ranges and YM-80A (JIS3312 G78AUMN5C1 M3T) with diameter of 1.6 mm was used for high-speed range. Since as this experiment has an objective for the screen out welding parameters then an appropriate size of filler

metal was also studied on stable hot-wire feeding conditions. The chemical composition of base metal and filler metal were presented on Table 5.1.
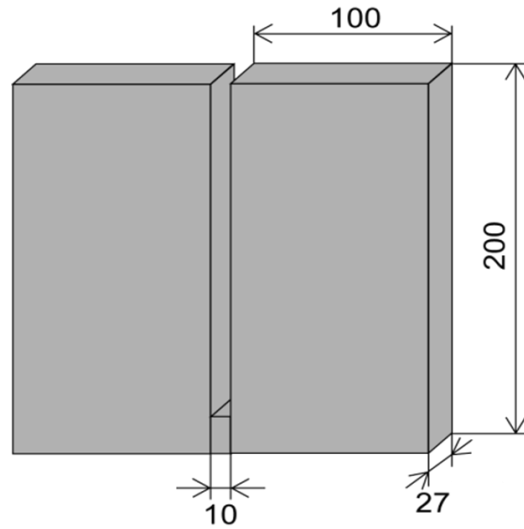
Figure 5.1 Specimen dimension and weld joint configuration

Table 5.1 Chemical compositions of materials used

Material	Chemical Composition, wt%											
	C	Si	Mn	P	S	Al	Cu	Ni	Nb	Ti	Cr	Mo
KE-40	0.11	0.285	1.31	0.008	0.003	No data						
YM-1N	0.04	0.46	1.35	0.01	0.007	-	0.17	1.07	-	0.7	-	0.26
YM-80A	0.07	0.5	1.6	0.009	0.004	-	0.03	-	-	-	-	-

5.2.2 Methodology of the twin laser beams and studied parameters design

The twin laser beams method was shown as schematic illustration on Fig. 5.2. The primary laser beam irradiated by diode laser source was utilized for main heat source. The secondary laser beam irradiated by fiber laser source was used of compensate the energy at the joint edge at the side of the diode laser access.
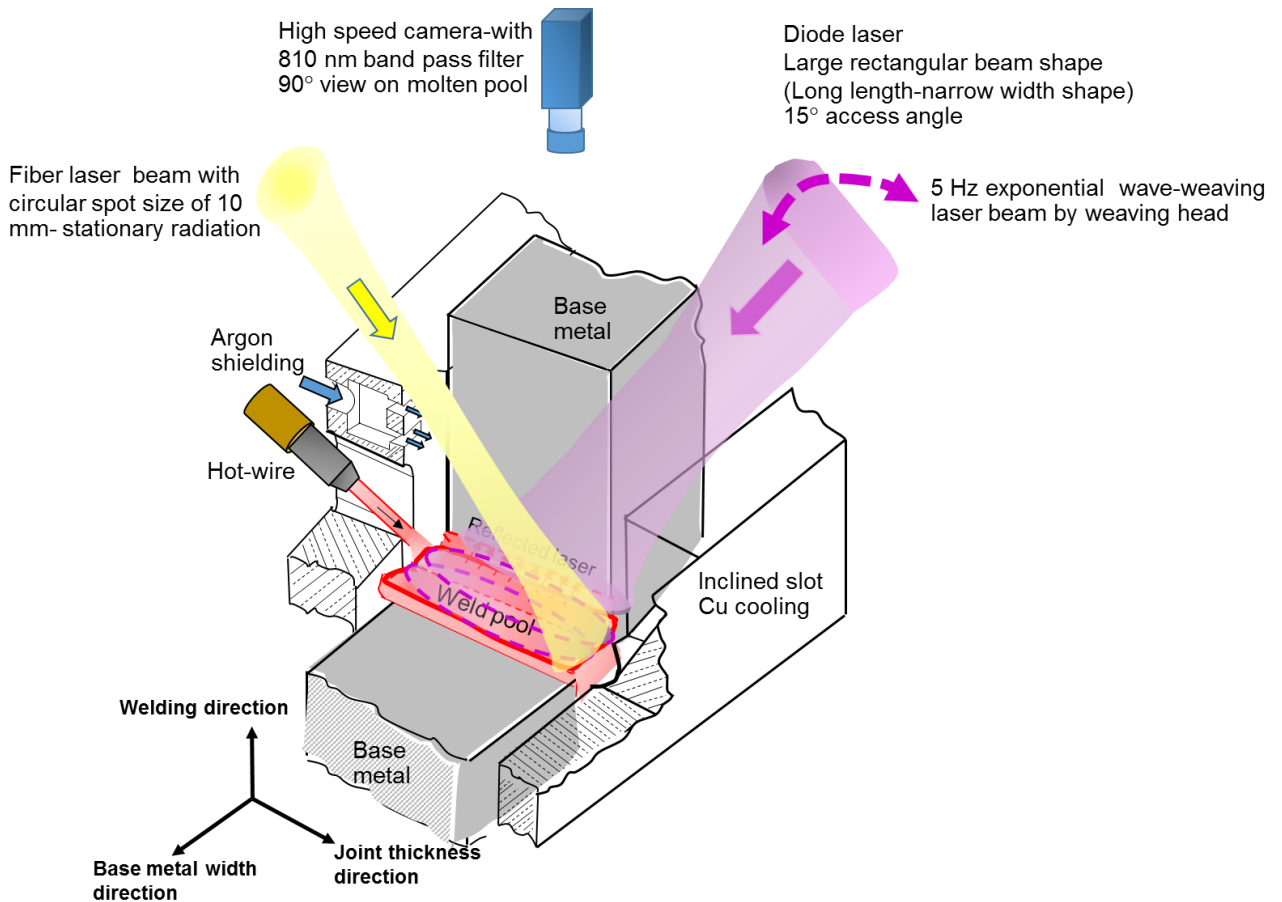
Figure 5.2 Schematic illustration of the twin laser beams method

Laserline LDF 6000-40 (6.0 kW) continuous wave (CW) Diode Laser (LD) was used as the main heat source. The twin laser beams method provided the weaving diode laser method for joining by reason of appropriate irradiating method for wide gap size. Weaving parameter set was 5 Hz-exponential waveform with parameter W_L/W_G ratio of 0.4 by the spot size of 4 mm x 27 mm. This parameter was evaluated as optimize in the previous chapter. The oblique laser access with tilt angle 15° of the weaving head was set for shoot the weaving beam through the joint target by defocus 20 mm.

Fiber laser beam source is YLR-300-S (IPG 3.0 kW. It irradiated by Yb-YAG (Ytterbium-Yttrium Aluminum Garnet, Y3Al5O12) with the wavelength of 1070 nm. In this basic experiment of the twin laser beams, the stationary fiber laser was irradiated as circular spot size of 10 mm and shoot through the edge region opposite side which laser head was handled by tilt angle of 13°. The handling laser heads by two robots showed in Fig. 5.3.
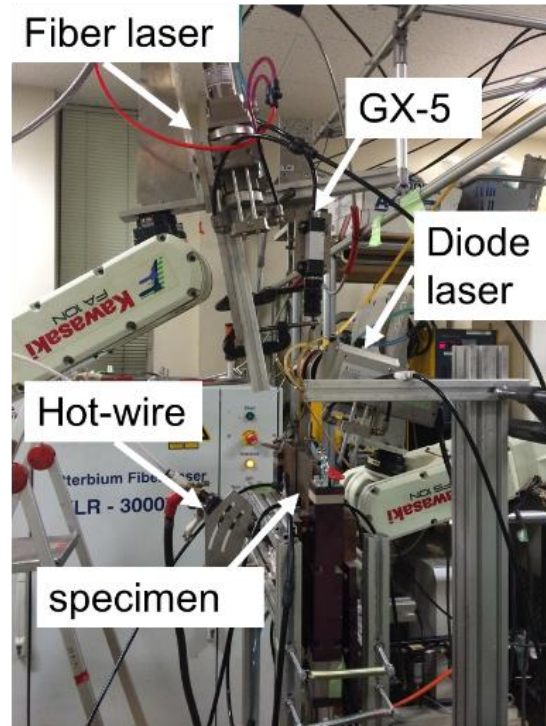
Figure 5.3 Set up the twin laser beams experiment.

One hot-wire feed system was set in a copper cooling jig which is opposite side the diode laser access side. The feeding angle was set at 35 degree to get feeding position of 5 mm from the joint edge. The environment was shielded by argon gas with flow rate 10 l/min from the same side of the hot-wire torch. Set of studied welding parameters was shown in the matrix design on Table 2 and welding parameters were shown on Table 5.3.

Studied parameters for the twin laser method were compensated laser power levels and welding speed ranges. Table 5.2 shows the levels of studied parameters. Compensate laser powers were 1, 2 and 3 kW by fixed welding speed of 3.33 cm/min (2m/h). For the study of welding speed effect, the speed of 3.33, 5.00 and 6.67 cm/min (2, 3 and 4 m/h) by fixed a compensated laser power of 3 kW. The results of weld characteristics will be performed and evaluated the appropriate level for prepare the experiment for parameter optimization.

Table 5.2 Studied welding parameters

Compensate laser power, kW	Welding speed, cm/min (m/h)		
	3.33 (2)	5.00 (3)	6.67 (4)
1	O		
2	O	-	-
3	O	O	O

In-situ observation by the high-speed camera with 810 nm band pass filter was associated in this experiment to investigate and make a supporting evidence of the weld pool phenomena under the influence of laser energy compensation. Fig. 5.4 showed Fig. 5.5 shows a schematic layout and explanation of weld pool view. The camera can be set at 90° from the plane of the weld pool, so the behavior of weld pool can be seen entirely in both axes. Table 5.4 presents high-speed monitoring condition.

The photograph of weld pool phenomena be presented by original high-speed photograph to observe the liquid metal filling through the gap and the relative intensity image was transformed from the original high-speed photograph to obtain visualized evidence on weld energy respond. The jet color image was used for compare high temperature zone and low temperature zone on each welding condition. It was noted that the limitation of this single wavelength band pass filter is proper detection the temperature in the qualitative method. Spatial analysis and temporal analysis could be used for discuss only one set condition. Comparison the effect of welding parameter is not a proper way by single wavelength band pass filter because an out intensity unit is not absolute unit which able to compare the effect of change condition.

Welded specimens were evaluated to obtain the weld joint characteristics by a macro cross section which is cut in perpendicular welding direction. 3% solution was used for etching to reveal weld morphology.

Table 5.3 Welding parameters

Main heat source			
Laser type	Diode laser		
Laser irradiation type	Weaving		
Fiber core, mm	1.0		
Homogenizer	LL3		
Focus lens, mm	400		
Laser power, kW	6		
Laser irradiation angle, degree	15°		
Defocus, mm	20		
Spot size, mm x mm	4.5^w x 27^l		
Power density, W/mm^2	55		
Weaving wave form	Exponential		
Weaving frequency, Hz	5		
Compensate heat source			
Laser type	Fiber		
Compensated laser power, kW	Table 5.2		
Defocus, mm	200		
Spot diameter, mm	10		
Laser irradiation angle, degree	13		
Compensated pre-irradiation, s	10		
Hot-wire parameter			
Filler wire diameter, mm	1.2		1.6
Welding speed, cm/min (m/h)	3.33 (2)	5.0 (3)	6.67 (4)
Wire feed speed, m/min	8.91	12.25	9.94
Wire current, A	137	149	239
Wire feeding angle, degree	35		
Wire feeding position, mm	0		
Shielding gas (Argon), LPM	10		
Pre irradiation time, s	120		
Welding time, s	20		

Table 5.4 high speed monitoring condition

High speed camera	GX-5
Frame rate, fps	500
Aperture	Closed
Focus lens, focal length, mm	50
Band pass filter, nm/FWHM	810 / 10
Lighting	N/A
Shutter speed, s	1/20 k

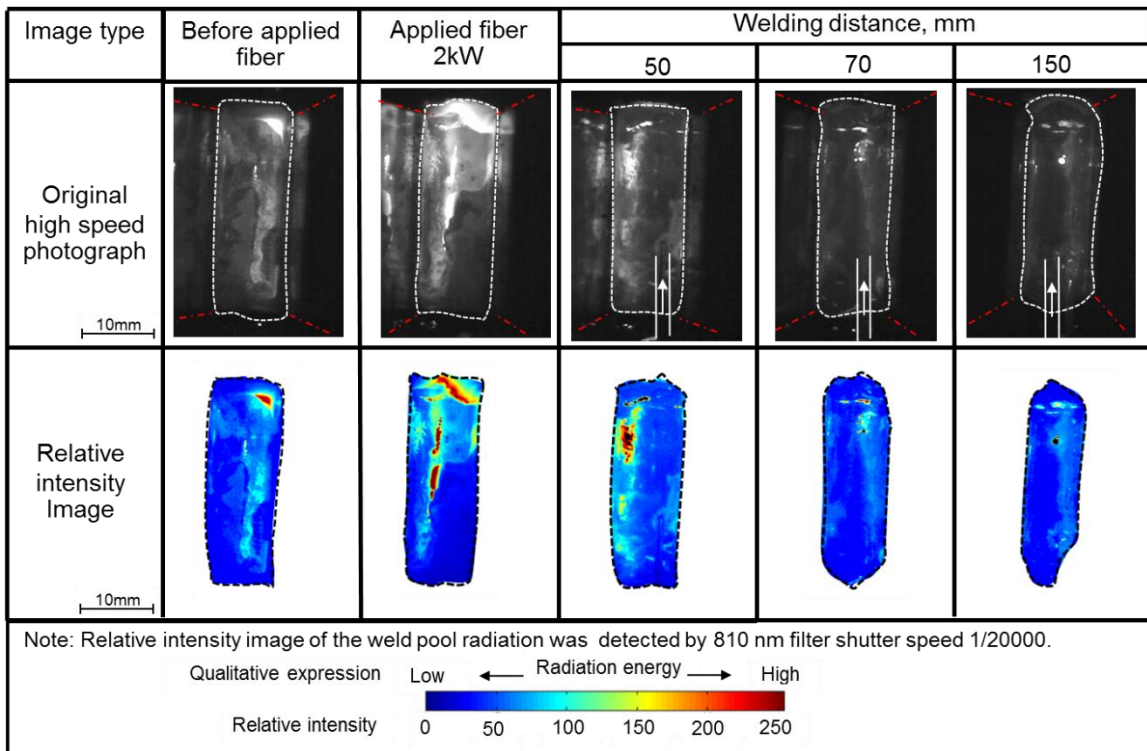### 5.2.3 Effect of compensate laser powers

Original captured high-speed images and relative intensity images of weld pool under three conditions of compensated laser power of 1, 2 and 3 kW were shown in Fig. 5.4 (a), (b) and (c), respectively. On each compensates laser power condition, weld pool situation was compared by the radiation energy on spatial (space) and temporal (time) perspective as a qualitative description.

In compensate laser power of 1 kW, it can be seen from Fig. 5.4 (a) that applied fiber laser on the edge side has affected radiation energy on the irradiated region. At the welding distance on 50 mm, the influence of applied laser power on edge side affected weld pool conduction and convection through the middle of joint thickness. However, after weld distance of 70 mm, radiate energy decreased but liquid metal still shows complete fulfill on the joint gap. Comparing on the weld pool radiation between the laser access side and wire access side, it was found that by compensation of 1 kW has the large gradient on weld pool radiation. It implies that weld penetration of this joint may show large penetration on the laser access side and narrow penetration on wire feeding side.

Image type	Before applied fiber	Applied fiber 1kW	Welding distance, mm		
			50	70	150
Original high speed photograph 10mm					
Relative intensity Image 10mm					
Note: Relative intensity image of the weld pool radiation was detected by 810 nm filter shutter speed 1/20000. Qualitative expression Low ← Radiation energy → High Relative intensity 0 50 100 150 200 250					

(a) Compensated laser power of 1 kW

Image type	Before applied fiber	Applied fiber 2kW	Welding distance, mm		
			50	70	150
Original high speed photograph 10mm					
Relative intensity Image 10mm					
Note: Relative intensity image of the weld pool radiation was detected by 810 nm filter shutter speed 1/20000. Qualitative expression Low ← Radiation energy → High Relative intensity 0 50 100 150 200 250					

(b) Compensated laser power of 2 kW

Image type	Before applied fiber	Applied fiber 3kW	Welding distance, mm		
			50	70	150
Original high speed photograph 10mm					
Relative intensity Image 10mm					
Note: Relative intensity image of the weld pool radiation was detected by 810 nm filter shutter speed 1/20000. Qualitative expression Low ← Radiation energy → High Relative intensity 0 50 100 150 200 250					

(c) Compensated laser power of 3 kW

Fig. 5.4 In-situed observation shows high speed photographs and relative intensity image of weld pool under influenced of compensated laser power by fixed welding speed of 3.33 cm/min (2m/h).

Compensation 2 kW (Fig 5.4 (b)) laser power showed the shading color of weld pool which used for represents radiate energy level more brightness than 1 kW laser power. It is not only region of the irradiated area but also overall weld pool area. When weld time increased (wire feeding and specimen moving) radiate energy has decreased similar case of 1 kW laser power. The gradient of radiate energy between laser access side and wire feeding side showed smaller than the case of 1 kW compensation. However, wire side has a trend of hard fulfill and energy decreased when welding time increasing.

Influenced of compensated laser power levels showed clearly when applied 3 kW laser power. The relative intensity image showed strong radiate energy or brightness shade overall weld pool. This welding condition has the potential of the large amount of base metal melting over joint thickness. Since as it was shown that overall energy distribution has almost high radiate energy even though welding time increased. Even though, the gradient of weld pool showed strongest radiate energy on laser irradiated region and low energy on wire feeding side when welding time increasing, overall radiate energy of weld pool still has a higher energy compared with 1 and 2 kW compensations.

By qualitative expression, in-situe observation showed the potential of compensation laser power level affected overall weld pool radiate energy or weld pool temperature. Increasing laser power on the edge side has affected weld pool energy increased.

Weld bead morphology and bead penetration on horizontal cross section were observed as shown in Fig. 5.5. Welded distance of 50 and 70 mm were used to investigate their effects. It is obviously shown that twin laser method or laser power compensation on the edge region of joint thickness could fixed insufficient fusion problem. All of compensated laser power levels showed complete fusion on the irradiated region. It was found from observation on the weld bead morphology that weld bead sizes on the laser access side has wider bead size than wire feeding side. It could be related through the result of in-situ observation on relative intensity image (Fig. 5.4) that wire feeding side showed the lower radiate energy of weld pool. Only condition of 3 kW compensation shows small differences weld bead sizes. On the other hands, 1 kW and 2 kW have been shown small imperfection on the edge region of wire feeding side. There are the small lock of fusion in the case of 1 kW and underfill weld for 2 kW compensation.

For investigation of the effect of laser power levels for compensation, Fig 5.6 shows measurement results of weld bead penetration along thickness distance. The results were obtained from 50 mm and 70 mm cross sections. For the section of 50 mm of 1 kW compensation shown complete fusion over joint thickness and has a maximum weld bead of 14.8 mm at the distance of 6 mm which was measured from the edge of laser side. While the section of 70 mm shown the maximum bead width of 14.7 mm on the distance of 6 mm, bead width became smaller when the distance over 20 mm, which showed only 9.0 mm or equal final gap size (gap had shrinkage during weld). Moreover, lack of fusion 3 mm length occurred on the edge of wire feeding side.

Bead width of 2 kW compensation (Fig. 5.6 (b)) shows both of sections have almost same of bead sizes, but the small imperfection of underfill size about 1 mm occurred on wire feeding side.

Highest level power of 3 kW compensation (Fig. 5.6 (c)) shows complete fusion and wider bead width sizes (large amount of base metal melting) of both sections. The maximum bead width of 18 mm (section of 70 mm) occurred at the edge of the specimen. However, overall bead width size of the section of 50 mm has larger section of 70 mm.
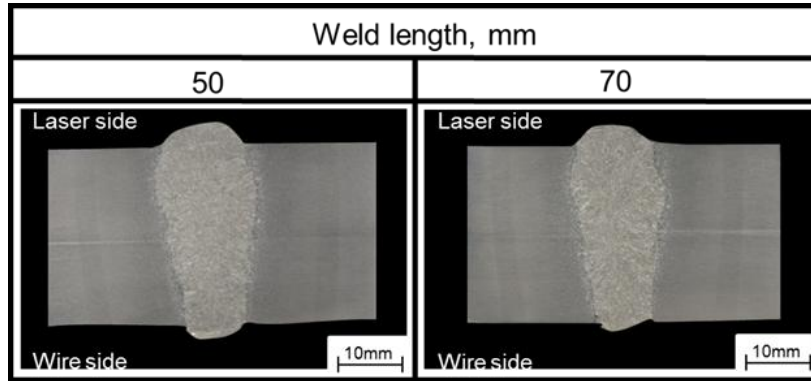
(a) Compensate laser power 1 kW
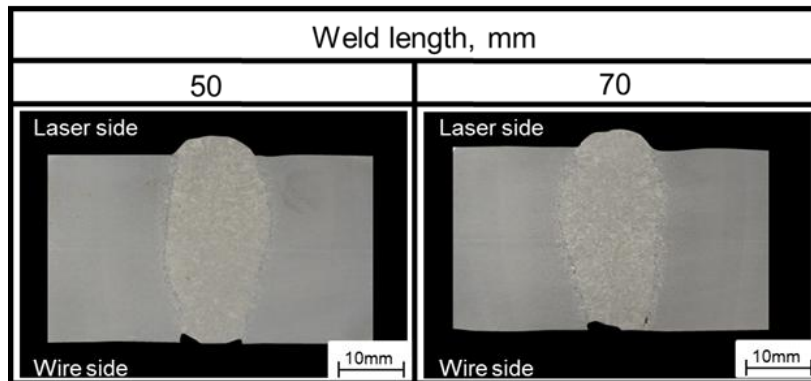
(b) Compensate laser power 2 kW
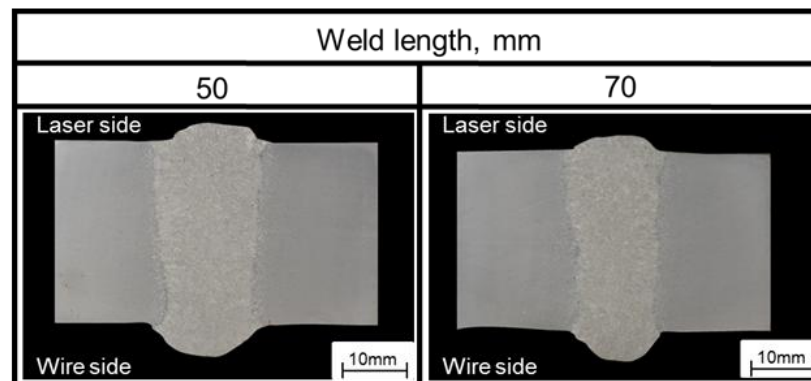
(c) Compensate laser power 3 kW

Fig. 5.5 Horizontal cross sections of twin laser method under influenced of compensated laser powers by fixed welding speed of 3.33 cm/min (2 m/h)
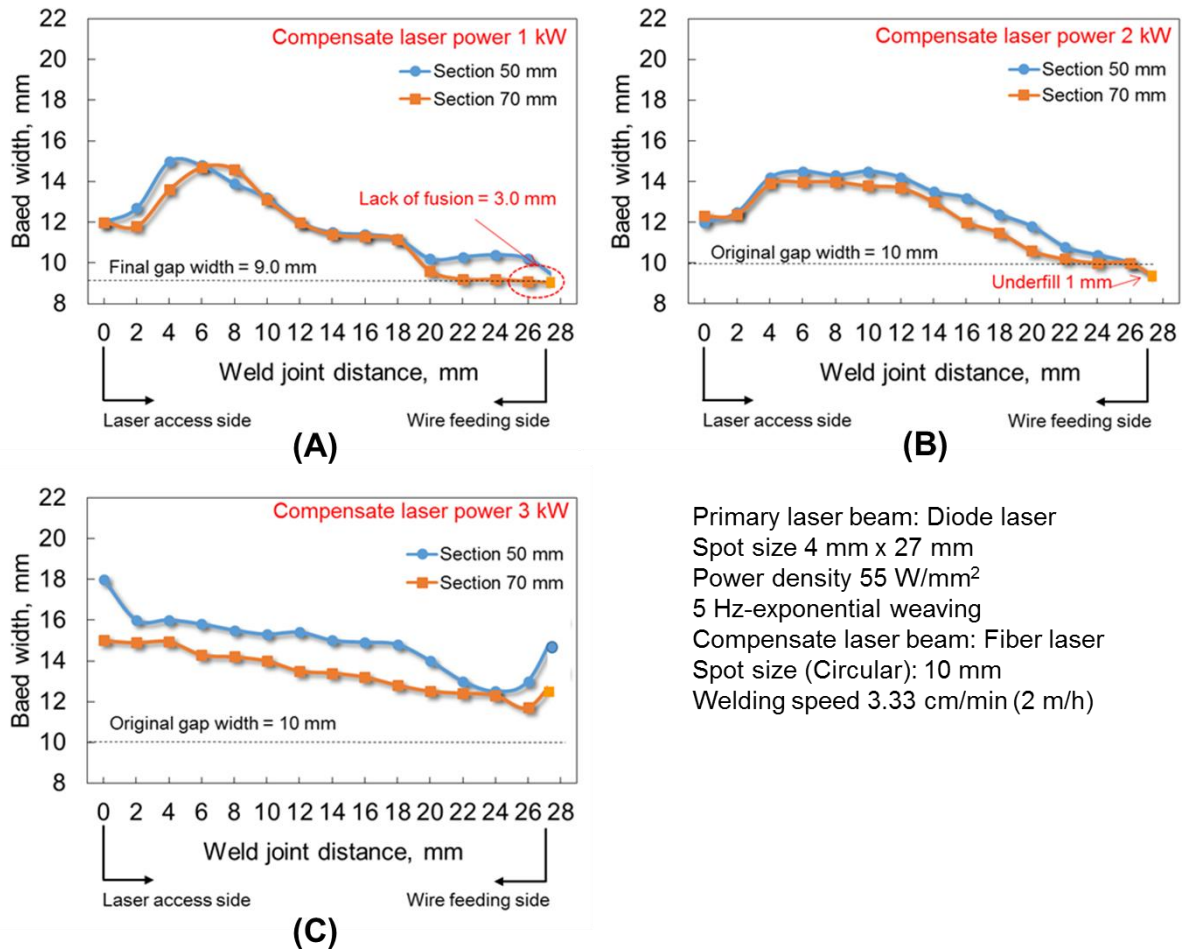
Fig 5.6 Measured results of bead width of weld metal of twin laser under influenced of compensated laser powers

5.2.4 Effect of welding speeds

According to the previous experiment, laser power for compensation of 3 kW has been showing complete fulfill and complete fusion. Then this condition was used for study welding speed effects on welded characteristics.
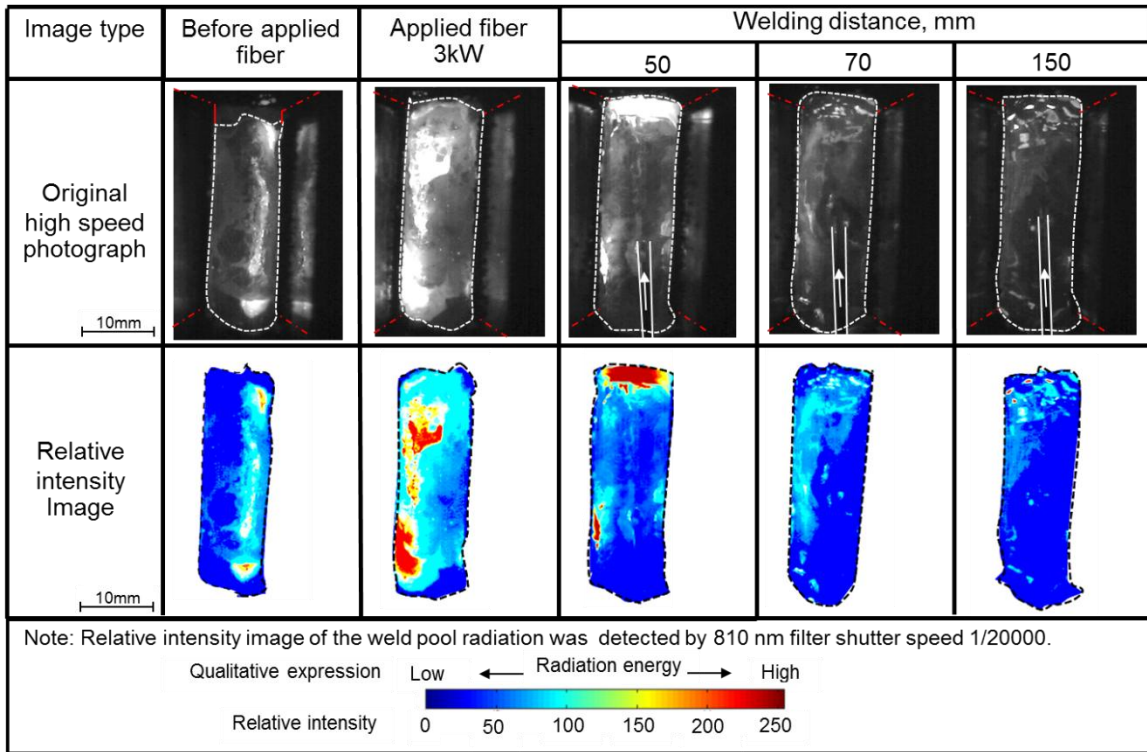
Fig. 5.7 (a), (b) and (c) show weld pool phenomena of welding speed of 3.33, 5.00 and 6.67 cm/min (2, 3 and 4 m/h), respectively. Original high-speed images show during hot wire feeding that welding speed does not strong affected weld metal fulfill. Relative intensity images show that welding speed affected the radiated energy of weld pool. It could be observed that increasing welding speeds the radiation on weld pool from the laser beam and radiate energy decreased, obviously. As for qualitative expression, they are a trend of increasing welding speeds have resulted of weld penetration decreased.

Welded specimens were cut and observed to obtain the effects of welding speed on weld bead morphology and bead width as shown in Fig. 5.8. All of welding speed ranges show complete weld metal fulfill. Welding speed does not affect weld metal fulfill in the case of 3 kW laser power. However, welding speed strongly affected weld penetration or melting efficiency, obviously. Increasing welding speed, weld penetration decreased. Especially, highest welding speed of 6.67 cm/min (4 m/h), both sections have weld bead size almost same groove width size. They have a trend of lack of fusion occur.
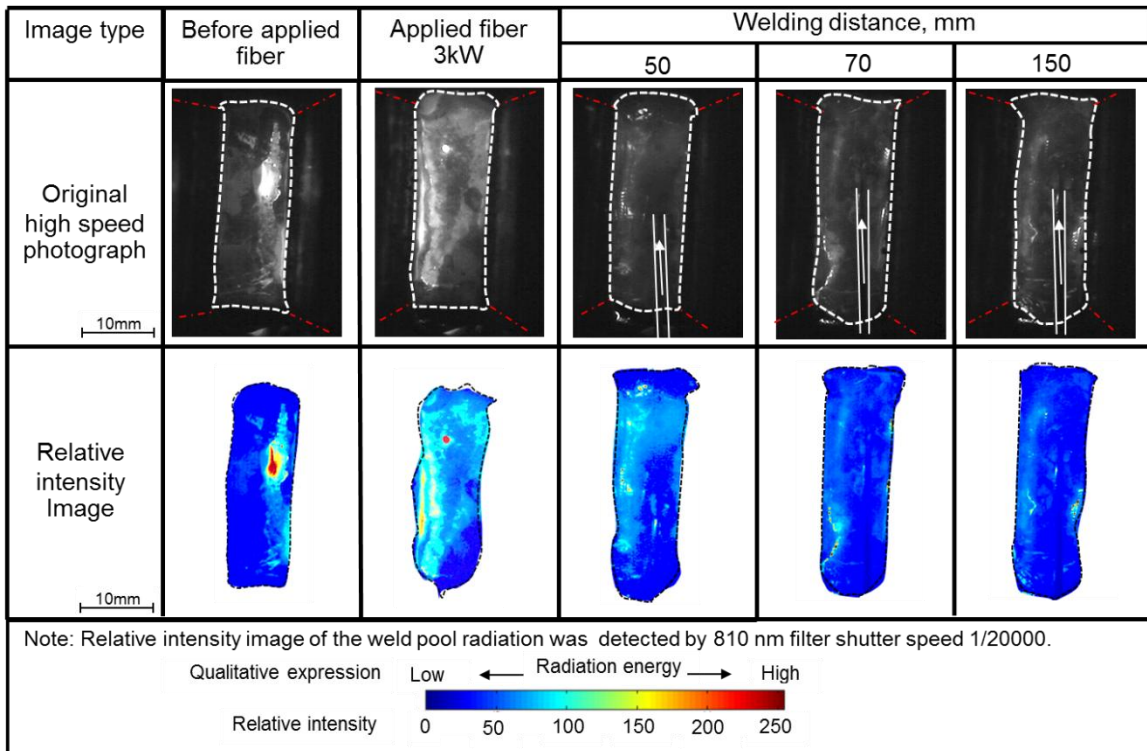
Measured results of weld bead width that shown in fig 5.9. The result of welding speed of 3.33 cm/min was used the data from the previous section (Fig 5.9 (a)). The welding speed of 5.00 cm/min showed both sections have results of complete fusion. Welded distance increasing (welding time), weld penetration few decreased, but they have almost same of the maximum bead width of 11.9 mm at edge region (laser side) and middle of joint thickness. Morphology of the section shows it has more penetration on the middle region of thickness. And it has low penetration under complete fusion on wire feeding side.

For welding speed of 6.67 cm/min (4 m/h), fig 5.9 (c) shows this condition has melting efficiency only half joint thickness for one side laser power compensation. Once of half side of wire feeding has low weld penetration and lack of fusion occurred on length of 5 mm on both sections. It was noticed that one side laser compensate hard achieved complete fusion for high-speed welding such 6.67 cm/min (4 m/h).

(a) Welding speed of 3.33 cm/min (2m/h)

(b) Welding speed of 5.00 cm/min (3m/h)

| Image type	Before applied fiber	Applied fiber 3kW	Welding distance, mm		
			50	70	150
Original high speed photograph 10mm					
Relative intensity Image 10mm					
Note: Relative intensity image of the weld pool radiation was detected by 810 nm filter shutter speed 1/20000.					
Qualitative expression Low ← Radiation energy → High					
Relative intensity 0 50 100 150 200 250					
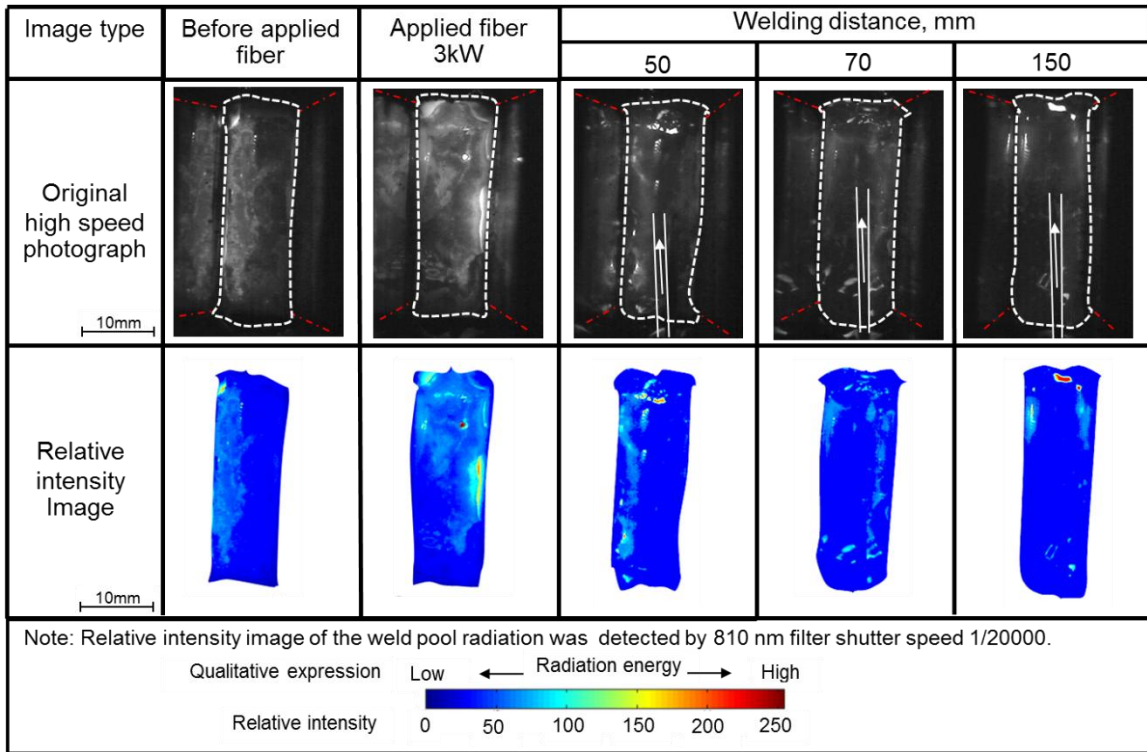
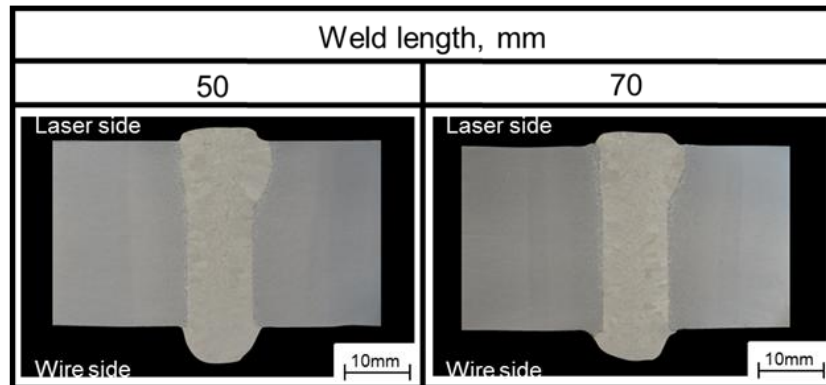(a) Welding speed of 6.67 cm/min (4m/h)

Fig. 5.7 In-situed observation shows high speed photographs and relative intensity image of weld pool under influenced of welding speed ranges by fixed compensated laser power of 3 kW.
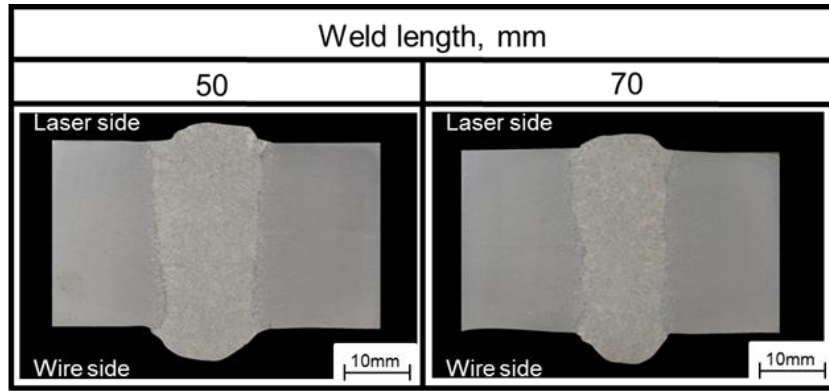
(a) Welding speed 3.33 cm/min (2 m/h)
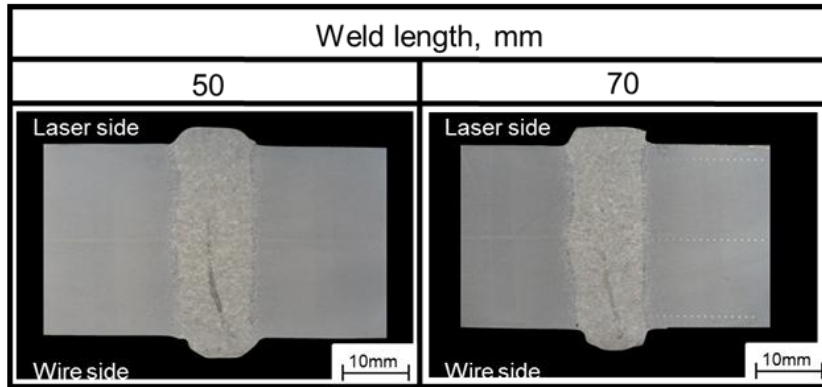
(b) Welding speed 5.00 cm/min (3 m/h)

(c) Welding speed 6.67 cm/min (4 m/h)

Fig. 5.8 Horizontal cross sections of twin laser method under influenced of welding speed ranges by fixed compensated laser power of 3 kW

(A)

(B)

Primary laser beam: Diode laser
Spot size 4 mm x 27 mm
Power density 55 W/mm^2
5 Hz-exponential weaving
Compensate laser beam: Fiber laser
Spot size (Circular): 10 mm
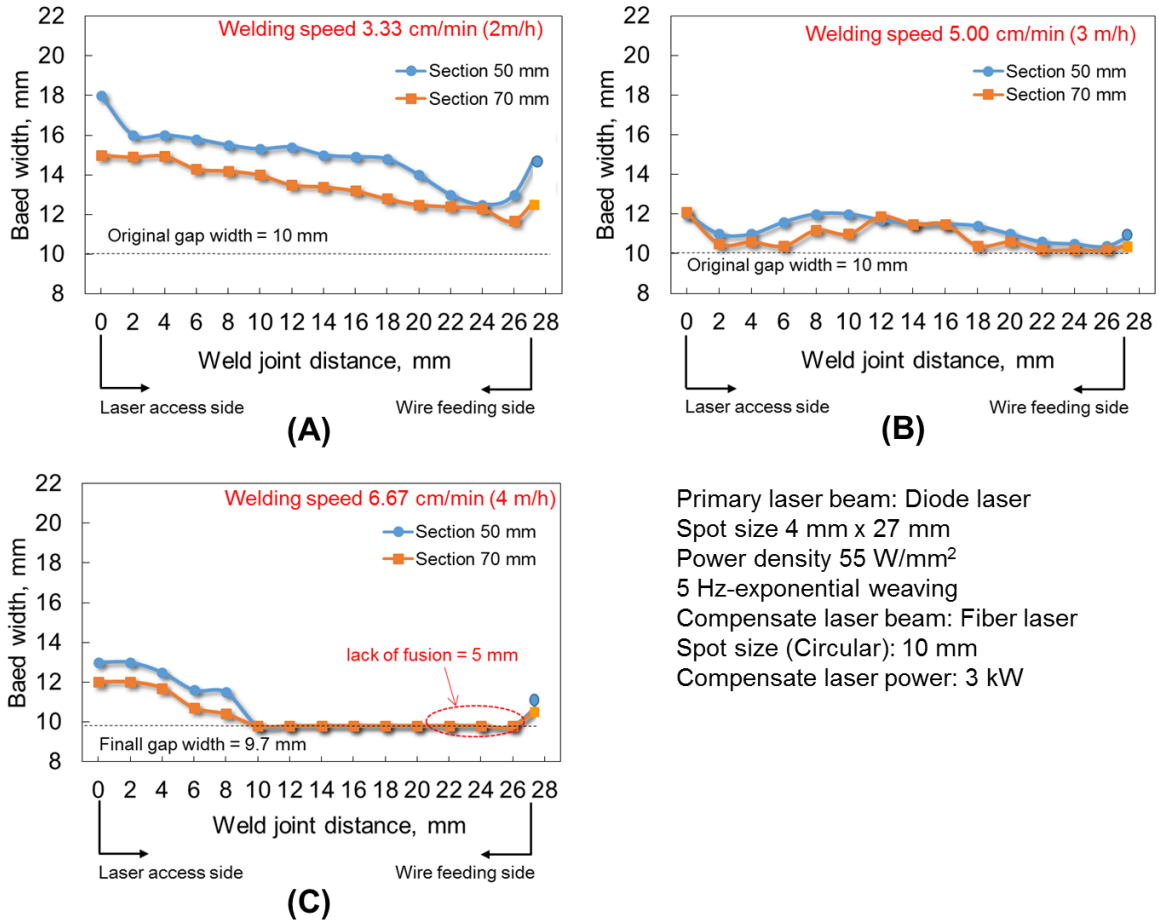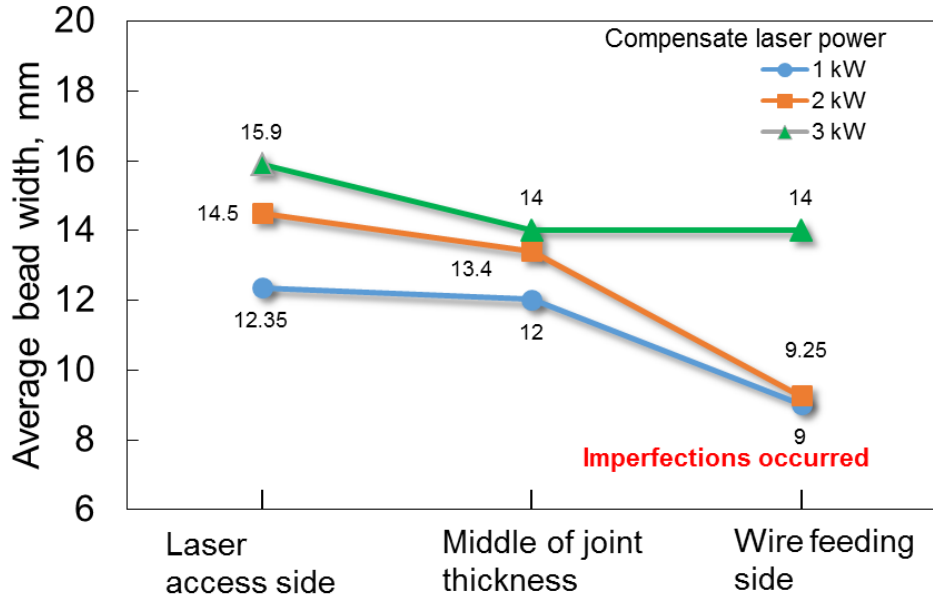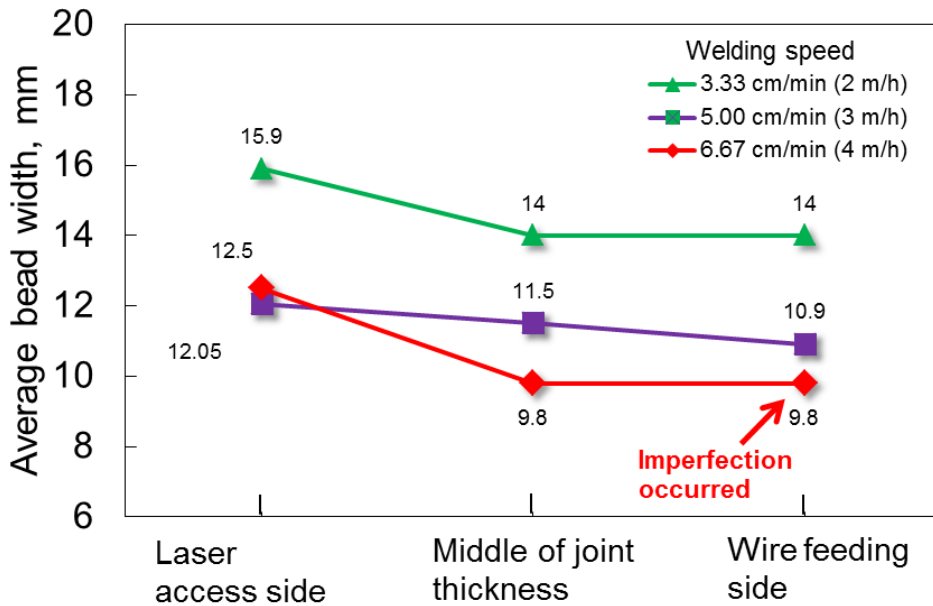Compensate laser power: 3 kW

(C)

Fig 5.9 Measured results of bead width of weld metal of twin laser under influenced of welding speed ranges

5.2.5 Parameter screen out of twin laser method with one edge side laser power compensation

By evaluating main effect of welding parameter of twin laser on melting phenomena, Fig. 5.10 shows the effect of compensate laser power levels (Fig. 5.10 (a)) and the effect of welding speed ranges (Fig 5.10 (b)) on the average bead width. The average bead widths were calculated from the measured results on cross-sections shown on fig 5.5 and 5.8. They were plotted as a function of 3 regions which were the laser access side, middle of joint thickness and wire feeding side to investigate the welding parameter effect on each location.

(a) Effect of compensated laser powers, fixed welding speed 3.33 cm/min

(b) Effect of welding speed range, fixed compensate laser power of 3 kW

Fig. 5.10 Main effect plot s to evaluate welding parameters

Fig 5.10 (a) shows the main effects of compensated laser power on the average bead width (melting amount of base metal). All of compensated laser power levels could fix insufficient fusion on the edge region. The edge region where compensated laser energy irradiated by fiber laser has more melting amount than that on middle zone and wire feeding side. The compensated laser power strongly

affected the melting amount. Increase of the compensate laser power by fiber laser resulted in base metal melting increase. Use of 3kW compensated laser power showed strong influence of the melting amount through the opposite side (wire feeding side) and this condition showed complete fulfill and complete fusion in the weld joint. In the case of compensated laser power of 1 and 2 kW, smaller influence of the melting amount slightly over half thickness (from the laser access side through the middle thickness, around 70% of joint thickness). Imperfections such as lack of fusion and underfill occurred on the edge of wire feeding side, and the maximum size was only 3 mm (Fig. 5.5 (a)). It can suggest that sound joint can achieve if compensate laser power at least 1 kW laser power irradiate on the both sides of edge regions. To control amount of base metal melting (dilution ration), compensate laser power of 3 kW is not necessary in case joining on thickness of 26 mm with welding 3.33 cm/min (2m/h). Moreover, it has a potential to reduces the laser power of original weaving beam for reduce the primary laser power level. As above mentioned, the experiment of twin compensate lasers on two edge sides should be performed to investigate the optimum energy profile of laser beam on the base metal melting characteristics. The optical equipment can be design for advanced joining on the heavy thick joint in the proposed welding process.

Since compensated laser power of 3 kW have high efficiency of joining, sound joint could be obtained by the large amount of base metal melting even though fiber laser applied only one edge side. Then this laser power compensation could be used for joining in the higher speed range to control the amount of melting (dilution ratio of weld metal) and heat input for joining (cooling rate). Fig 5.10 (b) shows the effect of welding speed range using fixed compensated laser power of 3 kW. Only welding speed of 6.67 cm/min (4 m/h) shows a small lack of fusion on the wire feeding side. Other speed ranges got the sound joint. Base on this result could be used to determine the optimization of welding speed range was investigated on the next experiment.

5.3 Optimization the laser parameters to achieve sound joint for twin laser method with one side laser power compensation

5.3.1 Materials used and specimen dimension

KE-47 steel plates were used in this study, the dimension of the specimen was 100 (width) x 200 (height) x 28 mm (thickness). Plates were fixed and aligned as a vertical joint configuration. The gap width was set by spacer (dimension of 10 (width) x20 (height) x 28 (thickness)). Fig. 5.11 shows specimen dimensions. The filler metal YM-80A (JIS3312 G78AUMN5C1 M3T) with a diameter of 1.6 mm was used since this size of filler wire could obtain stable feed over welding speed range for the experiment. The chemical composition of base metal and filler metal were presented on Table 5.5.
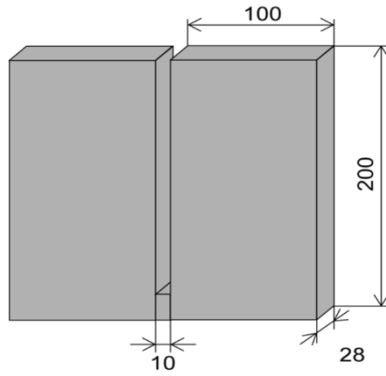
Figure 5.11 Specimen dimension and weld joint configuration

Table 5.5 Chemical compositions of materials used

Material	Chemical Composition, wt%											
	C	Si	Mn	P	S	Al	Cu	Ni	Nb	Ti	Cr	Mo
KE-47	0.09	0.364	1.56	0.01	0.002	No data						
YM-80A	0.07	0.5	1.6	0.009	0.004	-	0.03	-	-	-	-	-

5.3.2 Methodology of the twin laser beams and studied parameters design

The twin laser beams method was shown as a schematic illustration on Fig. 5.12. The primary laser beam irradiated by the diode laser source was utilized for main heat source for welding. The secondary laser beam irradiated by the fiber laser source was used for compensate energy ay the joint edge on the diode laser access side.
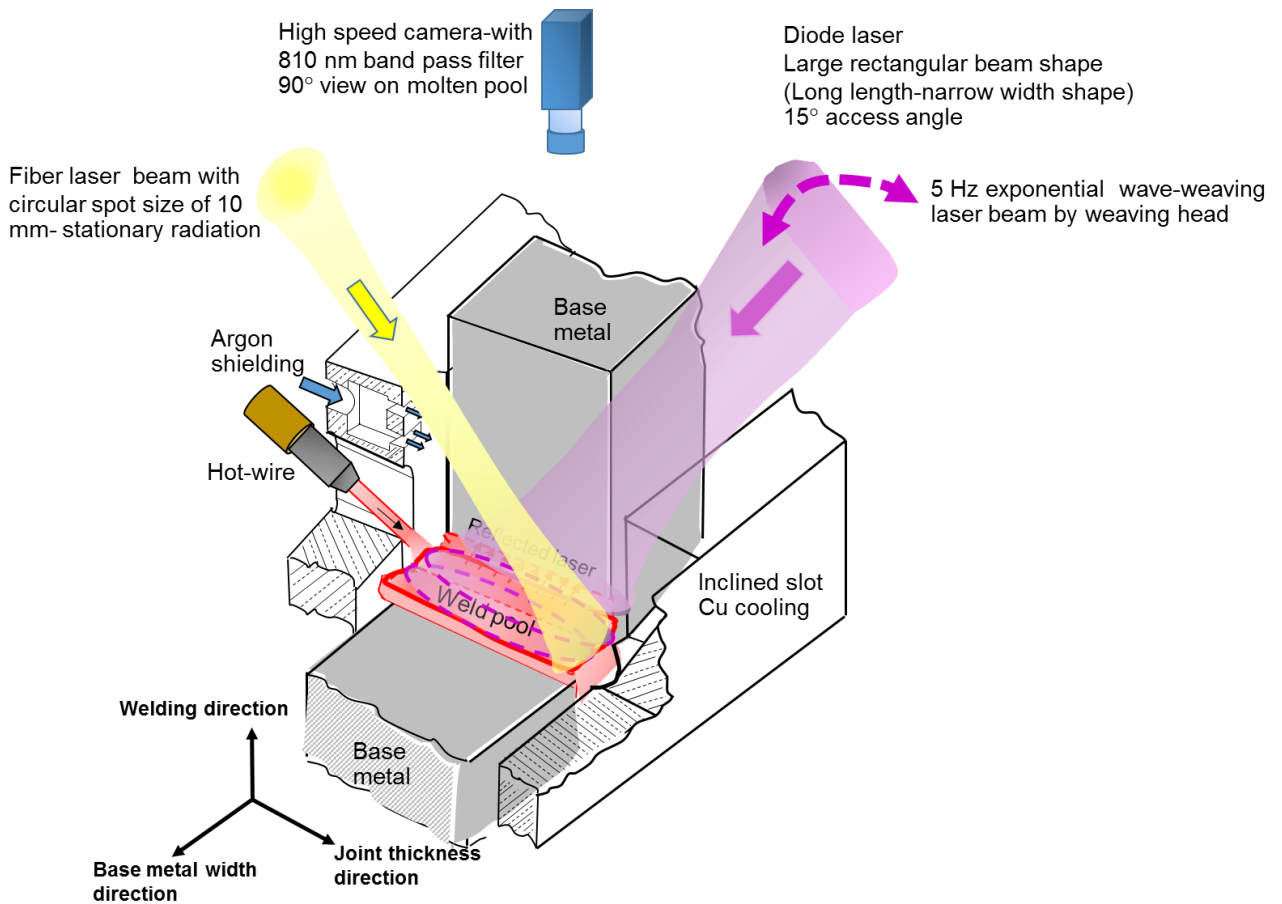
Figure 5.12 Schematic illustration of the twin laser beams method

Laserline LDF 6000-40 (6.0 kW) (continuous wave (CW) Diode Laser (LD)) was used to irradiate the diode laser beam. The twin laser beams method provided the weaving diode laser method for joining by reason of appropriate irradiating method for a wide gap size. The weaving parameter was set as 5 Hz-exponential waveform with parameter W_L/W_G ratio of 0.4 by the spot size of 4 mm x 27 mm. This optimum parameter was evaluated in the previous chapter. The oblique laser access with tilt angle 15° of the weaving head was set for shoot the weaving beam through the joint target by the defocus amount of 20 mm.

The fiber laser beam source is YLR-300-S (IPG 3.0 kW. It was irradiated by Yb-YAG (Ytterbium-Yttrium Aluminum Garnet, Y3Al5O12), with wavelength irradiates is 1070 nm. In this basic experiment of the twin laser beams, the stationary fiber laser was irradiated as circular spot shape with diameter of 10 mm and shoot through opposite side which laser head was handled by tilt angle of 13°. The centerline of the beam spot of the fiber laser was set at 3.33 mm from the outer edge of the specimen. The handling laser heads by two robots showed in Fig. 5.13.
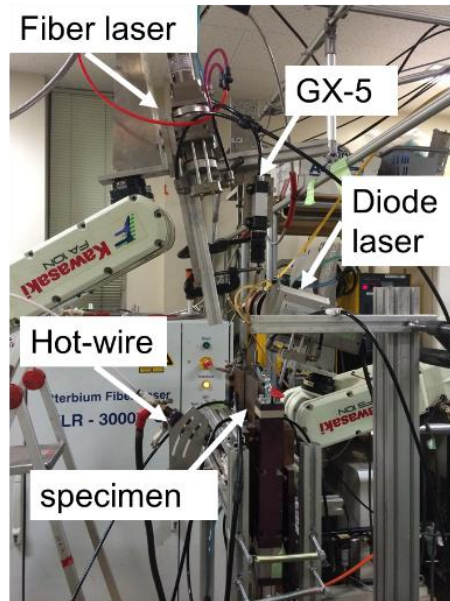
Figure 5.13 Set up the twin laser beams experiment.

One hot wire feeding system was set in the copper cooling jig which is located at the opposite side of the diode laser access side. The feeding angle was set at 35° to get feeding position of 5 mm from the joint edge. The environment was shielded by argon gas with flow rate 10 l/min from the same side of the hot-wire torch. The welding parameters was shown on Table 5.6 and welding conditions were shown on Table 5.7.

Studied parameters for the twin laser method was varied as welding speed ranges. The welding speed 3.33, 5.00 and 6.67 cm/min (2, 3 and 4 m/h) by fixed compensated laser power of 3 kW. The evaluation of weld characteristics was performed for the parameter optimization.

Table 5.6 Studied welding parameters

Compensate laser power, kW	Welding speed, cm/min (m/h)		
	3.33 (2)	5.00 (3)	6.67 (4)
3	O	O	O

Table 5.7 Welding parameters

Main heat source			
Laser type	Diode laser		
Laser irradiation type	Weaving		
Fiber core, mm	1.0		
Homogenizer	LL3		
Focus lens, mm	400		
Laser power, kW	6		
Laser irradiation angle, degree	15°		
Defocus, mm	20		
Spot size, mm x mm	4.5^w x 27^l		
Power density, W/mm^2	55		
Weaving wave form	Exponential		
Weaving frequency, Hz	5		
Compensate heat source			
Laser type	Fiber		
Compensated laser power, kW	3		
Defocus, mm	200		
Spot diameter, mm	10		
Laser irradiation angle, degree	13°		
Compensated pre-irradiation, s	10		
Hot-wire parameter			
Filler wire diameter, mm	1.6		
Welding speed, cm/min (m/h)	3.33 (2)	5.0 (3)	6.67 (4)
Wire feed speed, m/min	5.11	7.67	9.93
Wire current, A	174	208	245
Wire feeding angle, degree	35		
Wire feeding position, mm	0		
Shielding gas (Argon), LPM	10		
Pre irradiation time, s	90		
Welding time, s	20		

5.3.3 Investigation of weld appearances under influence of welding speed ranges

The first stage of investigation effect of welding speed, weld appearances on both side of the specimen (laser side and wire side) were investigated by visual inspection. Fig 5.14 shows selected weld specimen of welding speeds of 3.33, 5.00 and 6.67 cm/min (2, 3 and 4 m/h). It can be seen that the proposed process which improved by twin laser method has a good potential to be used for single-pass vertical joining. The recorded imperfections on each welding speed were shown in Fig 5.15. The Low welding speed (3.33 cm/min) has imperfection type of underfill when welding time increased since large gap shrinkage occurred on this condition. It was resulted in the laser beam could not access through the wire feed side because of gap closed. Then underfill occurred on the wire feeding side. However, it must be noted that this problem is caused from inadequate fixing parts on small specimens. For actual situation in ship construction (large structural sizes) does not occur the shrinkage problem. Welding speed 5.00 cm/min (3 m/h) shows the sound appearances on the both sides. It implies that this speed matches with laser power because welded appearances show stable formation overall the weld length. In case of the high welding speed of 6.67 cm/min (4 m/h), the small size of insufficient fusion occurred along edge region on the wire feeding side when welding distance over 100 mm.

5.3.4 Investigation of weld morphology under influence of welding speed ranges

Horizontal macro cross sections were shown in Fig 5.16. They were cut in the position of 50 mm to investigate the effect of welding speed on weld penetration. It can be seen that the increased welding speed resulted in the decreased weld bead sizes. Bead width morphology of welding speeds of 3.33 cm/min and 5.00 cm/min show a gradient change in the thickness direction. The bead width of the laser side is larger and the trend of its decrease toward the wire feeding side. Only welding speed of 6.67 cm/min, uniform bead width as same as groove width was decreased. Moreover, lack of fusion occurred along fusion boundaries in this side. These macro sections could be used for one confirmation that of the twin laser method has a stability to create weld joint under various welding speed ranges. Since as they had been shown same welded morphology on Fig 5.8.
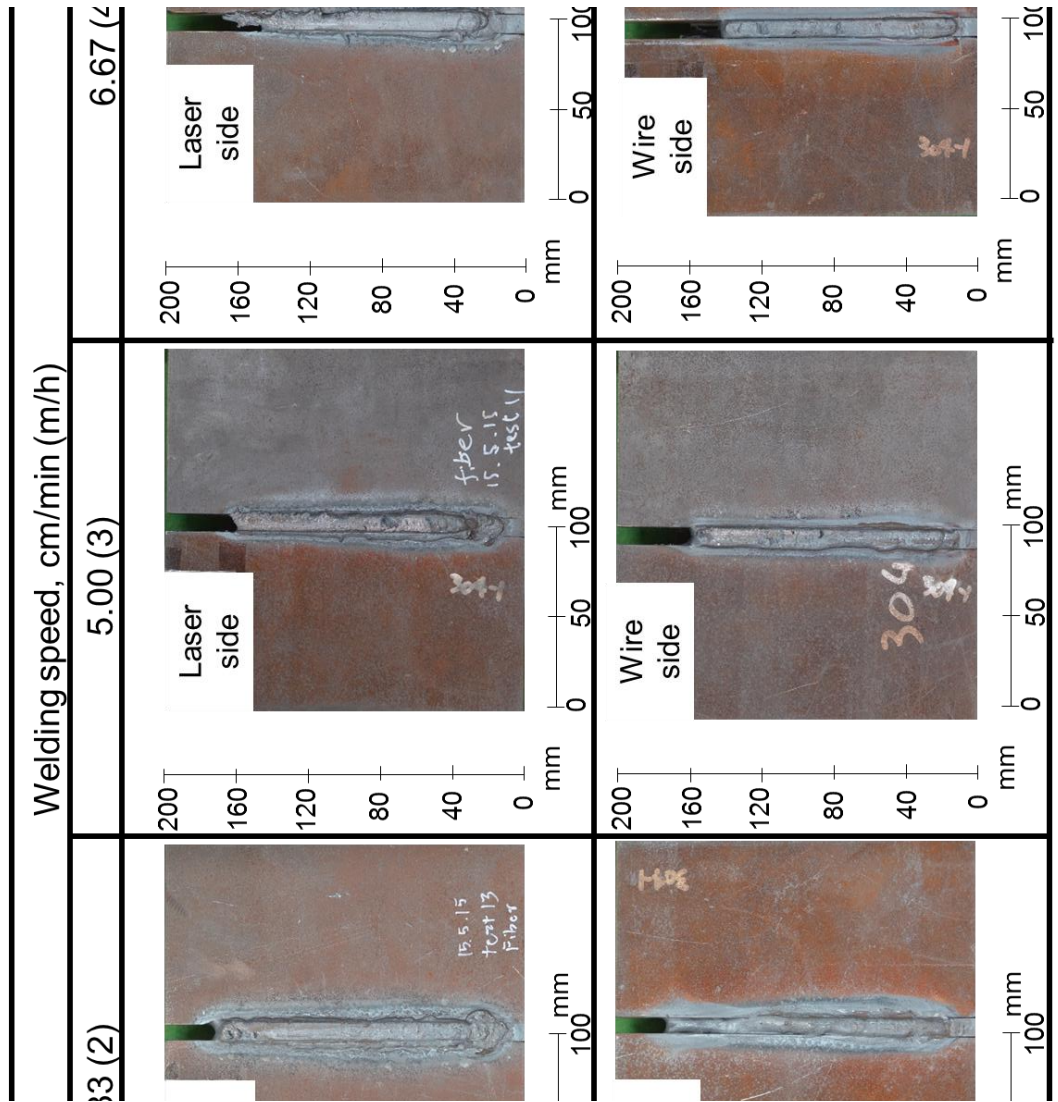
Fig.5.14 Appearances of welded specimens of twin laser method under welding speed affected
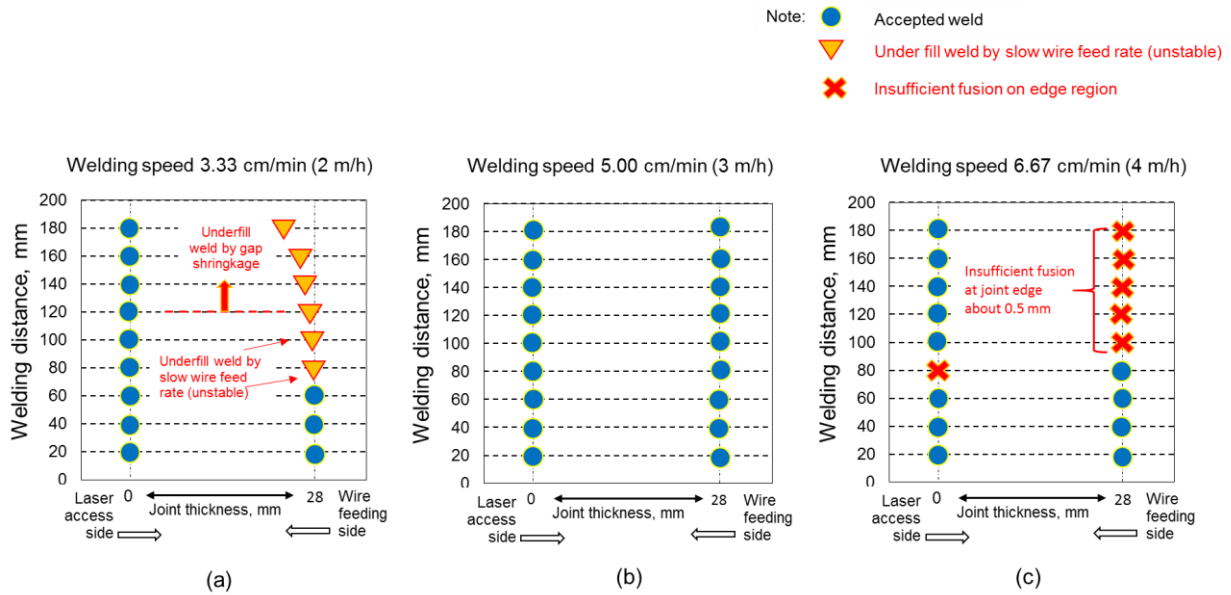
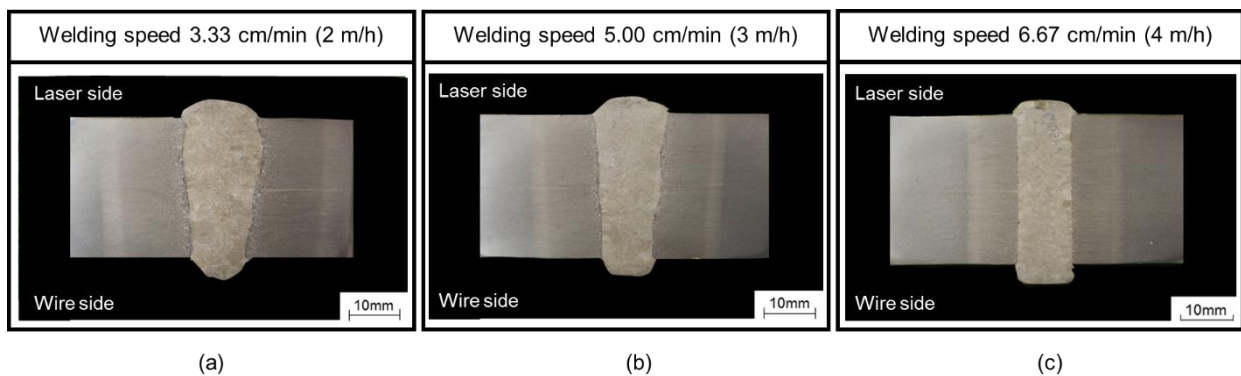Fig 5.15 Visual inspected results of weld appearances of twin laser method under welding speed affected.

Fig 5.16 Horizontal cross sections of twin laser method under welding speed affected. Sections cut at weld distance of 50 mm.

Measurement results of the bead width and imperfection under each welding speed were shown in Fig 5.17. The welding speed of 3.33 cm/min has the maximum bead width of 16.5 mm at the edge region of laser access side and minimum bead width of 10.6 mm at the opposite wire feeding side, distance of 26 mm (from laser edge side). The welding speed of 5.00 cm/min (3 m/h) has a maximum and minimum bead width of 15 mm and 10.2 mm, respectively, their locations are same as the welding speed of 3.33 cm/min. In case of welding speed of 6.67 cm/min (4 m/h), the maximum bead width of 12.5 mm was obtained at the edge region of laser side. Almost of the weld bead width was achieved but it contained the lack of fusion along fusion lines.

Primary laser beam: Diode laser
Spot size 4 mm x 27 mm
Power density 55 W/mm^2
5 Hz-exponential weaving
Compensate laser beam: Fiber laser
Spot size (Circular): 10 mm
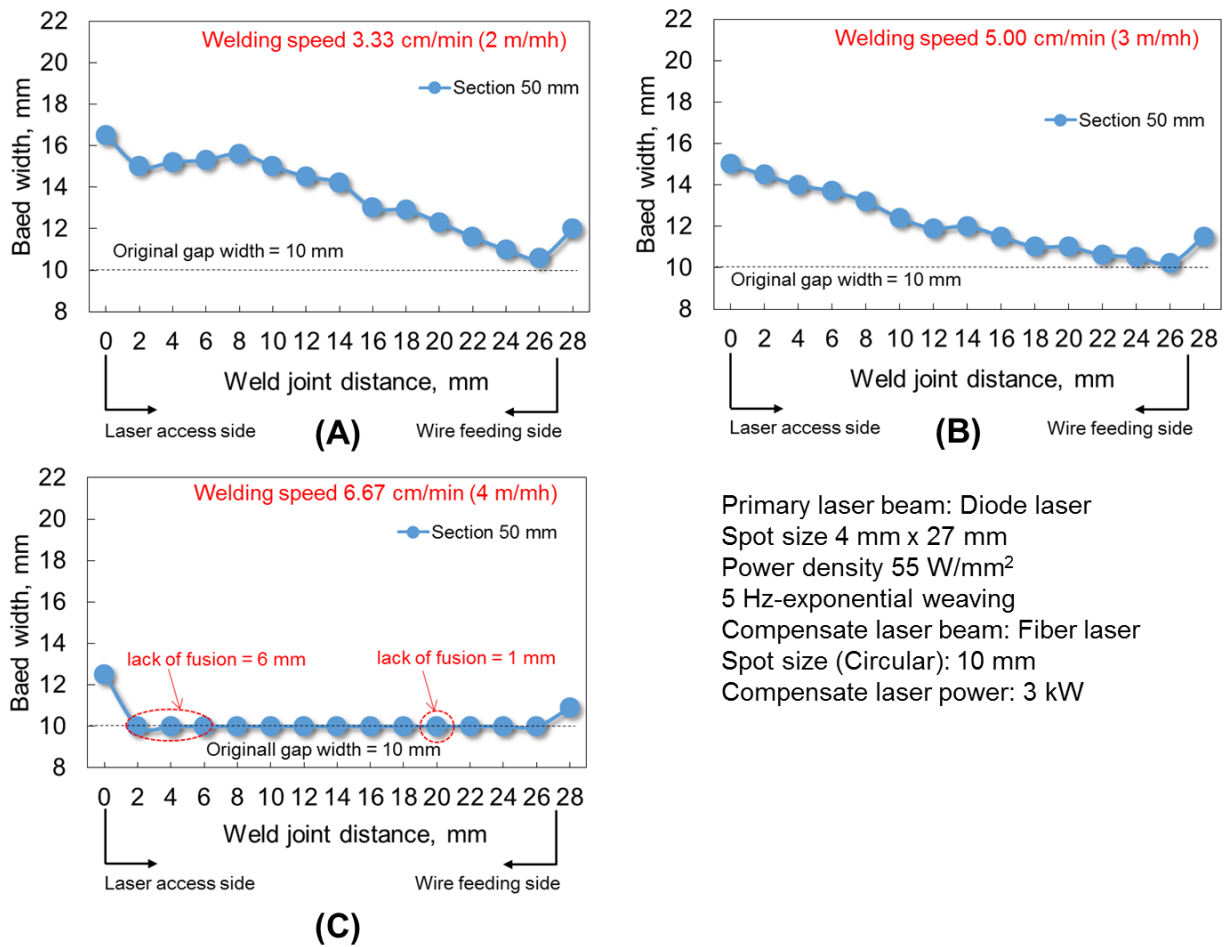Compensate laser power: 3 kW

Fig. 5.17 Measured results of bead width of weld metal of twin laser under influenced of welding speed ranges. Results were obtained from sections cut at weld distance of 50 mm.

5.4 Optimization of welding speed for twin laser method with one edge side laser power compensation

Combination results of weld appearances (visual inspection) and weld bead width (cross section) were used to discuss an optimization of the welding speed range. Fig 5.18 shows the average bead width and accumulated imperfection as a function of the welding speed. An optimized welding speed is 5.00 cm/min since it is free from defect occurrence and provides adequate melting amount or weld penetration.

Consider on the low welding speed of 3.33 cm/min that is also the achievement of sound weld joining. However, consideration of the optimization of joining process, it was shown that exceed dilution or large amount of base metal melting due to joining by the high heat input condition (high power input and low welding speed). Thus, this welding speed is an improper condition for compensate laser power of 3

kW. On the other hands, applying lower laser power of compensate such as 1 or 2 kW on both sides on edge region may proper than 3 kW by fixed this welding speed.

The high welding speed of 6.67 cm/min (4 m/h) shows lack of fusion and low dilution under the weaving parameter of 5 Hz-exponential waveform with W_L/W_G ratio of 0.4 by the spot size of 4 mm x 27 mm, using 6 kW irradiating power and compensate laser power of 3 kW. However, it shows lack of fusion occurred because of limited interaction time for base metal melting for this welding speed. To achieve the high welding speed such 6.67 cm/min (4 m/h), an advanced technique must be required precise control of the energy distribution along joint thickness direction by the special optical technique or higher power laser source.
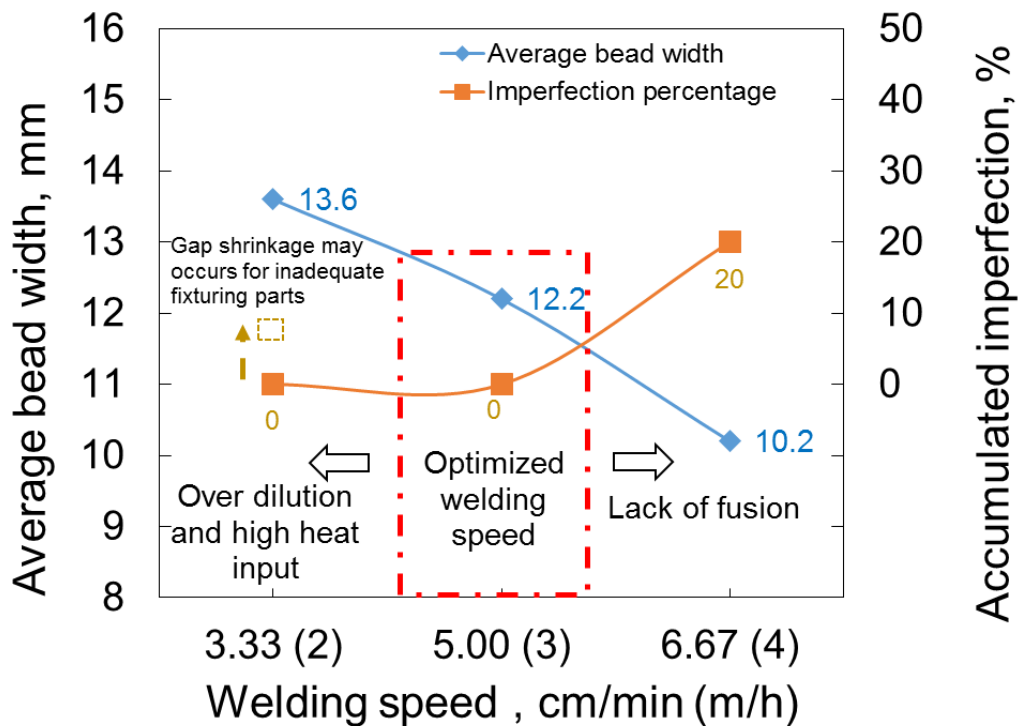

Fig. 5.18 Optimization of welding speed with average weld bead width and imperfection on twin laser welded joint.

5.5 Summary

In this chapter twin laser method was performed to improve weld joint quality for sound weld achievement. They could be drawn summary as follows.

1) Twin laser method has successfully applied on one pass vertical joining. Imperfection on edge region could be fixed by compensate laser power on the edge region.
2) For one side of compensate laser power, laser power levels strongly affected the melting amount of base metal. In the case of compensated laser power of 1 and 2 kW, smaller influence of the melting amount slightly over half thickness. Lack of fusion and underfill occurred on the edge of the wire feeding side, and the maximum size was only 3 mm. It can suggest that sound joint can achieve if compensate laser power at least 1 kW laser power irradiate on the both sides of edge regions.
3) Using 3 kW compensate laser power achieved complete fulfill weld metal and complete fusion of weld joint under fixed welding speed 3.33 cm/min (2 m/h). It was performed to study of welding speeds effects to optimize welding parameters.
4) The optimized welding speed for twin laser with one side compensation is 5.00 cm/min (3 m/h). It obtained complete fulfill and adequate weld penetration.
5) The low welding speed of 3.33 cm/min is also the achievement of sound weld joining. However, it was shown that the excessive weld dilution or large amount of base metal melting due to joining by the high heat input condition.
6) The high welding speed of 6.67 cm/min (4 m/h) shows lack of fusion and low dilution occurred because of limited interaction time for base metal melting. To achieve joining by this welding speed, an advanced technique must be required precise control of the energy distribution along joint thickness direction by the special optical technique or higher power laser source.

From the information of this chapter, it can be suggested that homogenizer for create laser beam shape should distribute higher energy on the edge tails on the laser beam. The center region can irradiate by lower energy since during joining heat conduction form both tail sides can provide adequate energy for fusion base metal.

Chapter 6

Weld metal characteristics

6.1 Introduction

This chapter has two main parts to study on a fusion zone for development on the proposed process. The first part, weld metal properties were obtained by twin laser parameters. Effect of welding speed on transformation cooling rate was investigated. The relationship between cooling rate in weld metal and microstructure was described to suggest a suitable filler metal for the proposed process. The Charpy impact test, the weld metal of the trial filler metal with high welding speed condition was performed. And the test result was evaluated with the relationship of welding condition and microstructure properties.

The second part was a feasibility study for suggestion the research method to develop the filler wire for the proposed process. For this section, the single diode laser method with low welding speed condition was employed to study the weld metal properties for the long cooling time condition. For the trial experiments, there are two experiment were performed. The experiment of investigation of the effect of the carbon equivalent of the weld metal microstructure and mechanical properties. And the experiment of the shielding condition with varied the oxygen content was performed to investigates the effects.

6.2 Study of metallurgical characteristics under influenced of welding parameters of the proposed welding process

Since the vertical joining by hot-wire laser method is original process, characteristics of cooling time range and transformation behaviors of fusion zone never established. Welding conditions have a feasibility area for joining (speed range could be varied) according to achievement of perfect joining by twin laser method. Therefore, this section has an objective to investigate the basic information of the relationship between the cooling time from 800-500 °C (hereafter will use as Δt8/5) and microstructure characteristics for the proposed welding process. The transformation cooling time, Δt8/5 is priority data for development of a matching filler metal for the proposed process. Filler metal type of JIS3312 G78AUMN5C1 M3T is trial filler metal in this section because filler metal could form finer microstructure and provide appropriate toughness value of weld metal from the previous experiment. Microstructure under various cooling rate from this experiment with YM-80A (JIS3312 G78AUMN5C1 M3T) are shown by associated results of Δt8/5, microstructure, the average size of prior austenite grain size and hardness.

6.2.1 Materials used and specimen dimension

KE-47 steel plates were used in this study, the dimension of the specimen was 100 (width) x 200 (height) x 28 mm (thickness). Plates were fixed and aligned as a vertical joint configuration. The gap width was set by spacer (dimension of 10 (width) x20 (height) x 28 (thickness)). Fig. 6.1 (a) shows specimen dimensions. Preparation for measurement of the cooling rate of fusion zone (weld metal) by thermocouple was shown on Fig. 6.1 (b). Small size hole at the center of base metal thickness was made. A thermocouple R type with diameter of 0.5 mm was preferential selected to monitor $\Delta t8/5$. A Tip of the thermocouple was set at around interface to make proper dip and read the temperature of the fusion zone. Ceramic insulator tube was used for the guide and protect another thermal effect in base metal during monitoring. By monitoring process, the thermocouple was connected to specified amplifier and PCD box. The sampling rate of 200 Hz was used to record the cooling rate.

The filler metal of YM-80A (JIS3312 G78AUMN5C1 M3T) with a diameter of 1.6 mm was used since this size of filler wire could obtain sTable feed on all welding speed range for the experiment. The chemical composition of base metal and filler metal were presented on Table 6.1.
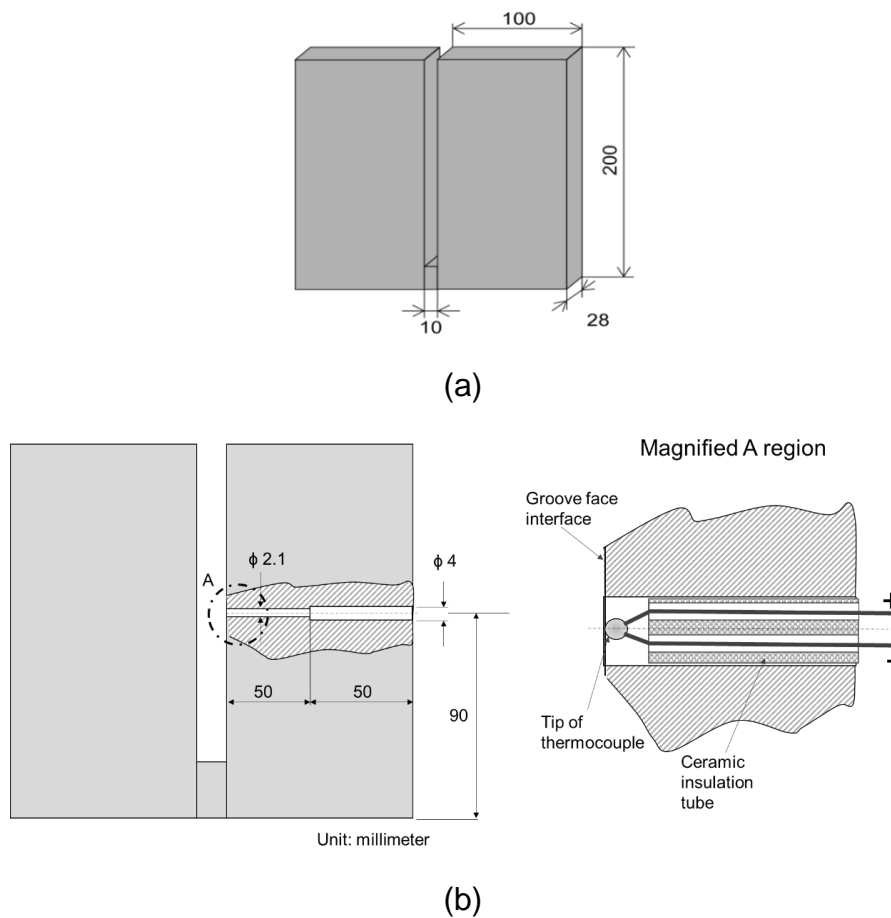

(a)

(b)

Fig. 6.1 Specimen dimension and weld joint configuration (a) and schematic illustration of a preparation of temperature (cooling) measurement for fusion zone (b)

Table 6.1 Chemical compositions of materials used

Material	Chemical Composition, wt%											
	C	Si	Mn	P	S	Al	Cu	Ni	Nb	Ti	Cr	Mo
KE 47	0.09	0.07	1.52	0.007	0.002	0.014	0.32	0.69	0.01	0.01	0.02	0.00
YM-80A	0.06	0.4	1.69	0.006	0.003	-	0.20	3.01	-	0.05	0.46	0.29

6.2.2 Methodology of the twin laser beams method

The experiment of this section uses welding parameters set same as welding parameters of the chapter 5 section 5.2.5. Since that is feasible welding range of twin laser method.

The twin laser beams method was shown schematic illustration on Fig. 6.2. The primary laser beam irradiated by diode laser source was utilized for main heat source for welding. The secondary laser beam irradiated by fiber laser source was used as the compensate energy at the joint edge of the diode laser access side (one-side laser power compensation). Table 6.2 showed welding parameters for joining in the experiment. Welding speeds of 5.00 and 6.67 cm/min were investigated in this study.
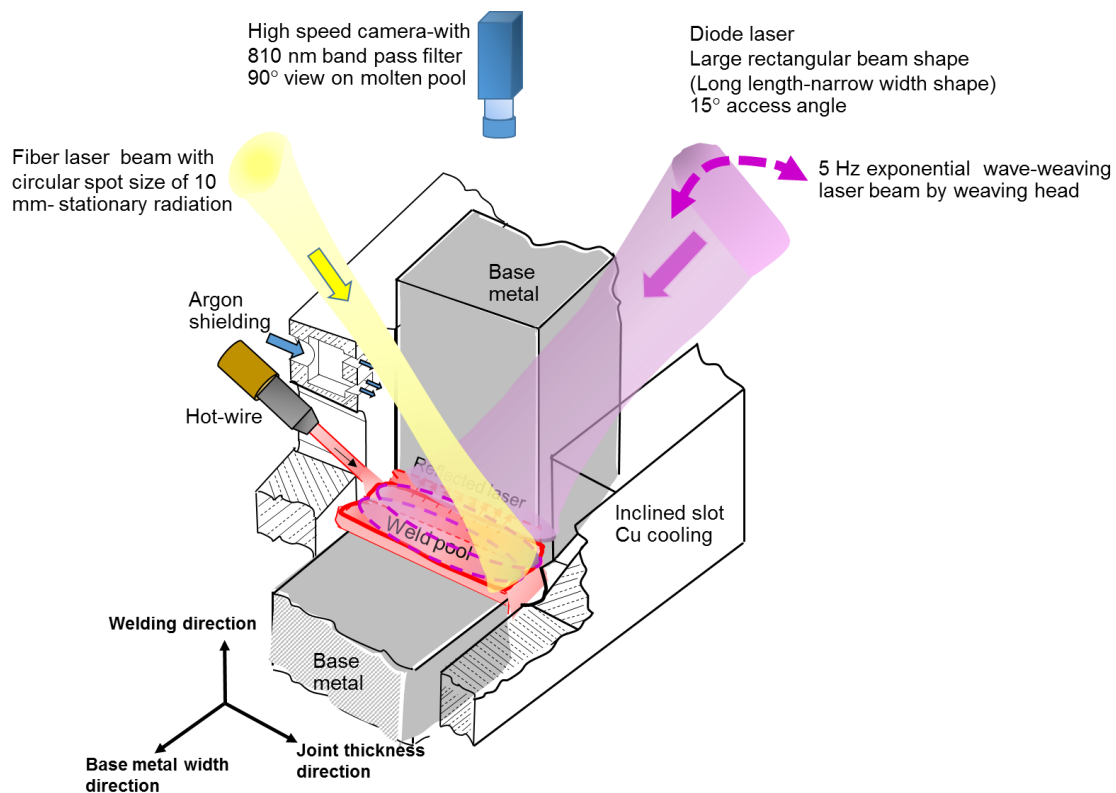

Figure 6.2 Schematic illustration of the twin laser beams method

Table 6.2 Welding parameters

Main heat source			
Laser type	Diode laser		
Laser irradiation type	Weaving		
Fiber core, mm	1.0		
Homogenizer	LL3		
Focus lens, mm	400		
Laser power, kW	6		
Laser irradiation angle, degree	15°		
Defocus, mm	20		
Spot size, mm x mm	4.5^w x 27^l		
Power density, W/mm^2	55		
Weaving waveform	Exponential		
Weaving frequency, Hz	5		
Compensate heat source			
Laser type	Fiber		
Compensated laser power, kW	3		
Defocus, mm	200		
Spot diameter, mm	10		
Laser irradiation angle, degree	13°		
Compensated pre-irradiation, s	10		
Hot-wire parameter			
Filler wire diameter, mm	1.6		
Welding speed, cm/min (m/h)	3.33 (2)	5.0 (3)	6.67 (4)
Wire feed speed, m/min	5.11	7.67	9.93
Wire current, A	174	208	245
Wire feeding angle, degree	35		
Wire feeding position, mm	0		
Shielding gas (Argon), LPM	10		
Pre irradiation time, s	90		
Welding time, s	20		

6.2.3 Cooling curve of weld metal of twin laser beams method

The thermal history of weld metal of 2 welding speeds (raw temperature cycle chart) were obtained and presented on Fig. 6.3. It can be seen that original two cooling history have a difference of temperature depended on welding speed ranges. They were satisfied the cooling from the experiment that be able to evaluate in material transformation characteristics.
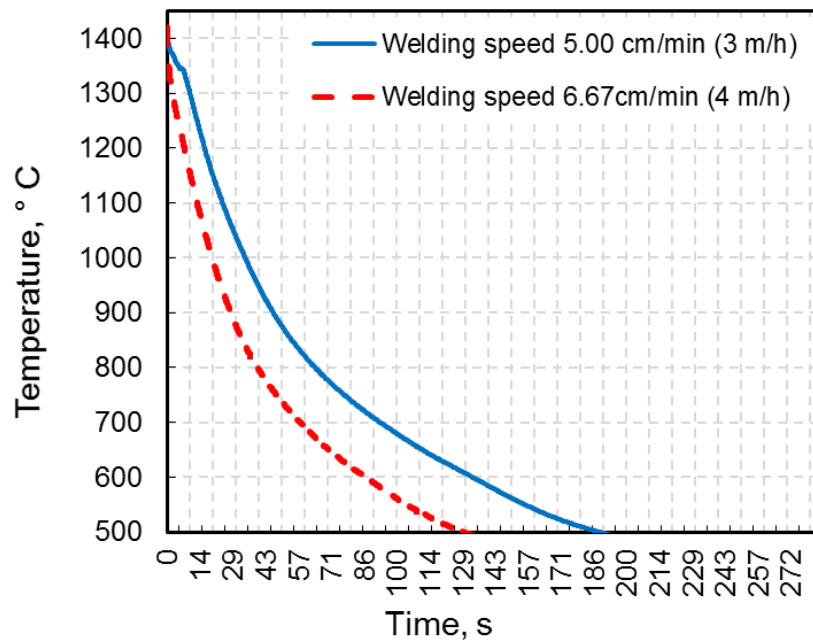

Fig 6.3 Thermal (cooling) history of welding speed of 5.00 cm/min and 6/67 cm/min (3 and 4 m/h)

Fig. 6.4 (a) shows the original result of 2 cooling curves under of the welding speed of 5.00 cm/min and 6.67 cm/min (3 and 4 m/h). The cooling curves were plotted in the temperature range from 800 to 500 °C which is useful information to evaluate phase transformation and mechanical properties of weld metal. Cooling curve for the welding speed of 3.33 cm/min (2 m/h) was obtained because of unsTable condition such as gap shrinkage and unsafe condition on present equipment due to high heat input condition. Then the original results could be obtained by the middle-speed range and high-speed range. However, Fig. 6.4 (a) shows clearly good resolution of significant differences of their cooling times (Δt8/5), 84 second is cooling time for the welding speed of 6.67 cm/min and 123 second is cooling time of welding speed of 5.00 cm/min. It is implied that the low welding speed of 3.33 cm/min (2 m/h) would has longer cooling time from their results. Therefore, estimated cooling curve for the welding speed of 3.33 cm/min was presented which

composed on two original cooling curves in Fig. 6.4 (b). Cooling time over 200 seconds was expected for the low welding speed of 3.33 cm/min.

This cooling curve of the proposed process pattern for consider of filler metal development. Since as these welding conditions are a feasible condition to joining. The continuous cooling curves will be related with corresponding results of microstructure constituents, hardness and so on which they depend on the type of filler metal (chemical composition) and dilution amount of weld metal.
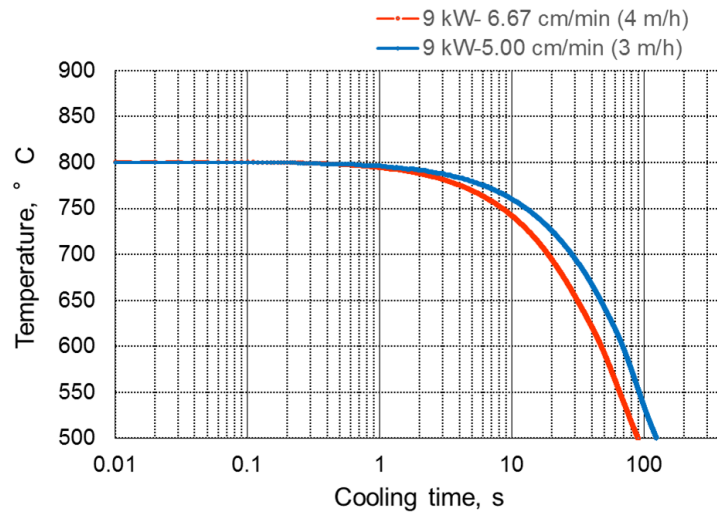
(a)
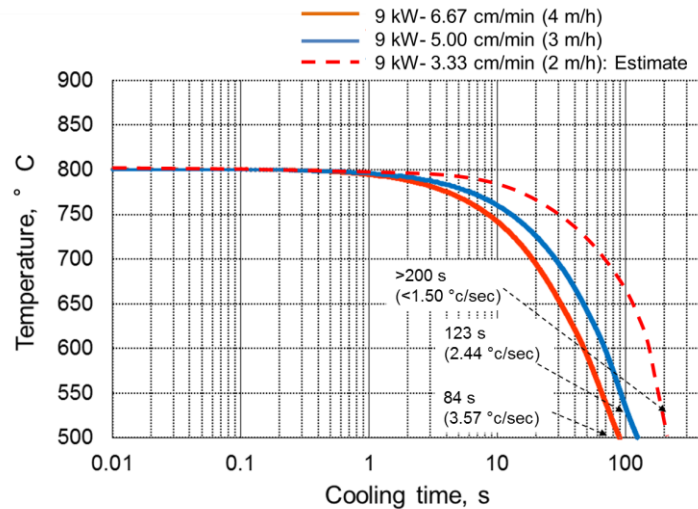
(b)

Fig. 6.4 Continues Cooling diagram of twin laser beams method with welding speed ranges of (a) 5.00 and 6.67 cm/min and (b) modified diagram for estimation of welding speed of 3.33 cm/min.

6.2.4. The relationship between cooling time and metallurgical characteristics of weld metal

This section has an objective investigate the relation of cooling time and microstructure characteristics using the selected filler metal for joining by the proposed welding process. YM-80A (JIS3312 G78AUMN5C1 M3T) is selected as a filler metal to study weld metal characteristics and properties in preliminary experiment. This filler metal has been investigated by K. Hashida [89] and Masuda [90], it provided intragranular microstructure type which desired microstructure of high-performance weld metal structure. Consequently this filler metal provided good potential of mechanical property such toughness value on the proposed process under 5 mm gap size situation (speed 3 m/h).

The welded results from the experiment using the twin laser method which followed the procedure as previous were obtained with filler metal of JIS3312 G78AUMN5C1 M3T. Fig. 6.5 (a), (b) and (c) show horizontal cross sections, measure values of dilution ratio and cooling time:Δt8/5 for welding speeds of 3.33, 5.00 and 6.67 cm/min (2, 3 and 4 m/h), respectively. These results showed that dilution amounts decreased with the increase of welding speed. However, in this study need to neglect the effect of the dilution ratio in order to discuss only effect of welding speed.

Microstructures on weld metal (fusion zone) under each welding speed were presented by OM (optical microscopic) image and SEM image on Fig. 6.6 and 6.7, respectively. 3 regions of the laser access region, middle of joint thickness and wire feeding regions were observed. Sections were etched by 3% Nital solution to reveal primary microstructures. Magnification of 500 x was used to observe to overall investigate microstructure outcomes.

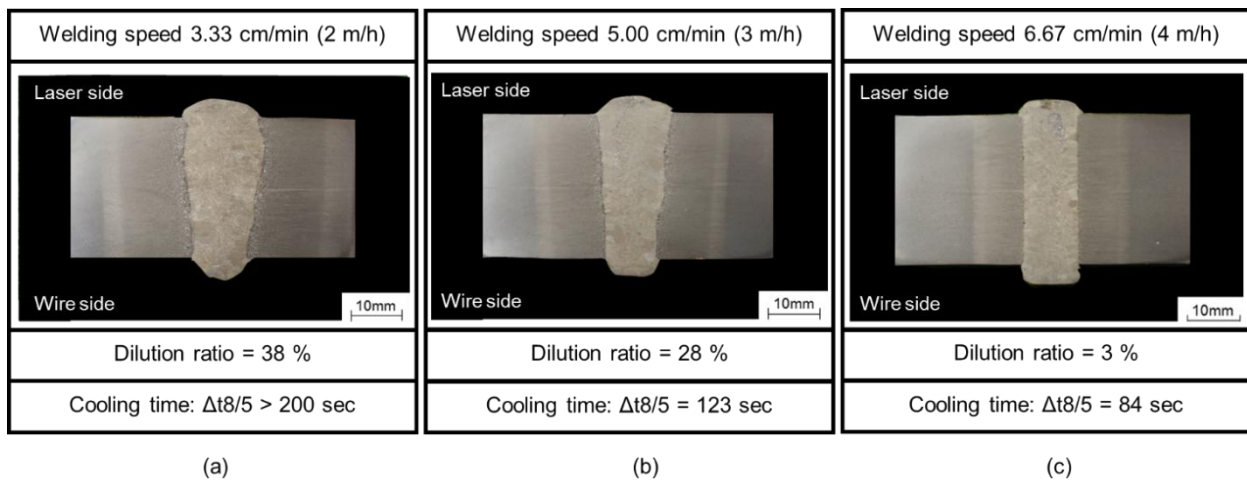| Welding speed 3.33 cm/min (2 m/h)	Welding speed 5.00 cm/min (3 m/h)	Welding speed 6.67 cm/min (4 m/h)
Laser side … Wire side … 10mm	Laser side … Wire side … 10mm	Laser side … Wire side … 10mm
Dilution ratio = 38 %	Dilution ratio = 28 %	Dilution ratio = 3 %
Cooling time: Δt8/5 > 200 sec	Cooling time: Δt8/5 = 123 sec	Cooling time: Δt8/5 = 84 sec
(a)	(b)	(c)

Fig 6.5. Horizontal cross sections of welding speeds of (a) 3.33, (b) 5.00 and (C) 6.67 cm/min.

In Fig. 6.6 of OM image, upper bainite (UB) which morphology of ferrite (white) plate –with aligned carbide or non-aligned carbide was clearly observed. On the other hand, finer black phase was not identified clearly by OM observation but SEM investigation could identify it as martensite phase (M). Fig. 6.7 shows enhance microstructure morphology between upper bainite and martensite. Fine lower bainite (LB) was also observed by high magnification of 5,000 x as shown in Fig. 6.8. It can be seen that nonlamellar aggregate carbide occurs in the small size of ferrite plate which formed in the main part of martensite (M). However, for phase counting in this case, martensite and lower bainite was preferentially combined as M+LB. Because, the objective of phase counting is to relate the fraction of brittle phase and non-brittle phase to toughness property. Then, the simple way for identification, it could be mentioned that upper bainite (UB) and martensite+lower bainite (M+LB) are predominantly microstructures in the weld metal of the selected filler metal. As for quantitative descriptions on metallurgical properties the fraction of these two major phase was used to analyze the effect of welding conditions. Prior austenite grain boundary was obtained by this etched and it will be also used for quantitative descriptions (size) on the future parts.

The use of filler metal of YM-80A (JIS3312 G78AUMN5C1 M3T) for joining in this process. Intergranular formation such GB allotriomorphic ferrite and widmanstatten ferrite never been observed all of welding speed conditions. Even though the low welding speed was used, intergranular microstructures never occured.

Observation of welding speed effect by OM images and SEM images that found that the increase of welding speed resulted in the increase of martensite phase. Moreover, it can be seen that upper bainite became small when welding speed increases. By observation of differences regions, there are not significantly differences of type and size (visual observation) of microstructures on each welding speed.

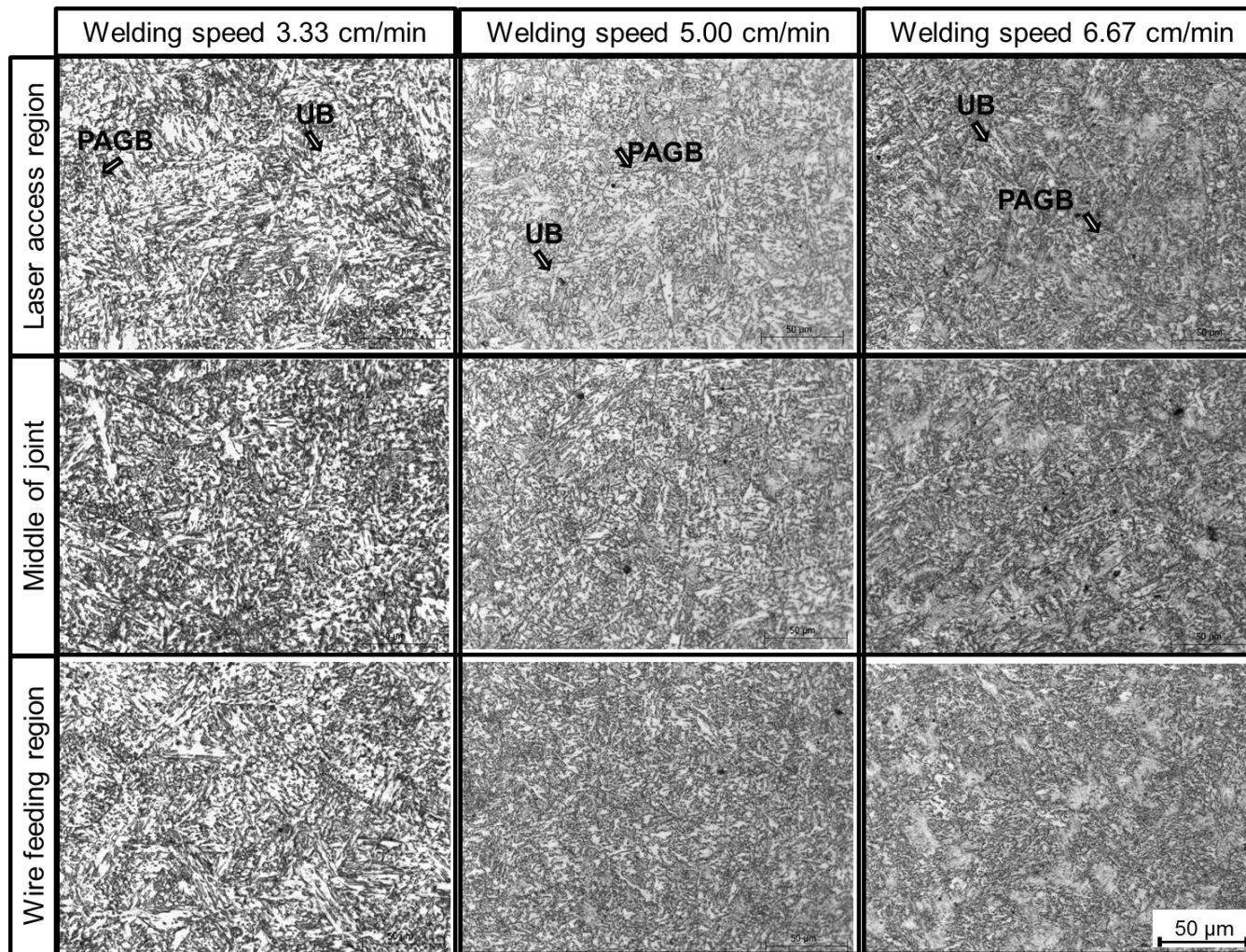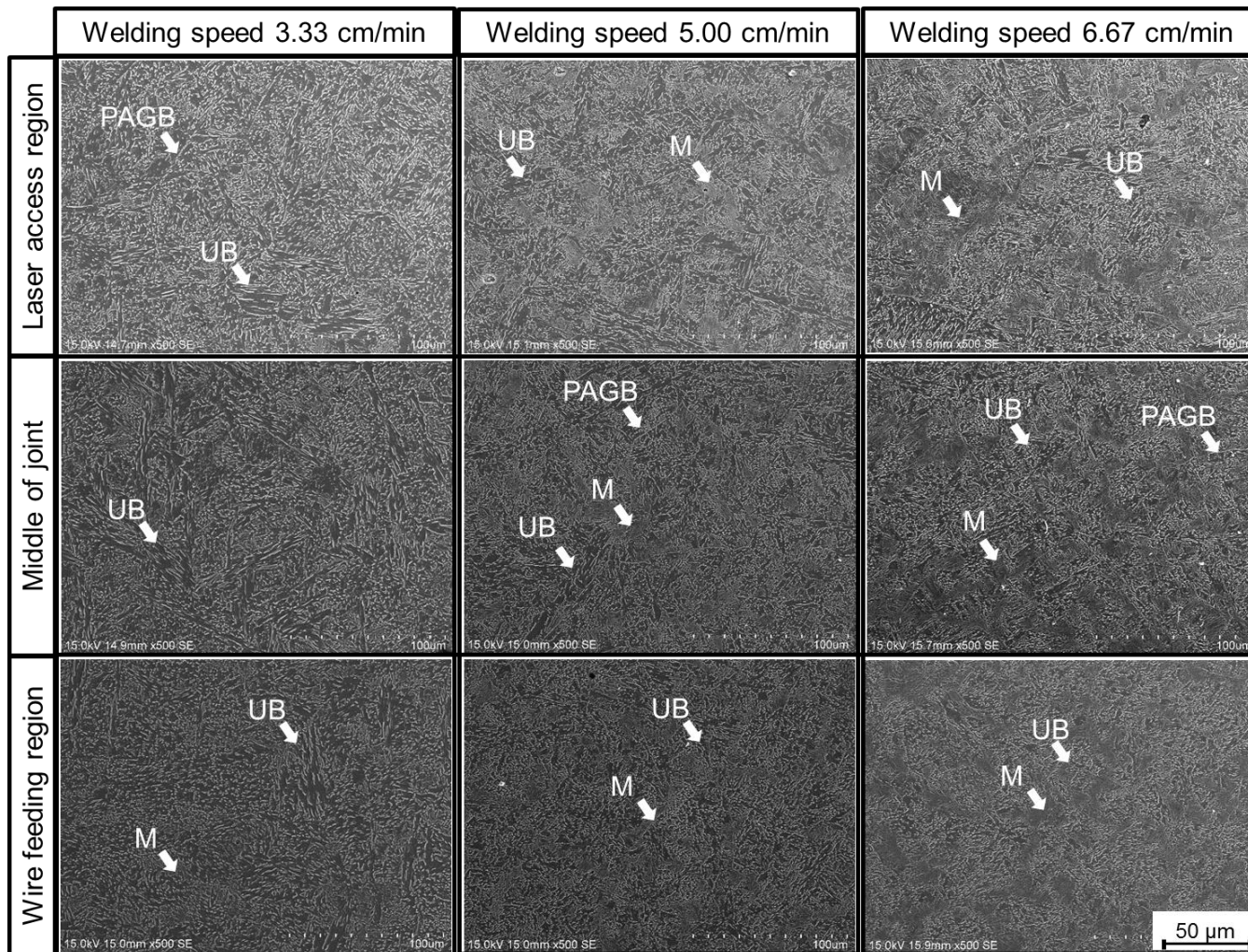| Welding speed 3.33 cm/min	Welding speed 5.00 cm/min	Welding speed 6.67 cm/min

Fig.6.6 OM images of twin laser method under influenced of welding speeds. PAGB, UB and M are prior austenite grain boundary, upper bainite and martensite, respectively. 3% Nital solution etched.
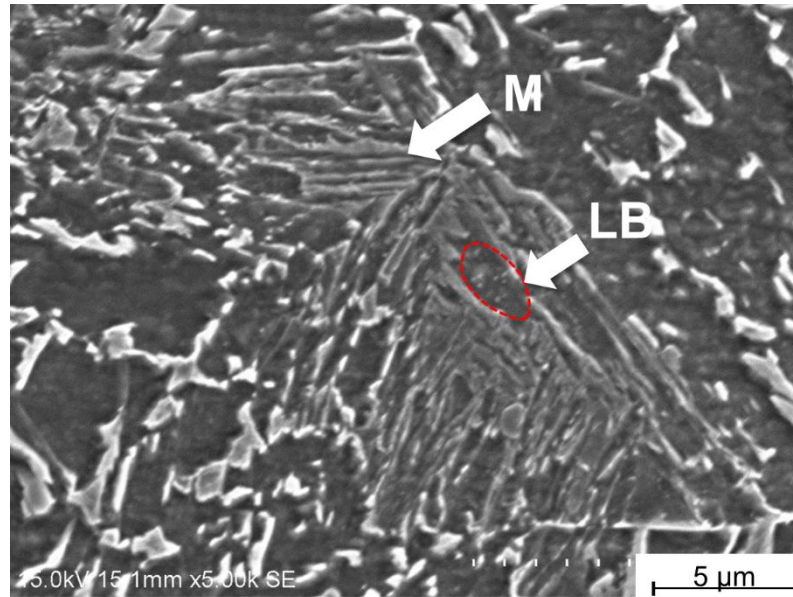
Fig. 6.7 SEM images of twin laser method under influenced of welding speeds. PAGB, UB and M are prior austenite grain boundary, upper bainite and martensite, respectively.3% Nital solution etched.

Fig 6.8 Martensite phase (M) and lower binite (LB) were identified on YM-80A weld metal. 3% Nital solution etched.

In order to evaluate the effects of welding speeds on metallurgical properties and the relation between cooling time and microstructure characteristics by the quantitative method, using high magnification of SEM images in order to measure the phase fraction. Magnification of 1000X SEM of 12 pictures of per one welding speed were measured.

Results of microstructure constituents (phase fraction %) showed in Fig. 6.9. The cooling time: $\Delta t8/5$ clearly affected phase constituents in wed metal. The shortest cooling time has a result of the high fraction of martensite and lower bainite (M+LB) phase and once of long cooling time that result of upper bainite (UB) formed on more fraction. Microstructure constituents (M+LB %-UB %) as a cooling times of 84, 123, 200 s were 23%-77%, 11%-89% and 4%-96%, respectively.
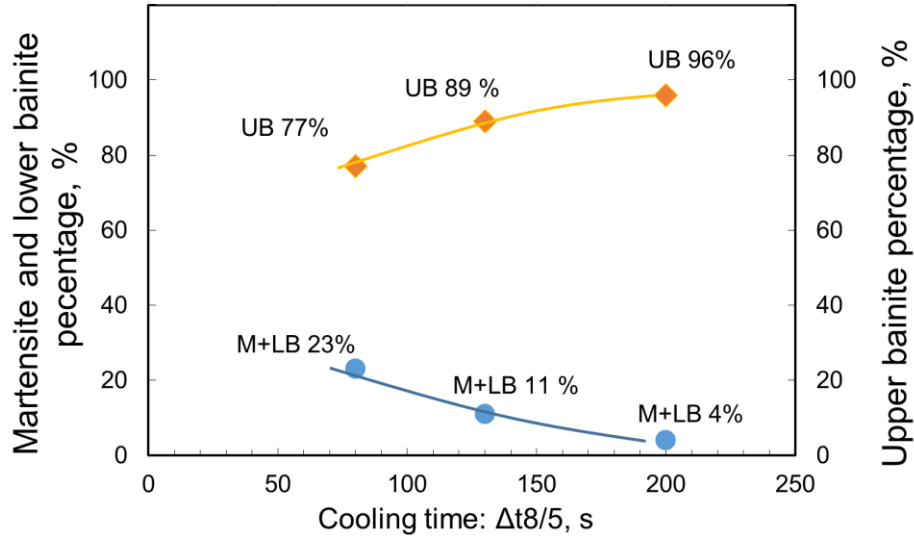
Fig 6.9 Microstructure constituents of weld metal under difference cooling time (Δt8/5)

6.2.5. The relationship between cooling time and hardness distribution across weld metal

Vicker hardness wiht load 10 kg was performed with scaning on weld metal by cross direction. Three scan lines (observe) location were shown in Fig. 6.10. L1 is the laser access region, L2 is middle of joint thickness and L3 is wire feeding region.

Results of hardness test for 3 cooling times were shown in Fig. 6.11. In this section would be explained hardness only the fusion zone. The distribution of hardness all of the conditions showed that almost uniform in the cross direction and three lines scan. Obviously, fast cooling time of Δt8/5 of 84 seconds has a high hardness level by an average around 305 HV. Meanwhile Δt8/5 of 123 and 200 second have average hardness level of 286 and 261 HV.

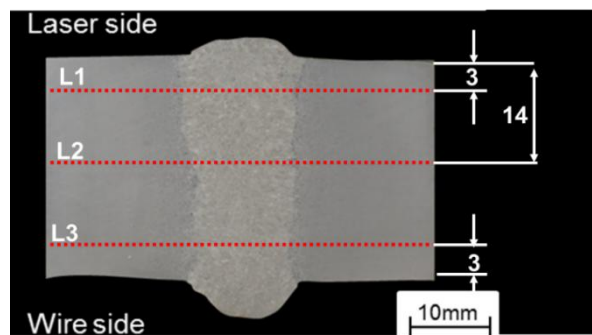Fig. 6.10 Location of Vicker hardness scan across weld joint.
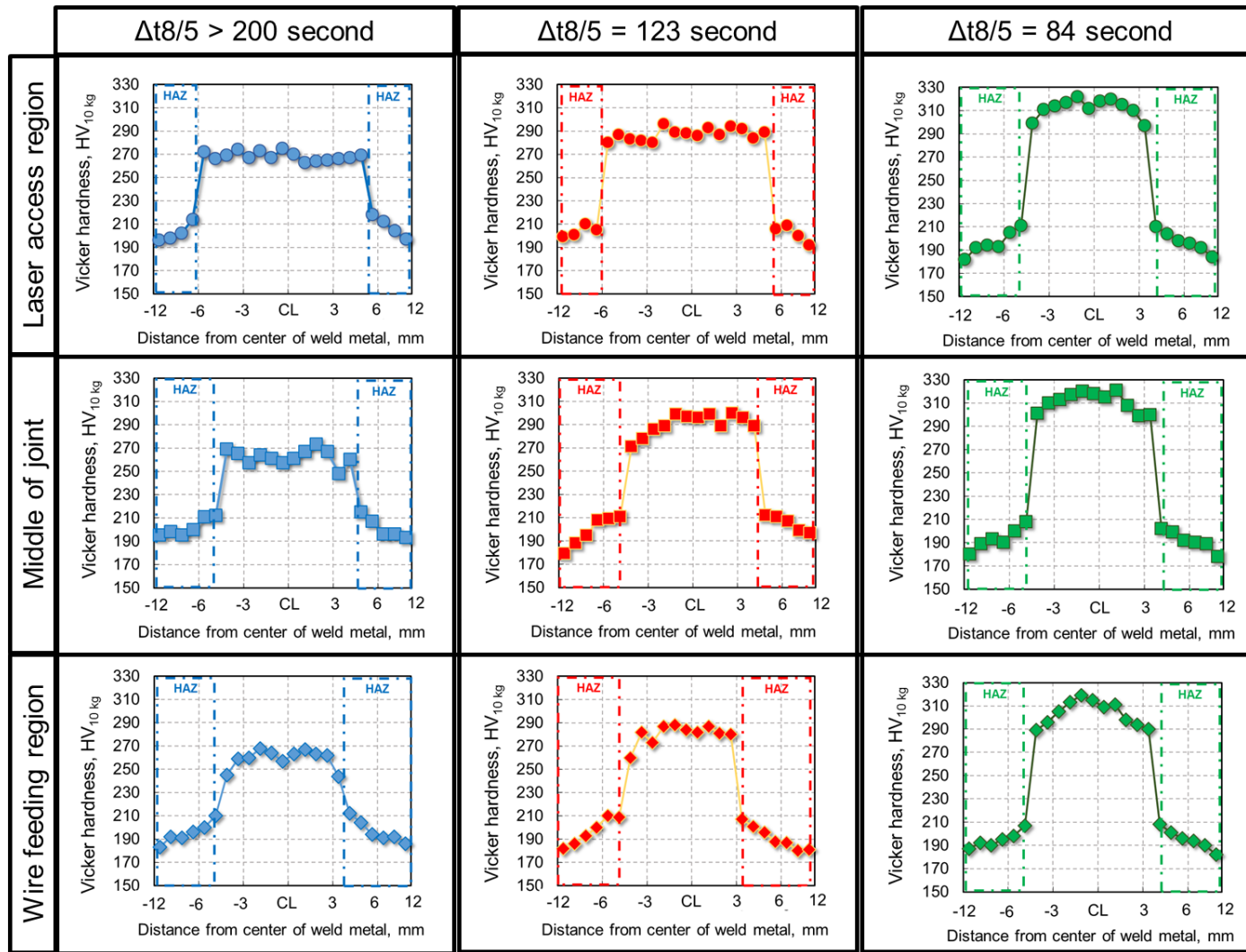
Fig. 6.11 Vicker hardness (10 kg) distribution of weld metal under influenced of differences Δt8/5.

6.2.6. The relationship between transformation cooling time and microstructure characteristics for twin laser method

According to the experiment of welding speed effects, the investigated results with consists of weld metal cooling time (Δt8/5), microstructure outcomes, phase fractions and hardness of weld metal was summarized as the relation of cooling time and microstructure characteristics diagram. The diagram was shown in Fig 6.12. The cooling time from 84 seconds to 200 s was obtained from working range of the twin laser and this cooling diagram was related to metallurgical characteristics which are specified for filler metal of YM-80A (JIS3312 G78AUMN5C1 M3T). The diagram can be used for prediction the microstructure and hardness by controlling weld metal cooling time which is a function of welding speed.
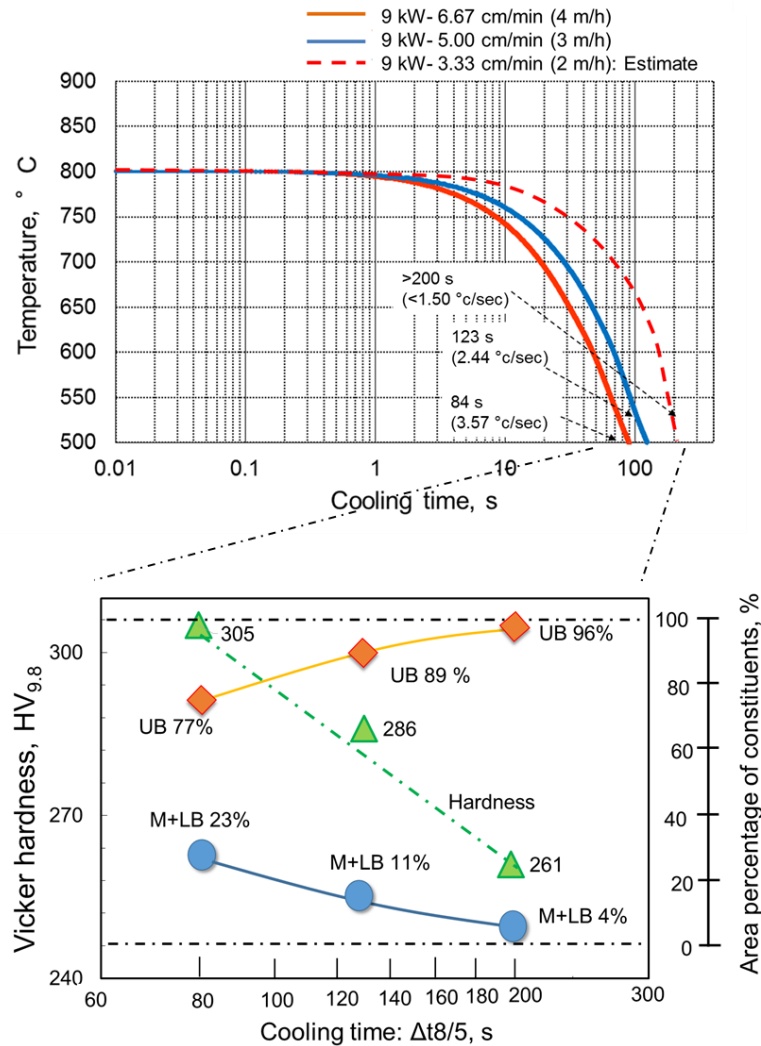
Fig. 6.12 Diagram of the relationship between Δt8/5, microstructure constituents and hardness of weld metal of twin laser method.

However, it must be discussed for this information can be used only the effect of cooling rate but for metallurgical characteristics is only make clear that this working range has clearly affected microstructure and hardness changing. Because it can be observed from two major parts. First microstructure on weld metal is bainitic-martensitic base mainly but for steel structure application need acicular ferrite predominately form on weld metal. Since as acicular has a high performance on strength, toughness [91] and crack arrest properties. On the other hands, upper bainite has many drawback for ship structure. Second, the hardness of these weld metal have over matching lever (high hardness) with KE-47 steel. On the practical side, filler metal should promote the hardness of weld metal be around 190-220 HV as is hardness on an appropriate microstructure such acicular ferrite. Therefore, information of the diagram can be used for develop an appropriate filler metal for the proposed process in the future. By the information of cooling time range (84-200 second), filler metal should promote the formation of acicular ferrite and get the fine size of this microstructure to get good properties of weld metal.

### 6.2.7. The effect of cooling time and metallurgical characteristics of weld metal

Prior Austenite Grain (PAG) size and phase sizes were associated with the metallurgical characteristic to inform and relate to mechanical properties of weld joint. SEM image of 1000 x magnification (clearly observed) were performed by 150,000 μm^2 per each condition (12 pictures per one welding speed).

PAG size were determined by ASTM linear intercept method and the measurement of phase fraction used grid counting and the measurement of phase size. Typical SEM image of Δt8/5 of 200, 123 and 84 second were shown in Fig. 6.13 (a), (b) and (c) respectively. P-UB is packet size of upper bainite and P-M is packet size of martensite and lower bainite. They were reported [91-92] as the packet size is one of parameters for controlling the mechanical properties (DBTT). Then PAG, P-UB and P-M were measured to investigate and discuss the effect of cooling time and estimate the tendency of weld joint properties.
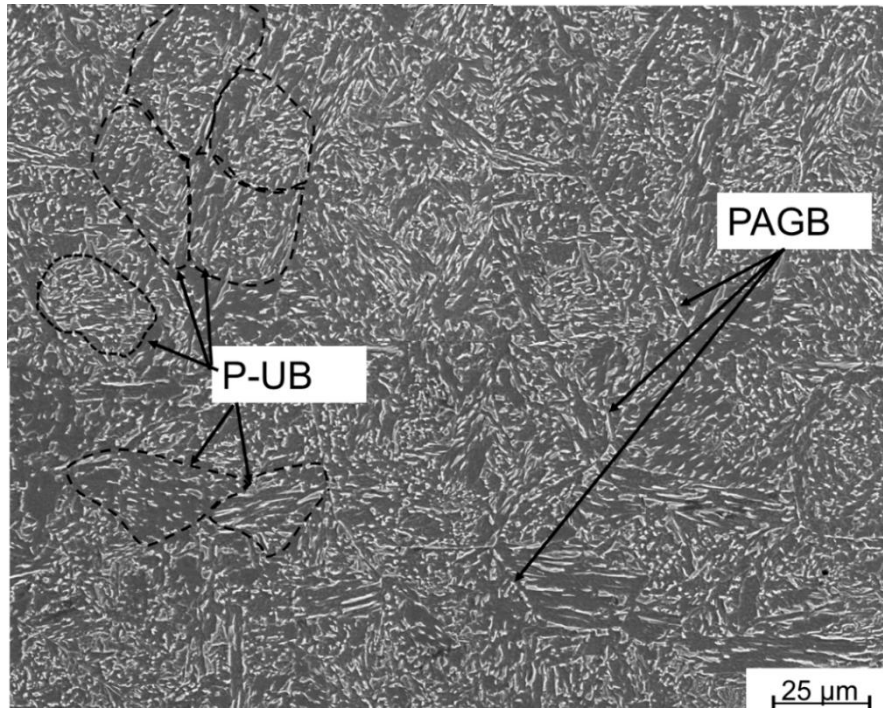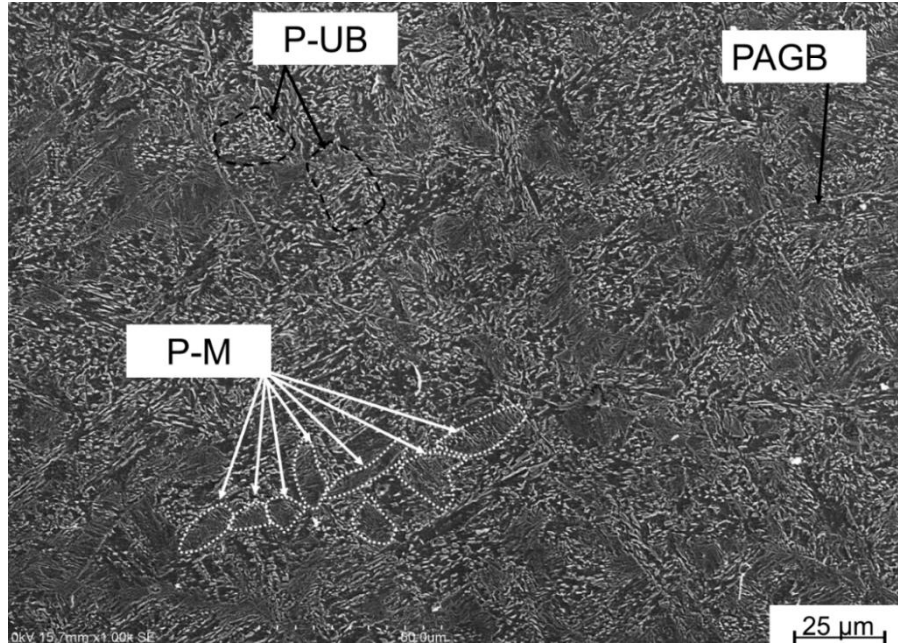
(a) Cooling time: Δt8/5 > 200 second
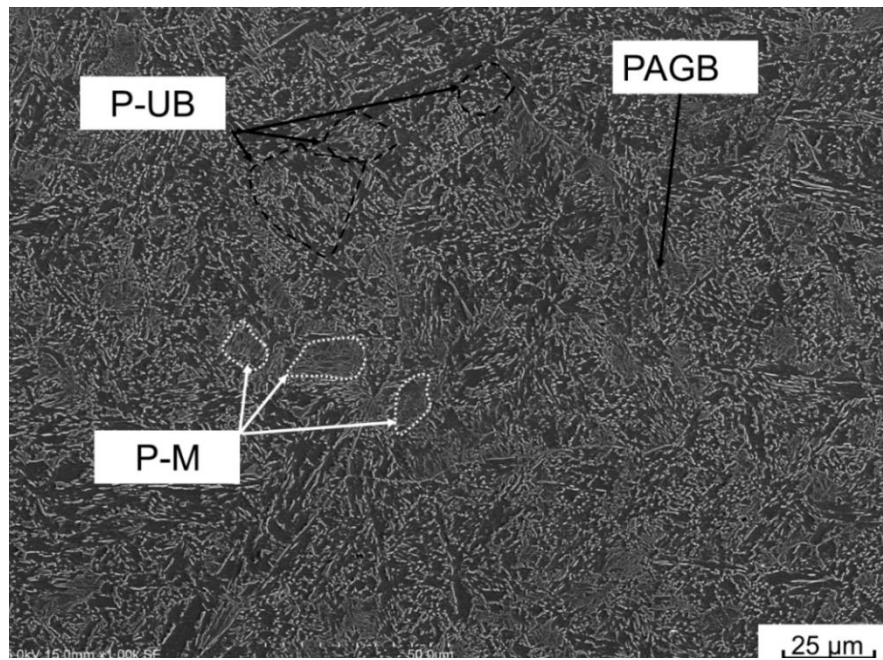
(b) Cooling time: Δt8/5 =123 second

(c) Cooling time: Δt8/5 = 84 second

Fig. 6.13 Typical SEM images to investigate effect of cooling time on PAG size and microstructure packet size. Note: PAGB is prior austenite grain boundary and PAG is prior austenite grain size.

Fig. 6.14 shows PAG size and P-UB size as a function of Δt8/5. It can be seen that Δt8/5 which was controlled by welding speed has direct affected PAG size and U-PB size. High welding speed or high cooling rate made PAG size. U-PB size has a same tendency similar to PAG size. By the behavior of the selected filler metal, the increase of PAGB and P-UB were not linear when Δt8/5 range increase. PAG and P-UB sizes on the cooling time of 84 and 123 s (by welding speeds of 4 and 3 m/h, respectively) does not have long period. When cooling time became longer than 200 seconds (welding speed of 2 m/h), PAG and P-UB increased around 1.5 times.

Not only PAG size plays a role in controlling the mechanical properties but also the packet size of the matrix such P-UB and P-M have influences on weld joint properties. Then, PAG and P-UB as a function of cooling time was used to investigate the formation of upper bainite phase under the effect of cooling time Δt8/5 and also to discuss a tendency of toughness property. From the measured results in Fig. 6.14 showed that P-UB has behaviors of formation closed to PAG when cooling time increased. For cooling time more than 200 s, P-UB has increases largely closed to PAG. It is implied that long cooling time creates a coarse matrix and result in weak toughness property. It is couple relations of their sizes controlling and toughness

properties. The coarse size of P-UB over PAG size has strong affected brittle crack of weld joint. Moreover, when upper bainite phase (ferrite facet size) has a packet size become near PAG size, the fracture is brittle cleavage type.
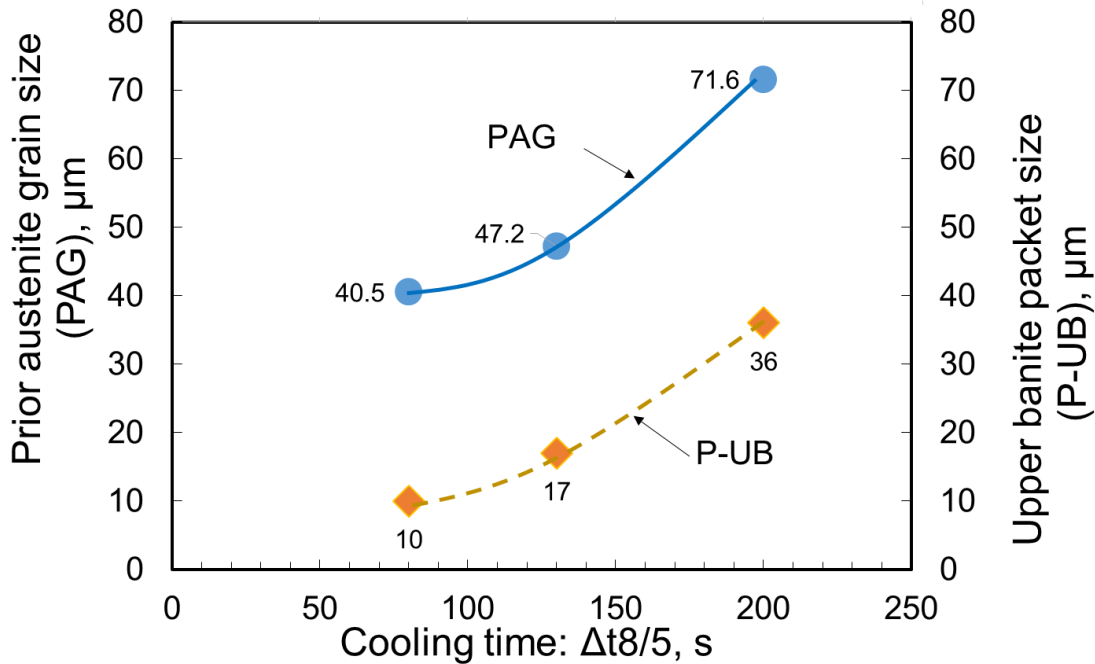

Fig 6.14 Relations of PAG and P-UB as a function of cooling time Δt8/5

As for discussion on the welding process aspect, the effect of welding speed range which has been already optimized in chapter 5, showed welding speed of 5.00 cm/min (3 m/h) is optimization of welding parameter. This parameters has a result of good welding time, completely fulfill, complete fusion and adequate dilution of the weld joint. In this section, the result of cooling time Δt8/5 of 123 second also showed an advantage of phase sizes since as it has size of PAG, P-UB almost same of high welding speed case (6.67 cm/min or 4 m/h) and finer more case of low welding speed (3.33 cm/min) around 2 times. Therefore, this speed is still optimized of welding condition.

Behavior of P-UB and P-M size were shown in Fig. 6.15 with cooling time Δt8/5. P-M sizes slightly increased with an increase Δt8/5. It was noticed that the selected filler metal could formed uniform size of martensite and lower bainite under cooling time of 84-200 second. Comparing P-UB and P-M, short cooling times Δt8/5 of 84 and 123 second have almost same sizes. However, case of long cooling time of 200 second that has a large differential phase size.
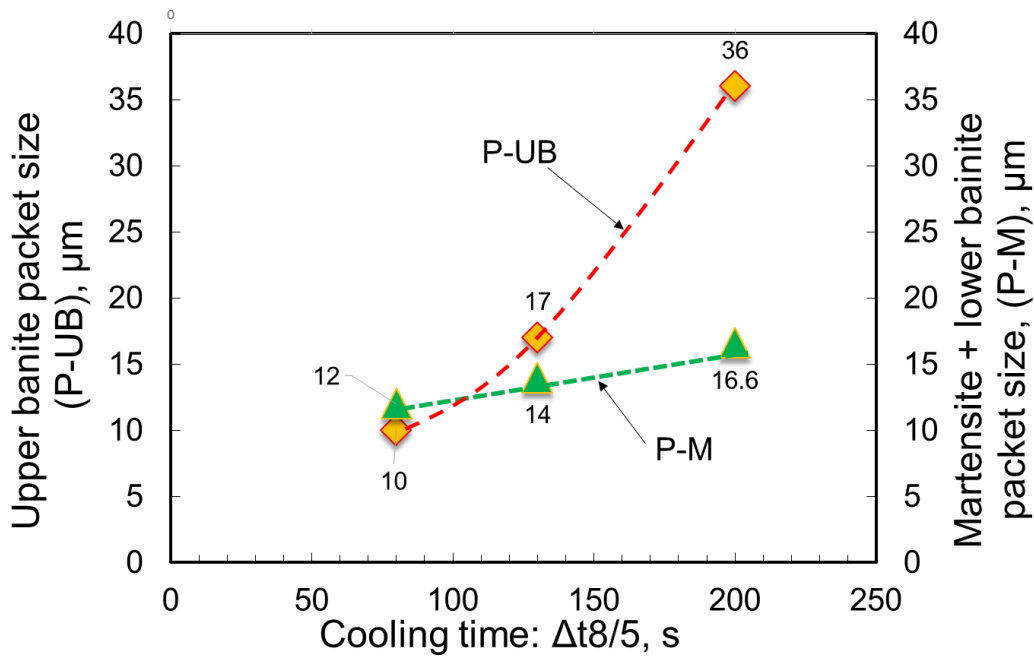
Fig 6.15 Relations of P-UB (upper banite) and P-M (martensite and lower bainite) as a function of cooling time Δt8/5

6.3 Investigation of toughness property of fusion zone with the selected welding condition

6.3.1 Welding Condition

According to section 6.2.7 that investigated sizes of microstructure with cooling time Δt8/5 and get the finest sizes of PAG, P-UB and P-M under cooling time Δt8/5 of 84 seconds. This cooling time result by welding speed 6.67 cm/min (4 m/h). Then, trial investigation a toughness property would perform this welding condition. The welding condition of twin laser method was same previous section. It must be noted that for welding speed 3.33 and 5.00 cm/min will be also tested in the future in order to investigate the cooling rate effect on toughness property.

6.3.2 The Charpy specimen preparation and test method

The standard full size of Charpy V-notch specimens were cut in welded specimen as same as a cutting plan on Fig. 6.16. Testing temperature of -20°C was selected to test for decide the toughness value for the selected welding condition. NK rules

assigned acceptance criteria for Charpy V-Notch at -20°C shall be over 64 Joule. The Charpy impact machine has a hammer weight of 45.26 kg, arm radius of 0.65 meter.
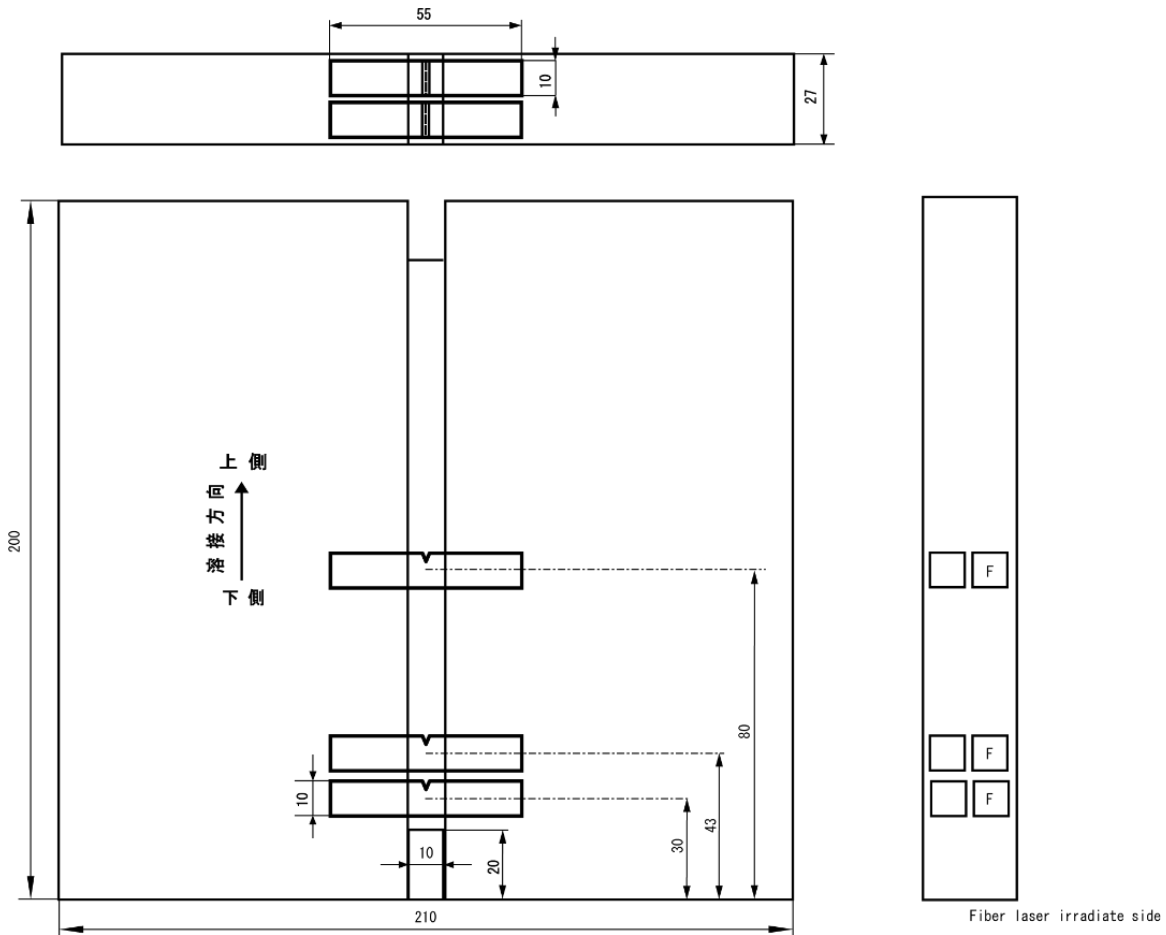

Fig. 6.16 Cutting plan for preparation of Charpy V-Notch specimen.

6.3.3 The Charpy impact test result

The Charpy test result was presented on Fig. 6.17. It can be seen that high absorbed energy was obtained by welding condition with welding speed 6.67 cm/min (4 m/h). The average of absorbed energy is about 159 Joule at -20°C test temperature. And each specimen has over 120 Joule. In comparison with this result seem to be high toughness properties for service condition when compare on the requirement of NK rule (minimum absorbed energy of 64 Joule at testing temperature of -20 °C). The related reason of this good toughness properties is fine microstructure of PAG, P-UB and P-M size on the selected welding condition. The adequate fraction of martensite and lower banite phase has influenced good toughness property.
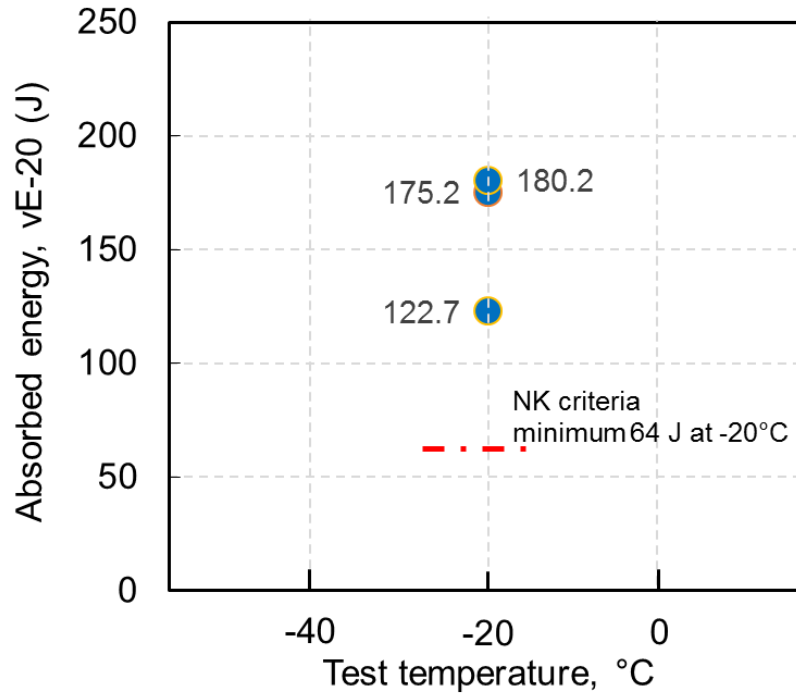
Fig. 6.17 Absorbed energy of Charpy V-notch test at -20°C.

6.4 Trial experiment to study the effects of carbon equivalent factor on weld metal properties

Since the filler wire of YM-80A (JIS3312 G78AUMN5C1 M3T) made weld metal having over matching hardness, even though it could provide a good toughness property. Carbon equivalent (CE) is usually used to predict hardenability in HAZ [93]. Normally, high CE% has a high hardness value. In this report, we tentatively used CE to predict hardenability in weld metal. CE% value of the selected filler metal was calculated by WES method [94] as equation as:

$$CE = \%C + \left(\frac{Si}{24}\right) + \left(\frac{Mn}{6}\right) + \left(\frac{Ni}{40}\right) + \left(\frac{Cr}{5}\right) + \left(\frac{Mo}{4}\right) + \left(\frac{V}{14}\right) \qquad (6.1)$$

The calculated result of CE was0.59%, it implies that is a high value like a brittle of weld joint property. This section is trail experiment which has an objective to study the effect of CE factor on weld metal by 2 hot-wires method. The original selected filler wire of JIS3312 G78AUMN5C1 M3T was used as the reference to compare its effect when it was diluted by other filler wire. The result of welded specimen will be observed on microstructure outcome and hardness of weld metal. The Charpy V-notch testing was also performed to evaluate the effect of CE value changing.

6.4.1 Methodology of 2 wires method and welding condition

Specimen dimension for the experiment of 2-wires method was shown in Fig. 6.18. Base metal dimension is 50 (width) x 100 (height) x 26 mm (thickness) and gap width of 10 mm. The base metal is KE 47 steel. Original filler metal of YM-80A (JIS3312 G78AUMN5C1 M3T (Martensitic-bainitic base)) was provided to joining by 2-wires method for reference of the weld characteristic. Two kind of filler wires were used to make the dilution weld metal. The filler metal A is YM-80A (JIS3312 G78AUMN5C1 M3T) and filler metal B is YM-24S (JIS Z 3312 G43A2Mo (Ferritic base)). Table 6.3 shows the chemical compositions of welding materials for this experiment. The feeding ratio of filler A to filler B is 2:1 is trial feed rate for investigation the effect of chemical dilution. Estimate the chemical composition of the dilute weld metal was also shown in Table 6.3. For CE value of welding materials were calculated follow the equation of 6.1 and shown on Table 6.4. It can be seen that dilute weld metal by filler A: filler B ratio of 2:1 has a result of CE of 0.61% (decreased about 19%).

Vertical laser access (laser irradiation angle of 0 degree) with 2 hot wires was employed as shown schematic in Fig. 6.19 and the parameter of the optical apparatus were shown on Table 6.5. The weaving parameter was 5 Hz-exponential waveform with parameter W_L/W_G ratio of 0.4 by the spot size of 4 mm x 27 mm.

For selection of welding speed for welding, the high speed of 6.67 cm/min (4 m/h) was not used in this experiment. Even through, this welding speed could obtain good toughness property from the previous section it also showed the imperfection on the weld joint. Moreover, this experiment must be used the laser irradiating parameter as above mentioned to access two hot wires. That welding parameter could obtain the best sound joint by the low welding speed condition. Then, the low welding speed of 3.33 cm/min (2 m/h) was used to welding in this experiment because it could obtain sTable welding condition and achieved a sound weld.
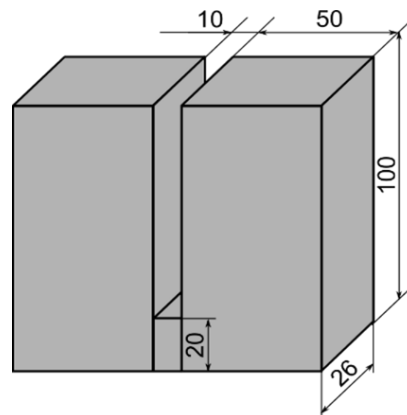

Fig 6.18 Specimen used for the experiment of 2-wires method.

Hot-wire parameters on each filler sides were shown in Table 6.5. All of welding parameters are associated in Table 6.5. Fig. 6.19 shows the schematic of the 2-wires method. Argon gas was used for shielding the weld pool with flow rate of 10 l/min.

Table 6.3 Chemical composition of welding materials

Material	Chemical Composition, wt%											
	C	Si	Mn	P	S	Al	Cu	Ni	Nb	Ti	Cr	Mo
KE 47	0.09	0.07	1.52	0.007	0.002	0.014	0.32	0.69	0.01	0.01	0.02	0.00
Filler A	0.06	0.4	1.69	0.006	0.003	-	0.20	3.01	-	0.05	0.46	0.29
Filler B	0.08	0.24	1.09	0.013	0.016	-	0.27	-	-	-	-	-
Estimate filler	0.07	0.35	1.49	0.01	0.01	-	0.09	2.02	0	0.03	0.31	0.19

Table 6.4 Calculated result of %CE by WES method

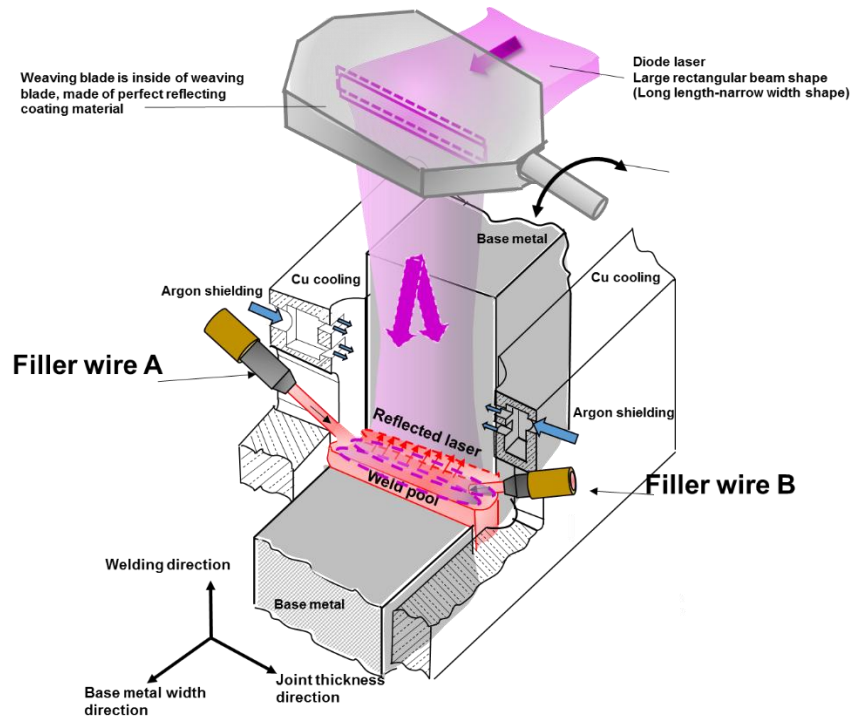| Material	CE%
KE 47	0.36
Filler A	0.59
Filler B	0.27
Estimate filler	0.49

Fig. 6.19 Schematic illustration of process methodology of the weaving laser irradiating method by vertical laser access with 2 hot-wires feed.

Table 6.5 Welding parameters for two wires method

Feeding ratio	Filler A 100%		Filler A : Filler B	
	1	1	2	1
Fiber core, mm	1.0			
Homogenizer	LL3			
Focus lens, mm	400			
Laser power, kW	6			
Laser irradiation angle, degree	90°			
Defocus, mm	20			
Spot size, mm x mm	4^w x 27^l			
Power density, W/mm^2	55			
Weaving condition	5 Hz, exponential waveform			
Filler wire diameter, mm	1.6			
Welding speed, cm/min (m/h)	3.3 (2)			
Wire feed speed, m/min	1.24	1.24	5.94	2.97
Wire current, A	93	93	114	75
Wire feeding angle, degree	45			
Wire feeding position, mm	0			
Shielding gas (Argon), LPM	20			
Pre irradiation time, s	120			

6.4.2 Result of microstructure characteristics on weld metal

The results of microstructure observation of both conditions were shown in Fig. 6.20. Reference weld metal (100% filler A) shows quite coarse upper bainite as a predominated microstructure. While the dilute case (2:1 of A:B) shows mixed of acicular ferrite and few parts of upper bainite. This result indicates that alloy dilution significantly affected microstructure formation in the proposed process. It was noticed that microstructure still shows quite a small size formation even though it was diluted. Formation of acicular ferrite that implies that weld metal may has a better toughness than upper bainite base.
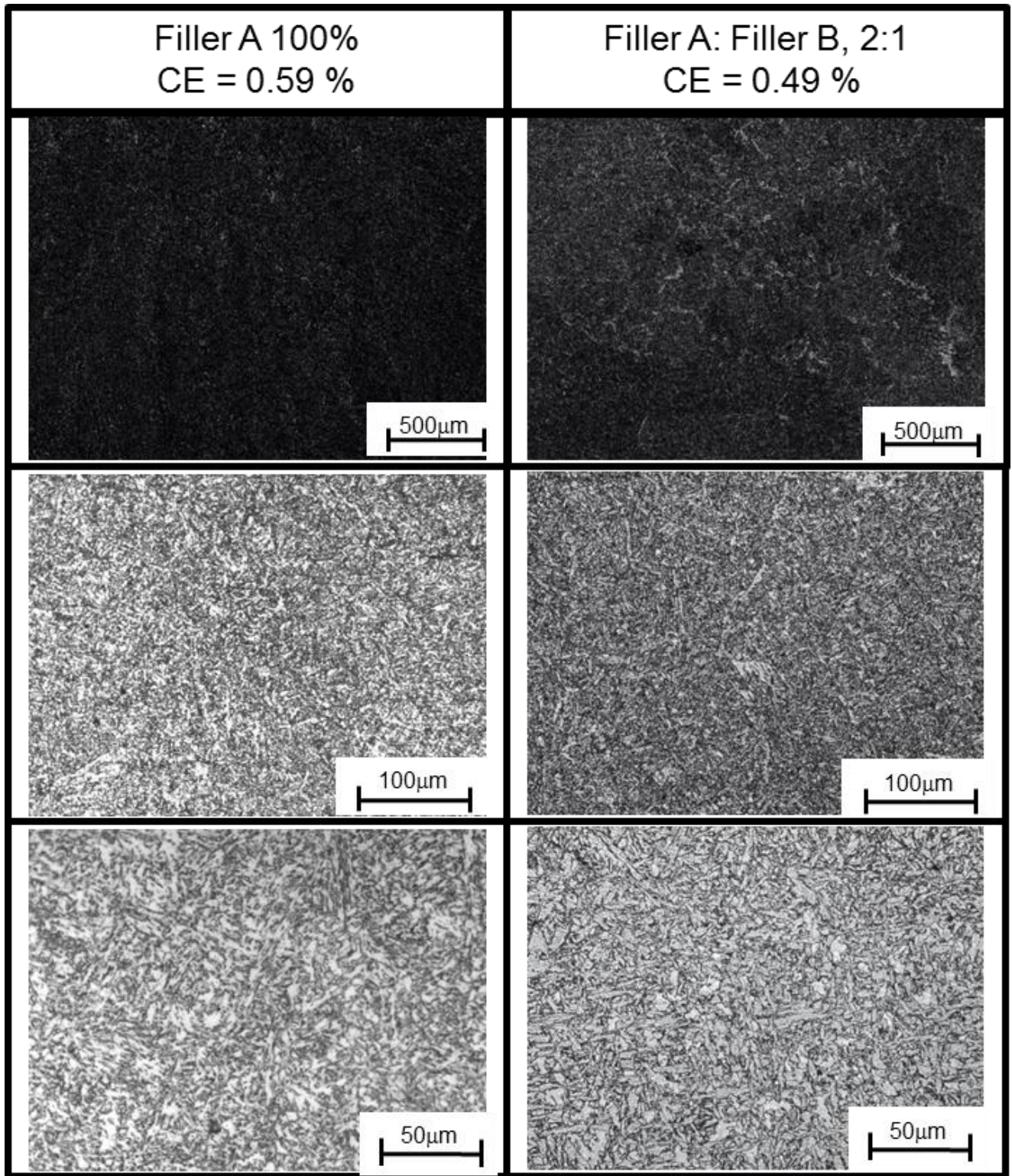
Fig. 6.20 Microstructure of Filler A 100% and A:B ratio of 2:1

6.4.3 Result of hardness level on weld metal

Weld metal of reference weld metal (100% filler A) and dilute case (A:B of 2:1) were investigated by Vickers hardness with 10 kg. The results were shown in Fig. 6.21 with the base on CE% value. Base on the proposed process, it was shown that CE value (factor of chemical compositions) significantly affected the hardness of weld metal. For CE of 0.49 % an average is about 183 HV while CE of 0.59 % has an average about 220 HV. By this result with a consistency with microstructure (previous section), metallurgical basis, upper bainite has a higher hardness than acicular ferrite. Usually, the relationship between hardness and CE is used under comparatively faster cooling rate condition. However, in the proposed process has a slower cooling rate compare with conventional welding process. Then, this experimental result has a relationship between CE value and weld metal hardness difference form other condition.
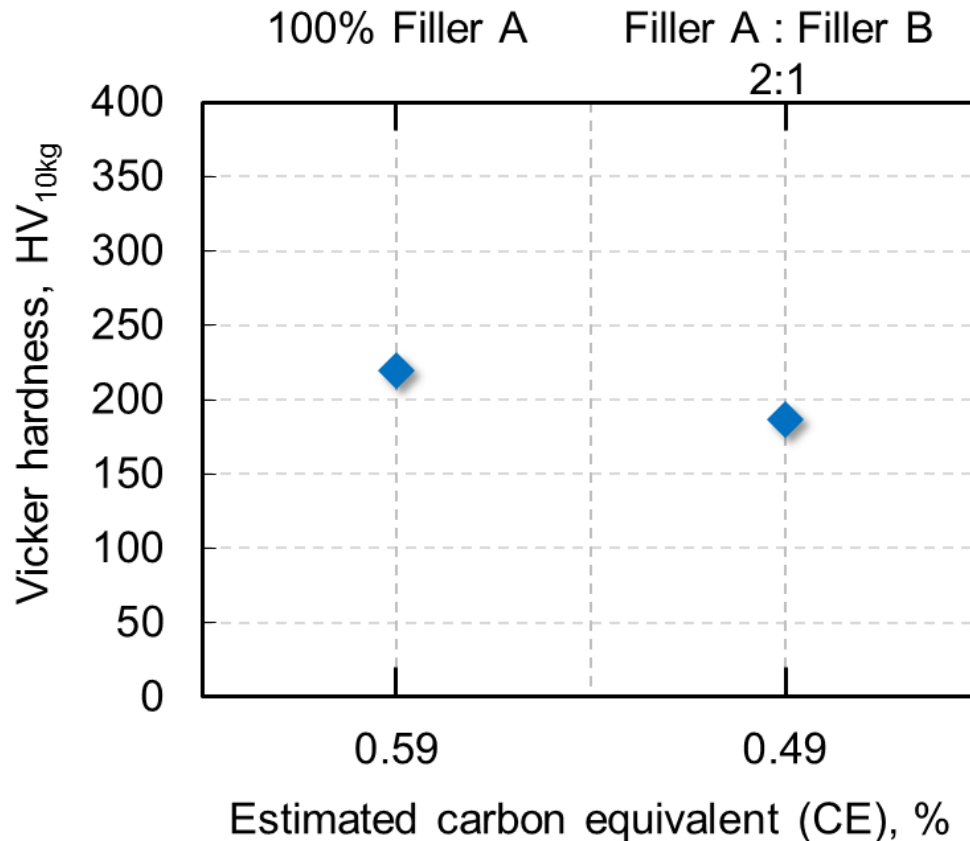
Fig. 6.21 Hardness, HV_{10kg} with carbon equivalent on weld metal

6.4.4 The Charpy specimen preparation and test method

According to results that microstructure and hardness value were controlled by chemical compositions (CE value also was controlled) from trial experiment and result has been shown a significant difference. Impact test was performed using welded specimens, and test coupon were cut as shown in Fig. 6.22. 3 specimens for each condition tested. The Charpy impact machine has a hammer weight of 45.26 kg, arm radius of 0.65 meter. Testing temperature is -20°C.
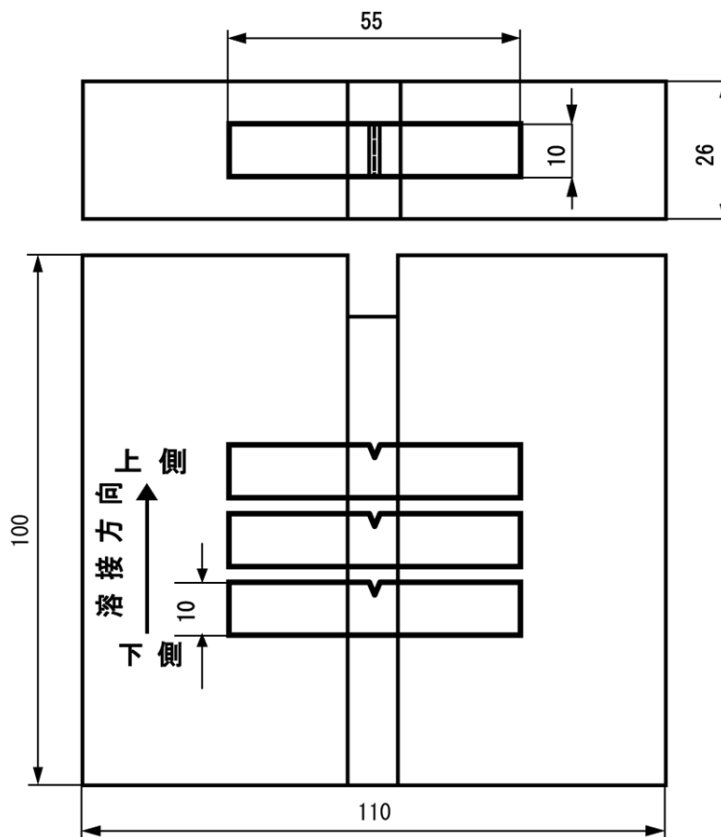

Fig. 6.22 Cutting plan of welded specimen for the charpy impact test.

6.4.5 The Charpy impact test result

The tested results of the Charpy test were shown in Fig. 6.23. Significant differences toughness levels of 2 cases. Low CE value (0.61%) of weld metal has a better trend of toughness properties than the high CE value (0.76%). However, most results show low toughness level or have brittle behavior. For discussion, there are two

assumptions on this result. First, upper bainite microstructure type may affect crack propagation in case of weld metal has it as predominate formation. Basically, acicular ferrite has a chaotic texture to deflect crack direction and it makes crack speed slow. Second, alloying element changes the chemical affinity of the bulk body. Chemical affinity is the basis of the attractive bonding for material and the main factor for their properties. Changing chemical compositions is atomic bonding degree changed. According to the level of the toughness results, base on the selected filler metal almost showed low energy. It implies taht, the chemical composition level of this filler wire of YM-80A (JIS3312 G78AUMN5C1 M3T) is mismatching for the proposed process. On the other hands, the trial experiment of dilution of chemical compositions could suggested that the proper filler wire should be able to promote tough microstructure type such acicular ferrite and promote the CE% value should be lower than 0.61%.
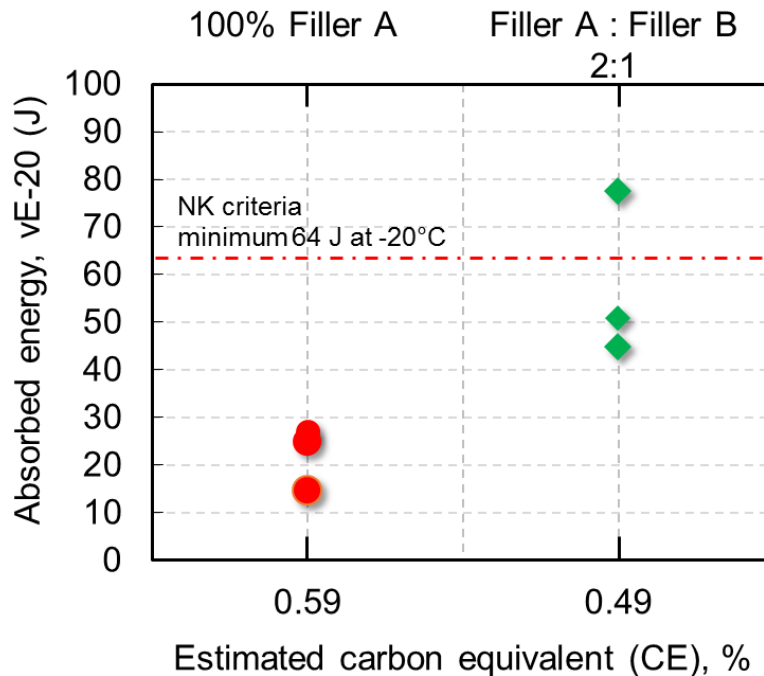

Fig. 6.23 Absorbed energy at -20 °C with differences of CE %.

6.5 Investigation of effect of oxygen content on weld joint toughness

Many researcher has investigated the effect of oxygen contents on the toughness properties on weld metal. Arc welding process [95], carbon steel weld metal which has contained the oxygen content around 200-300 ppm, can promote good toughness properties. However, it is totally difference the behaviors for the proposed process because, on the historical experiment, the proposed process (hot-wire laser method) used 100% argon gas for shielding. Then oxygen content never determined on the

proposed process. Therefore, the experiment of the effect of oxygen contents on toughness property was performed. The objective on this section is determination oxygen content on weld metal from differences of shielding type. Oxygen content is measured and related with microstructure and Impact toughness.

6.5.1 Material used and welding condition

KE-47 steel plates were used in this study, the dimension of the specimen was 50 (width) x 200 (height) x 26 mm (thickness). Plates were fixed and aligned as a vertical joint configuration. The gap width was set by spacer (dimension of 10 mm (width) x20 mm (height) x 26 mm (thickness)). The filler metal YM-80A (JIS3312 G78AUMN5C1 M3T) with a diameter of 1.6 mm was used. The chemical composition of base metal and filler metal were presented on Table 4.9.

The welding method was the oblique laser access method (Tilt angle of 15 degree) with weaving irradiating method in this experiment. Beam spot size of 4 x 27 mm, power density of 55 W/mm^2 was irradiated. Single hot-wire was used for deposit weld metal and hot-wire feeding parameters were set depend on the welding speed of 3.33 cm/min (2.0 m/h). Since the welding parameter for this study is the single laser method as above mention then a suitable welding speed is 3.33 cm/min.
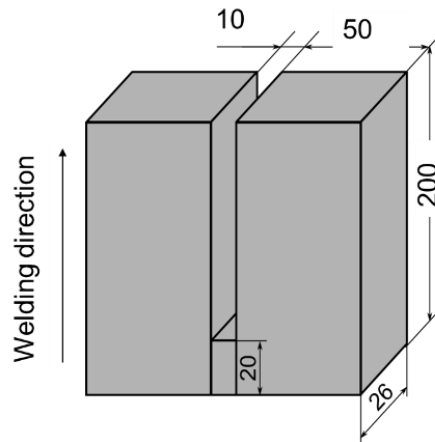

Fig. 6.24 Specimen dimension

Table 6.6 Chemical compositions of materials used

Material	Chemical Composition, wt%											
	C	Si	Mn	P	S	Al	Cu	Ni	Nb	Ti	Cr	Mo
KE 47	0.09	0.07	1.52	0.007	0.002	0.014	0.32	0.69	0.01	0.01	0.02	0.00
YM-80A	0.06	0.4	1.69	0.006	0.003	-	0.20	3.01	-	0.05	0.46	0.29
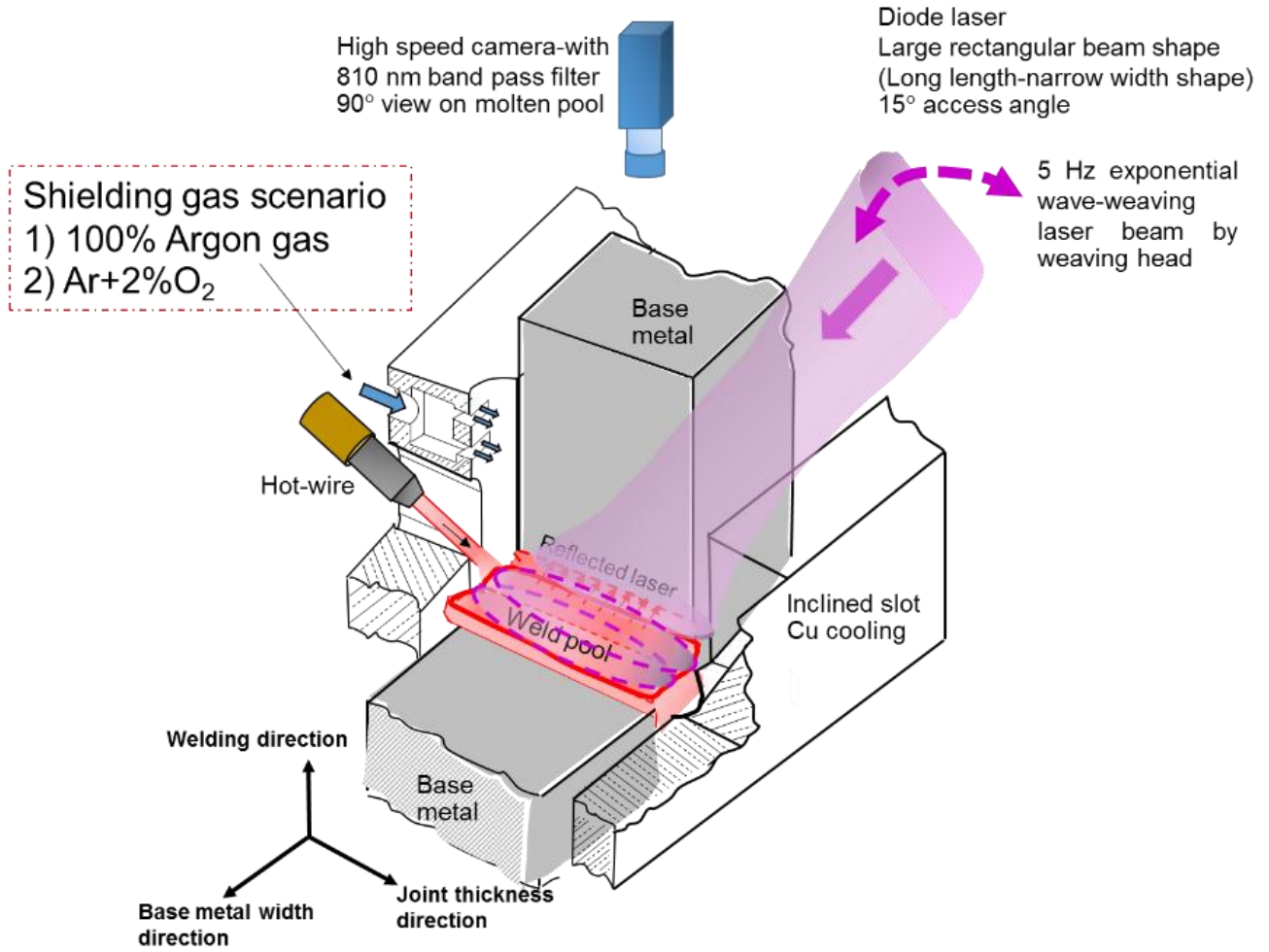
Fig. 6.25 Schematic illustration of the proposed process

Table 6.7 Welding condition

Laser source	LD	
Fiber core, mm	1.0	
Homogenizer	LL3	
Focus lens, mm	400	
Laser power, kW	6	
Laser irradiation angle, degree	15°	
Defocus, mm	20	
Spot size, mm x mm	4^w x 27^l	
Power density, W/mm^2	55	
Weaving condition	5 Hz, exponential waveform	
Filler wire diameter, mm	1.2	
Welding speed, cm/min (m/h)	3.3 (2)	
Wire feed speed, m/min	8.26	
Wire current, A	123	
Wire feeding angle, degree	45	
Wire feeding position, mm	5	
Shielding gas,	Pure Argon	Ar+2%O_2
LPM	10	
Pre irradiation time, s	120	

6.5.2 Effect of oxygen content on weld metal microstructures

Fig. 6.26 shows microstructure on weld metals with different shielding types. Measured oxygen contents were obtained. Shielding by argon has the oxygen content of 40 ppm and Ar+2%O_2 shielded has the oxygen content of 60 ppm. These oxygen values small affected overall microstructure formation. Most of microstructure is upper bainite. In addition, hardness test by Vicker hardness 10 kg was also obtained. Weld metal which was shielded by argon type has an average of HV10kg of 280 HV. While shielding by Ar+2%O_2 type that weld metal has an average of HV10kg of 300 HV. It was shown that 2%O_2 add on argon base small affected both of microstructure formation and hardness level.
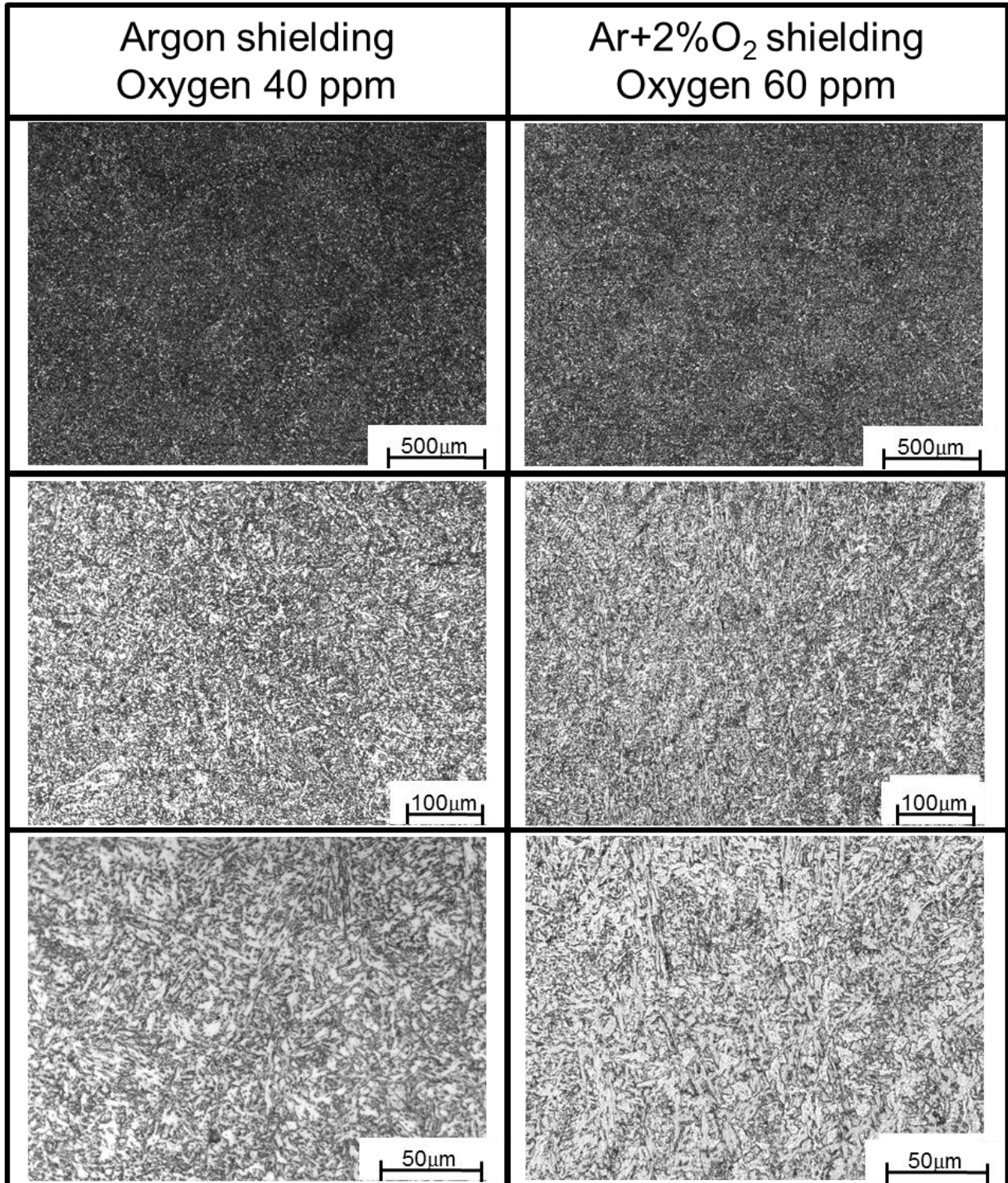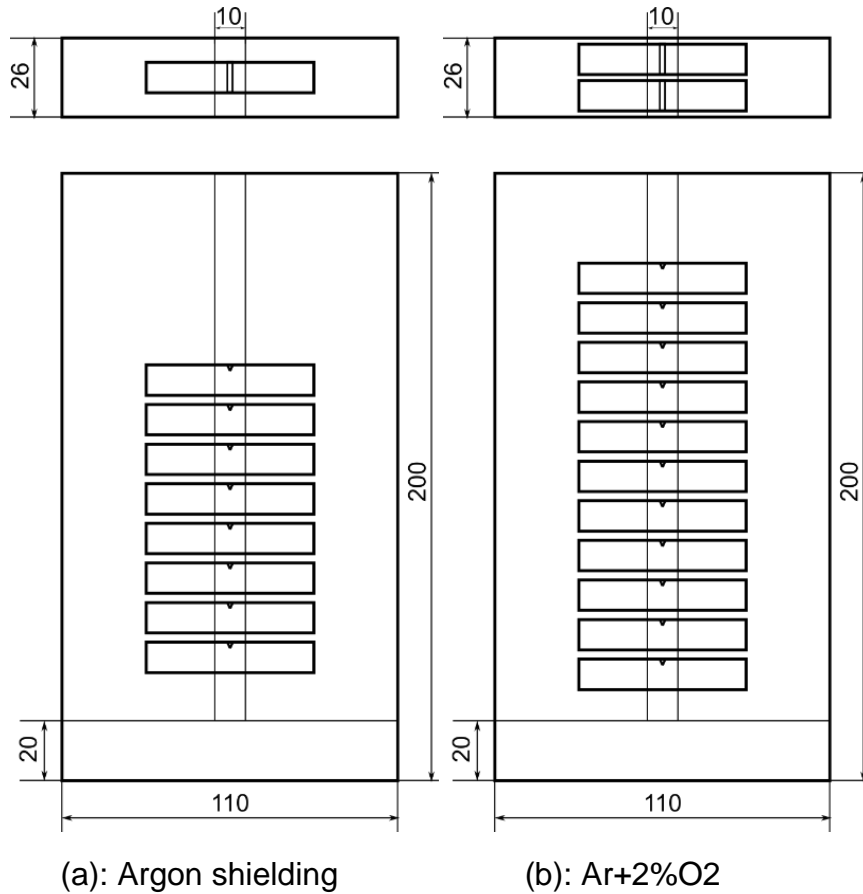
Fig. 6.26 Microstructure of weld metals with different shielding gas

6.5.3 The Charpy specimen preparation and test method

Fig. 6.27 shows cutting plan for impact specimen's preparation. Fig. 6.27 (a) is argon shielding type and Fig. 6.27 (b) is Ar+2%O_2 shielding type. The Charpy impact machine has a hammer weight of 45.26 kg, arm radius of 0.65 meter. Testing temperature is -20°C.

(a): Argon shielding   (b): Ar+2%O2

Fig. 6.27 Cutting plans for the Charpy specimen.

6.5.4 The Charpy impact test result

Results of absorbed energy at -20°C , Vicker hardness results with difference oxygen contents were shown in Fig. 6.28. Both of low oxygen content have almost low absorbed energy. However, it was noticed that 60 ppm has a potential to increase absorbed energy. The oxygen content slightly affected weld metal hardness. By this small experiment could be suggested to the future study of the effect of oxygen contents on weld metal toughness. Since, it has a feasibility to improve a toughness property on fusion zone by varies oxygen contents. Absorption of oxygen content in the proposed

process never studied then investigation of this aspect should be also considered for the research.
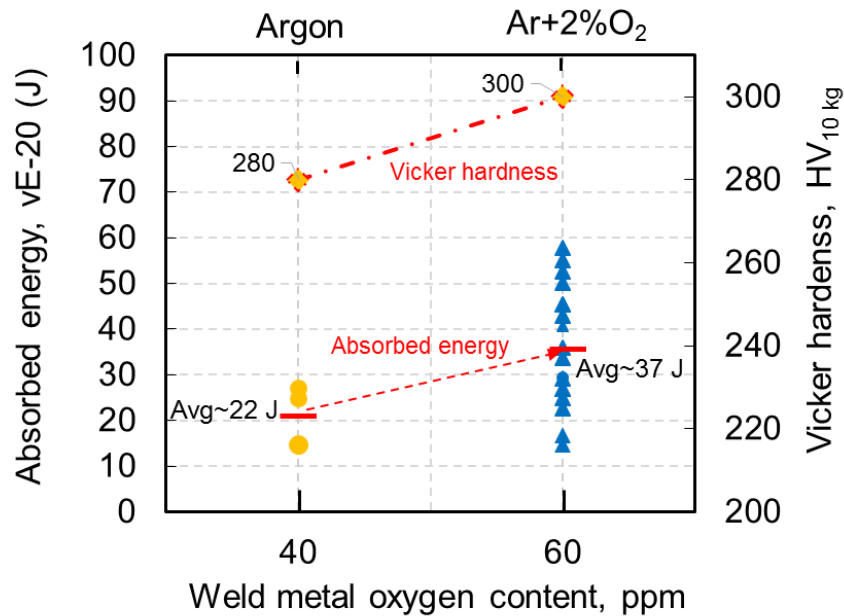

Fig.6.28 Absorbed energy at -20 °C, Vicker hardness result with weld metal oxygen content

6.6 Summary

In this chapter, the fusion zone characteristics were investigated. There are two main parts for studied and could be concluded as:

First parts: 1) Cooling transformation time, Δt8/5 were obtained and related with microstructure and toughness. The cooling characteristic of the twin laser method has the Δt8/5 range of 84 to 200 second. The selected filler metal of YM-80A (JIS3312 G78AUMN5C1 M3T) provided martensitic-bainitic base of microstructures transformation. Increasing welding speed resulted in cooling time became short and resulted in the fine martensite phase formed. On the other hand, long cooling time by low welding speed resulted in coarse upper bainite formed.

2) The finest microstructure of cooling time of 84 s was performed on the Charpy V-notch test. Absorbed energy more than 100 Joule at test temperature -20 °C could be obtained by this condition.

Second part: 1) Trial experiment to study the effects of carbon equivalent factor on weld metal properties showed a potential to improve toughness property by controlling the carbon equivalent factor. Low carbon equivalent has a higher toughness and also promoted acicular ferrite on weld metal.

2) The effect of oxygen content was studied and showed small effects microstructure and hardness changing. On the other hand, toughness properties of added $2\%O_2$ on argon base shielding type has a trend to increase toughness property.

Chapter 7

Heat affected zone (HAZ) characteristics

7.1 Introduction

According to chapter 5, the twin laser method using compensate laser power of 3 kW on one side edge region provides feasible welding speed ranges and sound joints. Adjusting welding speed in the proposed process using the twin laser method can control heat input level. Therefore, in this chapter the characteristics of heat affected zone (HAZ) under several heat input levels of the proposed process was described. Microstructure and grain sizes were investigated. Furthermore the results of CGHAZ width were competitively compared with VEGA ® which is an advanced heavy thickness joining process for the present. Hardness on HAZ was also investigated to make clear influence of heat input of the proposed process. Finally, the requirement of heat input for the proposed process was estimated to compare with other processes.

7.2 Material used and welding parameters

KE-47 steel plates were used in this study, the dimension of specimen was 100 mm (width) x 200 mm (height) x 28 mm (thickness) for twin laser method (Fig 7.1(a)) and dimension of once 50 mm (width) x 200 mm (height) x 26 mm (thickness) for weaving laser method (Fig 7.1(b)). Plates were fixed and aligned as a vertical joint configuration. The filler metal YM-80A (JIS3312 G78AUMN5C1 M3T) with a diameter of 1.6 mm was used since this size of filler wire could obtain stable feed over welding speed range for the experiment. The chemical composition of base metal and filler metal were presented on Table 7.1.
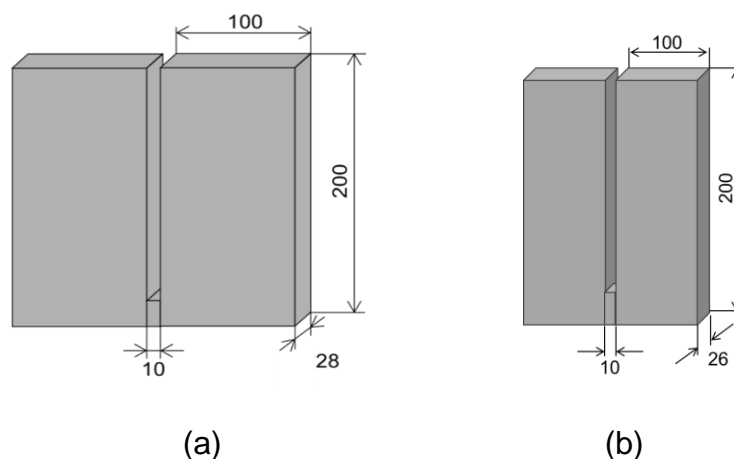

(a)   (b)

Fig 7.1 Specimen dimension for (a) Twin laser method and (b) Weaving laser method

Table 7.1 Chemical composition of welding materials

Material	Chemical Composition, wt%											
	C	Si	Mn	P	S	Al	Cu	Ni	Nb	Ti	Cr	Mo
KE 47	0.09	0.07	1.52	0.007	0.002	0.014	0.32	0.69	0.01	0.01	0.02	0.00
YM-80A	0.06	0.4	1.69	0.006	0.003	-	0.20	3.01	-	0.05	0.46	0.29

Table 7.2 Welding parameters of Twin laser method

Main heat source			
Laser type	Diode laser		
Laser irradiation type	Weaving		
Fiber core, mm	1.0		
Homogenizer	LL3		
Focus lens, mm	400		
Laser power, kW	6		
Laser irradiation angle, degree	15°		
Defocus, mm	20		
Spot size, mm x mm	4.5^w x 27^l		
Power density, W/mm^2	55		
Weaving wave form	Exponential		
Weaving frequency, Hz	5		
Compensate heat source			
Laser type	Fiber		
Compensated laser power, kW	3		
Defocus, mm	200		
Spot diameter, mm	10		
Laser irradiation angle, degree	13°		
Compensated pre-irradiation, s	10		
Hot-wire parameter			
Filler wire diameter, mm	1.6		
Welding speed, cm/min (m/h)	3.33 (2)	5.0 (3)	6.67 (4)
Wire feed speed, m/min	5.11	7.67	9.93
Wire current, A	174	208	245
Wire feeding angle, degree	35		
Wire feeding position, mm	0		
Shielding gas (Argon), LPM	10		
Pre irradiation time, s	90		
Welding time, s	20		

Table 7.3 Welding parameters of Weaving laser irradiating method

Laser irradiation method	Weaving 5 Hz-exponential wave
Fiber core, mm	1.0
Homogenizer	LL3
Focus lens, mm	400
Laser power, kW	6
Laser irradiation angle, degree	15°
Defocus, mm	20
Spot size, mm x mm	4^w x 27^l
Power density, W/mm^2	55
Filler wire diameter, mm	1.6
Welding speed, cm/min	3.3
Wire feed speed, m/min	5.31
Wire current, A	181
Wire feeding angle, degree	45
Wire feeding position, mm	5
Shielding gas (Argon), LPM	10
Pre irradiation time, s	120

Table 7.2 and 7.3 present welding parameters of twin laser and weaving laser method, respectively. Based on the aforementioned results, perfect fusion of weld joints that 3 speed levels (3.33, 5.00 and 6.67 cm/min) of twin laser method and 1 speed level (3.33 cm/min) of weaving laser were used.

7.3 Metallurgical preparation for grain size measurement

In order to measuring prior austenite grain boundary on HAZ, Marshall's reagent was used for reveal prior austenite grain boundary (PAGB) and for observation of microstructure on the same time. Etching recipes is 2 main parts of the solution. Part A is mixing of 5 mL of sulfuric acid, 8 g of oxalic acid and 100 mL. Part B is 30% solution of hydrogen peroxide. Mixing Part A and B by 1:1 ratio and hold the specimen in a vertical direction in the etching solution. Post etching by 3% nital solution for reveal interior microstructure.

Optical microscopic was used to observe and obtain a microscopic image on the etched specimen. HAZ grain size was investigated from fusion boundary to unaffected zone (base metal). Continuous (20% lapping) images were assembly by 50 X magnification. 5 images of 200X magnification with same position from fusion boundary were used for measurement of PAGB. Linear intercept method was used

to obtain average grain size. Evaluated length of liner intercept is 28,000 μm (28 mm) on each position.

7.4 Investigation of effect of heat input levels on HAZ characteristics

Fig. 7.2 shows macro cross sections of 50 mm weld distance. Complete fulfill and complete fusion (macro scale observation) were achieved, then the effect of heat input was compared. Simple heat input calculation (Heat input = laser power / welding speed) was used to compare with other processes such as conventional EGW or VEGA ® process. Results of the calculation are 162, 108 and 81 kJ/cm for welding speeds of 3.33, 5.00 and 6.67 cm/min with the twin laser of 9 kW. For weaving laser (single diode laser) method, 108 kJ/cm for welding speed of 3.33 cm/min with laser power 6 kW was obtained.
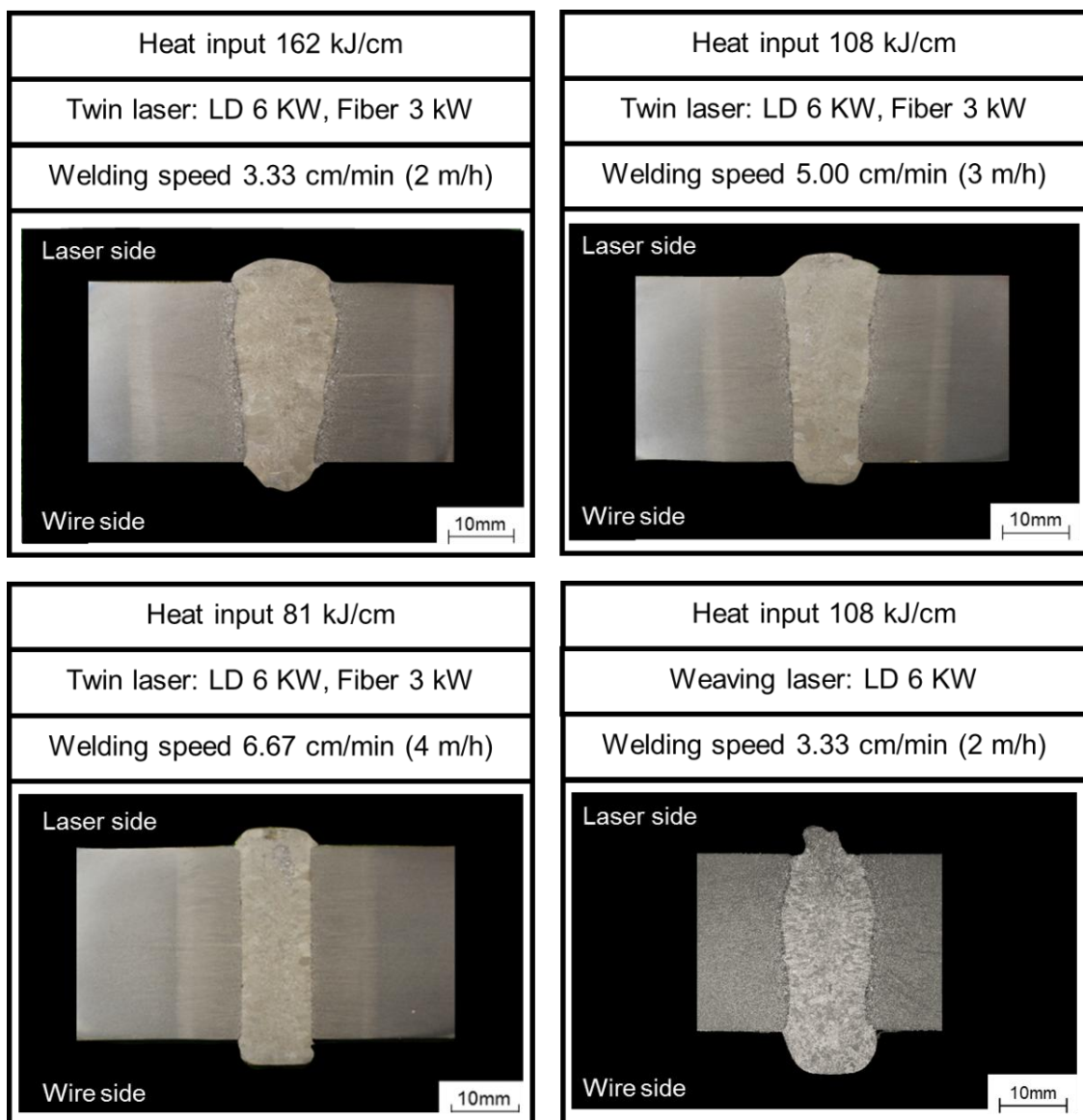
Fig. 7.2 Horizontal cross sections of weld specimen under influenced of heat input levels.
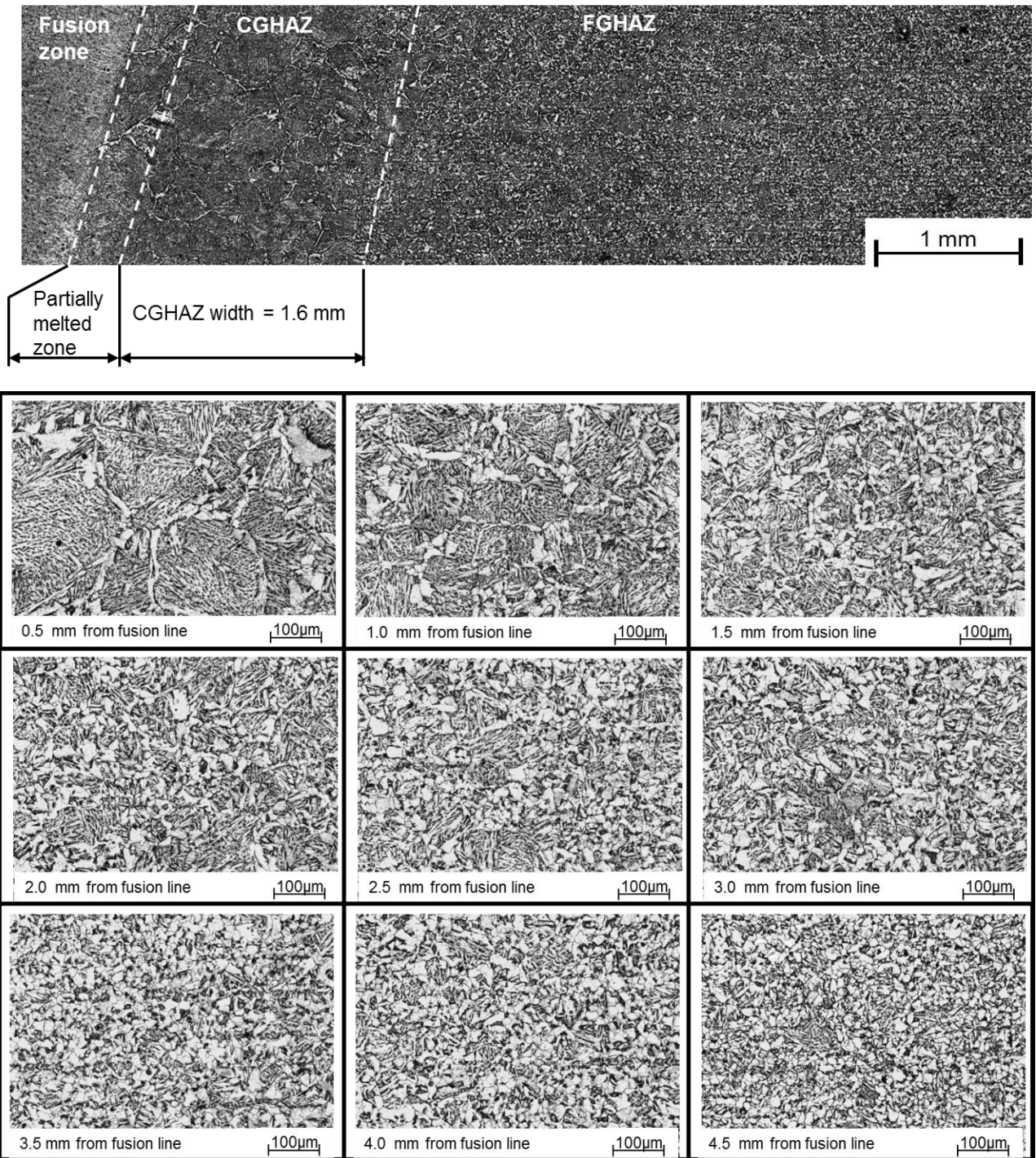
Fig. 7.3 HAZ microstructure of weld heat input of 162 kJ/cm (9kW, 3.33 cm/min)

Half melted grain | CGHAZ width =0.7 mm

0.5 mm form fusion line   100μm

1.0 mm form fusion line   100μm

1.5 mm form fusion line   100μm

2.0 mm form fusion line   100μm

2.5 mm form fusion line   100μm

3.0 mm form fusion line   100μm

3.5 mm form fusion line   100μm

4.0 mm form fusion line   100μm

4.5 mm form fusion line   100μm

175
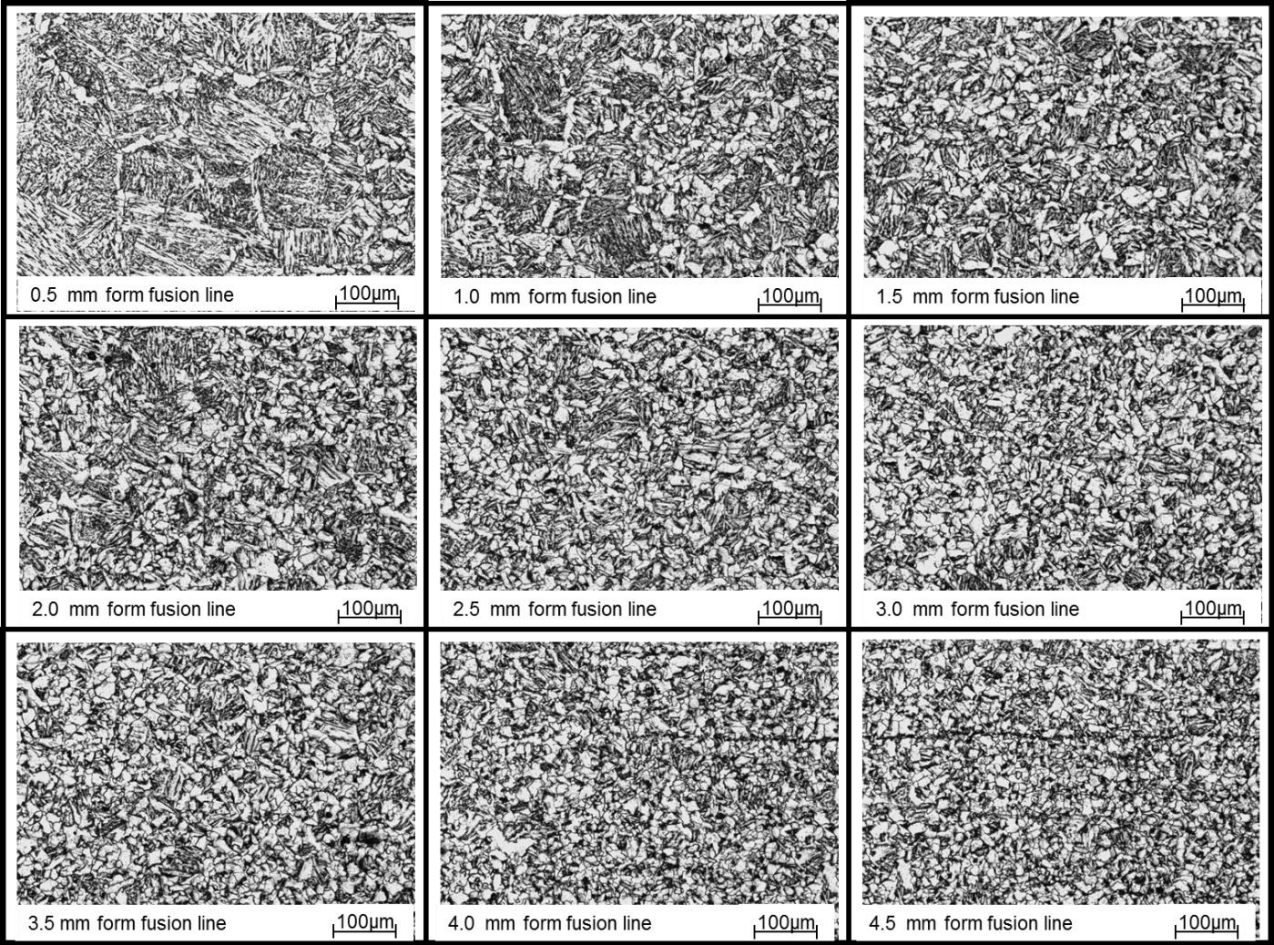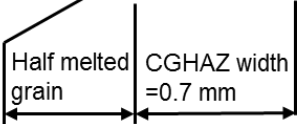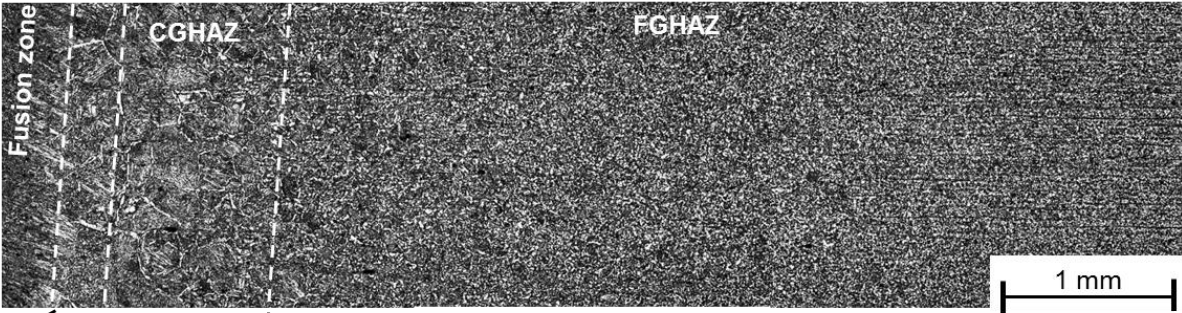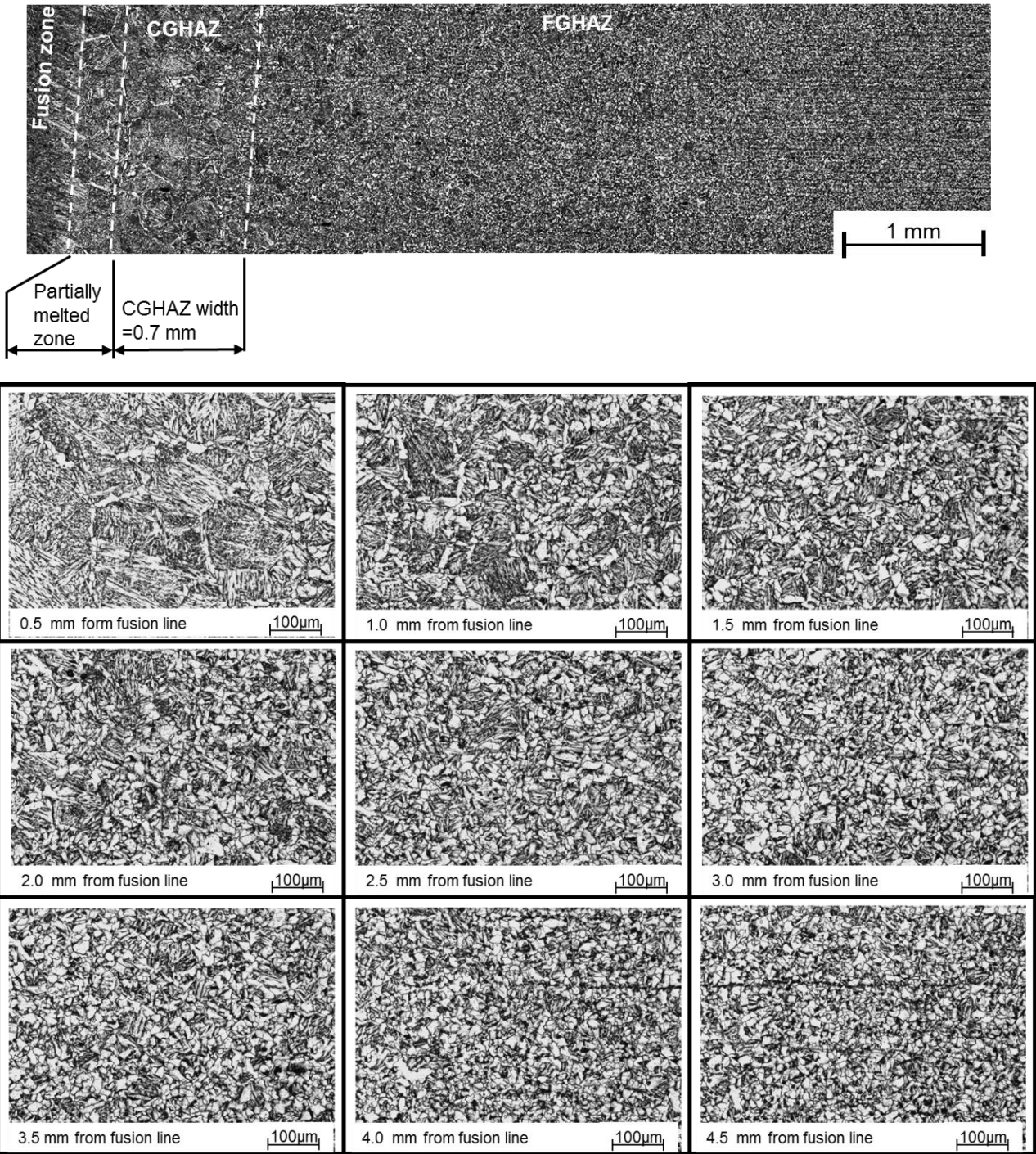
Fig. 7.4 HAZ microstructure of weld heat input of 108 kJ/cm (9kW, 5.00 cm/min)
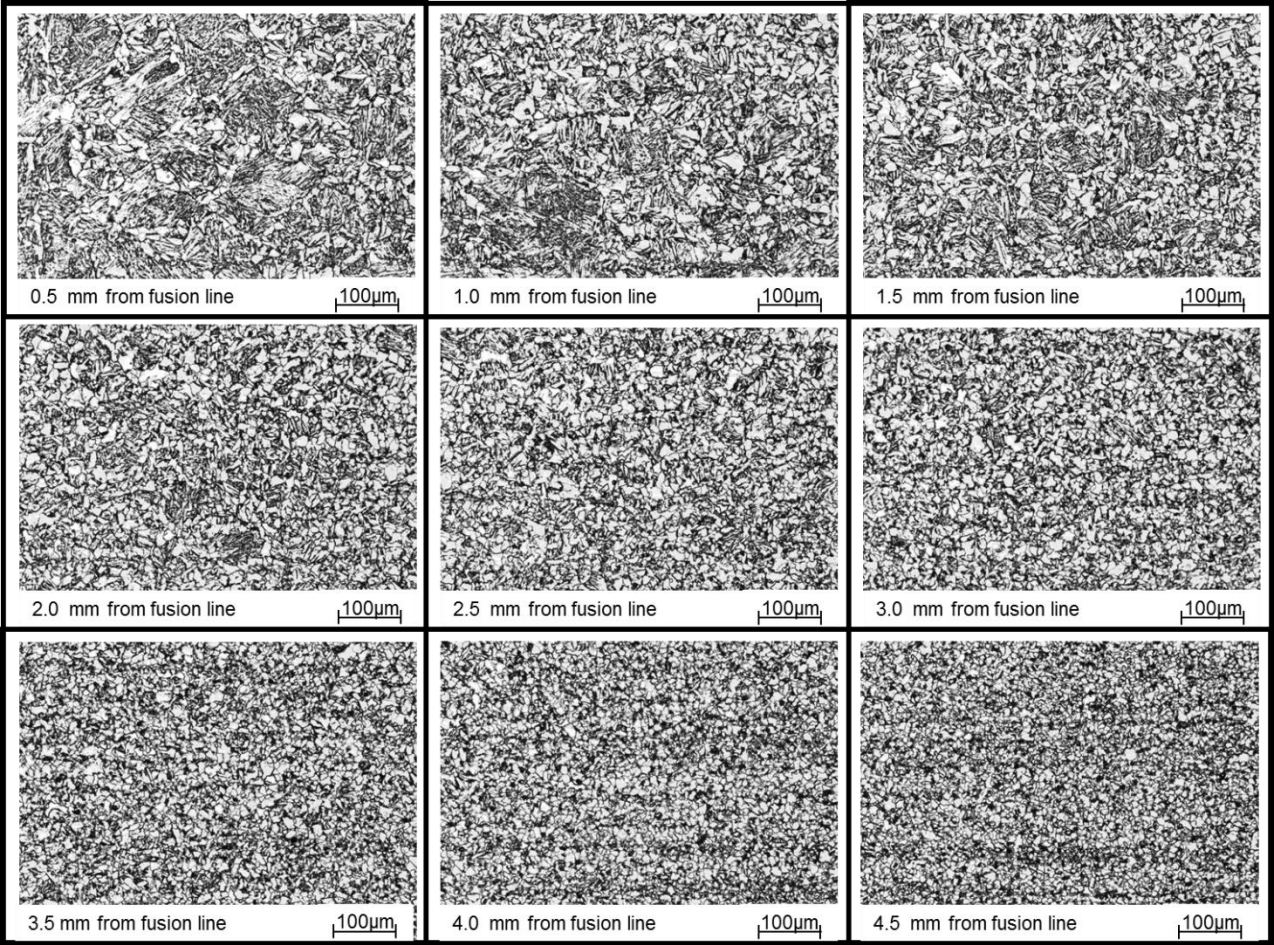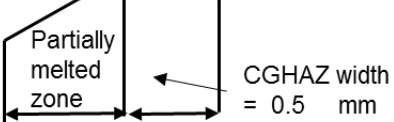
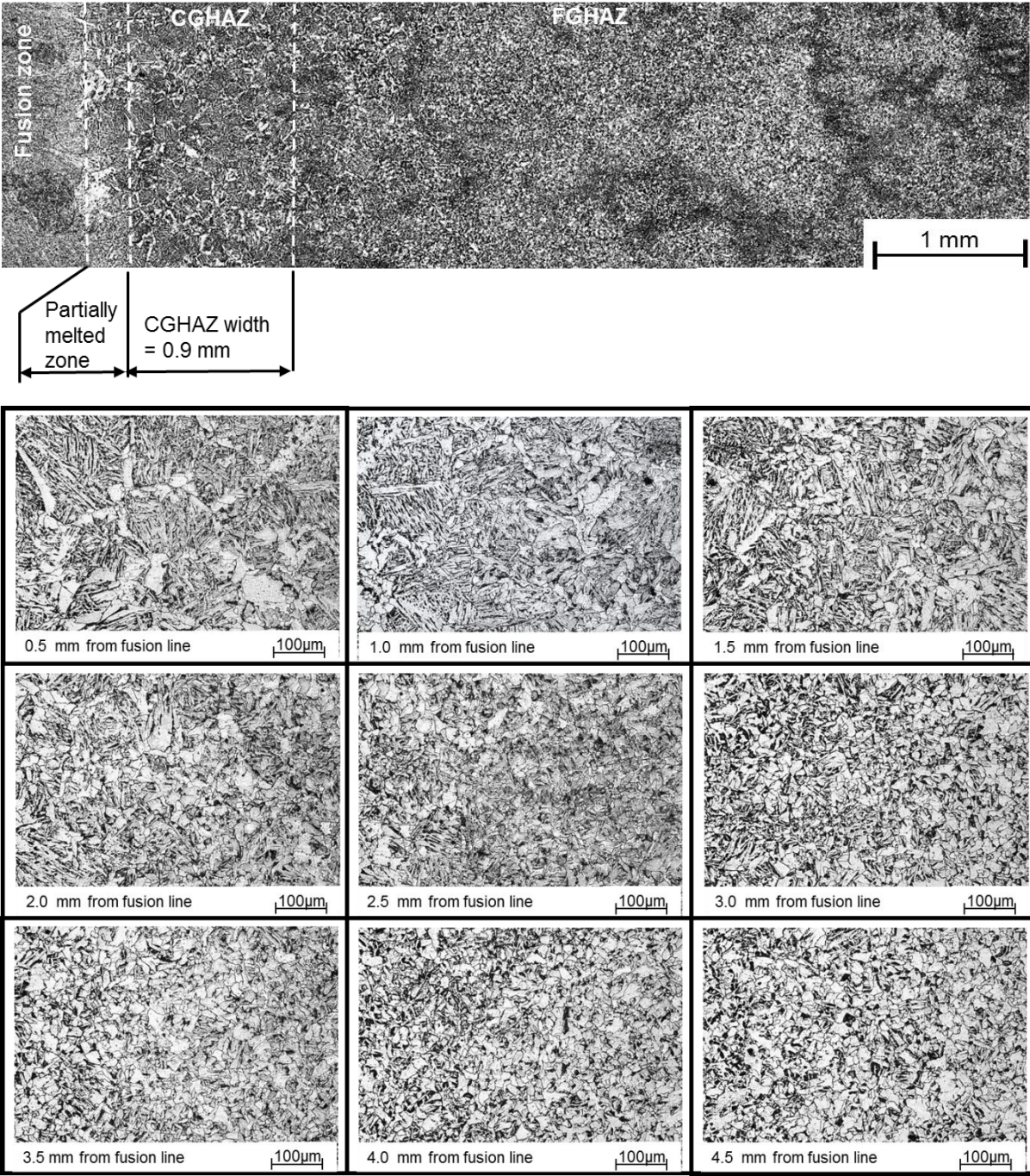Fig. 7.5 HAZ microstructure of weld heat input of 81 kJ/cm (9kW, 6.67 cm/min)

Fig. 7.6 HAZ microstructure of weld heat input of 108 kJ/cm (6 kW, 3.33 cm/min)
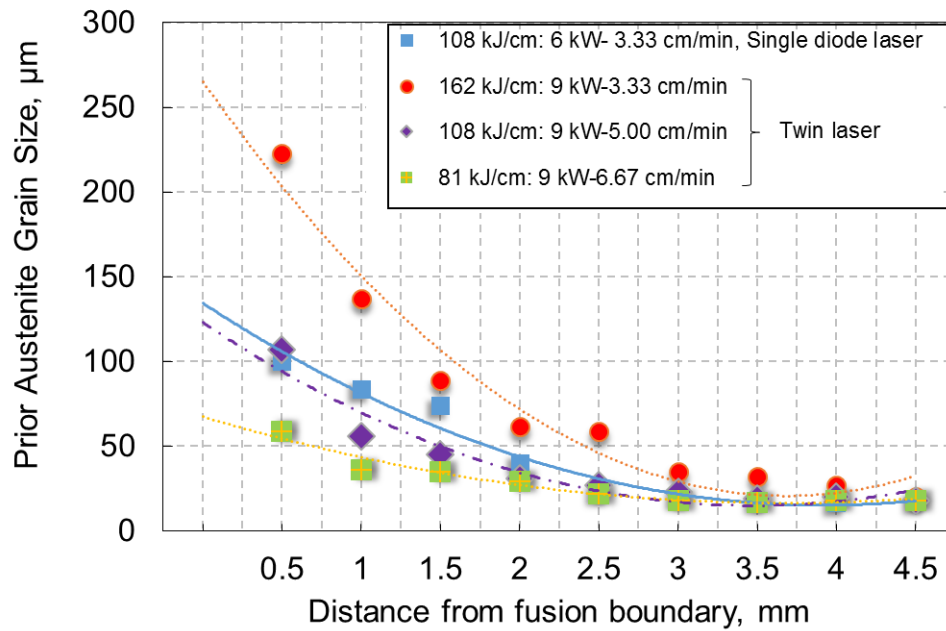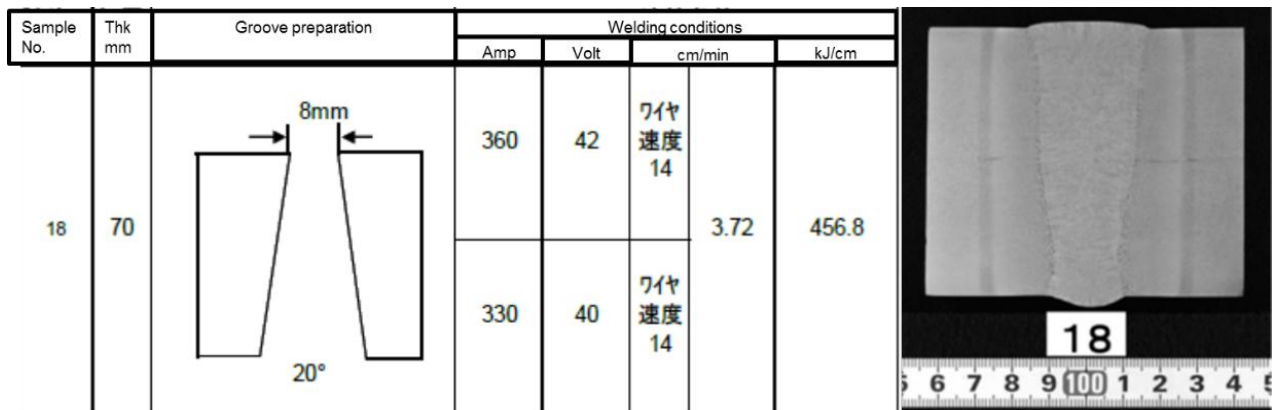
Fig. 7.7 Grain size distributions under influenced of welding heat input.

Results of microstructures of HAZ for the twin laser 162, 108 and 81 kJ/cm were shown on Fig. 7.3, 7.4 and 7.5, respectively. Fig. 7.6 shows microstructures of heat input of 108 kJ/cm for the weaving laser method. In qualitative comparison, it could be seen that higher heat input has wider coarse grain heat affected zone (here after call as CGHAZ) and low heat input level has narrower CGHAZ.
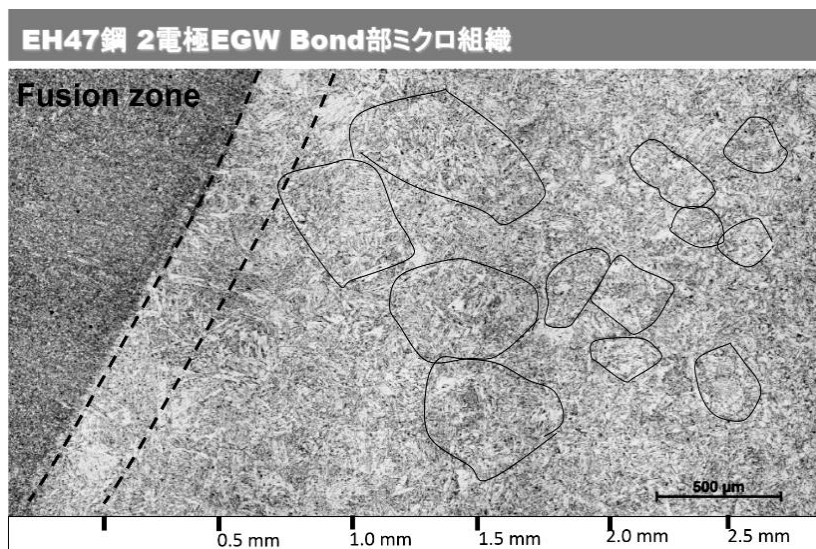
Clear microstructures of grain growth region can be observed to measure PAGB. The result of grain size distribution for each welding conditions were plot along measured distance from fusion boundary in Fig. 7.7. It was clearly seen that the grain size increased when heat input increasing. The highest heat input of 162 kJ/cm has an average grain size at 0.5 mm is 223 µm and gradually decreased when the distance is far from fusion boundary more 1.5 mm. Decreasing heat input by increasing welding for the twin laser from 3.33 cm/min to 5.00 cm/min and 6.67 cm/min (108 and 81 kJ/cm) resulted in smaller grain size than 150 µm at distance of 0.5 mm.

For weaving laser method which has heat input of 108 kJ/cm, same tendency of grain growth was obtained as that of the twin laser of 9 kW with welding speed of 5.00 cm/min, and the maximum grain size has a same size together. The distribution of weaving laser shows wider CGHAZ than twin laser case because may be affected by the width of the specimen. However, it has the same trend of the distribution when welding heat input is the same level.

All of welding condition, the grain size became smaller than 50 µm when distance is far from 2 mm. It was mean that the proposed process provides low heat input since CGHAZ width is narrower than 2 mm.

Sample No.	Thk mm	Groove preparation	Welding conditions				
			Amp	Volt	cm/min	kJ/cm	
18	70	8mm 20°	360	42	ワイヤ速度 14	3.72	456.8
			330	40	ワイヤ速度 14		

(a) Welding procedure and macro cross section

(b) Microstructure of HAZ

Fig 7.8 Two electrode VEGA® with joining on thickness of 70 mm, base metal type EH 47 steel, Heat input of 456 kJ/cm. (Resource from Nippon Steel and Sumitomo Metal Cooperation)

To compare with the best condition of vertical joining process on the present, the result of two electrodes VEGA® was used. Fig 7.8 (a) showed the welding condition of two electrodes VEGA® for joining on the thickness of 70 mm, base metal type EH 47 steel (same grade of the experiment). Heat input of 456.8 kJ/cm was applied to achieve single pass joining on the thickness of 70 mm. Fig 7.8 (b) showed HAZ microstructure and marks PAGB in HAZ. It can be seen that coarse grain occurred in this process although this case is the beast condition for joining. Grain sizes were obtained, and the result was plotted on Fig. 7.9.
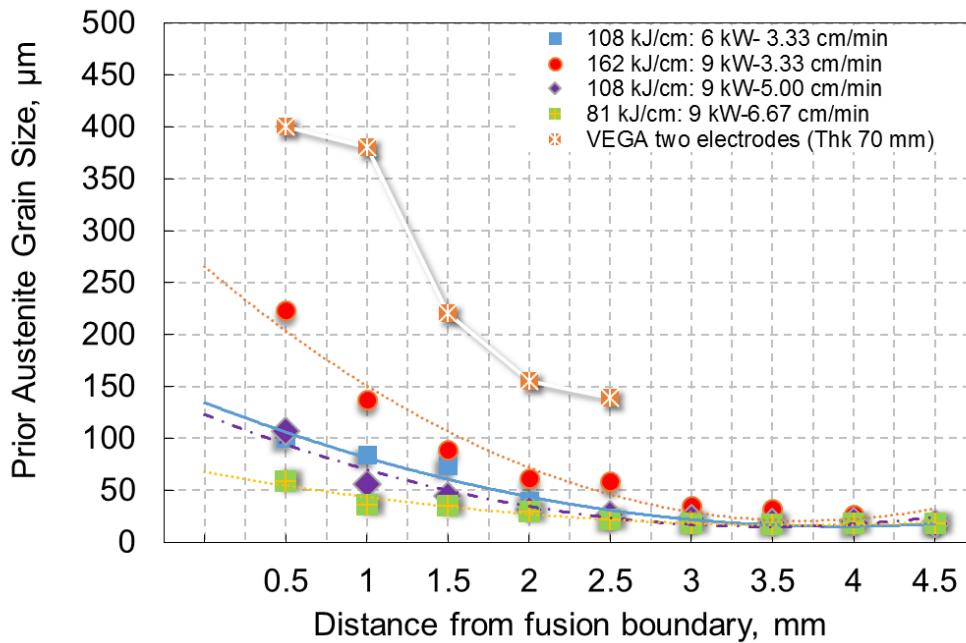
Fig. 7.9 Comparison of grain size distribution between the proposed process and VEGA® process

Fig. 7.9 shows results of a comparison of grain size distribution between the proposed process and VEGA ® process. Coarse grain behavior extremely occurred over the VEGA ® process. Although distance is far over 2.0 mm from fusion boundary, the grain size was over 100 µm. This is clear evidence that the proposed process can provide joining condition with low heat input level. By this comparison, EH-47 steel has a good property for retard austenite grain growth then it was applied to the structure for support high heat input joining. However, EH-47 steel is not used over wide fields of fabrication industries. It must be noted that high heat input process is not adequate joining process for sensitive steel on grain growth or conventional steel. Therefore, the proposed process has a good potential to apply joining over wide steel grades and wide fields of heavy joint fabrication industries in the present and the future.

Fig 7.10 shows the microstructure of CGHAZ for the proposed process and Fig. 7.11 shows the width of CGHAZ with as a function of heat input. CGHAZ could be controlled by welding speed controlling. High welding speed could provide the narrow width and small grain size of CGHAZ. Moreover, Fig. 7.1 shows clearly evidence that low heat input could be controlled by increasing welding speed but not need to decrease laser power. Since as the proposed process, especially the twin laser method, has a working range on both of modulation modes of laser power and welding speed to maintain the sound joint result.
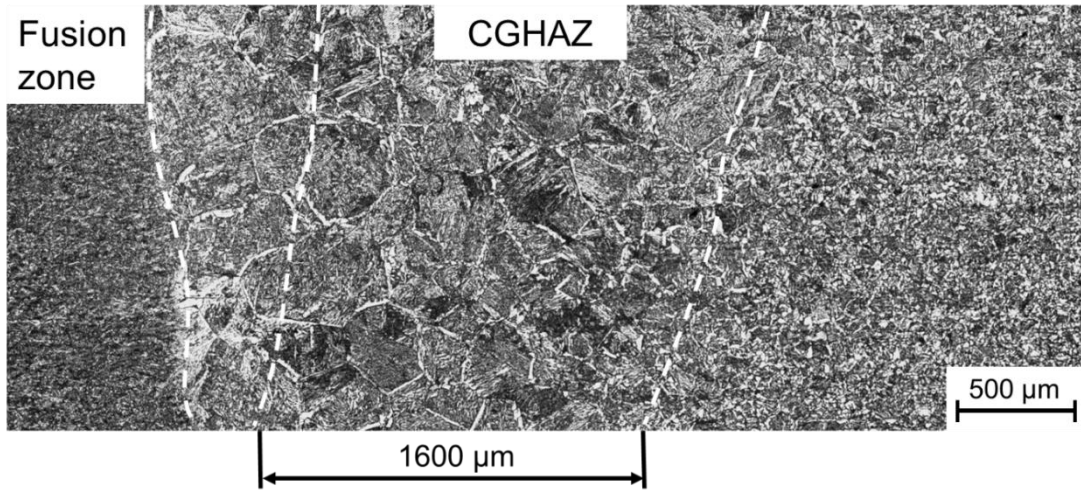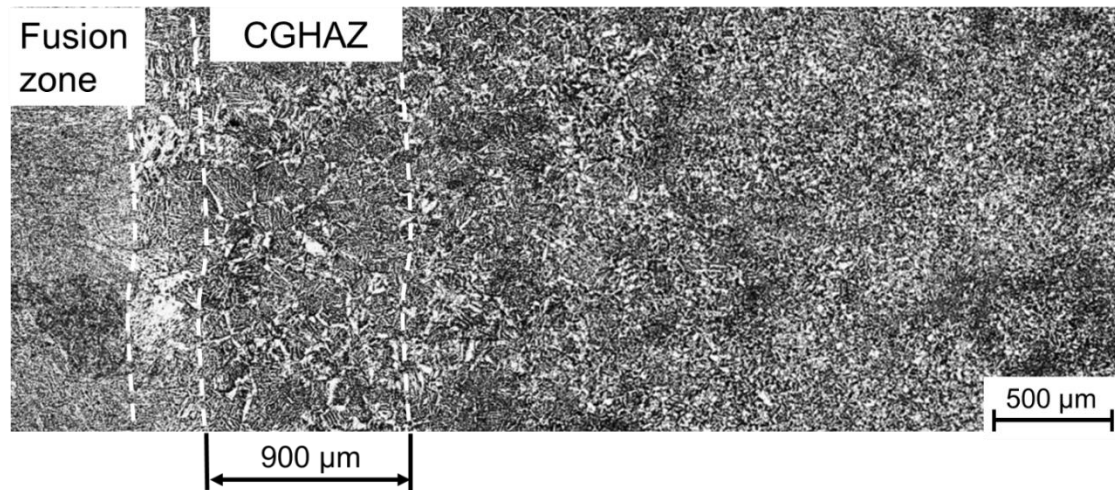
(a) Heat input 162 kJ/cm with twin laser 9 kW, welding speed 3.33 cm/min
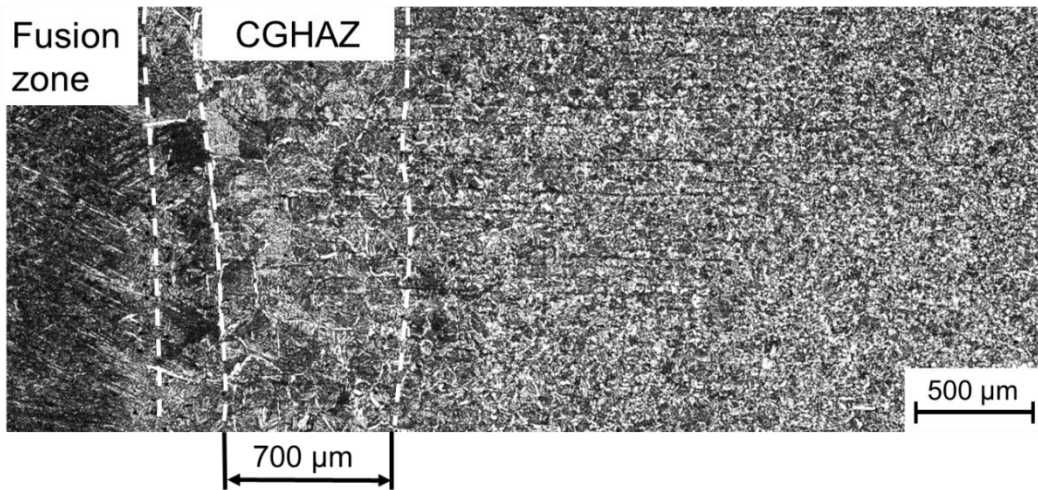
(b) Heat input 108 kJ/cm with twin laser 9 kW, welding speed 5.00 cm/min
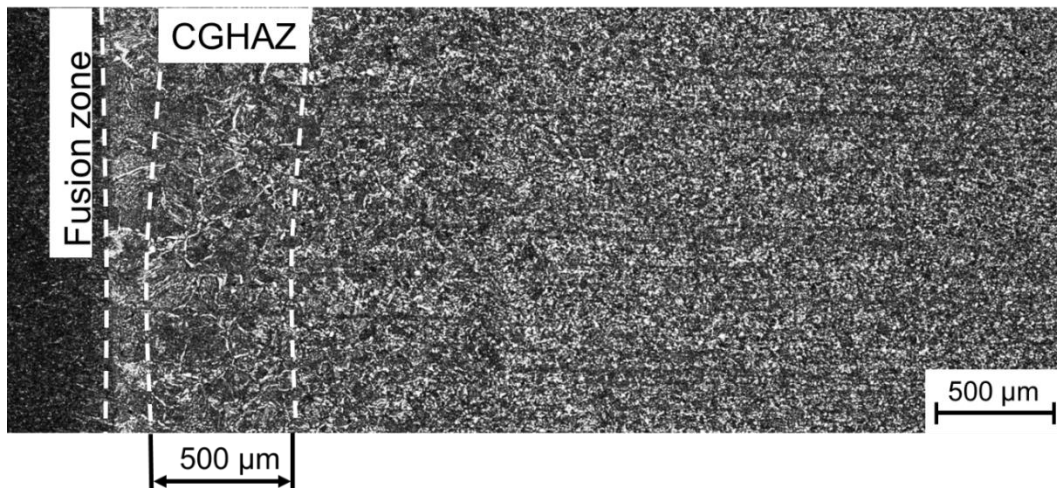
(c) Heat input 81 kJ/cm with twin laser 9 kW, welding speed 6.67 cm/min

(d) Heat input 108 kJ/cm with single diode laser 6 kW, welding speed 3.33 cm/min

Fig. 7.10 Observation coarse grain heat affected zone (CGHAZ) for the proposed process.

Increasing welding speed provides decreased of heat input for joining and smaller HAZ size. Welding speed of 5.00 cm/min (3 m/h) has an advantage of the narrow CGAHZ and small grain size compared with low welding speed case of 3.33 cm/min (2 m/h). The width of CGHAZ of 700 µm could be obtained by welding speed of 5.00 cm/min while the speed of 3.33 cm/min has the width of CGHAZ of 1600 µm. In case of welding speed of 6.67 cm/min (4 m/h) it must be note that this speed condition was a boundary of fusion) critical speed then it has drawback on the robust process side than speed 5.0 cm/min. By comparing the width of CGAHZ of the proposed process with VEGA®, it was clearly seen that narrower grain size could be obtained with narrower 2 mm by the proposed process while VEGA obtained the width of CGHAZ wider 2.5 mm as shown in Fig. 7.12. In addition, the proposed process could be controlled CGHAZ width to become narrower by controlling welding speed. If possible provide high power laser source can be employed, CGHAZ width will be narrower.
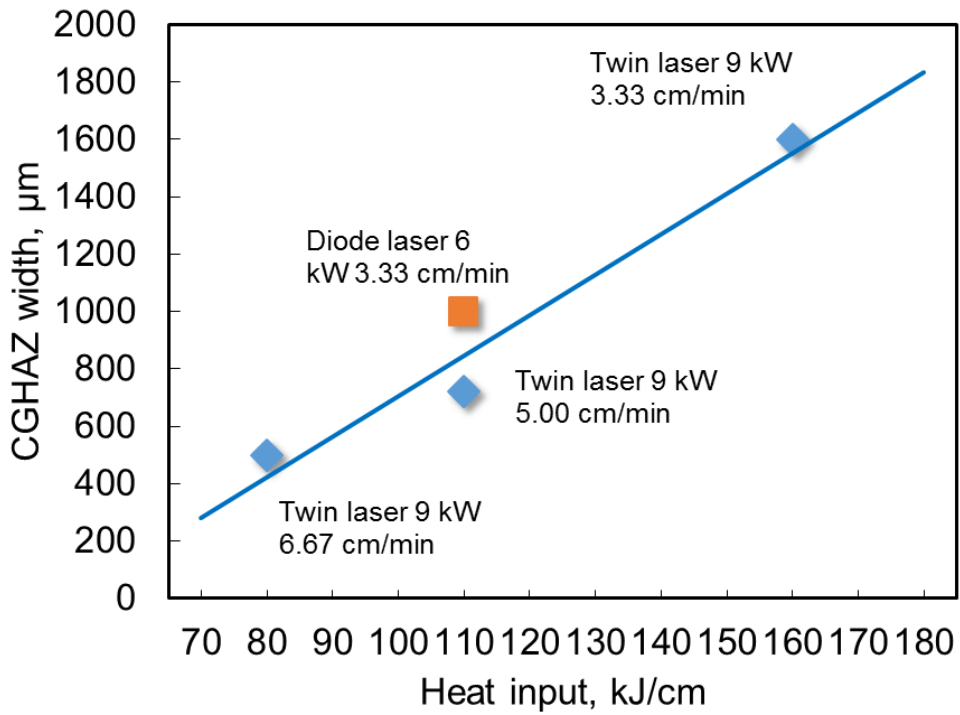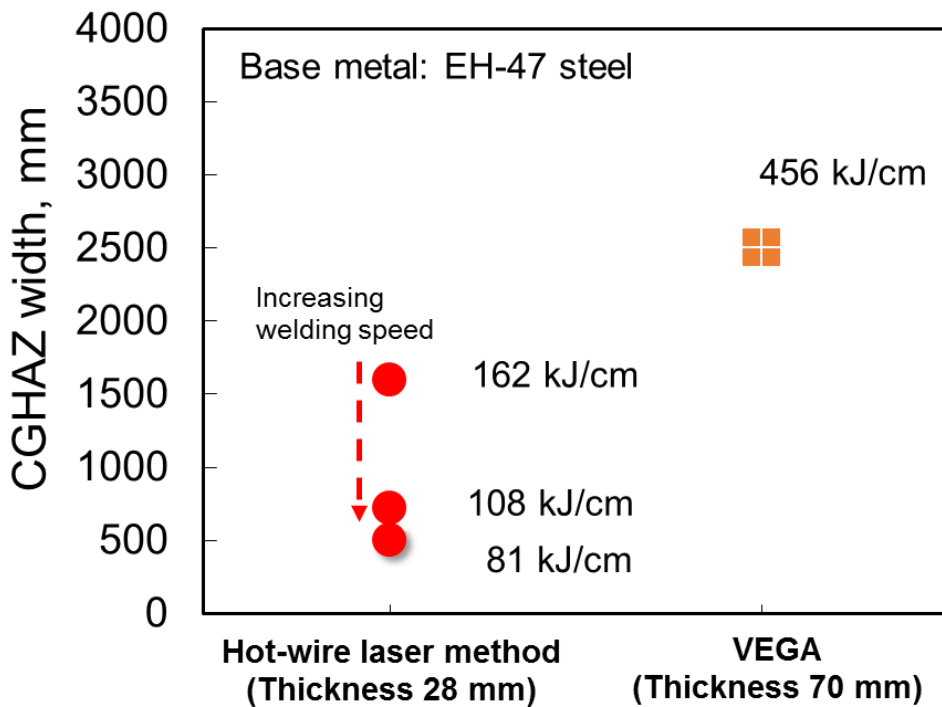
Fig. 7.11 CGHAZ width as a function of heat input.

Fig. 7.12 Comparison CHAZ width between the proposed process and VEGA

7.5 Hardness distribution on HAZ

To investigate the heat input effect on base metal, Vicker hardness test was performed with 10 kg load and indentation time of 10 second. Measurement line across the weld joint with the effect of heat input levels (average from 3 line same position of section 6.2.5) were shown in Fig. 7.13. As for HV of base metal about 200 HV, it can be seen that increasing heat input resulted in wider hardness changed. Moreover, It has a trend of softening behaviors occurred when used low welding speed or high heat input of 162 kJ/cm. On the other hands, low heat input condition (high welding speed used) shows narrow HV changed and small difference on hardness levels. It was noticed that the proposed process does not provide harder zone over working range conditions.

Hardness results of the VEGA with 501 kJ/cm was also compared. It can be seen that wide softening zone and large significant differences of hardness levels on HAZ and base metal. It cases of the same speed (same interaction time) the proposed process with 168 kJ/cm obtain narrow and shallow softening region than VEGA, obviously. By this result mention the proposed process has advanced of controllable a welding speed to get small hardness fluctuation.
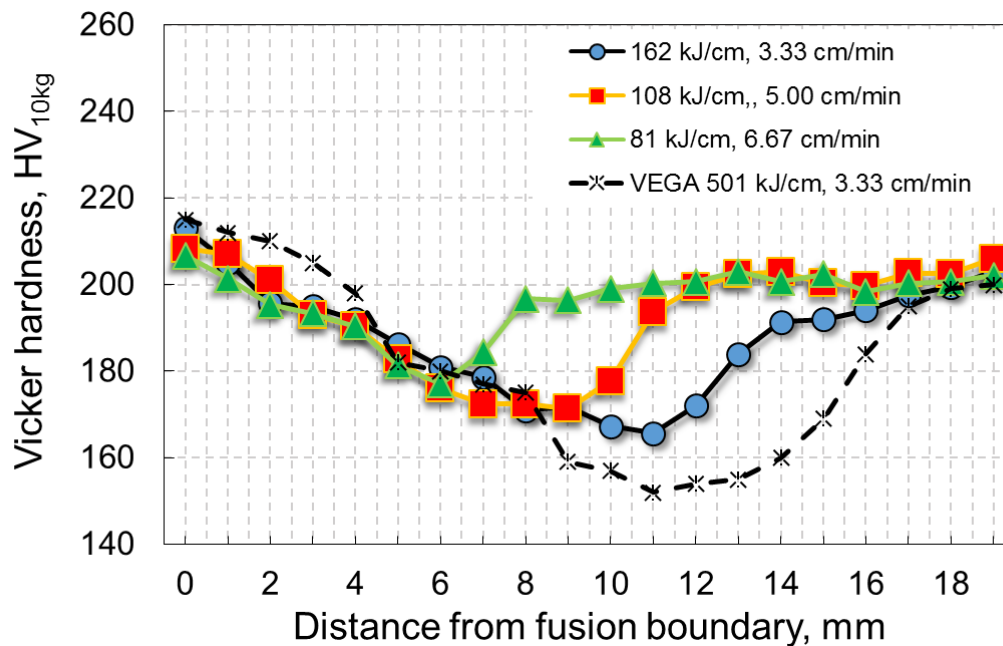
Fig. 7.13 Hardness distribution on HAZ by differences heat input levels.

7.6 Comparison of heat input requirement for joining with other joining processes

Analysis of possible joining over many joint metal thickness with the heat input of welding process, Fig. 7.13 showed requirement of heat input for conventional EGW, single electrode VEGA, two electrodes VEGA and the hot-wire laser method (the proposed process) over joint thickness. The heat input level on each process were obtained from the literature which were mentioned in chapter 2 and the hot-wire laser method follows heat input as aforementioned. Conventional EGW required energy input of 227 kJ/cm for joining on thickness only 19 mm and may be much energy requirement for joining over plate thickness of 50 mm. Single electrode VEGA that could reduce heat input for joining thickness of 19 mm by used only 72 kJ/cm but must be used 258 kJ/cm for plate thickness of 50 mm. However, it has been reported that single elected VEGA difficulty joins on heavy joint thickness (over 50 mm) because imperfections such lack of fusion was found on those joints. Two electrodes VEGA process has been using for heavy thickness joining such 50 mm plate thickness by high heat input over 280 kJ/cm. In case of 70 mm plate thickness that over 380 kJ/cm (welding speed of 5.00 cm/min) of heat input was applied. And heat input of 456 kJ/cm is the best condition (free defect condition) for two electrodes VEGA with welding speed of 3.72 cm/min.
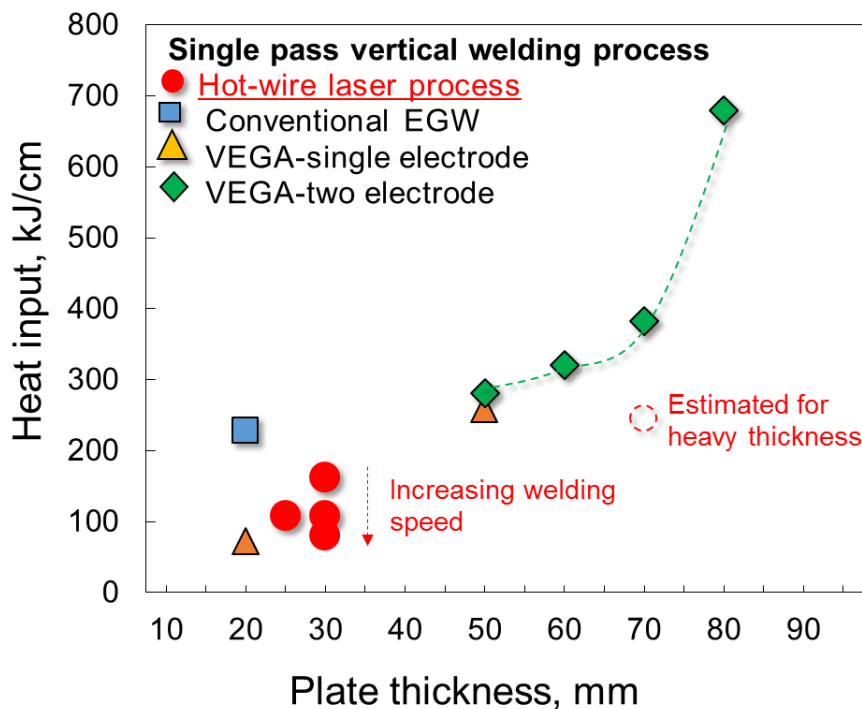

Fig 7.13 Comparison specified heat input for single pass vertical joining processes over joint thickness.

On the other hands, the hot-wire laser method has a good potential for the lower requirement of the heat input for joining over plate thickness and could be reduced heat input by increasing welding speed. AS for estimate laser power source for joining over plate thickness of 70 mm, keep power density of 55 W/mm2 with laser beam spot size of 4 x 27 mm and weaving by 5 Hz exponential wave that required 18 kW laser power and compensate laser power of 1 kW on both edge sides. Total laser power of 20 kW with the welding speed of 3.33 cm/min (worth case) has a calculated heat input of only 360 kJ/cm or lower than two electrodes VEGA than 1.5 times. It is be able to reduce the heat input by increasing welding speed by same trend from the experiment (chapter 5) such optimized welding speed of 5.00 cm/min that will have the heat input of only 240 kJ/cm or 1.58 times reducing from two electrode VEGA under same welding speed. The open mark with a broken line is represented the estimated heat input for the hot-wire laser method for 20 kW with the welding speed of 5.00 cm/min.

AS aforementioned, the hot-wire laser method has a good potential to be single pass vertical joining method on heavy joint by keep a lower heat input for joining. It is a good tendency for maintain properties of the parent metal since as the low heat input for joining has the few effects on grain growth and toughness of weld joint.

7.7 Summary

Investigation of heat input effects on HAZ's characteristics could be draw conclusion as:

1)   For twin laser method, heat input was controlled by welding speed ranges. Increasing welding speed resulted in heat input was decreased thereby grain size on CGHAZ became smaller.

2)   CGHAZ width of the proposed process has narrower 1,600 μm and could narrower than 700 μm by using the welding speed of 5.00 cm/min which was optimized welding speed for sound weld condition.

3)   Compare HAZ's characteristics of the proposed process with two electrode VEGA, the proposed process has an advantage of both of grain size and CGHAZ over two electrode VEGA.

4)   HAZ hardness fluctuation of the proposed process has a narrower and shallower that VEGA method. The proposed process has the advantage of welding speed controllable to obtain small hardness fluctuation.

5)   The requirement of heat input of the proposed process has lower level of heat input when comparatively compared with other vertical welding process.

Chapter 8

Summary and future work

Development of the low heat input process for single-pass vertical joining on thick steel plates is the main propose of this study. Originality idea by a combination of hot-wire method and laser heat source was expected to provide low heat input joining, high-efficiency weld deposition and appropriate weld joint properties. Thick steel plates of high strength steel grade of YP-47 steel is used material for high efficiency hull structure, was used as base metal in order to compare weld joint properties with high heat input process such as VEGA® process. A high-power laser diode is used as the main heat source. A large-rectangular spot-shape, which fits a groove width (gap) dimension and plate thickness, is irradiated to make a weld pool. Reflected laser on the molten pool surface is used to melt groove surfaces in front of the molten pool, efficiency. Laser irradiating methods were developed and studied welding phenomena during vertical welding.

The background statement and the research objective were discussed. The present research and technical reports were reviewed on the meet requirement of high-performance fabrication technology.

Next, the basic idea of the proposed process was created and investigated the welding phenomena. Irradiating of large rectangular laser spot size to crates weld pool is possible and able to make weld joint by hot-wire feeding as single pass vertical joining. In-suit observation by the high speed camera, reflected laser beam was investigated and obtained the evidence of it could make the initial melting on groove surfaces. From the study of the stationary laser beam was irradiated over narrow gap width (5 mm gap) and welding speed ranges were varied. Power density is the primary parameter to obtained base metal melting. Critical power densities with relative to welding speeds were obtained, which is about 25 and 35 W/mm^2 for each welding speed of 1.7 and 3.3 cm/min, respectively.

The weaving laser beam irradiating method by was developed to obtain adequate fusion of base metal over large gap size (10 mm) instead of the low power density stationary laser beam. The narrow-width long-length sweep in the gap width direction provided an appropriate laser power density can improve a joining fulfill and amount of base metal melt. While the stationary laser beam has a low power density over wide laser spot width due to the limit of laser power source, resulting a low melting amount of base metal and large size of lack of fusion occurred. The welding phenomena of weaving laser method, the value of power density largely affects initial melting of base metal. However, large amount of base metal or final melting volume of weld metal was strongly affected by the weld pool heat

conduction. The wide laser spot size-W_L/W_G =0.4 could maintained a high temperature weld pool and resulting on large melting volume (larger weld bead size). Meanwhile, laser beam W_L/W_G = 0.2 has resulted on large difference the liquid weld pool energy when laser beam moving, although narrower laser beam width irradiated by higher power density. It was mentioned that using long length laser beam size for joining resulted of much low energy on the beam tails (edge region). Frequently imperfection such incomplete fulfill or lack of fusion occurred on this region. An important idea that problem is a compensation the laser energy on the both tails for troubleshooting for the imperfection occurring.

Then, the twin laser method was performed to improve weld joint quality for sound weld achievement. Twin laser method has successfully applied on one pass vertical joining. Imperfection on edge region could be fixed by compensate laser power on the edge region. For one side of compensate laser power, laser power levels strong affected melting amount of base metal. 3 kW compensate laser power provided complete fulfill weld metal and complete fusion of weld joint under fixed welding speed 3.33 cm/min (2 m/h). It was performed to study of welding speeds effects to optimized welding parameters. The optimized welding speed for twin laser with one side compensation is 5.00 cm/min (3 m/h). It provided complete fulfill and adequate weld penetration. From the information of this chapter, it can be suggested that homogenizer for create laser beam shape should distribute higher energy on the edge tails on the laser beam. The center region can irradiate by lower energy since during joining heat conduction from both tail sides can provide adequate energy for fusion base metal.

The weld joining properties were studied. The fusion zone characteristics were investigated. Cooling transformation time, Δt8/5 were obtained and related with microstructure and toughness. The cooling characteristic of the twin laser method has Δt8/5 range of 84 to 200 second. The selected filler metal of JIS3312 G78AUMN5C1 M3T provided martensitic-bainitic base of microstructures transformation. Increasing welding speed resulted in cooling time became short and resulted in the fine martensite phase formed. On the other hand, long cooling time by low welding speed resulted in coarse upper bainite formed. The finest microstructure of cooling time of 84 second was performed on the Charpy V-notch test. Absorbed energy more than 100 Joule at test temperature -20 °C could be obtained by high-speed condition.

According to the main target of low heat input delivered to base metal, heat input effects on HAZ's characteristics was investigated. Twin laser method, heat input was controlled by welding speed ranges. Increasing welding speed resulted in heat input was decreased thereby grain size on CGHAZ became smaller. CGHAZ width of the proposed process has narrower 1,600 micron and could narrower than 700 micron by using the welding speed of 5.00 cm/min which was optimized welding speed for sound weld condition. Compare HAZ's characteristics of the proposed

process with two electrode VEGA, the proposed process has an advantage of both of grain size and CGHAZ over two electrode VEGA. It was clearly evidence of the proposed process provide low heat input welding for single-pass vertical joining. The requirement of heat input of the proposed process has the lower level of heat input when comparatively compared with other vertical welding processes.

The novel welding process has been successfully developed on the lab-scale specimen size. Therefore, the future work is an experiment on large-scale specimen size to physically simulate welding condition like a real field situation. New optical homogenizer to provide optimized laser energy distribution will be obtained and used on the experiment. Thermal behaviors on the large-scale specimen will be performed to investigate realized heat flow during welding. The appropriate filler metal will be developed for the proposed process by obtaining the high strength and high toughness properties.

Acknowledgements

.

Reference

1)　　山口欣弥，北田博重，矢島浩，廣田一博，白木原浩：『超大型コンテナ船の開発　−新しい高強度極厚鋼板の実用−』日本船舶海洋工学会誌 第 3 号 (2005)，p70-76

2)　　岡野重雄，大番屋嘉一，阿部研吾，細井宏一：『厚板需要業界の技術動向と当社の対応状況』神戸製鋼技報 Vol.58 No.1 (2008)，p2-7

3)　　木治昇，豊田昌信：『船舶　−溶接技術による安全・環境性能向上−』

4)　　溶接学会誌 No.3 (2012)，p21-24

5)　　船津裕二：『船舶(材料編)』溶接学会誌 No.4 (2012)，p41-47

6)　　中島善之，岡田哲男：『船舶(日本造船工業界)』溶接学会誌 No.1 (2013)，p24-28

7)　　白幡浩幸，皆川昌紀，井上健裕，大谷潤，船津裕二：『超大型コンテナ船厚手高靭性 YP47 鋼の開発』まてりあ Vol.51 No.2 (2012)，p76-78

8)　　一宮克行，角博幸，平井龍至：『「JFE EWEL®」技術を適用した大入熱溶接仕様 YP460 級 鋼板』JFE 技報 No. 18 (2007)，p13-17

9)　　廣田一博，中川隆，武田信玄，橘吉美，多田益男：『世界初の船体用降伏応力 47kgf/mm^2 級 高張力鋼板の開発と実船適用』三菱重工技報 Vol.44 No.3 (2007)，p28-32

10)　　金子雅人，泉学，吉川直宏，阿部研吾：『超大型コンテナ船向け大入熱溶接用 YP460MPa 級 厚肉鋼板の開発』神戸製鋼技報 Vol.58 No.1 (2008) p39-41

11)　　材料艤装部，技術研究所：『造船分野における高機能鋼板の実用化』

12)　日本海事協会会誌 No288 (2009)，p1-7

13)　溶接学会編：『新版溶接・接合技術入門 (2008)，p50-51

14)　佐藤正晴：『エレクトロガスアーク溶接法の施工技術』

15)　溶接学会誌 第 66 巻 第 4 号 (1997)，p54-58

16)　鈴木伸一，一宮克行，秋田俊和：『溶接熱影響部靭性に優れた造船用高張力鋼板 −大入熱溶接部の高品質化を実現する JFE EWEL 技術—』JFE 技報 No. 5 (2004)，p19-24

17)　小野守章：『最近の厚板溶接技術および熱影響部組織制御技術の進歩』

18)　JFE 技報 No.18 (2007)，p7-12

19)　金沢正午，中島明，岡本健太郎，金谷研：『微細 TiN による溶接ボンド部靭性の改善と 大入熱溶接用鋼の開発』鉄と鋼 第 11 号 (1975)，p65-79

20)　皆川章，寺嶋久栄，西山昇：『50kgf/mm^2 級高張力鋼大入熱溶接ボンド部の低温靭性改善に 関する一考察』溶接学会全国講演概要 No.37 (1985)，214-215

21)　弟子丸慎一，平井征夫，天野虔一，上田修三，上村尚志，坪田一哉：『氷海域海洋構造物向 大入熱溶接用厚肉鋼板の製造』川崎製鉄技報 Vol.18 No.4 1986)，p295-300

22)　児島明彦，植森龍治，皆川昌紀，星野学，市川和利：『微細粒子による溶接熱影響部の組織 微細化技術『HTUFF』を適用した厚鋼板の開発』まてりあ 第 42 巻 第 1 号 (2003)，p67-69

23)　児島明彦，清瀬明人，植森龍治，皆川昌紀，星野学，中島隆雄，石田浩司，安井洋二：微細粒子による HAZ 細粒高靭化技術"HTUFF$^®$"の開発』 新日鐵技報 第 380 号 (2004)，p2-5

24)　木谷靖，池田倫正，一宮克行：『溶接金属中 B の拡散を利用した大入熱溶接熱影響部の 高靭性化』JFE 技報 No.18 (2007)，p47-52

25)　伊藤実，児島明彦，田中洋一，皆川昌紀，小関敏彦：『低炭素鋼の大入熱溶接 HAZ 靭性に及ぼすオーステナイト中のボロン存在状態の影響』材料とプロセス Vol.17 (2004)，p1376

26)　船越督巳，田中智夫，上田修三，石川正明，腰塚典明，小林邦彦：『希土類元素と B 添加による高張力鋼の大入熱溶接ボンド部の組織と靭性改良』鉄と鋼 第 2 号 (1977)，p303-312

27)　稲垣道夫，寺井清，岡西達也：『立向き自動溶接：エレクトロスラグ溶接/
28)　エレクトロガス溶接』(1966)，p151

29)　笹木聖人，須田一師，元松隆一，橋場裕治，大北茂，今井嗣郎：『高能率 2 電極エレクトロ ガスアーク溶接法の開発』新日鉄技報 第 380 号 (2004)，p57-63

30)　豊原力，辻井浩，太田昌宏，大北茂，今井嗣郎，笹木聖人，本江敦忠，須田一師：『高能率自動立向エレガス溶接法の開発』溶接学会全国大会講演概要 No.70 (2002)，p38-39

31)　植森龍治，藤岡政昭，井上健裕，皆川昌紀，白幡浩幸，野瀬哲郎：『海運や建設現場を支える鋼材(造船・建産機分野)』新日鉄技報 第 391 号 (2011)，p37-47

32)　小川一郎，稲田達夫，伊藤保，渡邊光三，倉持貢：『(仮称)丸の内 1 丁目 1 街区開発計画(C 棟)の設計と高性能鋼材の適用(その 1．構造設計概要)』日本建築学会大会学術講演梗概集 (2002)，p757-758

33)　金沢武，町田進，矢野清之助，田中潔，山本辰一，松村裕之，糸賀興右 9%Ni 鋼の脆性破壊発生靭性と停止靭性の関係に関する実験的検討』日本造船学会論文集 第 153 号 (1983)，p306-315

34)　星野学，斎藤直樹，村岡寛英、佐伯修 :『LNG タンク用高靱性スーパー9%Ni 鋼の開発』新日鉄技報 第 380 号 (2004)，p17-20

35)　掘勝義，渡辺浩，明賀俊治，草野和喜 :『ワイヤ加熱にパルス電流を用いたホットワイヤ TIG 溶接法の開発-パルス　通電加熱ホットワイヤ TIG 溶接法の研究(第 1 報)- 』溶接学会論文集 第 21 巻 第 3 号 (2003)，p362-373

36)　長光勇輔 :『パルス通電加熱ホットワイヤ TIG 溶接を用いた超高速溶接技術の開発 広島大学大学院 工学研究科 修士論文 (2007)

37)　片山聖二 :『レーザ溶接技術開発の最新動向』溶接学会誌 第 80 巻 第 7 号 (2011)，p11-19

38)　片山聖二 :『レーザ溶接』溶接学会誌 第 78 巻 第 2 号 (2009)，p40-54

39)　片山聖二 :『鉄鋼材料のレーザ溶接およびハイブリッド溶接』
40)　日本船舶海洋工学会誌 第 51 号，p23-29

41)　古賀宏志，郷田穂積，寺田伸，廣田一博，中山伸，坪田秀峰 :『レーザ・アークハイブリッド溶接の初の一般商船への適用』三菱重工技報 Vol.47 No.3 (2010)，p86-91

42)　橋田光栄 :『ホットワイヤ・レーザ溶接法による高張力・高靱性極厚鋼板立向き溶接技術の 開発』広島大学 工学部 卒業論文 (2012)

43)　橋田光栄，Warinsiriruk Eakkachai，山本元道，篠崎賢二，門井浩太，矢島浩，谷野忠和 福井努，中山伸，野瀬哲郎，土谷祥子，渡辺浩，金沢辰徳 :『ホットワイヤ・レーザ溶接法 による厚鋼板立向き溶接プロセスの開発』溶接学会全国講演概要 No.95 (2014)，p246-247

44)　Hashiba Yuuji, Sasaki Kiyohito, Kasuya Tadashi, Inoue Takehiro, Funatsu Yuuji, DEVELOPMENT OF WELDING MATERIALS FOR HIGH HEAT INPUT WELDING COMPATIBLE WITH THICK STEEL PLATES OF 460MPa YIELD POINT CLASS FOR VERY LARGE CONTAINER SHIPS』Welding in the world Vol.54 (2010)

45)　『日本海事協会　鋼船規則　M編　溶接』

46)　Bill Addis. *Building: 3000 years of Design Engineering and Construction*. Phaidon. 2007. p. 632

47)　R. Uemori, M. Fujioka, T. Inoue, M. Minagawa, K. Ichikawa, H. Shirahata, T, Nose: Steels for Marine Transportation and Construction, Nippon Steel Technical Report, (2012), No. 101, 37-41.

48)　J. William Cofer, presentation to Virginia Port Authority Virginia's Offshore Fairways , November 27, 2012.

49)　S. Suzuki, K. Ichiyama, T. Akita: High Tensile Strength Steel Plates with Excellent HAZ Toughness for Shipbuilding - JFE EWEL Technology for Excellent Quality in HAZ of High Heat Input Welded Joints -, JFE Technical Report, 5 (2005), 24-29

50)　S. Suzuki, K Oim, K. Kitani, Y. Murakami, Y. Materia. Vol. 43, no. 3, 2004, p. 232-234.

51)　O. Haida, T. Emi, G. Naito, M. Moriwaki, S. Tetsut-Hagane. Vol. 66, 1980, p.354-362.

52)　S. Kanazawa, A. Nakashima, K. Okamoto, K. Kanaya, Tetsut-Hagane. Vol. 61, 1975, p. 2589-2603.

53)   Y. Kasamatsu, S. Takashima, R. Hosoya, Tetsut-Hagane. Vol. 65 no. 8, 1979, p. 1232-1241.

54)   K. Ichimiya, H. Sumi, T. Hirai: 460MPa-Yield-Strength-Class Steel Plate with JFE EWEL® Technology for Large-Heat-Input Welding, JFE Technology Report 2008, No. 11, 7-12.

55)   K. Sakaguchi, M. Toyoda, Y. Inukai: IHI Engineering Review. 2007, vol. 40, no.2, p. 49-53.

56)   S. Nagatsuka. Kanrin, 2007, no. 11, p. 12-16.

57)   S. Suzuli, K. Ichimiya, T. Akita. JFE Giho. 2005, no. 5, p. 24-29.

58)   S. Suzuki, K. Oi, K. Ichimiya, Y. Kitani, Y. Murakami. Materia. 2004, vol. 43, no. 3, p. 232-234.

59)   A. Kojima, A, Kiyose, M. Minagawa, A, Hirano, K. Yoshii, T. Nakashima, M. Hoshima, Y. Ueshima. CAMP-ISIJ. 2003, vol. 16, p. 360-363.

60)   A. Kojima, R. Uemori, M. Hoshino, K. Ishida, A. Kiyose, M. Minagawa, T. Nakashima, H. Yasui: Super High HAZ Toughness Technology with Fine Microstructure Imparted by Fine Particles, Nippon Steel Technical Report, (2004), No. 90, 2-6

61)   http://www.me-mechanicalengineering.com/2014/10/electrogas-welding.html . 15 July 2015.

62)   K. Sasaki, K Suda, R. Motomatsu, Y. Hashiba, S. Okita, S. Imai: Developmtnet of Two-electrode Electro-gas Arc Welding, Nippon Steel Technical

Report, 2004, No. 90, p. 67-74.

63)   K Hori, H Watanabe, K Kusano, T Myoga, "Development of hot wire TIG welding methods using pulsed current to heat filler wire – research on pulse heated hot wire TIG welding processes" Journal of Welding International, 2004, Vol. 18, Issure 6, p. 456-468.

64)   K. Shinozaki, M. Yamamoto, T. Uchida, K. Mitsuhata, T. Nagashima, T. Kanazawa, H. Arashin: Development of Ultra-High-Speed GTAW Welding Process Using Pulse-Heated Hot-Wire. National Conference 2008, Japan Welding Society. 2008, p.228-229.

65)   Cary, Howard B. and Scott C. Helzer (2005). *Modern Welding Technology*. Upper Saddle River, New Jersey: Pearson Education. ISBN 0-13-113029-3.

66)   K. Shinozaki, M. Yamamoto, K. Morinaga, D. Yagi, Y. Katakamim T. Ozaki, "Development of remote laser welding method using long focal-distance lens for automobile galvanized steel". J. The Japan Welding Society, 2009, 27(2), 60s-63s.

67)   J. Xie, "Dual beam laser welding", Welding Journal, 2002, pp 223s-230s

68)   K. Kadoi, K. Shinozaki, M. Yamamoto, K. Owaki, K. Inose, D. Takayanagi, " Development of high-efficiency/high-quality hot-wire laser fillet welding process" , Quarterly J. JWS, 29-3 (2011), p. 62s-65s.

69)   D. Okita, M. Yamamoto, K. Shinozaki, K. Kadoi, T. Sado: Weld Defect Prevention for Fillet Welded Joint on Steel Plate Coated with Shop Primer Using Hot-wire Laser Welding, The International symposium on Visualization in Joining & Welding Science through Advanced Measurements and Simulation (Visual-JW 2014), Joining and Welding Research Institute Osaka   University, 2014, Osaka, Japan, V(1), p.103-104.

70)   M. Yamamoto, K. Shinozaki, K. Kadoi, D. Fujita, T, Inoue, M. Fukahori, Y. Kitahara, " Development of hot-wire welding method for lap joint of steel sheet with wide gap" , Quarterly J. JWS, 29-3 (2011), p. 58s-61s.

71)   P. Rittichai, M. Yamamoto, K. Shinozaki, M. Yamamoto, and K. Kadoi: "Heat Source Model for Hot-wire Laser Narrow Gap Welding Process; Effects of Welding

Conditions on High-temperature Strain Initiation, Modeling of Thermal Elastic Plastic Analysis for Hot-wire laser Narrow Gap Welding Process (Part 2)", National Meeting of Japan Welding Society, 93(4) (2013), p.212-213

72) R. Phaoniam, R. Nakamura, K. Shinozaki, M. Yamamoto, K. Kadoi H. Yamamoto, and T. Nakajima: "Evaluation of solidification cracking susceptibility based on high-temperature strain analysis, Evaluation of hot cracking susceptibility on large scaled cast steel part for construction machinery during GMA welding (2nd report), National Meeting of Japan Welding Society, 93(4) (2013), p.210-211

73) Masayuki Yamamoto, Phanoniam Rittichai; Kenji Shinozaki; Motomichi Yamamoto; Kota Kadoi: "Development of High Efficient Hot-wire Laser Welding for Narrow Gap Joint", 7th Asia Pacific IIW International Congress, (2013), Document number: ICRA-2013-SING.211.

74) P. Rittichai, A.Nishijima, M.Yamamoto, K.Shinozaki, M.Yamamoto, and K.Kadoi: "Heat Source Model for Hot-wire Laser Narrow Gap Welding Process; Modeling of Thermal Elastic Plastic Analysis for Hot-wire laser Narrow Gap Welding Process (Part 1)", National Meeting of Japan Welding Society, 91(4) (2012), p.18-19

75) M. Yamamoto, R. Phaonaim, K. Shinozaki, M. Yamamoto, K. Kadoi, and A. Nishijima, and S. Tsuchiya: "Development of high efficient hot-wire laser welding for narrow gap joint", The International symposium on Visualization in Joining & Welding Science through Advanced Measurements and Simulation (Visual-JW 2012), Joining and Welding Research Institute Osaka   University, 2012, Osaka, Japan, V(1), p.73-74.

76) T. Okagaito, H. Watanabe, K. Shinozaki, M. Yamamoto, K. Kadoi, M. Yamamoto, and R. Phaonaim: "Strength evaluation of narrow gap hot wire laser welding joint of heat-resistant steel for boiler", National Meeting of Japan Welding Society, 91(4) (2012), p.16-17.

77) T. Okagaito, H. Watanabe, K. Shinozaki, M. Yamamoto, K. Kadoi, A. Nishijima, and R. Phaonaim: "Development of Narrow Gap Hot-Wire Laser Welding Process for Heat-Resistant Steel Pipe for Boiler", National Meeting of Japan Welding Society, 90(4) (2010), p.200-201.

78)   R. Phaonaim, K. Shinozaki, M. Yamamoto, and K. Kadoi, and A. Nishijima: "Development of a highly efficient hot-wire-laser hybrid process for narrow-gap welding; welding phenomena and their adequate conditions", Journal of welding in the world, (2013),p.607-613

79)   M. Kaviany. Principles of heat transfer, 2002, John Wiley&Sons,Inc., New York. P.306-311.

80)   J.T. Lui and D.C. Wu.

81)   J. Mazumder, W.M. Steen, Heat Transfer Model for CW Laser Material Processing, Journal of Applied Physics, 1980, No. 51, p. 941-947.

82)   V.N. Tokarev, A. F. H. Kaplan, An Analytical Modeling of Time Dependent Pulsed Laser Melting , Journal of Applied Physics, 1999, No. 86, p. 2846-2836.

83)   C. Konrad, Y. Zhang, B. Xiao, Analysis of Melting and Resolidification in a Two-component Metal Power Bed Subjected to Temporal Gaussian Heat Flux, Int. J. of Heat and Mass Transfer, 2005, No. 48, p-3932-3944.

84)   DJ. Abson, RJ. Pargeter. Factors Influencing As-Deposited Strength, Microstructure, and Toughness of Manual Metal Arc Welds Suitable for C-Mn Steel Fabrications. Int. Met. Rev, 1986, No. 31, p. 141-194.

85)   O. Grong, DK. Matlock. Microstructure Development in Mild and Low Alloy Steel Weld Metals. Int. Met. Rev. 1986, No. 31, p. 27-48.

86)   G. Thewlis. Classification and Quantification of Microstructures in Steels. Mater Sci Technol., 2004., No. 20, p. 143-160.

87)   H. Hommam S. Ohkita, S. Matsuda, K. Yamamoto, Improvement of HAZ Toughness in HSLA Steel by introducing Finely Dispersed Ti-Oxide. Weld J., 1987, No. 66, p.139s-149s.

88)   PL. Harison, RA. Farrar. Influence of Oxygen-Rich Inclusions on the γ to α Transformation in High Strength Low Alloy (HSLA) Steel Weld Metals. J Mater Sci. 1981, No.16, p. 2218-2226.

89)   Hashida Koei, Development of Vertical Welding process for Thick Steel Plates Using Hot-wire Laser Welding method, Master thesis, Mechanical system engineering, Hiroshima University, 2014.

90)   Masuda Kouhei, Development of Vertical Welding process for Thick Steel Plates Using Hot-wire Laser Welding method, Basehor thesis, Mechanical system engineering, Hiroshima University, 2014.

91)   S. Ohkita, Y. Horii, Recent development in controlling the microstructure and properties of low alloy steel weld metals, ISIJ Internatianal, 1995, Vol. 35, No. 10, p. 1170-1182.

92)   Y. Tomita, K. Okabayashi, Effect of microstructure on strength and toughness of heat treated low alloy structural steels. Metallurgical Transactions A, 1986, Vol. 17A, p. 1203-1209.

93)   F. Matsuda, K. Ikeuchi, J. Liao. Weld HAZ toughness and its improvement of low alloy steel SQV-2A for pressure vessels (Report 1): Effect of cooling time on microstructure and charpy impact value in single thermal cycle, Transactions of JWRI. 1993, Vol. 22, No. 2, p. 271-279.

94)   Yurioka, N (1990). "Weldability of Modern High Strength Steels". *First US-Japan Symposium on Advances in Welding Matallurgy* (American Welding Society): 79–100.

95)   http://www-it.jwes.or.jp/weld_simulator/en/cal1.jsp . 15 July 2015.

Published or submitted papers in regards to this thesis

1. **E. Warinsirirruk,** K. Hashida, M. Yamamoto, K. Shinozaki, K. Kadoi, T. Tanino, H. Yajima, T. Fuki, S. Nakayama, T. Nose, S. Tsuchiya, H. Watanabe,T. Kanazawa, Welding Phenomena during Vertical Welding Process on Thick Steel Plate Using Hot-wire Laser Welding Method, Quarterly J. JWS, 33-2 (2015), pp. 143-147. (Chapter 3 & 4).
2. **E. Warinsirirruk,** K. Hashida, M. Yamamoto, K. Shinozaki, K. Kadoi, T. Tanino, H. Yajima, T. Fuki, S. Nakayama, T. Nose, S. Tsuchiya, H. Watanabe,T. Kanazawa, Oblique Laser Irradiation Technique for Vertical Welding of Thick Steel Plates Employing Hot-wire Laser Welding Method, Quarterly J. JWS, 33 (2015),(Accepted). (Chapter 3 & 4).
3. **E. Warinsirirruk,** K. Hashida, M. Yamamoto, K. Shinozaki, K. Kadoi, T. Tanino, H. Yajima, T. Fuki, S. Nakayama, T. Nose, S. Tsuchiya, H. Watanabe,T. Kanazawa, Welding Phenomena during Vertical Welding Process on Thick Steel Plate using Hot-wire Laser Welding Method, The International symposium on Visualization in Joining & Welding Science through Advanced Measurements and Simulation (Visual-JW 2012), Joining and Welding Research Institute Osaka University, 2014, Osaka, Japan, V(1), pp. 99-100. (Chapter 3 & 4).
4. T. Tanino, H. Yajima,**E. Warinsirirruk,** K. Hashida, M. Yamamoto, K. Shinozaki, K. Kadoi, T. Fuki, S. Nakayama, T. Nose, S. Tsuchiya, H. Watanabe,T. Kanazawa, Development of Vertical Welding Process on Thick Steel Plate usinf Hot-Wire Laser Welding Method, Proceeding of the Symposium on Welding Mechanics & Design, 2014, pp. 13-16. (Chapter 3 & 4).

Presentations

1. K. Hashida, **E. Warinsirirruk**, M. Yamamoto, K. Shinozaki, K. Kadoi, T. Tanino, H. Yajima, T. Fuki, S. Nakayama, T. Nose, S. Tsuchiya, H. Watanabe,T. Kanazawa, Welding Phenomena during Vertical Welding Process on Thick Steel Plate using Hot-wire Laser Welding Method (Report 1), National Conference of JWS, 95 (2014), 243-245. (Chapter 3).

2. **E. Warinsirirruk**, K. Hashida, M. Yamamoto, K. Shinozaki, K. Kadoi, T. Tanino, H. Yajima, T. Fuki, S. Nakayama, T. Nose, S. Tsuchiya, H. Watanabe,T. Kanazawa, Welding Phenomena during Vertical Welding Process on Thick Steel Plate using Hot-wire Laser Welding Method (Report 2), National Conference of JWS, 95 (2014), 246-247. (Chapter 3 & 4).

3. **E. Warinsirirruk**, K. Hashida, M. Yamamoto, K. Shinozaki, K. Kadoi, T. Tanino, H. Yajima, T. Fuki, S. Nakayama, T. Nose, S. Tsuchiya, H. Watanabe,T. Kanazawa, Development of Vertical Welding Process on Thick Steel Plate using Hot-wire Laser Welding Method, The 7th International Congress on Laser Advanced Materials Processing (LAMP 2015), Kitakyushu International Conference Center, Kokura, Kitakyushu-city, Japan, 2015, p. 143. (Chapter 3 & 4).